ADDIS ABABA UNIVERSITY

ADDIS ABABA INSTITUTE OF TECHNOLOGY

SCHOOL OF CIVIL AND ENVIRONMENTAL ENGINEERING

COMPARISON AND EVALUATION OF SATELLITE-BASED RAINFALL PRODUCTS FOR HYDROLOGICAL MODELING *(*CASE OF WABE WATERSHED, ETHIOPIA*)*

A Thesis in Hydraulics Engineering

By: Kiduse Teshome

October 2019

Addis Ababa

A Thesis

Submitted in Partial Fulfillment of the Requirements for the Degree of Master of Science

The undersigned have examined the thesis entitled '**Comparison and Evaluation of Satellite Rainfall products for Hydrological Modeling (case of Wabe watershed, Ethiopia)**' presented by **Kiduse Teshome**, a candidate for the degree of **Master of Science** and hereby certify that it is worthy of acceptance.

Advisor	Signature	Date
Internal Examiner	Signature	Date
External Examiner	Signature	Date
Chairperson	Signature	Date

UNDERTAKING

I confirm that research work titled "**Comparison and Evaluation of Satellite Rainfall products for Hydrological Modeling (case of Wabe watershed, Ethiopia)**" is my own work. The work has not been presented elsewhere. Where material has been used from other sources it has been properly acknowledged.

Kiduse Teshome

This is to certify that the above certification made by the candidate is correct to the best of my knowledge

Signature

Fiseha Behulu (PhD)

ABSTRACT

Satellite-based Rainfall products have been playing an immense role and used as an alternative source of data in regions where conventional rainfall measurements are not readily available or inadequate.

The objective of this study is to evaluate and compare high-resolution satellite rainfall products such as CHIRPS, PERSIANN-CCS, RFE and TAMSAT with the ground-based observed rainfall data over the Omo-Gibe River Basin. For spatial assessment, a point to pixel approach at different temporal scale over the time window of 2003-2017 is used. Moreover, the capabilities, applicability, and limitations of satellite rainfall products were also evaluated by forcing the hydrological model (HBV-light) in Wabe Watershed from Omo-Gibe River Basin. Continuous statistics was used to assess their performance in estimating and reproducing rainfall amounts and categorical statistics was used to evaluate rain detection capabilities while Kling-Gupta Efficiency (KGE) is used for model performance evaluation.

At mean daily scale, a good correlation agreement was observed by Wolkite with TAMSAT, RFE, PERSSIAN-CCS, CHRIPS (r=0.769, r=0.686, r=0.627, r=0.543) respectively. While the remaining station with the products show a low correlation and the time step has an important influence. This showed when the time step increases the accuracy of satellite rainfall products to predict the rainfall event relative to the station value will increase.

The HBV model was simulated using datasets from 2003-2012 considering both satellite rainfall products and ground-based observed dataset. The model has shown good performance when calibrated with the gauged observed rainfall data. During calibration, the objective function showed KGE= 0.42 for daily, and KGE=0.61 for monthly time scale; whereas, the validation period showed KGE=0.54 and 0.71 for daily and monthly time scales respectively. The adjusted satellite rainfall estimates TAMSAT and RFE showed relatively good performance while adjusted PERSIANN-CCS and RFE relatively showed less performance. The adjusted TAMSAT data set perform the best result than that of the other dataset at daily and monthly time scale with KGE=0.39 and KGE=0.54 for calibration and KGE=0.6 KGE=0.72 for validation period respectively. Finally, this study reveals that besides the gauged observed rainfall data the bias-adjusted TAMSAT and RFE dataset can be used as an alternative dataset for hydrological modeling for the study area.

Keywords; Omo –Gibe, Wabe, HBV-light, CHIRPS, PERSIANN-CCS, RFE, TAMSAT, KGE,

ACKNOWLEDGMENTS

First of all my thanks to Above all, creator and governor of the two worlds, the almighty GOD, Jesus Christ, his mother Saint Marry, all his Angels and Saints for his priceless and miracle gifts to me. Next, I would like to express my appreciation to my thesis advisor Dr. Fiseha Behulu Muluneh. I have been lucky, having the chance to be advised and guided by someone so positive and so encouraging. Thank you Dr. Fiseha I would like also to thank Ministry of Water Irrigation & Energy and National Meteorological Service Agency for their cooperation in availing the necessary data then I would like to express my admiration to all my friends and course mates for their support and wonderful social atmosphere. Back home, I wish to express my deep gratitude to all my family members, their prayers for me when the main sources of inspiration, motivation, and encouragement to continue this work. Last of all, thanks to everyone who helped me and my thanks also go for those who showed me their immorality side their act wasn't limit my effort but alarms me to be stronger and I wish all of you wonderful happy life.

.

TABLE OF CONTENT

LIST OF TABLES

LIST OF FIGURES

ABBREVIATIONS

BETA	shape coefficient
CHRIPS	Climate Hazards Group Infra-Red Precipitation with Stations
DEM	Digital Elevation Model
E	Nash–Sutcliffe Efficiency coefficient
EWS	Early Warning System
FAR	False Alarm Ratio
FC	maximum value of soil moisture storage
HBV	*HydrologiskaByr°ansVattenavdelning*
K0	storage (or recession) coefficient 0
K1	recession coefficient (upper box)
K2	recession coefficient (upper box)
KGE	Kling-Gupta efficiency
LP	the fraction of FC above which actual ET equal potential ET
MAXBAS	length of triangular weighting function in routing routine
ME	Mean Error
MOWIE	Ministry of Water, Irrigation, and Energy
Net-CDF	Network Common Data Form
NMSA	Ethiopian National Meteorological Services Agency
NOAA-CPC	the National Oceanographic and atmospheric administration for climatic prediction center
PERC	the maximum rate of recharge between the upper and lower ground water boxes
PERSSIAN-CCS	Precipitation Estimation from Remotely Sensed Information using Artificial Neural Networks-Cloud Classification System
POD	Probability of Detection
RFE	African Rainfall Estimation
r	coefficient of correlation
RMSE	the relative root mean squared error
SMHI	Swedish Meteorological and Hydrological Institute
SRE	Satellite Rainfall Estimates

SRPs	Satellite Rainfall products
TAMSAT	Tropical Applications of Meteorology using Satellite
TRMM	Tropical Rainfall Measuring Mission
UZL	threshold parameter
WMO	World Metrologic Organization

1. INTRODUCTION

1.1 Background

Rainfall is a crucial resource in many socio-economic activities, particularly for those African countries relying predominantly on rain-fed agriculture. Many countries have been affected by rainfall variability and long-term changes in both rainfall amount and distribution over recent decades (T. Dinku et al., 2007); it is also an essential component of the hydrological cycle so accurate global rainfall coverage is necessary to improve short term, medium and long term weather forecasts, and Climate monitoring (Shrestha, 2011).

A sound water resource planning and management process requires reliable estimates of rainfall, traditionally these data are provided by networks of *in situ* monitoring stations, which are costly to maintain in vast and desert areas, such as the case of many African countries. (Sandra Pombo, 2014)

Even though rain gauge is a direct rainfall measuring instrument which is technologically mature, ease and widely used, it cannot reflect the spatial variation of rainfall effectively due to the very limited radius of point measurements (Collischonn, 2008).

In comparison with a rain gauge, the ground radar system can provide the instantaneous spatial distribution of rainfall over the basin indirectly and thus help to remove the bias of rain gauge observations partly. But, because of its problem of limited coverage area, high costs of establishing and maintaining infrastructure, there is no perfect radar network in many regions (Gu H.et al, 2010), It still cannot meet the requirements of a study carried out on large scale basins. These sorts of drawbacks clearly show that rainfall data availability and accuracy impose a notable limitation on the application of the hydrological model.

River flow measurements are critical for hydrological data assimilation and model calibration in flood forecasting and other water resource management issues in many parts of the world, however, *in situ* river discharge measurements are either completely unavailable or are difficult to access for timely use in operational flood forecasting and disaster mitigation. Hence Satellite-based Rainfall products have been regarded as an alternative source of data in regions where conventional rainfall measurements are not readily available or inadequate (Odai et al, 2018)

Recent advances in multi-satellite rainfall estimates have allowed uses of high-resolution satellite rainfall products in hydrological modeling for runoff simulations and predictions. The growing availability of high-resolution (and near real-time) satellite rainfall products are attracting the interest of hydrologists particularly in developing countries and remote locations where weather radars are absent and conventional rain gauges are sparse (Bitew et al, 2012)

However, SRPs are subjected to a variety of potential errors, which originate from discontinuous revisit time of observing sensors and weak relationships between remotely sensed signal and rainfall rate. Hence to ensure a justified usage of SRP as input to hydrological models, a systematic validation is required. There are two methods for validating SRFE: either through ground-truthing or through model-based applications. As many researchers (Worqlul A. W., 2014) (Hughes, 2006) (Gebremichael & Romilly, 2010) (Getachew T., 2017) and (M.dembele & S.J.Zwart, 2016) has done it the first method refers to the traditional approach comparing SRPs against ground observed precipitation. The second approach refers to the evaluation of SRPs by assessing their performance within a target application. An example of this approach is the evaluation of SRPs based on their capabilities to reproduce the observed streamflow, also referred to as ‘‘hydrological evaluation’’. Some of these works are done previously by (T. Cohen Liechti, 2012) (Bitew et al, 2012) (Vera Thiemig, 2013), (Vu Thi Thom, 2018), and (Bakary Faty, 2018). Even though both methods can be independently applied, they can be considered as complementary: the first one provides insight into the intrinsic data quality of the SRFE, whereas the second one assesses the usefulness of the SRP within a certain application

The HBV (*Hydrologiska Byr°ans Vattenavdelning*) model software provides Different functionalities, such as an automatic calibration using a genetic algorithm or a Monte Carlo approach, as well as the possibility to perform batch runs with predefined model parameters (Seibert & Vis, 2012)

The best product depends on the specific application and the time step has great importance in evaluating the quality of satellite products. Estimates at a daily or shorter time step are essential for driving rainfall-runoff models used for flood forecasting and river management (Grimes, Pardo-Igúzquiza, & Bonifacio, 1999)

Hence, this study was intended to investigate the performance of four operational high-resolution satellite-based rainfall products: Climate Hazards Group Infrared Precipitation with Stations (CHIRPS), Precipitation Estimation from Remotely Sensed Information using Artificial Neural

Networks-Cloud Classification System (PERSIANN-CCS), African Rainfall Estimation (RFE 2.0), and Tropical Applications of Meteorology using Satellite (TAMSAT) for hydrological modeling in Wabe watershed, Ethiopia.,

Using the above software Steam-flow simulation was carried out for various precipitation products that include gauge observation and gauge adjusted SRPs. Therefore the aim of this study is to assess the performance of various satellite precipitation data for the application of hydrological modeling in the Wabe Watershed, Ethiopia

1.2 Statement of the problem

A low network density and infrequent reporting rates present a serious challenge in monitoring rainfall events across Africa. As shown in Figure 1-1 below the African rainfall network is 8 times lower than WMO recommended level.

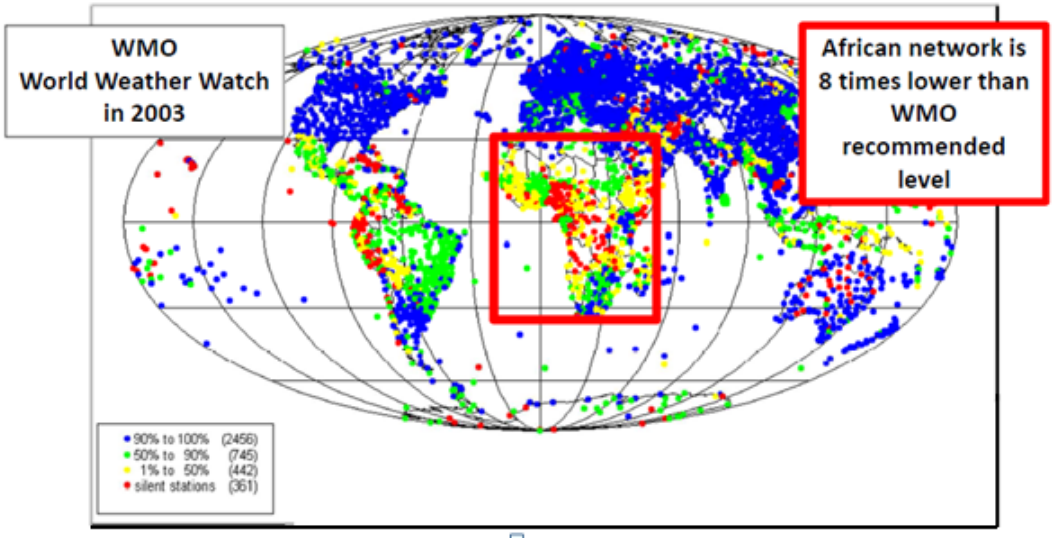

Figure 1-1 WMO World Weather Watch in 2003

Aspects of poor spatial distribution and non-existence of reliable rain gauge networks that apply to many catchments also apply to the Omo –Gibe basin As such, satellite-derived rainfall has emerged as a viable option to indirectly retrieve rainfall estimates. However, whether measured directly by rain gauges or indirectly by remote sensing techniques all are susceptible to uncertainty additionally; accuracies of the rainfall products as compared to gauge measurements are often not impressive, so bias correction that can potentially compensate for the systematic errors is essential.

Despite that most of the existing products are continuously improving their algorithms and data sources to adapt to particular environments, catchment-specific studies should still be carried out before any hydrological application. (Mauricio Zambrano-Bigiarini, 2017)

For rivers that cross international boundaries, inconsistencies in instrumentation and ground-based limitations to data access further hamper the effective use of hydrology models. These limitations are true for the Omo–Gibe basin. For this basin, the use of bias-corrected rainfall estimates in streamflow simulations is yet to be fully explored. Furthermore, and among other factors, many studies reveal that accuracies of SREs are affected by product type and area, yet very few studies have analyzed such aspects. Motivated by this existing gap, this study thus attempts to assess the effects of bias corrections of rainfall estimates from CHIRPS, PERSIANN-CCS, RFE 2.0, and TAMSAT, Intercomparison of different seasonal performance, and application of SRPs to streamflow simulations by applying HBV software.

1.3 Objective

1.3.1 General objective

The main objective of this research is to evaluate and determine the suitable type of satellite-based rainfall estimate for hydrological modeling in Wabe watershed.

1.3.2 Specific objective

- To evaluate the accuracy of satellite rainfall products over Omo- Gibe Basin using statistical approach;
- To identify the availability and reliability of satellite rainfall products for hydrological modeling;
- To do hydrological modeling using gauged observed rainfall data as well as satellite rainfall data as an input.

1.4 Research Questions

- Are satellite rainfall products effective in simulating stream flows for small watershed?
- Can high-resolution satellite-based rainfall estimates provide reliable rainfall information for streamflow simulation applications in this watershed?
- What is the most effective rainfall bias correction scheme for the watershed?

- Is there any significant difference using satellite rainfall products and rain gauge rainfall observation in hydrological modeling?

1.5 Scope of the study

The boundary of the study is the Omo-gibe basin, for this study the scope has been limited with respect to the stated objectives. Thus, gauged observed rainfall data were considered as a reference in the evaluation and assessment of satellite rainfall products. while The HBV-light model is applied to simulate the streamflow in the watershed and finally selecting the reliable rainfall estimation over the basin was the main target of the study.

1.6 Significance of the study

The study is highly significant and plays a vital role in the following concerns

- It is relevant in terms of providing flow information for the status of hydropower projects and irrigation projects in the cascade of Wabe watershed. Additionally, it will have a contribution to water resources development and feasibility studies
- It is important in finding the appropriate precipitation bias correction scheme for the Basin;
- It will serve as feedback to respective products' developers and end-users in understanding the errors and uncertainties involved and how they propagate in hydrological response applications.

1.7 Outline of the Thesis

This thesis is consists of five chapters. The first chapter presents an introduction section where the background, statement of the problem, objectives of the study, research questions, scope of the research and significance of the study are discussed while the second chapter deals with the literature review relating to the high resolution of satellite rainfall products. The third chapter delivers a brief history of the study area and material and methods of the research and model input data whereas the fourth chapter briefly presents results and discussions. Finally, the last chapter delivers the conclusions and recommendations of the study.

2. LITERATURE REVIEW

2.1 General

Sound predictions of hydrological models need an accurate spatial and temporal distribution of precipitation. Since African agriculture is predominantly rain-fed, and many regions are affected by high rainfall variability in both space and time, there is a pressing need for accurate gridded rainfall products for different applications, such as agricultural monitoring and yield prediction in remote areas. Rain gauges have been the main source of rainfall data, but in many countries, the rain gauge network is inadequate to produce reliable distributed rainfall maps (Toté et al, 2015). The emergence of the aforementioned near-global and high-resolution SREs opens up new possibilities for applications in data-scarce or ungauged regions.

This chapter describes the literature review related to the objective of this study. Therefore; first Global Satellite-Based Rainfall Estimation Methods are reviewed, the next literature on satellite rainfall Products was reviewed. Then review on Rainfall-Runoff Modeling was discussed. Finally, a review on the evaluation of the Performance of Satellite-Based Rainfall Products and their role for hydrological modeling was presented.

2.2 Review of Global Satellite-Based Rainfall Estimation Methods and Products

Since the launch of a meteorological satellite Television Infra-Red Observation Satellite (TIROS-1) in 1960, the study of the earth's atmosphere and oceans using data obtained from these remote sensing devices has advanced rapidly. Particularly, since the last two decades, there has been a lot of advancement in the estimation of rainfall from space. In the 1970s rainfall estimation using Infra-Red (IR) sensors on geostationary platforms to track cloud movement and advance climate and weather prediction was developed (Janowiak, 2001). Since then, this technology for monitoring precipitation from space obtained from satellites orbiting the earth has rapidly advanced. The primary scope of satellite rainfall monitoring is to provide information on rainfall occurrence, amount and distribution over the globe on a continuous basis from all areas including those inaccessible to gauges and radar for various applications in meteorology, climatology, hydrology, and environmental sciences. (Shrestha, 2011).

2.2.1 Satellite-Based Rainfall Estimation Methods

SRE is primarily from two types of meteorological satellites, geostationary satellites, and polar-orbiting satellites. Geostationary satellites provide continuous observation of the earth's surface and provide data on half-hourly or even lesser durations. Imagery obtained from these satellites are mainly visible (VIS) and IR at a resolution of about 4 km, with information on clouds, collected once every 15- 30 minutes. There are several operational geostationary meteorological satellites in orbit such as the MTSAT, GOES, METEOSAT, FY series, and INSAT.

The second type of satellites is the polar-orbiting satellites. Polar-orbiting satellites travel in a circular orbit from pole to pole orbiting at an altitude of about 800 km and use microwave (MW) channels. The orbits of these satellites are such that they pass the equator at the same local time on each orbit, providing about two overpasses each day. (Shrestha, 2011).a brief diagrammatical representation is shown in figure 2-1.

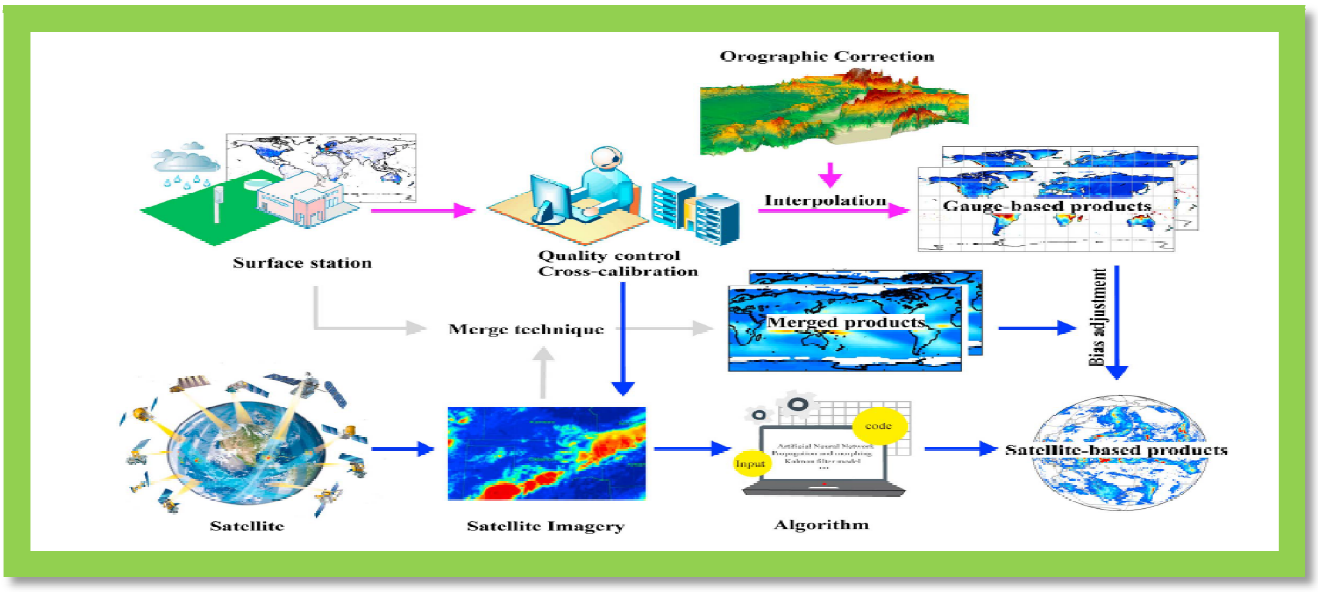

Figure 2-1 Flow chart for the precipitation products. The images for satellite adapted from (Hou et al. 2014).

2.2.2 Summary of some satellite rainfall products

A number of satellite precipitation data sets are currently available. Satellite observations provide precipitation information with homogeneous spatial coverage but contain non negligible random errors and biases owing to the indirect nature of the relationship between the observations and precipitation, in table 2-1 summary of SRPs is tabulated.

Table 2-1 Summary of Major Satellite-Related Precipitation Products Currently Available adapted from (Qiaohong Sun et al, 2017)

Summary of Major Satellite-Related Precipitation Products Currently Available

Data set	Adjusted	Res.	Freq.	Coverage	Period	Data source	Algorithm	Reference
GPCP	GPCC, GHCN	2.5°	Monthly	Global	1979–present	GPI, OPI, SSM/I scattering, SSM/I emission, TOVS		(Adler et al., 2003)
GPCP 1dd	GPCC, GHCN	1.0°	Daily	Global	1996–present	SSM/I-TMPI, TOVS		(Huffman & Bolvin, 2013)
GPCP_PEN_v2.2	GPCC, GHCN	2.5°	5-daily	Global	1979–2014	OPI, SSM/I, GPI, MSU		(Xie et al., 2003)
CMAP	GPCC, GHCN	2.5°	Monthly	Global	1979–present	GPI, OPI, SSM/I scattering, SSM/I emission, MSU, NCEP–NCAR		(Xie et al., 2003; Xie & Arkin, 1997)
CPC-Global	GTS, COOP, NMAs	0.5°	Daily	Global land	2006–present	GTS, COOP, NMAs		(Xie et al., 2010)
TRMM 3B43	GPCC	0.25°	Monthly	50°S–50°N	1998–present	TMI, TRMM Combined Instrument, SSM/I, SSMIS, AMSR-E, AMSU-B, MHS, and GEO IR	Probability Matching	(Huffman et al., 2007)
TRMM 3B42	X	0.25°	3 h/Daily	50°S–50°N	1998–present	TMI, TRMM Combined Instrument, SSM/I, SSMIS, AMSR-E, AMSU-B, MHS, and GEO IR	Probability Matching	(Huffman et al., 2007)
GSMaP	X	0.1°	1 h/daily	60°S–60°N	2002–2012	TMI, AMSR-E, AMSR-E, SSM/I, multifunctional transport satellites (MTSAT), Meteosat-7/8, GOES 11/12	Kalman filter model	(Ushio et al., 2009)
PERSIANN-CCS	X	0.04°	30 min/3, 6 h	60°S–60°N	2003–present	Meteosat, GOES, GMS, SSM/I, polar/near polar precipitation radar, TMI, AMSR	Artificial Neural Networks	(Sorooshian et al., 2000)
PERSIANN-CDR	GPCP	0.25°	3, 6 h/Daily	60°S–60°N	1983–present	GOES 8, GOES 10, GMS-5, Metsat-6, and Metsat-7, TRMM, NOAA 15, 16, 17, DMSP F13, F14, F15.	Artificial Neural Networks	(Ashouri et al., 2015)
CMORPH	X	0.25°/8 km	30 min/3 h/Daily	60°S–60°N	2002–present	TMI, SSM/I, AMSR-E,AMSU-B, Meteosat, GOES, MTSAT	Propagation & Morphing	(Joyce et al., 2004)
GPM		0.1°	30 min/3 h/daily	60°S–60°N	2015–present	GMI, AMSR-2, SSMIS, Madaras, MHS, Advanced Technology Microwave Sounder	IMERG	(Hou et al., 2008, 2014)
MSWEP	CPC, GPCC	0.1°/0.5°	3 h/daily	Global	1979–present	CPC, GPCC, CMORPH, GSMaP-MVK, TMPA, ERA-Interim, JRA-55		(Beck et al., 2017)

2.2.3 Selected Satellite Rainfall Products

Global and continental remote-sensing precipitation products are becoming increasingly available with reasonable spatial and temporal resolutions for application in hydrological and climate studies. These may provide an alternative for traditionally measured rainfall at weather stations (M.dembele & S.J.Zwart, 2016)

There are now several operational and semi-operational algorithms available from national centers and universities to produce rainfall estimates for time periods ranging from half-hourly to monthly (Shrestha, 2011), there are so many satellite-based rainfall products such as **(CHIRPS)**, **(PERSIANN-CCS)**, **(RFE 2.0)**, **and (TAMSAT)** Which are described briefly in the following section. Two of

them represent quasi-global rainfall product while the other two represent for Africa (local) respectively

2.2.3.1 The RFE

It is developed by the NOAA Climate Prediction Center (CPC) (M.dembele & S.J.Zwart, 2016). It is mainly produced for Famine Early Warning Systems Network to assist in disaster-monitoring activities over Africa.

The input data for RFE 2.0 comprise four operational sources:

I. daily Global Telecommunications System (GTS) rain-gauge data,
II. Advanced Microwave Sounding Unit (AMSU)-based rainfall estimates,
III. Special Sensor Microwave Imager (SSM/I)-based estimates, and
IV. The Geostationary Operational Environmental Satellite (GOES)

Precipitation index (GPI) calculated from cloud-top infrared (IR) temperatures on a half-hourly basis. The ARC is based on the same algorithm used in RFE. However, there are differences between ARC and RFE in the use of polar-orbiting PM and geostationary IR data. ARC uses only 3 hourly IR data instead of 30min and does not include PM estimates, which RFE does.

2.2.3.2 The TAMSAT

The **TAMSAT** ***(Tropical Applications of Meteorology using the Satellite data)*** approach is based on METEOSAT Thermal Infra-Red imagery to identify precipitating cumulonimbus clouds (deep convection) TAMSAT was established by the University of Reading in 1977. In the last three years, the group has developed close collaborations with the Climate Division of the National Centre for Atmospheric Science (NCAS) and the National Centre for Earth Observation (NCEO) to extend the range of climate services it provides. These collaborations are supporting the development of new datasets and other products, including rainfall estimate uncertainties, full column soil moisture, and probabilistic forecasts of drought.

2.2.3.3 The CHIRPS

This data set was developed by the US Geological Survey (USGS) and the Climate Hazards Group at the University of California, Santa Barbara (UCSB). The data inputs used for CHIRPS creation were:

I. the Climate Hazards Precipitation Climatology (CHPClim);

II. quasi-global geostationary TIR satellite observations from two NOAA sources, the CPC and the National Climatic Data Center (NCDC);
III. atmospheric model rainfall fields from the NOAA Climate Forecast System, version 2 (CFSv2);
IV. The TRMM 3B42 product from NASA; and
V. In situ precipitation observations obtained from a variety of sources including national and regional meteorological services (M.dembele & S.J.Zwart, 2016).

2.2.3.4 The PERSSIAN CCS

PERSIANN-Cloud Classification System (PERSIANN-CCS) is a real-time global high resolution(0.04° x 0.04° or 4km x 4km;) satellite precipitation product developed by the Center for Hydrometeorology and Remote Sensing (CHRS) at the University of California, Irvine (UCI).PERSIANN-CCS system enables the categorization of cloud-patch features based on cloud height, areal extent, and variability of texture estimated from satellite imagery. At the heart of PERSIANN-CCS is the variable threshold cloud segmentation algorithm. In contrast with the traditional constant threshold approach, the variable threshold enables the identification and separation of individual patches of clouds. The individual patches can then be classified based on texture, geometric properties, dynamic evolution, and cloud top height. These classifications help in assigning rainfall values to pixels within each cloud based on a specific curve describing the relationship between rain-rate and brightness temperature.

2.3 Review of hydrological Modeling

The term hydrology can be treated as an important subject for the people and their environment. It deals with water of the earth, their occurrence, circulation and distribution, their chemical and physical properties and their reaction with the environment including their relation to living things. It also deals with the relationship of water with the environment within each phase of the hydrologic cycle. (Gayathri K. Devi et al., 2015)

Nowadays, various hydrological models have been developed across the world to find out the impact of climate and soil properties on hydrology and water resources. Each model has got its own unique

characteristics. The inputs used by different models are rainfall, air temperature, soil characteristics, topography, vegetation, hydrogeology, and other physical parameters. (Gayathri K. Devi et al., 2015)

There are many different reasons why modeling of the rainfall-runoff processes of hydrology is needed. The main reasons behind are a limited range of hydrological measurement techniques and a limited range of measurements in space and time (Beven, K, 2000)

According to Seibert and Vis (2012) Models can contribute to a better understanding of hydrological variables and their interactions in a quantitative way.

Gayathri.et.al (2015) Stated that Hydrological models are now a day considered as an important and necessary tool for water and environmental resource management.

Lenhart (2002) Describe that hydrological modeling is a great method of understanding hydrological systems for the planning and development of integrated water resources management. The purpose of using a model is to establish baseline characteristics whenever data is not available.

As many types of research and the above literature explained the essence of hydrological modeling for characterization of the hydrological system is essential therefore conclusively dealing and considering such aspects in studies is vital.

2.3.1 Classification of Hydrological Models

Rainfall-runoff models are classified based on model input and parameters and the extent of physical principles. It can be classified as a lumped and distributed model based on the model parameters as a function of space and time and deterministic and stochastic models based on the other criteria. The deterministic model will give the same output for a single set of input values whereas, in stochastic models, different values of output can be produced for a single set of inputs. Another classification is static and dynamic models based on time factors. Static model excludes time while the dynamic model includes time (Gayathri K. Devi et al., 2015).

One of the most important classifications is an empirical model, conceptual models, and physically-based models.

According to Gayathri.et.al (2015) *Conceptual methods (Parametric models)* describes all of the component hydrological processes. It consists of a number of interconnected reservoirs which

represents the physical elements in a catchment in which they are recharged by rainfall, infiltration, and percolation and are emptied by evaporation, runoff, drainage, etc. Semi-empirical equations are used in this method and the model parameters are assessed not only from field data but also through calibration. A large number of meteorological and hydrological records is required for calibration additionally *Empirical models (Metric model)* are describes as observation oriented models which take only the information from the existing data without considering the features and processes of hydrological system and hence these models are also called data-driven models. It involves mathematical equations derived from concurrent input and output time series and not from the physical processes of the catchment. These models are valid only within the boundaries and physical-*based models* described as a mathematically idealized representation of the real phenomenon. These are also called mechanistic models that include the principles of physical processes. It uses state variables that are measurable and are functions of both time and space. furthermore, it can provide a large amount of information even outside the boundary and can apply for a wide range of situations.

2.3.2 Brief Description of Hydrological Models

2.3.2.1 Description of HBV Model

HBV model is named after the *Hydrologiska Byr°ans Vattenavdelning* unit at the Swedish Meteorological and Hydrological Institute (SMHI), where its development started in the1970s. The HBV model has become widely used and exists in several versions. The version HBV-light was developed at Uppsala University in 1993 using Microsoft Visual Basic and has become widely used in education at several universities (Seibert & Vis, 2012).

The HBV model is a semi-distributed conceptual rainfall-runoff model for continuous daily simulation of catchment runoff (Bergström, 1976.) It is a computerized system that converts precipitation, potential evaporation, and snowmelt, if applicable, into streamflow/reservoir inflow by simulating the natural hydrological processes. It is a semi-distributed conceptual rainfall-runoff model for continuous simulation of runoff, hydrological forecasting, design flood computations and climate change studies (Bergström, 1976.)

Different model versions are now available and are used in different countries with different climatic conditions. The degree-day method is used to simulate snow accumulation and snowmelt. Groundwater recharge, runoff, and actual evaporation are simulated as functions of actual water

storage. HBV-light is a new version of the HBV model and it uses a warm-up period, in which the state variables will get its appropriate values as per meteorological data and parameter values. (Gayathri K. Devi et al., 2015).

2.3.3 Model Selection

The best model is the one that gives results close to reality with the use of least parameters and model complexity. (Gayathri K. Devi et al., 2015).

In this paper, the selection of model taking into consideration the following three fundamental selection criteria in addition to project-specific criteria which are recommended by (Cunderlik, J. & Simonovia, S. P., 2007).

I. Required model outputs important for the needed purpose and therefore to be estimated by the model - does the model predict the variables required by the project such as inflow and sediment yield prediction?
I. Hydrologic processes that need to be modeled to estimate the desired outputs adequately - is the model, capable of simulating supposed physical and agronomic/vegetative erosion reduction measures over the area.
II. Availability of input data - can all the inputs required by the model be provided within the time and cost constraints of the project?

A study over HBV-light software was conducted by (Grillakis, I. K. Tsanis, & Koutroulis, 2010) to investigate the resultant flash flood in the study area, which consisted of five basins, was simulated with the conceptual distributed hydrological model HBV-light. The model was calibrated and validated with past rainfall-runoff events with satisfactory results-producing values of the Nash – Sutcliffe coefficient between 0.82 and 0.96. The validated model was applied to the flash flood case with stream gauge failure, driven by spatiotemporal precipitation produced by a set of rain gauges and radar data. The model delivered satisfactory results on three out of five basin outlets

Study on HBV-light model in different parts of Ethiopia was also made by (A. Y. JILLO ET AL., 2017), (Perera, 2017), (Endalkachew Abebe & Asfaw Kebede , 2019) and (Abebe Temesgen Ayalew, 2019). Results showed that the HBV-light model can be taken as a good source for hydrological modeling.

The conceptual models simplify the complex physical process and can be taken as an opportunity in catchment scale hydrological modeling. Model parameters can be optimized using different available hydrological modeling tools and remain constant as long as catchment property is not changed (Rientjes, 2011).The selection models mainly based on their input data requirement, computational power, the operating system, temporal and spatial scale, simplicity and output reliability. Therefore, since this model required few input data which are easily available it is apparently selected for this study.

As noted above among many hydrological models, the conceptual semi-distributed model HBV-light was used and tested for its applications runoff modeling in Ethiopia. For this reason, HBV-light was selected for this study based on the above-mentioned criteria.

2.4 Review on Evaluation of the Performance of Satellite-Based Rainfall Products and their use for hydrological modeling

2.4.1 Previous Studies around the World

Satellite-based rainfall data from PERSIANN and GPCP was compared by Hughes (2006) with gauge observed rainfall data in four basins with different climate regimes in southern Africa. They explored the use of SRP in hydrological models. Monthly time steps with simple statistics (visual interpretation, $r^{2,}$ and slope) were used in the comparison.

A bias-adjusted rainfall product for flood prediction was done by (Shrestha, 2011). Findings from this study indicate that the SRE underestimates rainfall significantly over Nepal but with a correlation higher than 0.70. The performance of the SRE is better in the flatter terrain than in the mountainous areas. The accuracy of SREs can be improved by applying a bias-adjustment. Prediction of discharge using bias-adjusted rainfall estimates can improve the accuracy of discharge prediction with a considerable increase in the predictive capability of flood prediction for which the hydrological model needs to be recalibrated.

Evaluation of the performance of five satellite rainfall estimation methods with ground-based precipitation over the Sahel region using the 10-day rainfall records from 1989-1993 at a 0.5^0 to 1^0 spatial resolution was conducted by (Laurent, 1998). This study is before the availability of high-resolution satellite-based products such as the TRMM. The study shows that the impact of calibrated and verified in sub-basin and basin using simultaneous historical observed data. For model evaluation

method, percent error in peak flow (PEPF), percent error in volume (PEV), coefficient of correlation (R^2) and the relative root mean squared error (RMSE) were used. In this research, the results show that the coefficient of correlation for all flood events was above 0.9, and the percent errors in peak flow and volume were all within the acceptable range (all values of PEPF < 10% and all value of PEV < 10%). However, the RRMSE for the basin was 21.9% in one event.

The reliability of ground-based measurements, different satellite products of rainfall and their combinations were tested for their impact on the discharge simulations of the Magdalena River. (Colombia) by (Amr Elgamala, 2016), they used Two different satellite rainfall products from the Tropical Rainfall Measuring Mission (TRMM), which have been compared and merged with the ground-based measurements and their impact on the Magdalena river flows quantified using the Representative Elementary Watershed (REW) distributed hydrological model.

Four gridded rainfall products, including APHRODITE, CFSR, PERSIANN, and TRMM, were used as input to the SWAT distributed hydrological model in order to simulate streamflow over the Srepok River Catchment in Vietnam. By (Vu Thi Thom, 2018) besides that, the available rain gauges data were also used for comparison. Amongst the four different datasets, the TRMM and APHRODITE data show their best match to rain gauges data in simulating the daily and monthly streamflow with satisfactory precision in the 2000–2006 periods. The result indicates that the TRMM and APHRODITE data have potential applications in driving hydrological models and water resources management in data-scarce and ungauged areas in Vietnam.

The performance of CHIRPS-based satellite precipitation estimates in Northeast Brazil for hydrological simulations was assessed by (Franklin, 2016). In this study, the monthly rainfall derived from the satellite-based rainfall product, Climate Hazards Group Infrared Precipitation with Stations (CHIRPS v.2), is compared with the observation from 21 ground stations in the NEB, for the period 1981-2013.

Comparison of two long-term and high-resolution satellite precipitation datasets in Xinjiang, China has been evaluated by (Feng Gaoa, 2018) the evaluation is performed at multiple temporal and spatial scales. Results based on comparisons with in situ measurements showed that PERSIANN-CDR and CHIRPS have similar correlations. However; both of the BIAS and RMSE, CHIRPS outperformed PERSIANN-CDR with smaller errors and bias. In terms of the long time-series comparison at

temporal scale, CHIRPS is more accurate with gauge observations at monthly and annual scales while PERSIANN-CDR tends to overestimate the precipitation in the rain season (from May to September). Furthermore, compared with PERSIANN-CDR, results show that CHIRPS is more accurate in reflecting the spatial distribution of average monthly and annual precipitation. In summary, the study shows that CHIRPS is a valuable complement to gauge precipitation data and provides useful guidance when choosing satellite precipitation products for hydro-meteorological applications in Xinjiang.

A Global-scale evaluation of 22 precipitation datasets using gauge observations and hydrological modeling was studied by (Hylke E. Beck1, 2017). They undertook a comprehensive evaluation of 22gridded (quasi-)global (sub-) daily precipitation (P) datasets for the period 2000–2016. Thirteen non-gauge-corrected P datasets were evaluated using daily P gauge observations from 76,086 gauges worldwide. Another nine-gauge corrected datasets were evaluated using hydrological modeling, by calibrating the HBV conceptual model against streamflow records for each of 9053 small to medium-sized(<50,000 km2) catchments worldwide and comparing the resulting performance. Marked differences in spatiotemporal patterns and accuracy were found among the datasets. Their results highlight large differences in estimation accuracy, and hence the importance of P dataset selection in both research and operational applications. The good performance of MSWEP emphasizes that careful data merging can exploit the complementary strengths of gauge-, satellite-, and reanalysis-based P estimates.

2.4.2 Previous studies in Africa

the performance of seven operational high-resolution satellite-based rainfall products – (ARC 2.0), (CHIRPS), (PERSIANN), (RFE 2.0), TAMSAT), TARCAT), and (TRMM) daily and monthly estimates – was investigated for Burkina Faso by (M.dembele & S.J.Zwart, 2016). These were compared to ground data for 2001–2014 on a point to- pixel basis at daily to annual time steps. Continuous statistics was used to assess their performance in estimating and reproducing rainfall amounts, and categorical statistics to evaluate rain detection capabilities. The north-south gradient of rainfall was captured by all products, which generally detected heavy rainfall events, but showed a low correlation for rainfall amounts. On a daily scale, they performed poorly. As the time step increased, the performance improved. All (except TARCAT) provided excellent scores for Bias and Nash–Sutcliffe Efficiency coefficients and overestimated rainfall amounts at the annual scale. RFE

performed the best, whereas TARCAT was the weakest. The choice of the product depends on the specific application: ARC, RFE, and TARCAT for drought monitoring, and PERSIANN, CHIRPS, and TRMM daily for flood monitoring in Burkina Faso.

An extensive evaluation of 10 different satellite rainfall products was performed using station network over a complex topography by (T. Dinku et al., 2007) where elevation varies from below sea level to 4620 m. The evaluation was for two groups of products. The first group had low spatial (2.5^0) and temporal (monthly) resolution and included the Global Precipitation Climatology Project (GPCP), the National Oceanographic and Atmospheric Administration Climate Prediction Center (NOAA-CPC) merged analysis (CMAP), and the Tropical Rainfall Measuring Mission (TRMM-3B43). The second group comprised products with relatively high spatial (0.1^0 to 1^0) and temporal (3-hourly to 10-daily) resolution. These included the NOAA-CPC African rainfall estimation algorithm, GPCP one-degree-daily (1DD), TRMM-3B42, Tropical Applications of Meteorology using Satellite and other data (TAMSAT) estimates, and the CPC morphing technique (CMORPH). These products were aggregated to a 10-day total and remapped to spatial resolutions of 1u, 0.5u and 0.25u. TRMM-3B43 and CMAP from the first group and CMORPH, TAMSAT and TRMM-3B42 from the second group performed reasonably well.

Three SRPs for the UZRB are bias-corrected and evaluated for use in real-time forecasting of daily stream flows: by (Rodrigo, 2016) using (1) CMORPH (Climate Prediction Center's morphing technique), (2) PERSIANN (Precipitation Estimation from Remotely Sensed Information using Artificial Neural Networks), and (3) TRMM-3B42RT (Tropical Rainfall Measuring Mission). Two approaches for bias correction (Quantile Mapping and a PrincgaugesComponent-based technique) are used to perform Bias Correction (BC) for the daily SPPs; for reference data, the Climate Hazards Group Infrared Precipitation with Stations (CHIRPS) was used. The two BC approaches were evaluated for the period 2001-2016. The bias-corrected SPPs were then used for real-time forecasting of stream flows at Katima Mulilo in the UZRB. Both BC approaches significantly improve the accuracy of the streamflow forecasts in the UZRB.

Three operational and acknowledged high resolution satellite-derived estimates: the Tropical Rainfall Measuring Mission product 3B42 (TRMM 3B42), the Famine Early Warning System product 2.0 (FEWS RFE2.0) and the National Oceanic and Atmospheric Administration/Climate Prediction Centre (NOAA/CPC) morphing technique (CMORPH)was analyzed in terms of spatial and temporal

repartition of the precipitations. By (T. Cohen Liechti, 2012) they compared the estimate with ground data for the wet seasons of the years 2003 to 2009 on a point to pixel basis at daily, 10-daily and monthly time steps and on a pixel to pixel basis for the wet seasons of the years 2003 to 2007at monthly time steps. FEWS pixels are much more inter-correlated than TRMM and CMORPH pixels. The volume ratio computation indicates that CMORPH is overestimating the rainfall by nearly 50 %. The statistics of TRMM and FEWS estimates show quite similar results. Due to its lower int,er-correlation and longer data set, the TRMM 3B42 product is chosen as input for the hydraulic-hydrologic model of the basin.

First validation of five different satellite-based precipitation products (TRMM-3B42 v6 & v7, RFE 2.0, PERSIANN-CDR, CMORPH 1.0 version 0.x) in the 1785 km² Makhazine catchment (Morocco) was assessed by (Yves Tramblay, 2016) result showed that among the different satellite-based precipitation estimates verified, the TRMM-3B42 v7 product is the closest to observed precipitation, and despite poor performance at the daily time step when used in the hydrological model, TRMM-3B42 v7 estimates are found adequate to reproduce monthly dynamics of discharge in the catchment. The results provide valuable perspectives for water resources modeling of data-scarce catchments with satellite rainfall data in this region.

Evaluation of Satellite Rainfall Estimates in the Pra Basin of Ghana was carried out by (Odai1 C. O., 2018) the accuracy of three satellite rainfall products, TMPA 3B42RT, TMPA 3B42, and CMORPH, in the Pra Basin of Ghana. Using the point-to-pixel method, following the analysis of the data at daily, monthly, annual and seasonal timescales, the result showed that TMPA products performed better on all timescales considered. CMORPH, on the other hand, showed overestimation at all gauge locations. The TMPA3B42 was seen to be the best amongst the three products. The overall rainfall in the basin was well depicted by the TMPA 3B42 and 3B42RT. Although there was not a perfect match between the 3B42RT and 3B42 products and the gauged rainfall, these products can be used to supplement gauged rainfall measurements in the basin and in the estimation of rainfall in ungauged basins with similar characteristics.

Evaluation of Satellite Rainfall Estimates for Drought and Flood Monitoring in Mozambique was evaluated by (Toté et al, 2015). they used Three decadal (10-day) gridded satellite rainfall products (TAMSAT African Rainfall Climatology And Time-series (TARCAT) v2.0, Famine Early Warning System Network (FEWS NET) Rainfall Estimate (RFE) v2.0, and Climate Hazards Group InfraRed

Precipitation with Stations (CHIRPS), then compared to independent gauge data (2001–2012). Overall, satellite products overestimate low and underestimate high decadal rainfall values. The RFE and CHIRPS products perform as good, generally outperforming TARCAT on the majority of statistical measures of skill. TARCAT detects best the relative frequency of rainfall events, while RFE underestimates and CHIRPS overestimates the rainfall events frequency.

Assessment of satellite rainfall products for streamflow simulation in Gambia watershed was carried out by (Bakary Faty, 2018) this study compared three SRE over a 12-year period (1998-2010), before and after their integration into the GR4J hydrological model over the Gambia Basin. The compared products are (CHIRPS), (PERSIANN-CDR) and TRMM 3B42v7. The calibration and validation of the GR4J model over the Gambia basin using a reference rainfall product (RRP) pointed out a very good performance. The correlation coefficient between simulated and observed daily discharge is higher than 0.8 both for calibration and validation. The inter-comparison of SRE against RRP and using them as forcing data into the calibrated GR4J hydrological model presented some coherence in the product performance. Finally, a bias correction is applied to the SRE using the RRP. The bias correction had significantly improved product performance. On average, the bias fell from 100 to 1.5% compared to the RRP, but the impact on the error is less significant. When using the corrected SRE in the hydrological model, the impact is very significant both on the bias and error. The overall performance of the different biases that corrected SRE is comparable.

2.4.3 Previous studies in Ethiopia

The capability of satellite rainfall products for monitoring meteorological droughts in upper Blue Nile basin of Ethiopia was assessed by (Yared B., 2017) ,The satellite rainfall product used in this study was selected through evaluation of five high-resolution products (Climate Hazards Group Infra-Red Precipitation with Stations (CHIRPS) v2.0, Precipitation Estimation from Remotely Sensed Information using Artificial Neural Networks (PERSIANN), African Rainfall Climatology and Time-series (TARCAT) v2.0, Tropical Rainfall Measuring Mission (TRMM) and Africa Rainfall Estimate Climatology version2 [ARC 2.0]).

The comparison and validation of eight satellite rainfall products (TRMM, CHIRPS, RFEv2, ARC2, PERSIANN, GPCP, CMAP and CMORPH) over the rugged topography of Tekeze-Atbara Basin was assessed by (Tesfay G., 2019). The performance was evaluated at various temporal (daily, monthly, seasonal) and spatial (point, sub-basin, basin) scale over the period 2002-2015. Results show that

CHIRPS, TRMM and RFEv2 performed well and were able to capture the rainfall measured by rain gauges. The Bias and correlation of these products were within 28 ±25% and >0.5over different time steps. The remaining products poorly performed at daily time step with higher Bias (up to ±200%) and lower correlation (<0.5). However, in this study, the spatial resolutions of the satellites are not relatively the same. For example, ARC2 – 0.1^{o} could not compare with TRMM-0.25^{0} of spatial resolution.

Satellite rainfall estimates over Ethiopian river basins were evaluated by (Gebremichael & Romilly, 2010). In this study; three SREs have been evaluated against collocated rain gauge measurements in Ethiopia across six river basins that represent different rainfall regimes and topography. The comparison was made using five-year (2003–2007) averages, and results are stratified by river basin, elevation and season.

The hydrologic applicability of a high-resolution satellite precipitation product (the Tropical Applications of Meteorology using Satellite and ground-based observations (TAMSAT) version 2 and 3 {TAMSAT 2 and TAMSAT 3}, the African Rainfall Climatology (ARC 2) products and CHIRPS) over the Upper Blue Nile Basin for the period of 2000 to 2015 was validated by (Getachew T., 2017) . From the overall analysis at decadal and monthly temporal scale, CHIRPS exhibited higher skills and the best bias value in comparison to ARC 2 but overestimates the frequency of rainfall occurrence particularly during the dry months. On the other hand, TAMSAT 3 has shown very comparable performance with that of CHIRPS product, particularly with regards to bias. The skill of CHIRPS is less affected by variation in elevation in comparison to TAMSAT 3 and ARC 2 product, while ARC 2 was found to be affected by elevation with the average biases of 1.53, 0.86 and 0.77 at lower (< 1000 m a.s.l), medium (1000 to 2000 m a.s.l) and higher elevation (> 2000 m a.s.l), respectively. Comparing the overall performance of the three products, CHIRPS exhibited the best performance followed closely by TAMSAT 3. Although in this study, the comparison of these three satellites was well performed with their spatial and temporal resolutions, the reason for the weakness of ARC 2 product to capture the rainfall was its higher spatial resolution of 0.1^{o} as compared to others.

satellite rainfall products for streamflow simulation in medium watersheds of the Ethiopian highlands has been assessed by (M. M. Bitew and Gebremichael, 2011) Results reveal that the utility of satellite rainfall products as input to SWAT for daily streamflow simulation strongly depends on the product type. The 3B42RTand CMORPH simulations show consistent and modest skills in their simulations

but underestimate the large flood peaks, while the 3B42 and PERSIANN simulations have an inconsistent performance with poor or no skills. Not only are the microwave-based algorithms (3B42RT, CMORPH) better than the infrared-based algorithm (PERSIANN), but the infrared-based algorithm PERSIANN also has poor or no skills for streamflow simulations. The satellite-only product(3B42RT) performs much better than the satellite-gauge product (3B42), indicating that the algorithm used to incorporate rain gauge information with the goal of improving the accuracy of the satellite rainfall products is actually making the products worse, pointing to problems in the algorithm. The effect of the watershed area on the suitability of satellite rainfall products for streamflow simulation also depends on the rainfall product. Increasing the watershed area from 299 km^2 to 1656 km^2 improves.

The performance of six satellite-based and three newly released reanalysis rainfall estimates at daily time scale and spatial grid size of 0.25 degrees over the Upper Blue Nile Basin, Ethiopia, was evaluated by (Dejene Sahlu et al, 2017). Among the six satellite-based rainfall products, adjusted CMORPH exhibits the best accuracy of the wet season rainfall estimate. In the secondary rainy season, unadjusted CMORPH and 3B42V7 are nearly equivalent in terms of bias, POD, and CSI error metrics. All error metric statistics show that MSWEP outperform both unadjusted and gauge adjusted ERA-Interim estimates. The magnitude of error metrics is linearly increasing with increasing percentile threshold values of gauge rainfall categories. Overall, all precipitation datasets need further improvement in terms of detection during the occurrence of high rainfall intensity. MSWEP detects higher percentiles values better than satellite estimate in the wet and poor in the secondary rainy seasons.

Validation of Global Precipitation Data Sets to Runoff Generation Using SWAT Modeling System was evaluated by (Fenet Tadese, 2015) in this study the performance of globally gridded high – resolution satellite rainfall products (TMPA 3B42V7, Corrected coarse CMORPH, and Adj-PERSIANN) under sparse ground based data and complex topography of Angar Watershed (3627.6 km2) in Upper Nile basin Ethiopia through semi-distributed hydrological model SWAT for monthly streamflow simulation was evaluated. Results reveal that the performance of the satellite rainfall products as input to SWAT for monthly stream flow simulation strongly depends on the product type. The application of these gridded data proves useful for hydrological studies in the absence of station data.

3. MATERIALS AND METHODS

3.1 Description of the study area

3.1.1 Location of the study area

The Omo Gibe River Basin is almost 79,000 km^2 in area and is situated in the southwestern part of Ethiopia, between 4°30’ and 9°30’ N and 35° and 38° E with an average altitude of 2800masl. It is Ethiopia's second-largest river system next to the Blue Nile, accounting for 14% of Ethiopian annual Runoff. It flows from the northern highlands through the lowland zone to discharge into Lake Turkana at the Ethio-Kenya border in the south and is nourished along its course by some important tributaries. The fundamental characteristic of the Omo Gibe River Basin is its complex topographic feature. Thus, the basin is divided sharply into the highlands in the northern half of the area and lowlands in the southern half.

The northern part of the catchment contains several tributaries emanating from the north-east, of which the largest is the Walga and Wabe rivers. (Gebresenbet, 2015).

The Wabe River catchment is located between 08°21′ and 08°30′ N and 38°05′ and 37°49′ E, and the elevation range is between 1014 and 3611 m above sea level and covers a drainage area of about 1860 km^2. (Mesfin Sahle, 2018).

3.1.2 Topography and River system of the basin

The topography of the Omo-Gibe basin as the whole is characterized by its physical variation. Two-third of the basin in its northern part has mountainous to hilly terrain cut by deeply incised gorges of the Omo, Gojeb and Gilgel-Gibe Rivers, the southern, which accounts for a third of the basin, is a flat alluvial plain punctuated by hilly geographies. The northern and central half of the basin lies at an altitude greater than 1500m a.s.l with a maximum elevation of 3360m a.s.l (located between Gilgel Gibe and Gojeb tributaries), the northern part of the catchment has a number of tributaries. Most of the rivers from the upper part of the catchment drain largely cultivated the land.

As shown in Figure 3-1 The Wabe River catchment is one of the tributaries of the Omo-Gibe River basin originating from the northeast part. The source of the Wabe River is the Gurage Mountain chain (Mesfin Sahle, 2018).

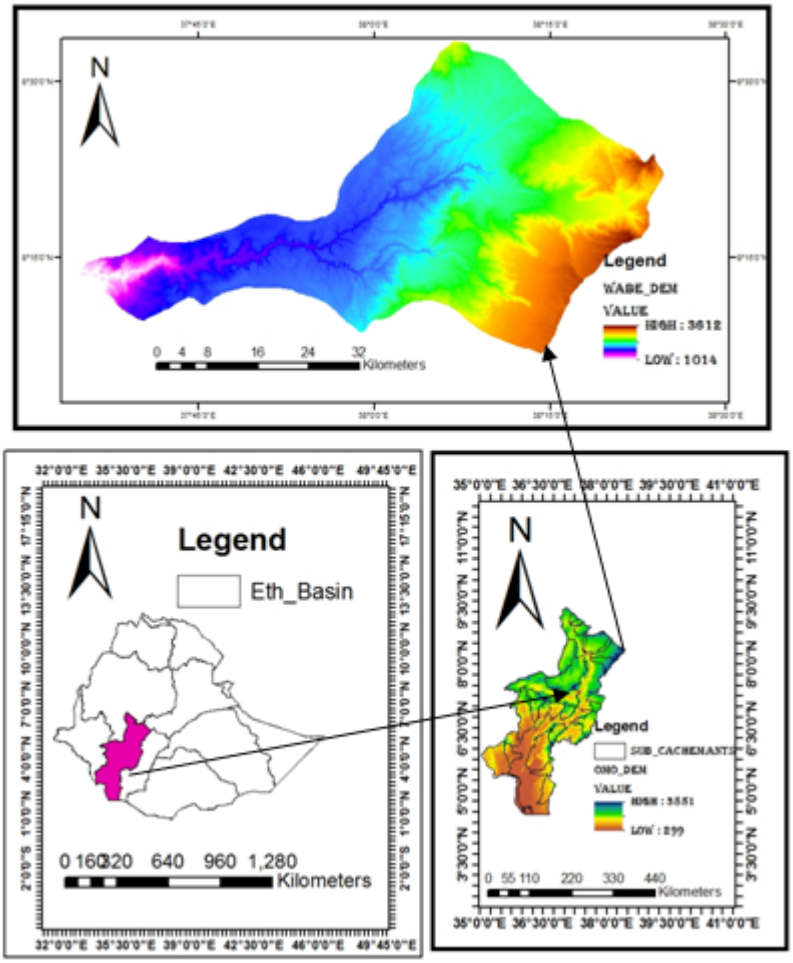

Figure 3-1 location of the study area

3.1.3 The climate of the Study Area

Omo Gibe River Basin has three distinct climate zones across the watershed in which it follows the country's climate classification, namely, Dega (cool zone), Weyna-Dega (temperate zone) and Kolla (hot zone). During the wet season, the area is under the influence of Atlantic equatorial westerly and southerly winds from the Indian Ocean, producing strong precipitation, mainly due to the Atlantic moisture component. (Gebresenbet, 2015)

As Ethiopia is situated within the tropical region, ITCZ is the principal factor that influences its weather system. The seasonal rainfall distribution within the Omo Gibe River Basin arises out of the annual migration of the ITCZ. Based on the rainfall distribution patterns, the Rainfall pattern strongly decreases from north to south of the watershed particularly less than 300 mm/year near Lake Turkana. (Gebresenbet, 2015)

Mean annual and monthly rainfall of the station in Omo-Gibe basin are shown in figure 3-2 and figure 3-3 below

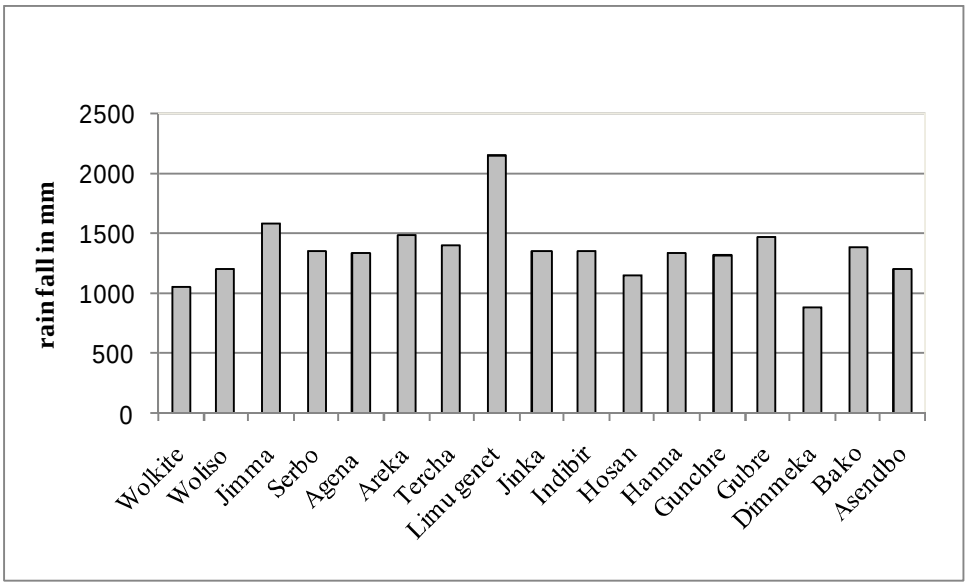

Figure 3-2 mean annual rainfall of stations (2003-2017)

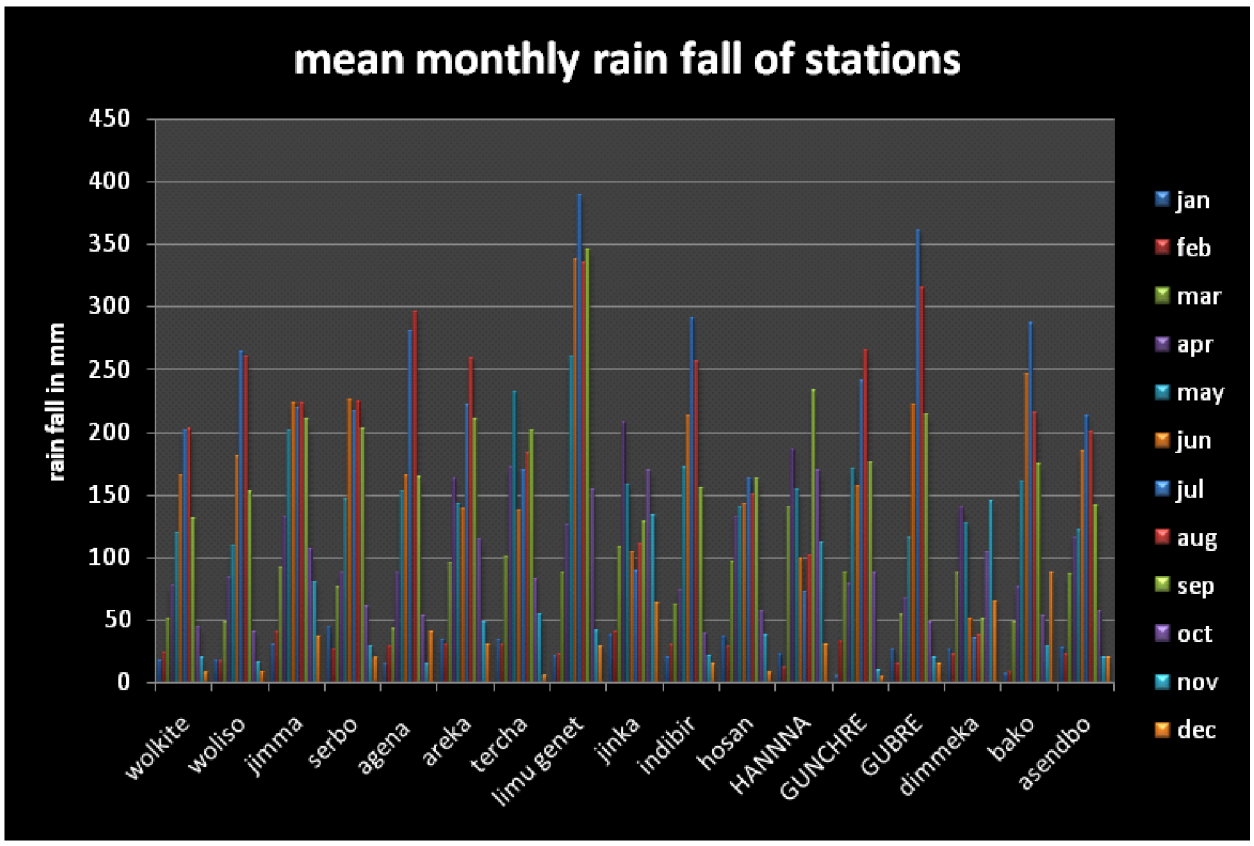

Figure 3-3 mean monthly rainfall of stations

3.1.4 Soil

The hydrological models need soil type of the study area either as the main input or as determining other parameters like curve number. The soils of the upper and middle reach of the basin are mainly permeable and well-drained while the valley bottoms have less permeable soils with impeded drainage. The dominant soils types in the basin are humic nitisol (27.4%) and humic alisol (18.1%).generally as shown in **f**igure 3-4 below the soil type of Wabe watershed reclassified as four type's loam, loam (cortisol), clay and sandy loam, the dominant soil types for the study area are clay and sandy loam

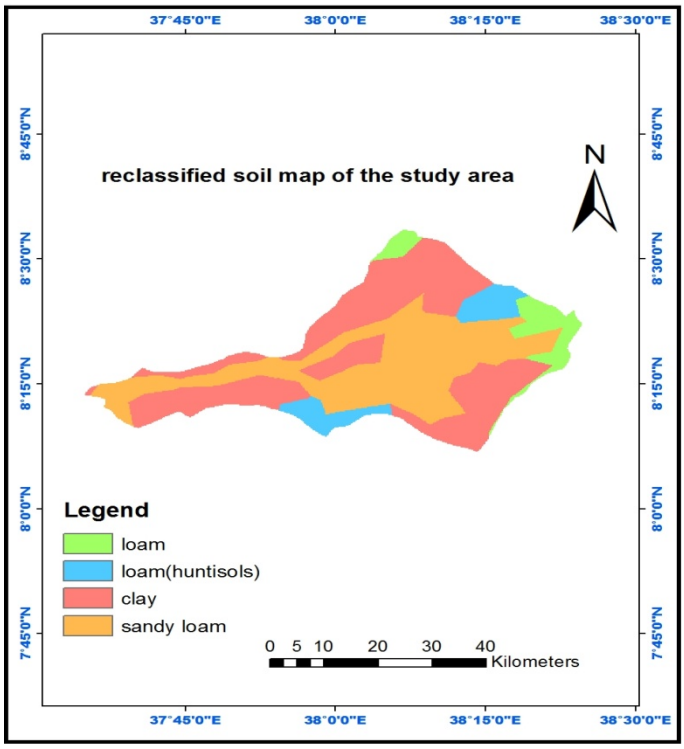

Figure 3-4 Soil Map of the Study Area

3.1.5 Land use land cover

The hydrological models need land use the land cover type of the study area either as main input or as determining other parameters like curve number, More than 76.14 % of the watershed land cover was agricultural land. As shown in figure 3-5 below. Land use/Land cover map of the study area is categorized mainly as agricultural 76.14%, Forest 0.13%, medium residential 18 %, water (5%) respectively; in figure 3-5 below the land use land cover of the study areas are described.

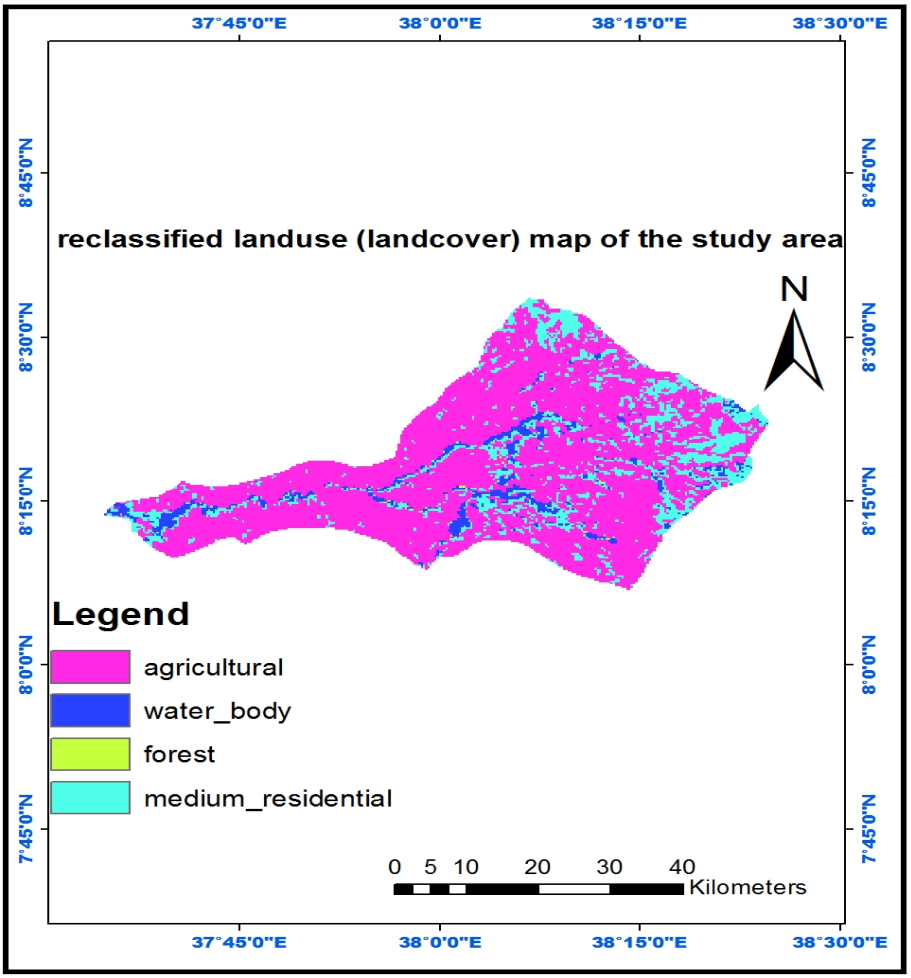

Figure 3-5 reclassified land use land cover map of the study area

3.1.6 Hydrology

Wabe near Wolkite is the gauging station of this river which is the contributor river flow of the watershed above the dam. For this reason, the Ethiopian Minister of Water Resources installed the gauging station downstream of the main route river near Wolkite. This flow data were obtained from MoWIE. Based on the data from 2003 - 2017 records the watershed has an average annual flow of 211.8m3/sec. The monthly average discharge at the Wabe gauging station is shown below in figure 3-6.

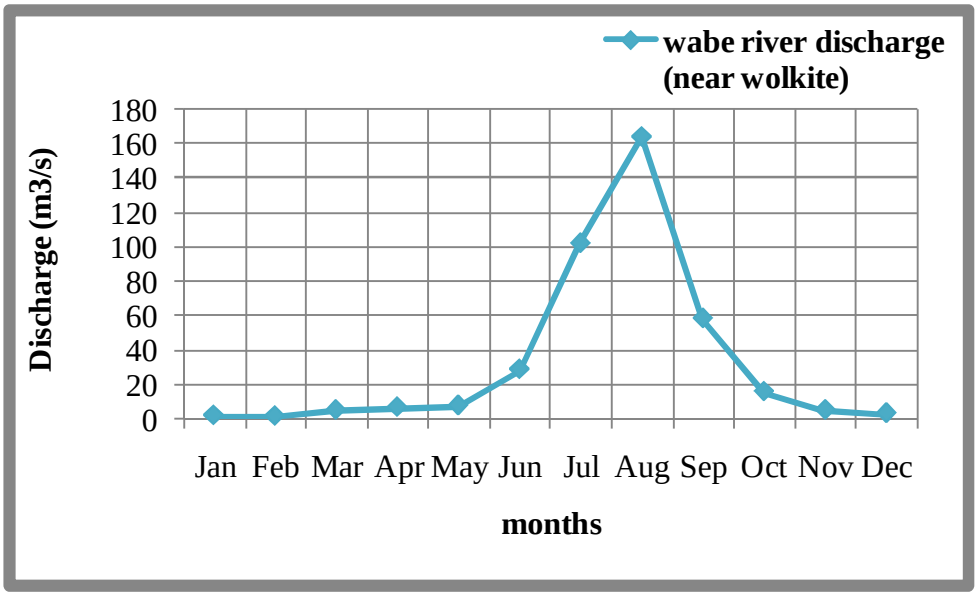

Figure 3-6 Monthly Average Discharge at Wabe gauging station

3.2 Data collection and analysis

In order to have reliability in this research work, having relevant information or data is mandatory. These data are Meteorological data (rainfall, temperature, relative humidity, wind speed and sunshine hour), hydrological data (streamflow), satellite precipitation product data (**CHIRPS**, **PERSIANN-CCS**, **RFE 2.0**, **and TAMSAT**.) and other data which is catchment physio-graphical data are required. With these, the HBV-light model requires climate and river flow data in daily time step including rainfall, temperature, and evapotranspiration. All data were arranged as per the requirement of the model in selected stations and the record length of these stations is 15 years.

3.2.1 Meteorological Variables

The HBV-light model needs climate data for hydrological simulation. In the study area, meteorological stations of different classes are found and collected from the Ethiopian National Meteorological Services Agency (NMSA). Based on the classification of the Agency there is principal, also termed as class one station, where precipitation, air temperature, wind speed, relative humidity, and sunshine duration measurements are taken every three hours. Another set of stations are class three stations (ordinary stations), where precipitation and air temperature measurements are taken daily. In addition, Class four stations only serve precipitation measurements on a daily base.

Based on this classification Jimma and Wolkite are principal stations whereas others are Class three stations. Measurements time series covers a period of 2003 – 2017.

The selection of the station was based on

- Their long-time data availability
- Their impact on the study area (weight)
- Stations that are around the study area with representative coverage was also selected
- Class (that was given by the agency)

Number of daily ground observations and aggregated totals per synoptic station used in the study are shown in Table 3-1

Table 3-1 Number of daily ground observations and aggregated totals per synoptic station used in the study

station name	Longitude	Latitude	**no days observation**	**expected**	**missed**
Agena	**38.004**	**8.135**	2780	5479	2699
Areka	**37.708**	**7.063**	3727	5479	1752
Assendabo	**37.217**	**7.75**	4369	5479	1110
Baco	**37.083**	**9.117**	4373	5479	1106
Dimeka	**36.533**	**5.167**	4704	5479	775
Genchile	**37.84**	**8.032**	1461	5479	4018
Gubre	**37.805**	**8.187**	4003	5479	1476
Hana	**36.129**	**6.223**	1820	5479	3659
Hosana	**37.854**	**7.567**	3483	5479	1996
Imdibir	**37.935**	**8.118**	2510	5479	2969
Jimma	**36.817**	**7.667**	5222	5479	257
Jinka	**36.55**	**5.767**	5434	5479	45
Limu-g	**36.95**	**8.067**	4247	5479	1232
Serbo	**36.967**	**7.7**	3828	5479	1651
Tercha	**37.168**	**7.149**	3885	5479	1594
Woliso	**37.97**	**8.54**	4980	5479	499
Wolkite	**37.75**	**8.27**	4563	5479	916

3.2.2 River Discharge Data

River discharge data of the basin were collected from the Ministry of Water, Irrigation, and Energy (MoWIE), Hydrology department for a period of 15 years (2003- 2017). The River Discharge data is then used for sensitivity analysis, calibration, and validation of the model.

As tabulated in table 3-2 the catchment has only one gauge station at the outlet of the Wabe River. As observed from historical flow data records, there is considerable fluctuation of flow due to rainfall and temperature variation. (Mesfin Sahle, 2018)

Table 3-2 Location of the hydrological gauging station (Wabe River)

River Name	Gauging Station (site)	Latitude (Degree)	Longitude (Degree)	Elevation(m)	Length of year
Wabe	Wabe	8.23	37.58	2150	10

3.2.3 Digital Elevation Model

A Digital Elevation Model (DEM) gives the elevation, slope and defines the location of streams network in a basin. The DEM used in this study was obtained from a digital elevation map of the area that was prepared using the Shuttle Radar Topography Mission (SRTM) with a resolution of 30 m x30m. The DEM was then used into hydrological models for watershed delineation.

3.2.4 Land Use/Land Cover Data and Soil data

This data are needed for the hydrological models to generate catchment delineation

3.2.5 Satellite Rainfall Products (SRPs)

.The SRFE evaluated in this study were selected based on their long time-series data availability; their spatial and temporal resolutions, which make them particularly suitable for hydrological applications and their near-real-time availability and their public domain availability (M.dembele & S.J.Zwart, 2016).

Sample daily estimates of the products are illustrated in figure 3-7.two of the products shown region-specific while the other two are quasi global.

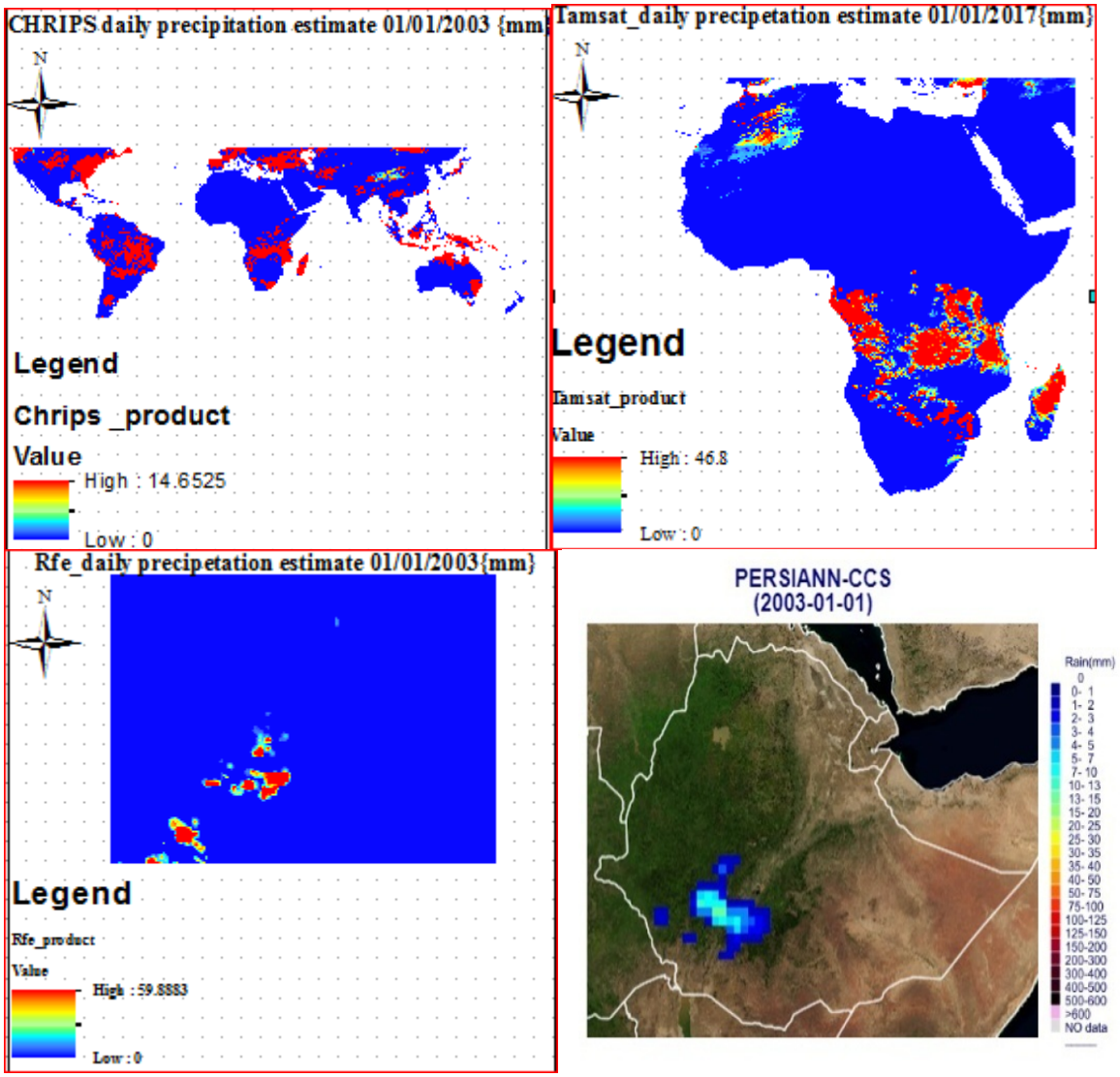

Figure 3-7 Sample Daily rainfall estimate of the products

Information about the four satellite products was illustrated by table 3-3 and it includes the website that they have been downloaded from

Table 3-3 Summaries of the four satellite products

Satellite product	Temporal coverage	Spatial coverage	Spatial resolution	Temporal resolution	Website data information
CHIRPS Version 2.0	1981–present	Near-global 50°N – 50°S, 0° – 360°E	0.05° (~5 km)	Daily	[1]
PERSIANN-CCS	1983–present	Near-global 60°N – 60°S, 0° – 360°E	0.04° (~4 km)	Daily	[2]
RFE Version 2.0	2001–present	Africa 40°N – 40°S, 20°W – 55°E	0.1° (~10 km)	Daily	[3]
TAMSAT Version 3.0	1983–present	Africa 38°N – 36°S, 19°W – 52°E	0.0375 °(~4 km)	Daily	[4]

3.2.6 Extraction of Satellite Rainfall Estimates

The satellite rainfall products used in this study were obtained on a Network Common Data Form (Net-CDF) gridded format from January 1st, 2003 to December 31st, 2017. These 5479 files (note that there are four more days because 2004, 2008, 2012 and 2016 are Leap Years) for each of the satellite product types were downloaded by the Net-CDF format. Then, in order to extract the rainfall data for the study area and to export the data in to excel for each pixel, GIS and OPEN NC FILE[5] software were used.

GIS and OPEN NC FILE[6] software were used to extract and export the rainfall data to excel for the study area and period for satellite rainfall estimates. Finally, with the use of this software fifteen years of daily satellite-based rainfall estimates were extracted in a suitable format for further analysis.

[1] ftp://ftp.chg.ucsb.edu/pub/org/chg/products/CHIRPS-2.0/africa_daily/tifs/p05/
[2] ftp://persiann.eng.uci.edu/CHRSdata/PERSIANN-CCS/daily/
[3] ftp://ftp.cpc.ncep.noaa.gov/fews/fewsdata/africa/rfe2
[4] http://researchdata.reading.ac.uk/112/
[5] http://agrimetsoft.com/open_nc_file_for_coordinates.aspx

[6] https://youtu.be/FAON53uUlLQ

3.2.7 Methodology for data comparison

Satellite-based rainfall estimates are continuous and represent areal rainfall while gauge observed rainfall is at a particular point in location. Hence, to make comparisons between the two it is necessary to convert the areal rainfall values into point, Following (T. Cohen Liechti, 2012) (M.dembele & S.J.Zwart, 2016) (Rodrigo, 2016) (Mauricio Zambrano-Bigiarini, 2017) (Odai1 C. O., 2018) (F.Gao et al, 2018) a point-to-pixel analysis was applied to compare time series of data observed at selected rain gauges to the corresponding SRE pixel. As it is illustrated in figure 3-8 All SRE products with a spatial resolution higher than 0.1_ (i.e. PERSIANN-CCS TAMSAT and CHIRPSv2) were upscaled to a unified grid of 0.1^0 in order to enable consistent point-to-pixel comparisons. The upscaling procedure applied in this work consisted of transferring values from the high-resolution raster cells to each one of the 0.1-degree grid cells, by using bilinear interpolations implemented in the Regrid function of the R package by[7] CDT.

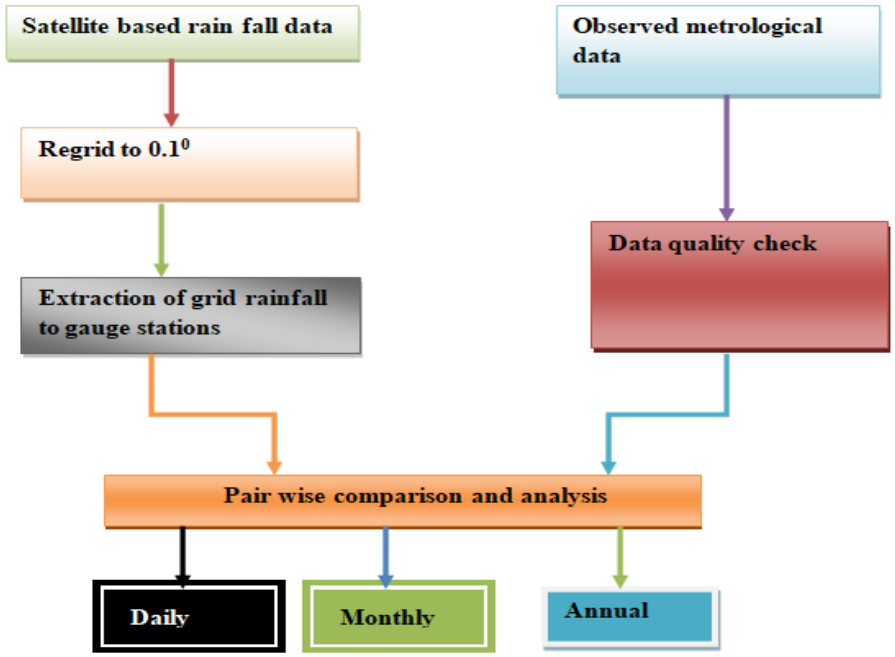

Figure 3-8 Flowchart of the methodology of rainfall analysis

[7] Climatic data tool (international research institutes for climate and society VERSION 5 Rija Fannianssoa,Tufa Dinku)

3.2.8 Methodology for Verification of Satellite-Based Rainfall Estimates

The method used in this study was based on the results of comparison of satellite rainfall products in Burkina Faso (M.dembele & S.J.Zwart, 2016) This method included pairwise comparison statistics, (continuous statistics) to evaluate the performance of the satellite products in estimating the amount of rainfall, and categorical statistics used to assess rain detection capabilities.

Five statistical indicators were computed for the pairwise comparison statistics **(**continuous statistics) In the statistical indicators that are described below S_i represent designates estimated value, S_{av} represent average satellite rainfall estimates, G_i represents Observed value at a given cell, G_{av} represent average satellite rainfall estimates and n represent the number of samples.

(1) **The Pearson correlation coefficient (*r*):** referring below equation 3-1 it is used to evaluate how well the estimates corresponded to the observed values;

$$r = \frac{\sum_{i=1}^{n}(G_i - G_{av})(S_i - S_{av})}{\sqrt{\sum_{i=1}^{n}(G_i - G_{av})^2}\sqrt{\sum_{i=1}^{n}(S_i - S_{av})^2}} \qquad \text{Equation 3-1}$$

(2) **The Mean Error (ME):** it estimates the average estimate error – as of equation 3-2 a positive ME shows that the estimated rainfall is generally overestimated, while a negative sign shows it is generally underestimated;

$$\mathbf{ME} = \frac{1}{n}\sum_{i=1}^{n}(S_i - G_i) \qquad \text{Equation 3-2}$$

(3) **The Bias:** as it is represented in equation 3-3 below it corrects the degree to which the measured value is over- or underestimated ;

$$\text{Bias} = \frac{\sum_{i=1}^{n} S_i}{\sum_{i=1}^{n} G_i} \qquad \text{Equation 3-3}$$

(4) **The root mean square error (RMSE):** it is a frequently used measure of differences between two variables – it measures the average magnitude of the estimate errors: below as defined in equation 3-4 lower RMSE values indicate greater central tendencies and generally smaller extreme errors;

$$RMSE=\sqrt{\frac{1}{n}\sum_{i=1}^{n}(S_i - G_i)^2} \qquad \text{Equation 3-4}$$

(5) **Nash–Sutcliffe Efficiency coefficient (E):** as it is marked in equation 3-5 below it shows how well the estimate predicted the observed time series, and it varies from minus infinity to one: negative values mean that the gauge means is better than the satellite-based estimate, zero means that the gauge mean is as good as the estimate, and 1 corresponds to a perfect match between gauge measurements and satellite-based estimates;

$$E= 1-\frac{\sum_{i=1}^{n}(S_i-G_i)^2}{\sum_{i=1}^{n}(G_i-G_{av})^2} \qquad \text{Equation 3-5}$$

As in table 3-4 shown two statistical indicators based on a contingency table were computed for two categorical statistics:

Table 3-4 Contingency table (Shrestha, 2011)

		satellite rainfall	
gauged /observed rainfall		no rain	yes rain
	no rain	correct negative (N)	false alarm (F)
	yes rain	Miss(M)	hit (H)

From the above table 3-4, we can infer that

a) 'hits' represents correctly estimated rain events by the product as well as the Insitu measurement,
b) 'false alarms' represents when rain is estimated by the product, but did not occur in reality,
c) 'misses' represents when rain is not estimated by the product, but did occur by the Insitu measurement, and
d) 'Correct negatives 'represents correctly estimated no rain events e by the product as well as the Insitu measurement. (Shrestha, 2011)

(6) **The Probability of Detection (POD):** as it is illustrated in table 3-6 it indicates what fraction of the observed events was correctly estimated,

$$POD=\frac{H}{H+M} \qquad \text{Equation 3-6}$$

(7) **The False Alarm Ratio (FAR):** as it is indicated below in above 3-7 it shows what fraction of the predicted events did not actually occur

$$FAR=\frac{F}{H+F} \qquad \text{Equation 3-7}$$

The above all explanation about the verification of satellite-based rainfall product can be summarized by the following table 3-5

Table 3-5 Continuous statistics and categorical statistics

statistics type	statical indicator	Formula	value range	perfect score
continuous statistics	Pearson correlation coefficient	$r\frac{\sum_{i=1}^{n}(G_i-G_{av})(S_i-S_{av})}{\sqrt{\sum_{i=1}^{n}(G_i-G_{av})^2}\sqrt{\sum_{i=1}^{n}(S_i-S_{av})^2}}$ Equation 3-1	−1 to 1	1
	Mean Error	$ME=\frac{1}{n}\sum_{i=1}^{n}(S_i-G_i)$ Equation 3-2	−∞ to ∞	0
	Bias	$Bias=\frac{\sum_{i=1}^{n}S_i}{\sum_{i=1}^{n}G_i}$ Equation 3-3	0 to ∞	1
	Root mean square error	$RMSE=\sqrt{\frac{1}{n}\sum_{i=1}^{n}(S_i-G_i)^2}$ Equation 3-4	0 to∞	0
	Nash–Sutcliffe Efficiency coefficient	$E=1-\frac{\sum_{i=1}^{n}(S_i-G_i)^2}{\sum_{i=1}^{n}(G_i-G_{av})^2}$ Equation 3-5	−∞ to 1	1
Categorical statistics	Probability of detection	$POD=\frac{H}{H+M}$ Equation 3-6	0 to 1	1
	false alarm ratio	$FAR=\frac{F}{H+F}$ Equation 3-7	0 to 1	0

Generally, Attention should be given to some statistics over others depending on the application of satellite products (Toté et al, 2015). For flood forecasting and hydrological purposes, it is important to avoid underestimations of rainfall events and rainfall amounts, and then avoid ME < 0 and low POD. In contrast, for drought monitoring, overestimations must be avoided, and then avoid ME > 0 and high

FAR. Products with high r and E and low RMSE have to be considered for general purposes (M.dembele & S.J.Zwart, 2016)

3.2.9 Bias Adjustment for the SRP

For different reasons SRP may under or overestimate the rainfall event when they compared with Insitu rainfall data due to this an adjustment(bias correction) is needed for the products, different scholars (eg.see (Shrestha, 2011), (B. Berhanu et al., 2016) , (Rodrigo, 2016)) were worked on bias adjustment of SRPs and reanalysis data's for this study From different bias adjusting methods, the linear scaling (LS) bias correction method was selected, as it aims to match the monthly mean of corrected values perfectly with that of the observed ones (B. Berhanu et al., 2016) .the linear scaling formula is illustrated in equation 3-8 below.

$$P_{d.cor}=P_{d.sat}*\left(\frac{\mathbf{P_{m.obs}}}{\boldsymbol{P_{m.sat}}}\right) \quad \text{Equation 3-8 where}$$

$P_{d.cor}$=represent corrected daily SRP

$P_{d.sat}$= represent uncorrected (raw) daily SRP

$P_{m.obs}$= represent long-term mean monthly observed rainfall data

$P_{m.sat}$= represent long-term mean monthly satellite rainfall data

3.3 General research methodology

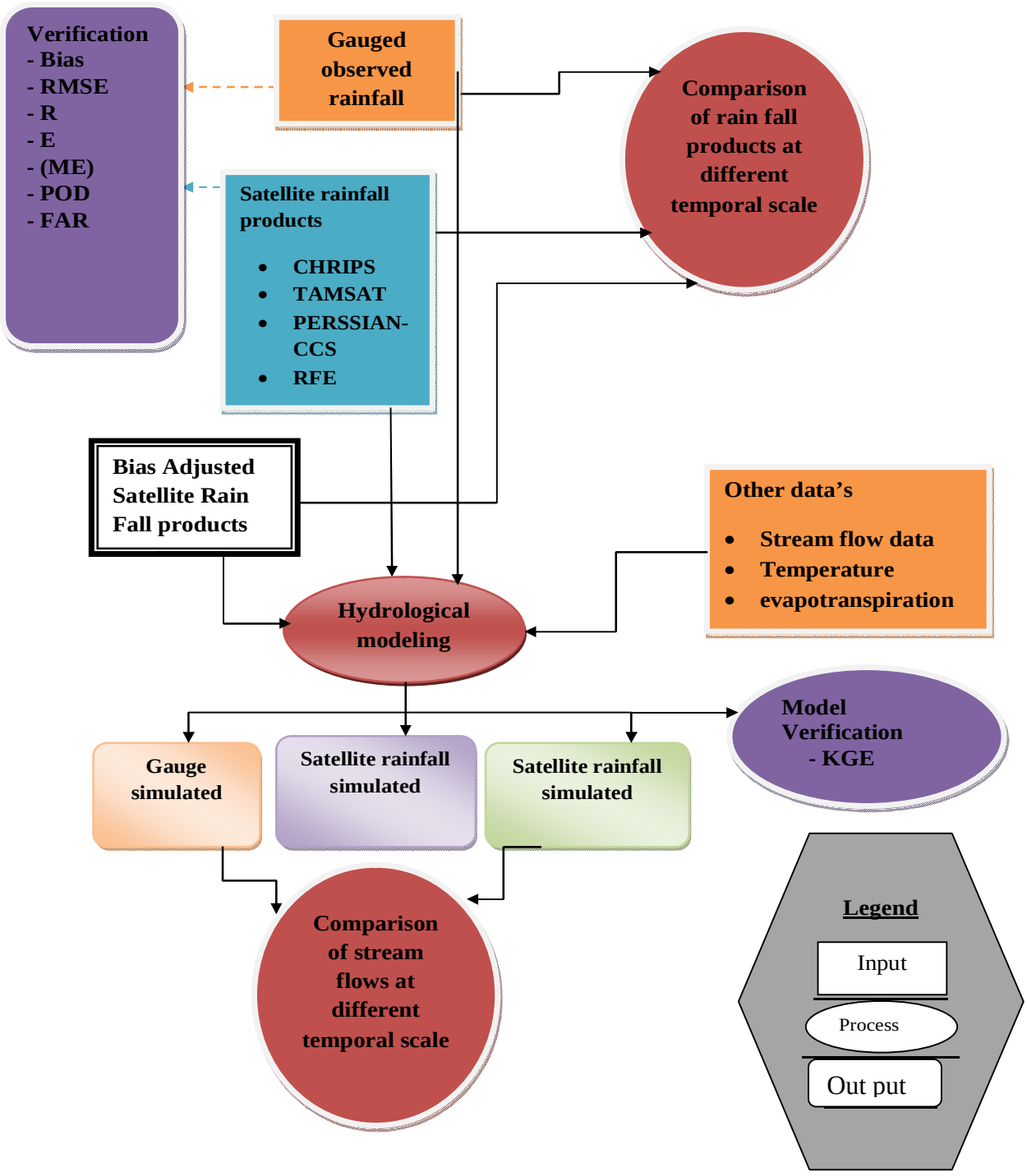

Figure 3-9 General framework of the study

3.4 Data Analysis

Before starting any model simulation, it is important to check whether the data are homogenous, consistence and sufficiently represent the purpose of the study.

3.4.1 Data quality tests for Stationary and Relative Consistency

Following E.R.Dahmen & M.J. Hall (1990) for all data; test for absence of trend was conducted using Spearman's Rank-Correlation Method while the test for stability of variance and mean was conducted by using the F-Test for Stability of Variance.

All data were satisfied with the conditions of the tests to use for frequency analysis or modeling.

3.4.2 Checking Homogeneity of Meteorological Stations

Homogeneity analysis is used to identify a change in the statistical properties of the time According to (Wijngaard, 2003)the recommended method to apply homogeneity has been tested with respect to neighboring stations that is supposedly homogeneous. The non-dimensionalizing of the month's value is carried out below in Equation 3-9

$$\mathbf{Pi} = \frac{\mathbf{Piav}}{\mathbf{pav}} *100 \quad \text{Equation 3-9}$$

As in equation 3-9 shown Pi represents Nondimensional value of rainfall for the month i, Piav represent Over years averaged monthly precipitation for the station I and Pav represent the over years average yearly precipitation and plotted to compare the stations includes in the computation of the area rainfall with each other in Figure 3-10 below. Since all the values of Pi are less than 30, it shows the result of homogeneity analysis and the selected stations are homogenous.

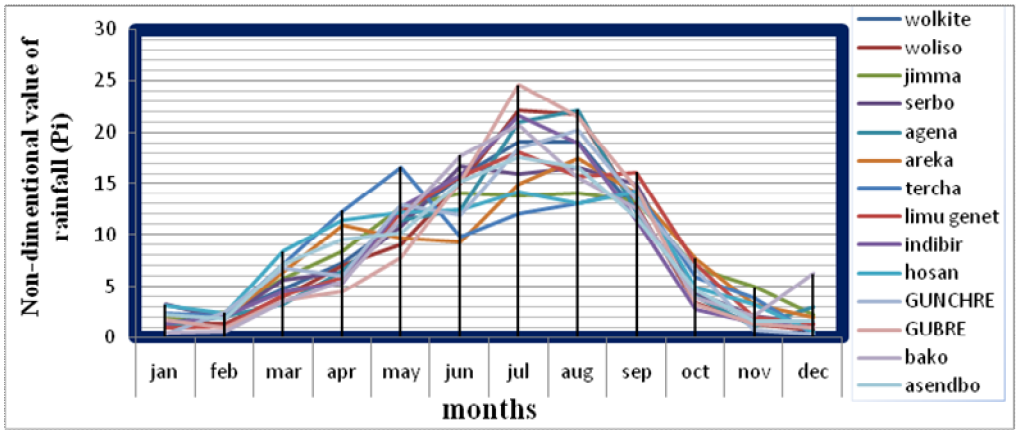

Figure 3-10 Homogeneity test for the selected fifteen meteorological stations in the area

As shown in the above figure 3-10 the selected rainfall stations were not-dimensionalized and plotted together to analyze their homogeneity. The maximum rainfall falls between May to September in all stations which shows the homogeneity of the stations. A time-series observational data is relatively homogeneous and consistent if the periodic data are proportional to an appropriate simultaneous period. This proportionality can be tested by double mass curve analysis in which accumulated rainfall data is plotted against the mean value of all neighborhood stations.

3.4.3 Checking Consistency of Stations data

According to (Subramanya, 1998), recording of the rain gauge stations has undergone a significant change during the period of record with various reasons; inconsistency would arise in the rainfall data of that station. This inconsistency of a record was done by the double mass curve technique.

Double-mass-curve analysis: - is the method that is used to check for inconsistency in a gauge record. The curve is a plot on arithmetic graph paper, of cumulative rainfall collected at a gauge where measurement condition may have changed significantly against the average of the cumulative rainfall for the same period of record collected at several gauges in the same region. If the station needs to be adjusted for the consistency of the records we can use the following equation

$$\frac{px}{py} = \frac{sx}{sy}$$ Equation 3-10

Where Px is the adjusted amount Py deviated amount for the concurrent period for which Px is desired; Sx: the slope of the mean double mass line to which the deviated data are to be adjusted Sy: the slope of the mean double mass line of the deviated data.

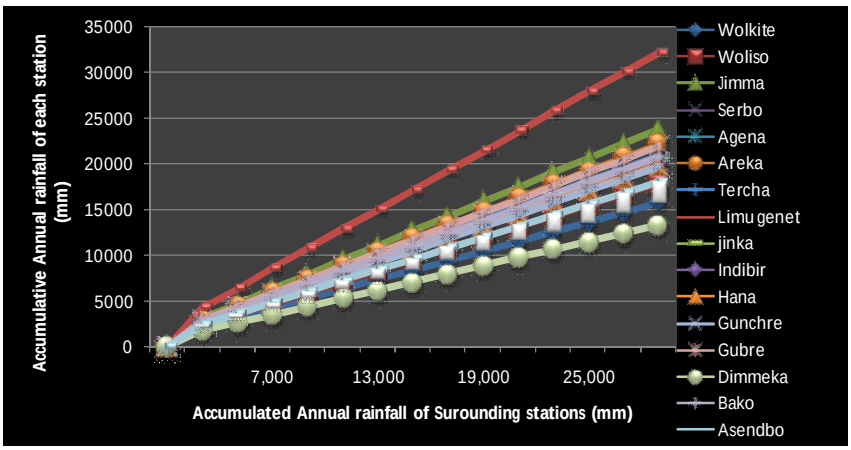

Figure 3-11 Double Mass Curves for the selected Meteorological Stations

A time-series plots of the annual cumulative rainfall (2003-2017) consistency for fifteen meteorological stations in Omo-Gibe Basin is shown above in figure 3-11

The graph of the cumulative data of one variable versus the cumulative data of a related variable is a straight line so long as the relation between the variables is a fixed ratio. Breaks in the double-mass curve of such variables are caused by changes in the relation between the variables. Thus, the 15 meteorological stations selected for this study are consistent since the graph of the plot forms is straight line without break.

3.4.4 Streamflow Homogeneity Test

Frequency analysis of data requires that the data be homogeneous and independent. The restriction of homogeneity assures that the observations are from the same population. One of the tests of homogeneity (Bushandi, 1982) is based on the cumulative deviations from the mean:

Rainbow[8] software has been used to check the homogeneity of the streamflow data. Frequency analysis of data requires that the data be homogeneous and independent. The restriction of homogeneity assures that the observations are from the same population as illustrated in equation 3-11.

$$\mathbf{Sk} = \sum_{i=1}^{k} [xi - x_{avg}] \quad \text{Equation 3-11}$$

Where Xi is the record from the series X1, X2…Xn and x_{avg} is the mean. The initial value of SK=0 and last value SK=n are equal to zero (as shown below in the Figure3-8). When plotting the Sk‘s (also called a residual mass curve) changes in the mean are easily detected. For a record Xi above normal the SK=i increases, while for a record below normal SK=i decreases. For a homogenous record, one may expect that the Sk‘s fluctuate around zero since there is no systematic pattern in the deviations of the Xi‘s from their average value X .k=1...n.

To test the homogeneity of the data set, the cumulative deviations are often rescaled. This is obtained by dividing the Sk‘s by the sample standard deviation value (s). By evaluating the maximum (Q) or the range (R) of the rescaled cumulative deviations from the mean, the homogeneity of the data of a time series can be tested: (Raes, 2006).

$$Q = MAX\left[\frac{Sk}{s}\right] \quad \text{Equation 3-12}$$

[8] a software package for hydro meteorological frequency analysis and testing the homogeneity of historical data sets

$$R = MAX\left[\frac{Sk}{S}\right] - MIN\left[\frac{Sk}{S}\right] \qquad \text{Equation 3-13}$$

When the deviation crosses one of the horizontal lines the homogeneity of the data set is rejected with respectively 90, 95 and 99% probability. As presented in Figure 3-12, the rescaled cumulative deviations from the mean would not cross one of the horizontal 90, 95 and 99% probabilities lines. The range of cumulative deviation and maximum cumulative deviation could not be rejected on 90%, 95% and 99% probability levels which show the homogeneity of the annual data series, assures that the observations are almost from the same population (Figure 3-13).

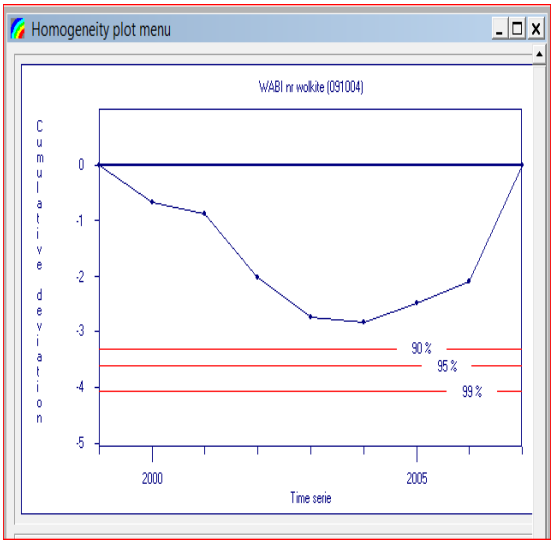

Figure 3-12 Rescaled Cumulative deviations for the total annual flow at Wabe

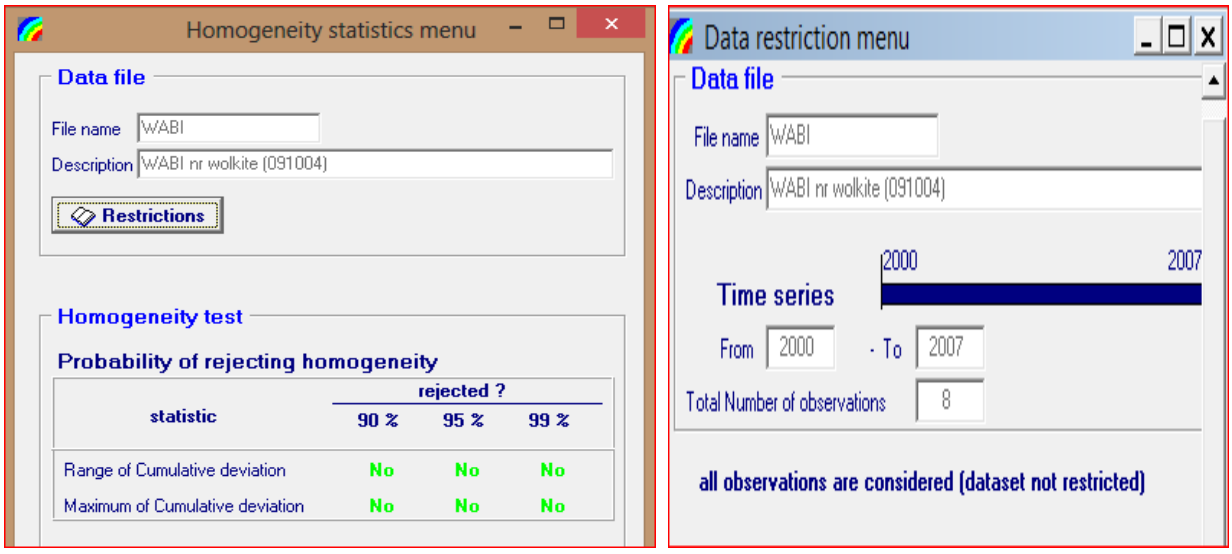

Figure 3-13 Probability of rejecting homogeneity of annual flow at Wabe station

3.5 Hydrological components of HBV- light Model

The HBV light model is a semi-distributed deterministic conceptual rainfall-runoff model. It was developed for educational purposes and includes a numerical description of hydrological descriptions at a catchment scale. The original HBV model ((Bergström, 1976.)Was developed by the SMHI (Swedish Meteorological and Hydrological Institute) and has become a standard model for simulating runoff in Nordic countries. Model development was driven by the goal to provide an easy to use and educational tool to represent runoff generation processes. It has been applied to many countries with different climatic conditions for research purposes and hydrological problems **(Seibert, 2005)**), the model uses sub-basins as primary hydrological units and within these, an area elevation distribution and a simple classification of land use is made. As shown in Figure 3-14 the model can be distinguished as four components: The snow, soil, groundwater (or response) and routing routine.

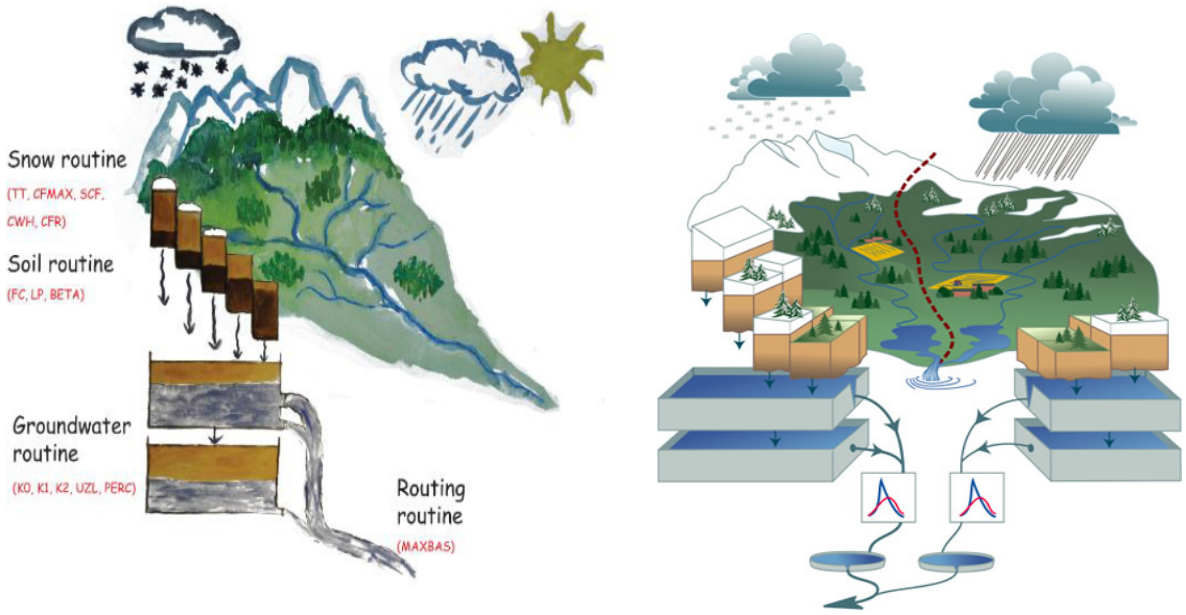

Figure 3-14 Schematic Structure of the HBV model ((Seibert & Vis, 2012)

3.5.1 Snow routine

The snow routine describes the accumulation of precipitation as snow. Since the study area does not experience any snowfall during the year, this component can be left out.

3.5.2 Soil Routine

In the **soil routine**, actual evapotranspiration, soil water content and groundwater recharge are calculated as a function of actual water storage in the soil. This routine is based on three parameters: The limit for potential evaporation (LP) which is the soil moisture value above which evapotranspiration reaches its potential value and the field capacity (FC) which is the maximum soil moisture storage Actual evapotranspiration equals the potential evapotranspiration rate as long soil moisture storage divided by FC is higher than LP. If it gets lower, a linear reduction is used (Figure 3-15, left). The shape parameter BETA (β) is responsible for the relative contribution to the response function and the rise in soil moisture storage caused by rainfall (Figure 3-15, right (Seibert & Vis, 2012).

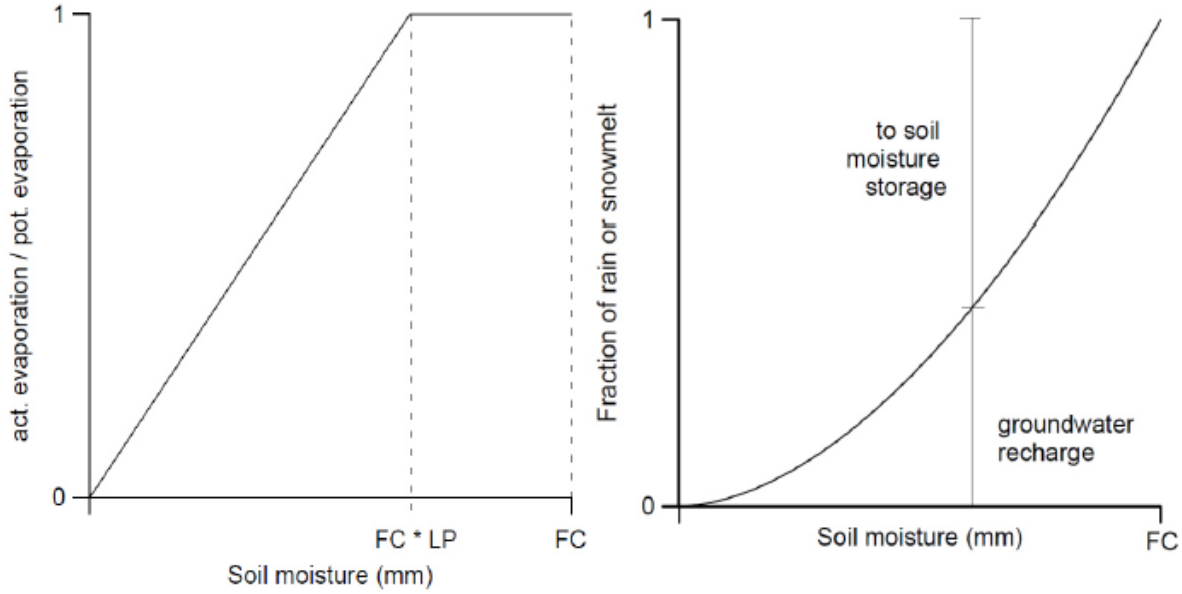

Figure 3-15 Soil routine: Left: Reduction of potential evapotranspiration depending on soil moisture storage. Right: Contribution from rainfall to soil moisture storage and groundwater recharge. Response routine (Seibert, 2005)

3.5.3 Response routine

Runoff generation is represented in the response function, which transforms excess water from the soil moisture zone to runoff. The function is structured by two conceptual groundwater storage reservoirs Figure 3-16 the water from the soil routine is added to the upper groundwater storage, therefore, the parameter PERC controls maximum percolation rate to the lower groundwater layer. Runoff is

calculated based on three linear reservoir equations: A fast, a slow and a very slow runoff component that is influenced by recession coefficients KO, K1, and K2. The fast component Q_0 contributes only to a runoff if a threshold parameter UZL in water storage is exceeded. (Seibert & Vis, 2012).

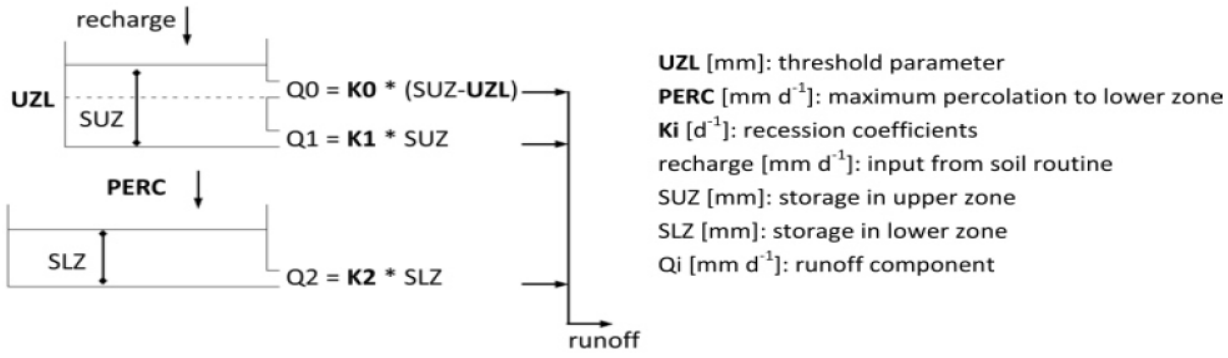

Figure 3-16 Response function (Seibert, 2005)

3.5.4 Routing Routine

Runoff transformation is done by combining the three runoff components with a triangular weighting function, where the generated runoff from one-time step is distributed over user-defined time steps with the parameter MAXBAS Figure 3-17 (Seibert & Vis, 2012).

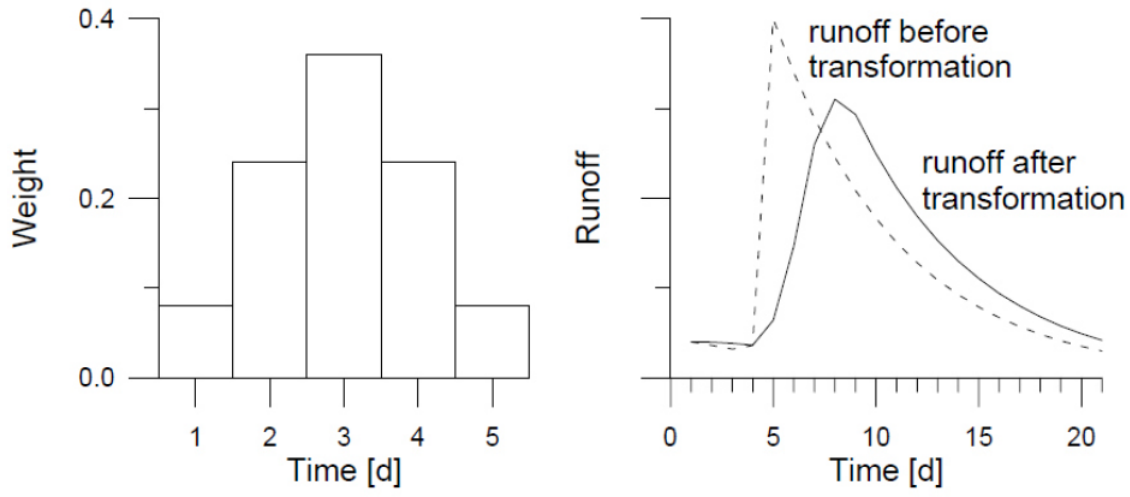

Figure 3-17 Routing routine (Example of runoff transformation with MAXBAS=5) (Seibert, 2005)

The runoff from an upstream sub-catchment is added to the runoff before the routing routine of the sub-catchment in question. The approach with the MAXBAS parameter is used to represent both: Routing through the sub-catchment of water from above and additional water entering the stream in

this sub-catchment. So when several sub-basins are used, the total runoff at the catchment outlet is simulated. (Seibert, 2005).

3.6 HBV Model Setup

Conceptual- semi-distributed HBV model requires a time series of daily rainfall, daily temperature, long-term potential evapotranspiration and daily time series of streamflow for calibration. Areal data is used for each of the sub-basin. Areal rainfall is computed by multiplying the rainfall by the weight of each of the stations for the sub-basin considered in the analysis from the Thiessen polygon. The time series of rainfall, temperature, and streamflow is prepared externally with format file.txt and imported to the model, while the data for long-term potential evapotranspiration and geographical zone, component is inferred directly into the model.

Based on land cover shapefile and DEM data with the use of ArcGIS, the Wabe watershed DEM data are delineated upstream of streamflow gauge stations. In ArcGIS, by using Reclassify tool 9 elevation zones are identified as the requirement of the HBV-light model and to analyze the hydro-meteorological element variation with elevation for the basin. These elevation zones and 3 land cover classes are intersected by using Raster Calculator Tool in ArcGIS to get the percentage of land cover coverage within each elevation zones.

Areal rainfall is computed by multiplying the rainfall by the weight of each of the stations for the sub-basin which is computed from the Thiesen polygon. Long-term potential Evapotranspiration is calculated using the FAO-ET_o calculator that uses the Penman-Monteith equation and as an alternative when solar radiation data, relative humidity data and/or wind speed data are missing. Therefore, reference Evapotranspiration, ET_O (mm d^{-1}), can be estimated using the Hargreaves equation which is previously used by (Endalkachew Abebe & Asfaw Kebede, 2019) & (Abebe Temesgen Ayalew, 2019). The FAO-56 Hargreaves equation for daily computation is given by;

$$ET_o = 0.0023[Ta + 17.8] * \sqrt{T_{\max} - T_{\min}} * Ra$$

Where T max (°C) is the maximum daily air temperature, T min (°C) is the minimum daily air temperature, Ra (MJ m^{-2} d^{-1}) is the extraterrestrial solar radiation. The parameters an (mm d^{-1}) and b are calibrated coefficients, determined on a monthly or yearly basis by regression analysis or visual fitting.

3.7 Sensitivity Analysis

A model sensitivity analysis can be helpful in understanding which model inputs are most important or sensitive and to understand the potential limitations of the model.

As shown in table 3-6 HBV-light model parameters can be grouped into (Soil Moisture Routine or volume controlling) (FC, LP and Beta) that influence the total volume and shape controlling parameters or response routine (K0, K1, K2, PERC) that distribute the calculated discharge in time and MAXBAS (routing routine).

Table 3-6 Parameters range considered in sensitivity analysis for the model (A. Y. JILLO ET AL., 2017)

	defination	unit	minimum value	maximum value
Soil routine				
FC	maximum value of soil mosture storage	mm	50	750
LP	fractioin of FC above which actual ET equalpotential ET	-	0.1	1
BETA	shape coficient	-	0.1	5
response routine				
UZL	treshold parameter	mm	0	50
PERC	maximum rate of recharge between the upper and lower gound water boxes	mm d^{-1}	1	25
K0	storage (or recession) coefficient 0	d^{-1}	0	1
K1	recession cofficient (upper box)	d^{-1}	0.01	0.4
K2	recession cofficient (upper box)	d^{-1}	0.001	0.15
routing routine				
MAXBAS	length of triangular weighting function in routing routine	d	1	7

The parameter range was considered and directly taken from (A. Y. JILLO ET AL., 2017) where previously analyze the parameters in the specified range in this study area.

Field capacity (FC) has an effect on partitioning (dividing) precipitation into soil moisture and runoff. When FC increases the recharge R decreases. When recharging increases the upper reservoir zone storage depth UZL increases this result in quick runoff increases. Therefore, when FC increased the soil storage will increase; hence the amount of water available for quick runoff generation is decreased. Similarly, BETA controls the response function of (R/IN) which is normally called a runoff coefficient or an increase of soil moisture. (J. Seibert and M. J. P. Vis, 2012). Some parameters have more impact on the model results than others so the objective here is to find those sensitive parameters. The knowledge of sensitive parameters is useful in model calibration where we try to match the model output with observed data; here we will try to do this automatically.

Through Monte Carlo simulation, the value of each model parameter was increased and decreased up to 60% by 20% interval and those having steep slopes are considered as most sensitive while those having moderate to gentle slopes are less sensitive (Abebe Temesgen Ayalew, 2019)

3.8 Model Calibration and Validation

All rainfall-runoff hydrological models (lumped or distributed) are simple representations of the real world processes. Besides this, the lumped model parameter represents an average value over the entire watershed. As a result, the model parameters cannot be measured and have to determine through model calibration. Calibration is a process in which parameter adjustment is made in order to simulate as closely as possible the hydrological behavior of the watershed. The goodness of fit is always determined by an objective function. Proper model calibration is necessary to consider a good fit between simulated and observed watershed runoff volume (water balance), the shape of the hydrograph, the peak flow, and the base flow. All these objectives are considered during model calibration because a single objective function cannot establish a reasonable match between simulated and observed data.

3.9 Model Performance Evaluation

The performance of a model must be judged on the extent to which it satisfies its objective of simulating the real world phenomena (accuracy), or the extent to which the achieved level of accuracy persists through different sample of data (consistency) and on the extent to which it can sustain the achieved level of accuracy when subjected to diverse application tests other than those used for calibrating the model (versatility).

To evaluate model simulation this study adopted using the Kling-Gupta efficiency (KGE). This was previously proposed by (Gupta,et al., 2009) and used by (A. Y. JILLO ET AL., 2017)

An additional reason for selecting KGE is that this allows for a multi-objective assessment of the model performance, by decomposing NSE in terms of mean bias, variability bias and correlation as separate criteria to be optimized (Gupta,et al., 2009), KGE is estimated by ;

KGE= $\mathbf{1-\sqrt{(cc-1)^2+(\alpha-1)^2+(\beta-1)^2}}$ Equation 3-14

As equation 3-14 state **cc** is the Pearson correlation coefficient between the observed (**qo**) and simulated (**qs**) runoff, **α** is the relative variability in the simulated and observed values (equal to the ratio of standard deviation of **qs** over the standard deviation of **qo**), and β is the ratio of the means of

simulated and observed flows (i.e. mean of qs over the mean of qo). During optimization, KGE is subject to maximization, with an ideal value at unity measures to determine the quality and reliability of predictions when compared to observed values.

3.10 HBV-light Model input data

The model input requirements for the HBV model are daily rainfall, temperature, estimates of potential evapotranspiration, and catchment characteristics of the area.

3.10.1 Catchment Data

Since the HBV-light model works as a semi-distributed conceptual model, the catchment area can be divided into different sub-basins and the sub-basins further be divided into different elevations and vegetation zones. Therefore a digital elevation map of the area was prepared using Shuttle Radar Topography Mission (SRTM) with a resolution of 30 m x30m.

3.10.2 Areal Rainfall

The HBV model requires daily rainfall as input. Hence rainfall data for the period of ten years (2003-2012) was prepared for seven meteorological stations in and around the catchment area. Areal rainfall in the model is computed by multiplying the rainfall by the weight of each station for the sub-basin considered in the analysis (figure3-18). As shown in table 3-7 the weight of each meteorological station was computed by the Thiesen polygon method.

Table 3-7 Thiessen polygon area ratio of the Wabe watershed

NO	sation name	Longitude	Latitude	Altitude	Anu_Rain	area_1	thiessen plolygon area ratio
1	Welkite	37.7727	8.2781	1809.03	1145.44	147.114	0.106366
2	Aqena	38.0998	8.1882	2688.09	1240.09	826.56	0.425815
3	Indibir	37.9294	8.1208	2048.57	1167.73	110.813	0.057056
4	Abelti	37.5602	8.1742	1634.06	1321.73	20.1357	0.030481
5	Gubre	37.802	8.1817	1839.28	1120.01	82.1956	0.049136
6	Weliso	37.9707	8.535	2028.08	1200.18	362.737	0.186791
7	Butajira	38.4214	8.174	2028.4	1114.05	212.458	0.144356

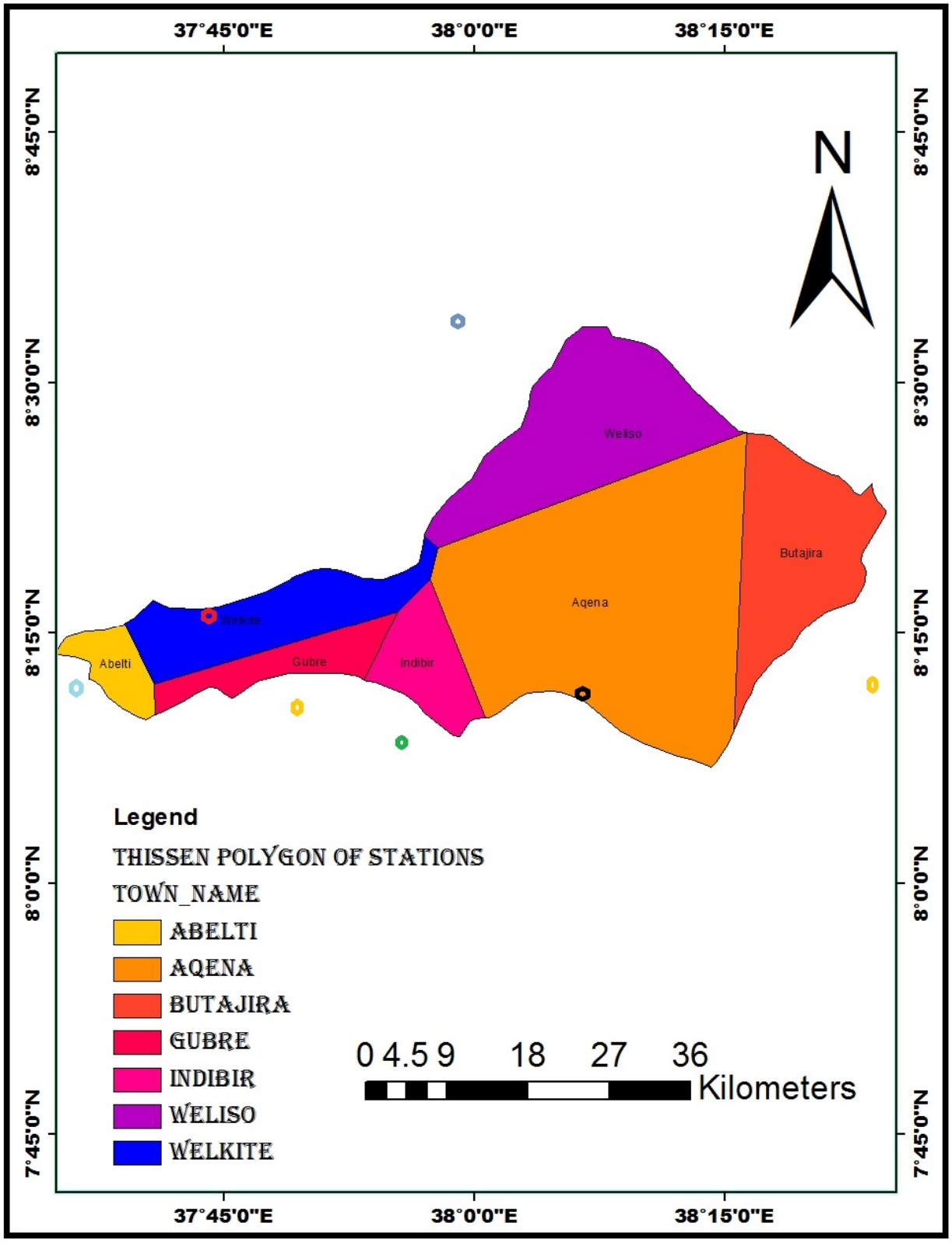

Figure 3-18 Thiesen Polygons for rainfall stations in Wabe watershed

4. RESULT AND DISCUSSION

This chapter presents the findings of this study and presented for each of the objectives proposed in the introduction section. The results are discussed with reference to other scientific works and also compared with findings from previous efforts in the study theme.

4.1 Comparisons of gauged and Satellite estimates rainfalls

As noted before the comparison were done between the gauged observed rainfall data and the four satellite rainfall products namely CHRIPS, PERSSIAN-CCS, TAMSAT, and RFE. In the present study, 17 rain gauge stations were selected at different parts of the Omo-gibe basin over the time period of, 2003 to 2017. The period of analysis was 15 years (5479 days) but only those days where ground observation are available with rainfall estimates were considered and the comparison was done at different temporal scale (daily and monthly).

4.1.1 Daily comparison

The study tried to see the comparisons of the products by the daily time series of the overlapping periods. The correlation result of the entire daily satellite product and the rain-gauge data were poor. As shown in figure4-1 and table 4-1 the best performance was observed for station Wolkite and TAMSAT (r=0.36, POD=0.74), and RFE data (r = 0.251, POD=0.81). However, the relationship was still very poor with the gauged observed rainfall data. The results obtained are similar to the findings by (M.dembele & S.J.Zwart, 2016) who compared SRP in Burkina Faso and also showed the similar result with that of which obtained by (T. Cohen Liechti, 2012) (Yves Tramblay, 2016) and (Odai1 C. O., 2018) Therefore, it could be expected that significant differences occur between rain-gauge and satellite data for daily time series data.

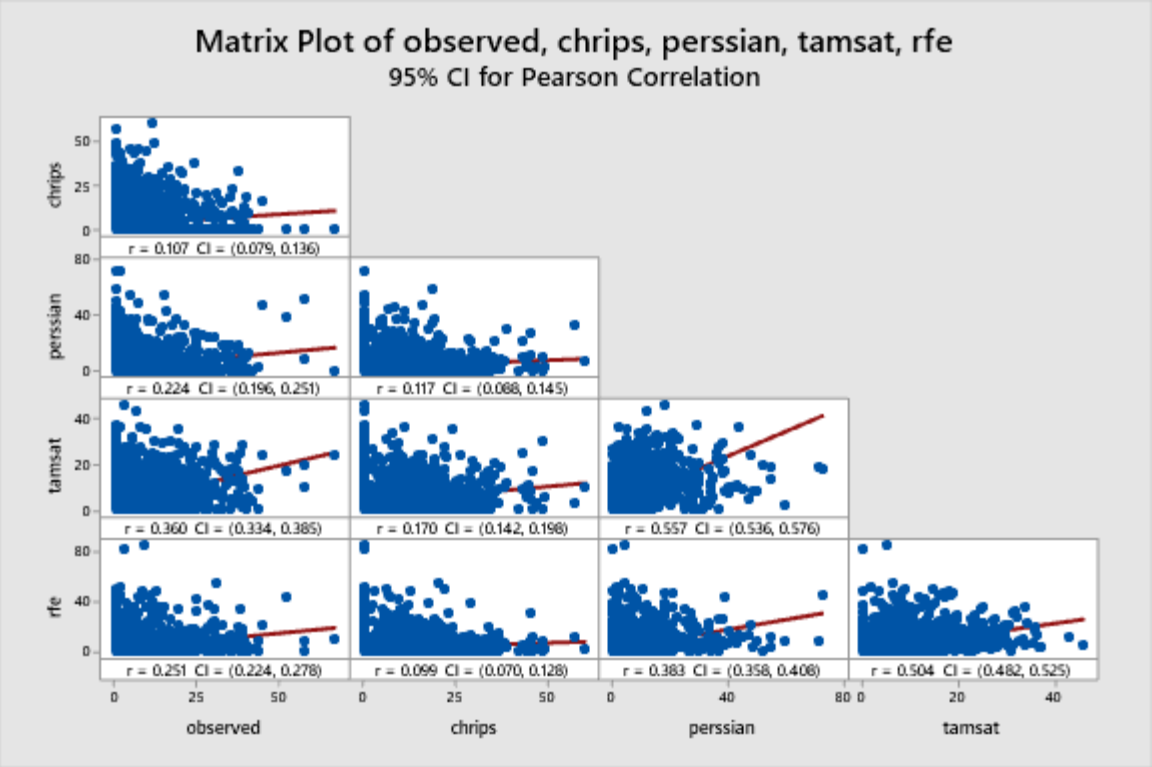

Figure 4-1 daily scatter plot for Wolkite station

Table 4-1 statical indicators for daily Wolkite observed against SRPs

wolkite observed						
	Bias	**ME**	**RMSE**	**E**	**POD**	**FAR**
chrips	1.14438	0.42474	9.02563	-0.96919	0.38568	0.54707
perssian	0.9278	-0.21218	7.90486	-0.5105	0.61301	0.43557
tamsat	1.23506	0.69077	7.07199	-0.20897	0.73587	0.43406
rfe	1.11481	0.33739	7.8544	-0.49128	0.80618	0.48162

- **N.B** (To see statical indicators for remaining station refer **Appendix I A**)

4.1.2 Mean daily comparison

The daily precipitation data were averaged to bring mean daily rainfall for the 365/366 days of a year, before any bias adjustment majority of the products shows low correlation. as shown by the scatter plot in figure4-2 a good correlation agreement was observed by Wolkite with TAMSAT, RFE, PERSSIAN-CCS, CHRIPS (r=0.769, r=0.686, r=0.627, r=0.543) respectively while the remaining station with the products show a low correlation (see appendix) however as shown in table most products were observed to score nearly good bias (B≥0.85) on the other hand relative to the other

products PERSSIAN-CCS data showed a low bias in most of the stations some of this are Agena (B=0.47) & jinka (B= 0.57) from the Stations comparing to the others Limugenet showed Less agreement with the products with CHRIPS (B=0.55) TAMSAT (B=1.03) RFE (B=0.62) PERSSIAN-CCS (B=0.67) and relatively the best Nash–Sutcliffe Efficiency(E) was achieved by Wolkite station with the products RFE(E=0.36), TAMSAT(E=0.36) PERSSIAN-CCS(E=0.27) and CHRIPS(E=-0.23), station Areka scored relatively higher POD with products RFE(POD=1), TAMSAT(POD =0.99) PERSSIAN-CCS(POD =0.97) and CHRIPS(POD =0.97) while gunchre station data showed the smallest but good POD with the products RFE(POD=0.85), TAMSAT(POD =0.71) PERSSIAN-CCS(POD =0.66) and CHRIPS(POD =0.61). Surprisingly CHRIPS data score (B=1) For Serbo station this showed CHRIPS can be taken as an alternative data source for Serbo station.

HANA station showed relatively high FAR value but low FAR which is CHRIPS (FAR=0.33), PERSSIAN-CCS (FAR=0.32), TAMSAT (FAR=0.28) and RFE (FAR=0.33).

Wolkite station relatively shows the lowest RMSE relative to the SRP which is CHRIPS (RMSE =3.22), PERSSIAN-CCS (RMSE =2.48), TAMSAT (RMSE =2.32) and RFE (RMSE =2.32).

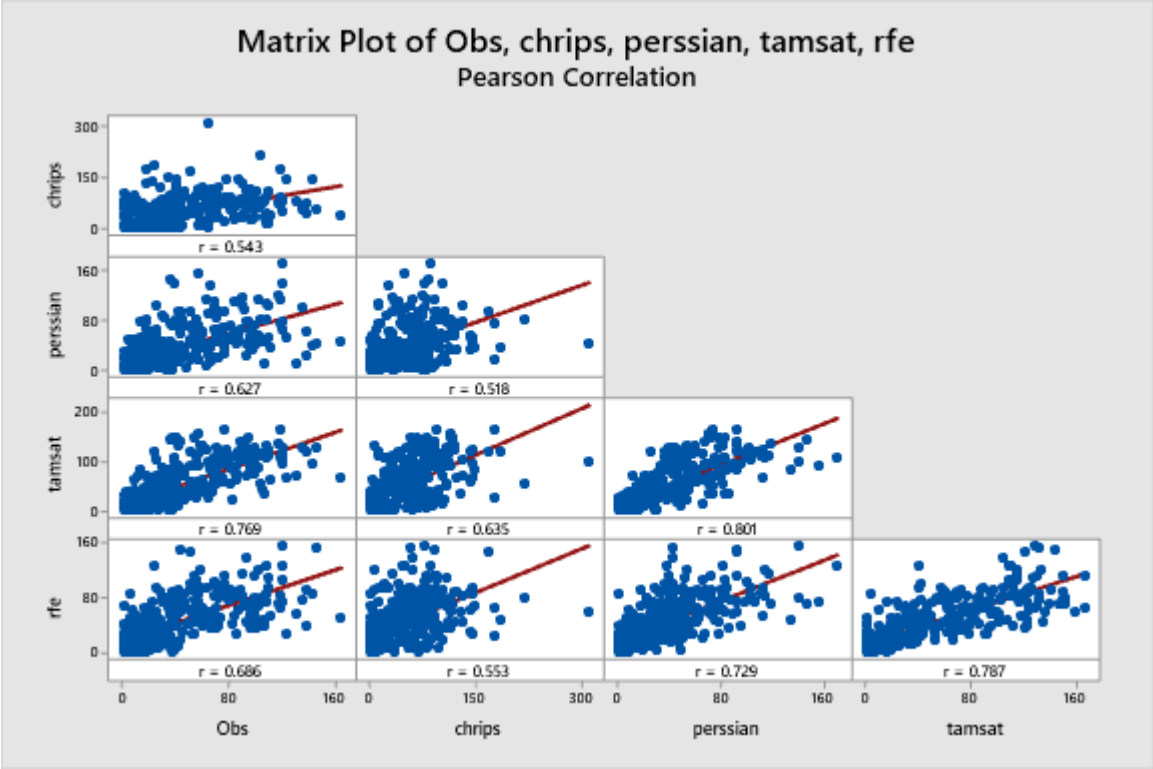

Figure 4-2 Mean daily scatter plot for Wolkite station

Table 4-2 some statistical indicators for mean daily station observed against SRPs

	station name		Jimma			
	statical indicators					
product type	Bias	ME	RMSE	E	POD	FAR
CHIRPS	0.85	-0.64	4.22	-2.81	0.89	0.00
co.CHIRPS	1.00	-0.01	4.31	-2.97	0.89	0.00
PERSIANN-CCS	0.71	-1.26	3.33	-1.37	0.95	0.00
co.PERSIANN-C	1.00	0.00	3.88	-2.22	0.95	0.00
TAMSAT	1.09	0.39	4.03	-2.47	0.89	0.00
co.TAMSAT	1.00	0.00	3.56	-1.71	0.89	0.00
RFE	0.85	-0.66	3.27	-1.29	0.99	0.00
co.RFE	1.00	-0.01	3.41	-1.49	0.99	0.00

	station name		Jinka			
	statical indicators					
product type	Bias	ME	RMSE	E	POD	FAR
CHIRPS	1.85	3.12	6.16	-7.44	0.97	0.00
co.CHIRPS	1.00	0.00	2.64	-0.55	0.97	0.00
PERSIANN-CCS	0.57	-1.57	3.46	-1.66	0.93	0.00
co.PERSIANN-CCS	1.00	0.01	3.81	-2.23	0.93	0.00
TAMSAT	1.12	0.44	3.33	-1.47	0.94	0.00
co.TAMSAT	1.00	0.00	3.01	-1.02	0.94	0.00
RFE	0.69	-1.15	3.35	-1.50	1.00	0.00
co.RFE	1.00	0.01	3.23	-1.32	1.00	0.00

It was also tried to analyze and evaluate the performance of the satellite products for different rain intensities on a daily scale.

The daily precipitations were grouped into seven classes, that is, 0, >0–3, >3–10, >10–25, >25–50, 50-100 and>100 mm day^{-1}. Figure 4-3 depicts the occurrence frequencies of daily precipitation at the point-based station locations scale in different precipitation intensity ranges and their relative contributions (RCs) to the total precipitation for rain-gauge(observed) data's, CHIRPS, PERSIANN-CCS, RFE, and TAMSAT. The occurrence frequency (OF) is equal to the number of rainy days within a class divided by the total number of rainy days. RC is equal to the sum of precipitation within a class divided by the total precipitation (LIUJunzhiet.al, 2012) and (M.dembele & S.J.Zwart, 2016).in most of the stations, the CHRIPS data set overestimate while RFE data set underestimate the occurrence

frequencies of zero precipitation. Only at station Hana, All the satellite-based rainfall products underestimated the occurrence frequencies of zero precipitation. The lowest difference was for PERSIANN-CCS (10–20%). The rain-gauge data showed an OF of 45%-80%, for the finest understanding see figure4-3.

All the satellite-based rainfall products and the rain-gauge data had the same trend in the RCs for all rainfall intensities classes. The trend presented an increase from 0 to 25mm day^{-1} with a decrease beyond (Figure 4-3). However, the RC of RFE products was the highest relative to all station during the increase, up to 25mm day^{-1}, and the lowest during the decrease, indicating that RFE detected little high-intensity rainfall, and thus must be avoided for flood monitoring, and extreme wet climate events in the basin this was the similar result was found for the TAMSAT in Burkina Faso found by (M.dembele & S.J.Zwart, 2016) and for Mozambique by. (Toté et al, 2015).

As with the rain-gauge measurements, all the satellite-based rainfall products presented a peak in rainfall intensity in the10–25 $mmday^{-1}$ class. Almost in All the satellite products and the stations indicated more than 40% of RC, accordingly, there was an insignificant difference between rain-gauge data and satellite products except for RFE for Jinka station (RC = above 50%). For the most of the stations, The contribution of RFE decreased quickly and indicated between 10 –20% for the 25-50 mm day^{-1} class, whereas PERSIANN-CCS showed about 15 - 25%, and CHIRPS and TAMSAT indicated approximately the same contribution of 20-25% as rain-gauge data (RC = between 25-30%). RFE contribution was null for rainfall intensity over 100 mm day^{-1}, while the other satellite-based rainfall products seemed to indicate the same values per pair of satellite products which is nearly less than 5%, Moreover, all of the satellite products indicated similar contribution as rain-gauge data, This leads to the conclusion that all the satellite products, except RFE, were capable of detecting high-intensity rainfall events over 100 mm day–1, and determining the rainfall amount of those events. The most likely reason for this is the poor capacity of the TIR sensor to estimate the actual rainfall amount since the sensor signal does not penetrate the clouds ((Toté et al, 2015), (M.dembele & S.J.Zwart, 2016)).

By and large further assessment is needed for performance evaluation of datasets for a given station to determine whether the given data set for the station used as flood or drought monitoring.

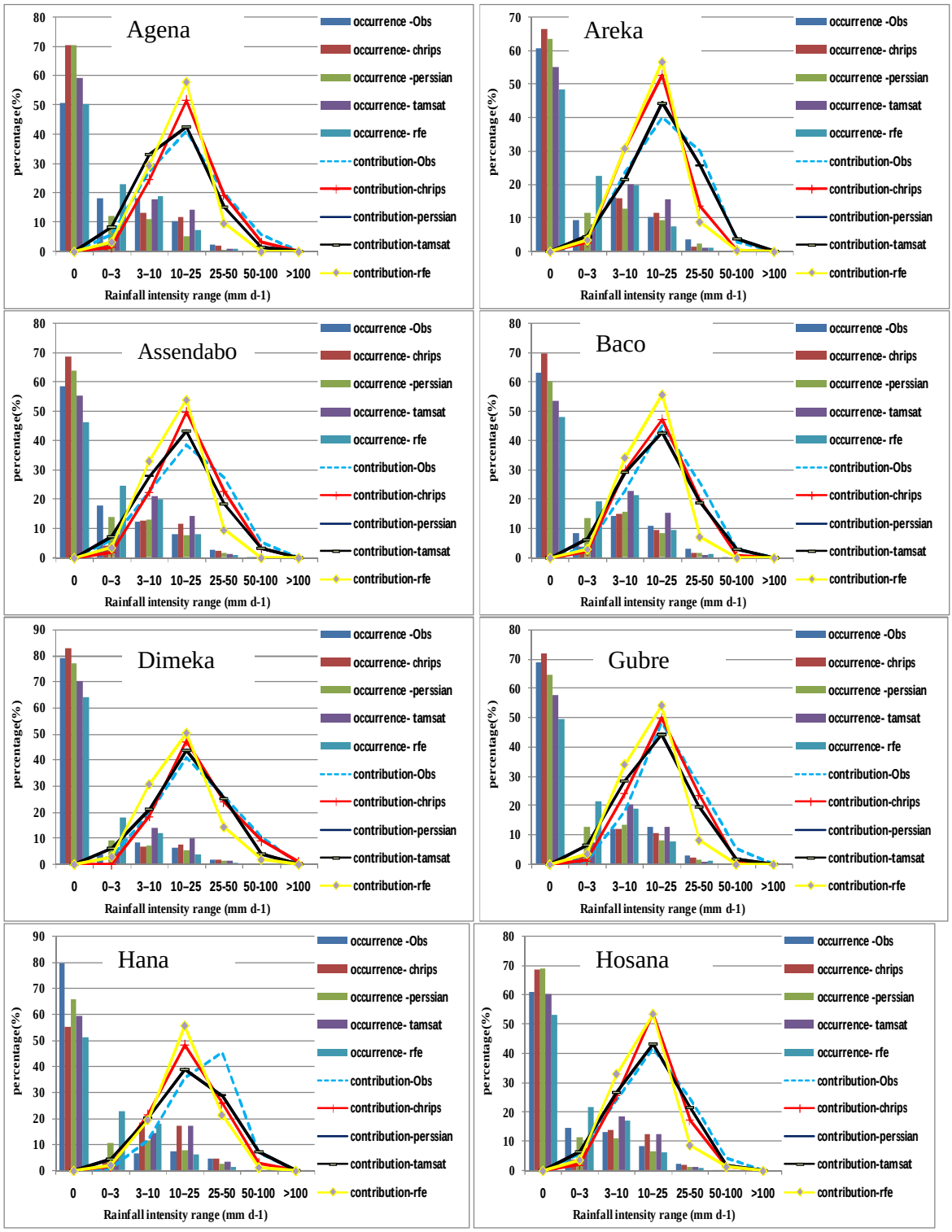

Figure 4-3 Occurrence frequencies of daily precipitation and their relative contributions to total precipitation

4.1.3 Mean monthly comparison

The mean daily satellite-based rainfall data were accumulated to monthly mean rainfall for rain gauge data, CHIRPS, PERSIANN-CCS, RFE, and TAMSAT. The mean monthly data sets were compared at the point-based station locations scale. Figure4-4 and Figure4-5 shows the scatter plots of data from rain-gauge stations (Wolkite and Gunchre for the remaining stations see appendix) against each of the satellite-based rainfall estimates. The statistical indicators are listed in Table4-3. Good agreement with the rain-gauge data was observed for all of the satellite products this result was previously observed by (M.dembele & S.J.Zwart, 2016) & (Odai1, 2018) .The best correlation was for station Wolkite with TAMSAT (r = 0.994) and the best bias score was observed for all stations with SRP. Whereas PERSSIAN-CCS with Agena station presented the weakest but still good score (B = 0.47). All SRP with station score POD =1 whereas TAMSAT for Gunchre presented the weakest but still excellent score (POD =0.92).

This higher accuracy at the monthly scale than at the daily scale is due to the fact that the errors at the sub-monthly scale are nearly symmetrical and thus can cancel each other out after the aggregation. As expected Wolkite station showed the best relationship with the SRPs while PERSSIAN-CCS with the station still estimates less relative to the other as a daily comparison, Serbo station showed a perfect match with the CHRIPS data set, followed closely by RFE. By and large TAMSAT data set showed a finer correlation with the stations and score good in continuous and categorical statics and nearly followed by RFE.

It is obvious that the time step has an important influence on the quality of the satellite estimates this showed when the time step increases the accuracy of SRP to predict the rainfall event relative to the station value will increase and this was also observed by (T. Cohen Liechti, 2012), (LIUJunzhiet.al, 2012)& (M.dembele & S.J.Zwart, 2016).

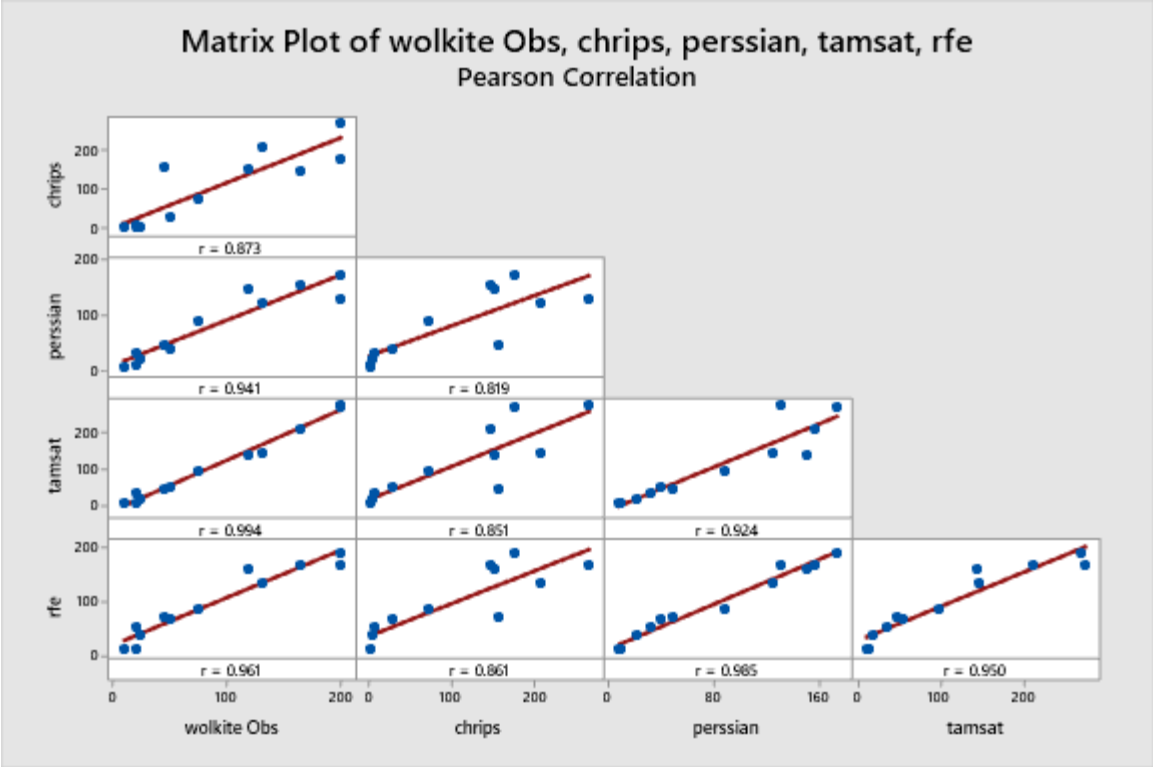

Figure 4-4 mean monthly scatter plot for Wolkite station against SRPs

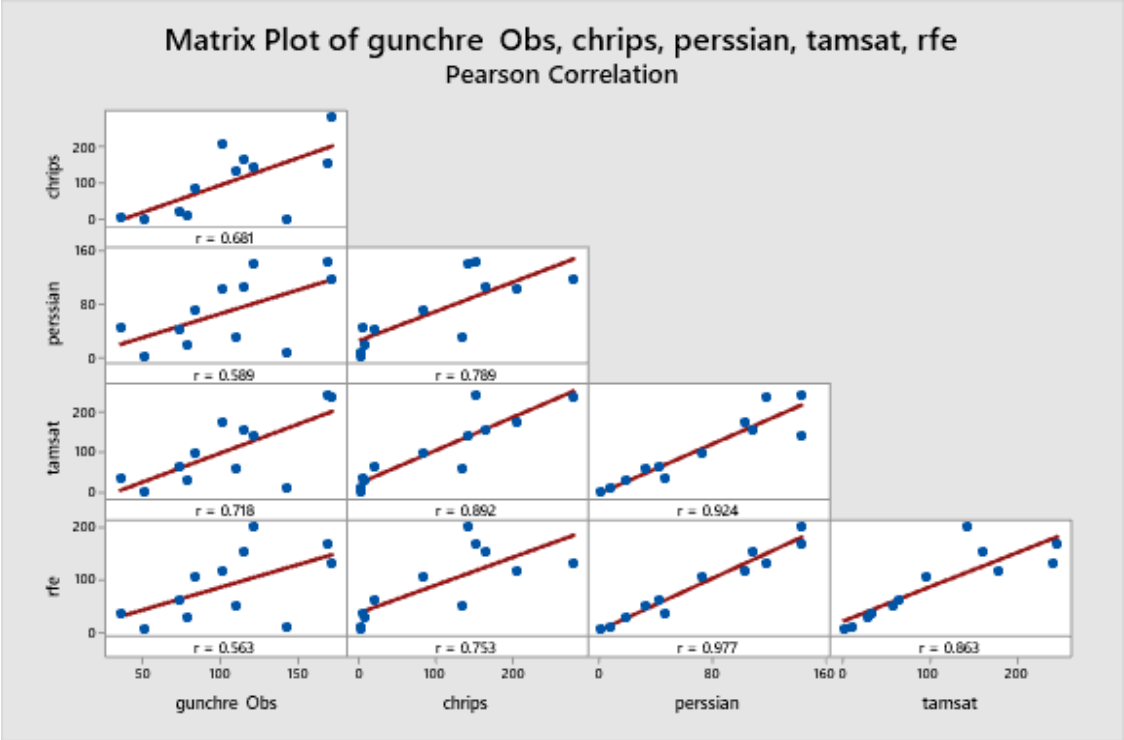

Figure 4-5 mean monthly scatter plot for gunchre station against SRPs

Table 4-3 some statistical indicators for mean monthly observed against SRPs

product type	station name	Jimma				
	statical indicators					
	Bias	ME	RMSE	E	POD	FAR
CHIRPS	0.85	-8.40	85.47	-23.66	1.00	0.00
co.CHIRPS	1.00	-0.32	0.96	1.00	1.00	0.00
PERSIANN-CCS	0.71	-38.47	64.08	-12.86	1.00	0.00
co.PERSIANN-CCS	1.00	-0.03	0.83	1.00	1.00	0.00
TAMSAT	1.09	15.04	90.17	-26.45	1.00	0.00
co.TAMSAT	1.00	-0.13	0.46	1.00	1.00	0.00
RFE	0.85	-20.17	56.53	-9.79	1.00	0.00
co.RFE	1.00	-0.27	0.89	1.00	1.00	0.00

product type	station name	Jinka				
	statical indicators					
	Bias	ME	RMSE	E	POD	FAR
CHIRPS	1.85	98.83	153.25	-41.66	1.00	0.00
co.CHIRPS	1.00	0.05	0.41	1.00	1.00	0.00
PERSIANN-CCS	0.57	-47.88	70.51	-8.03	1.00	0.00
co.PERSIANN-CC	1.00	0.22	0.61	1.00	1.00	0.00
TAMSAT	1.12	10.21	46.70	-2.96	1.00	0.00
co.TAMSAT	1.00	0.07	0.41	1.00	1.00	0.00
RFE	0.69	-35.14	62.15	-6.02	1.00	0.00
co.RFE	1.00	0.37	0.99	1.00	1.00	0.00

By observing the monthly statical indicators of each SRP with respect to gauged data (mainly the Bias and ME); the products for the station classified as underestimates (B<1 & ME<0) or overestimate (B>1 & ME>0). consequently, Agena, Areka, Gunchre, Gubre, Indibr underestimated by all products this may be due to lack of long term time series data for the stations and this information is summarized in figure 4-6 below.

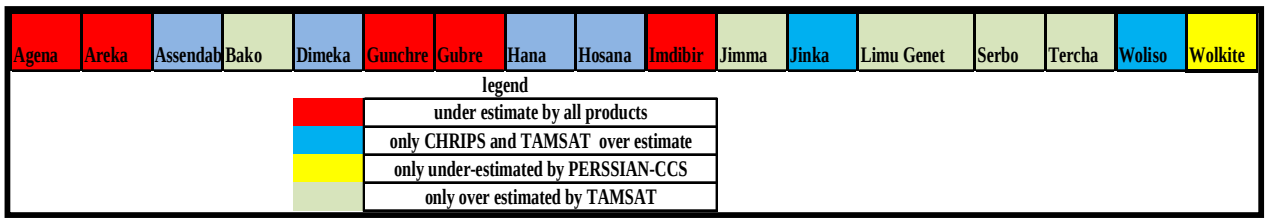

Figure 4-6 Aggregate results of the SRPs respect to the station observed

Relatively the TAMSAT data is the most to overestimate 12 stations out of 17 and which highly recommended for hydrological modeling and flood forecasting while PERSSIAN-CCS performed underestimate almost for all station this result contradicts with the result where previously found by (M.dembele & S.J.Zwart, 2016) which PERSSIAN-CCS data was overestimated for Burkina Faso and suggest it not use for drought monitoring this may arises due to geographical and elevation difference .

but after the adjustment (bias correction) literally to say a perfect correlation agreement was observed for all the products as shown in table 1and 2 of the statical indicators most observed data have nearly a Bias value of 1 and ME nearly approach to 0 and for categorical statics POD and FAR value of 1 and 0 respectively.

In (figure4-7 -4-8) below it was trying to see the comparison amongst the SRPs, the observed and the corrected SRPs through graphical interpretation and clearly shows how bias-adjusted value can be close to the observed values.

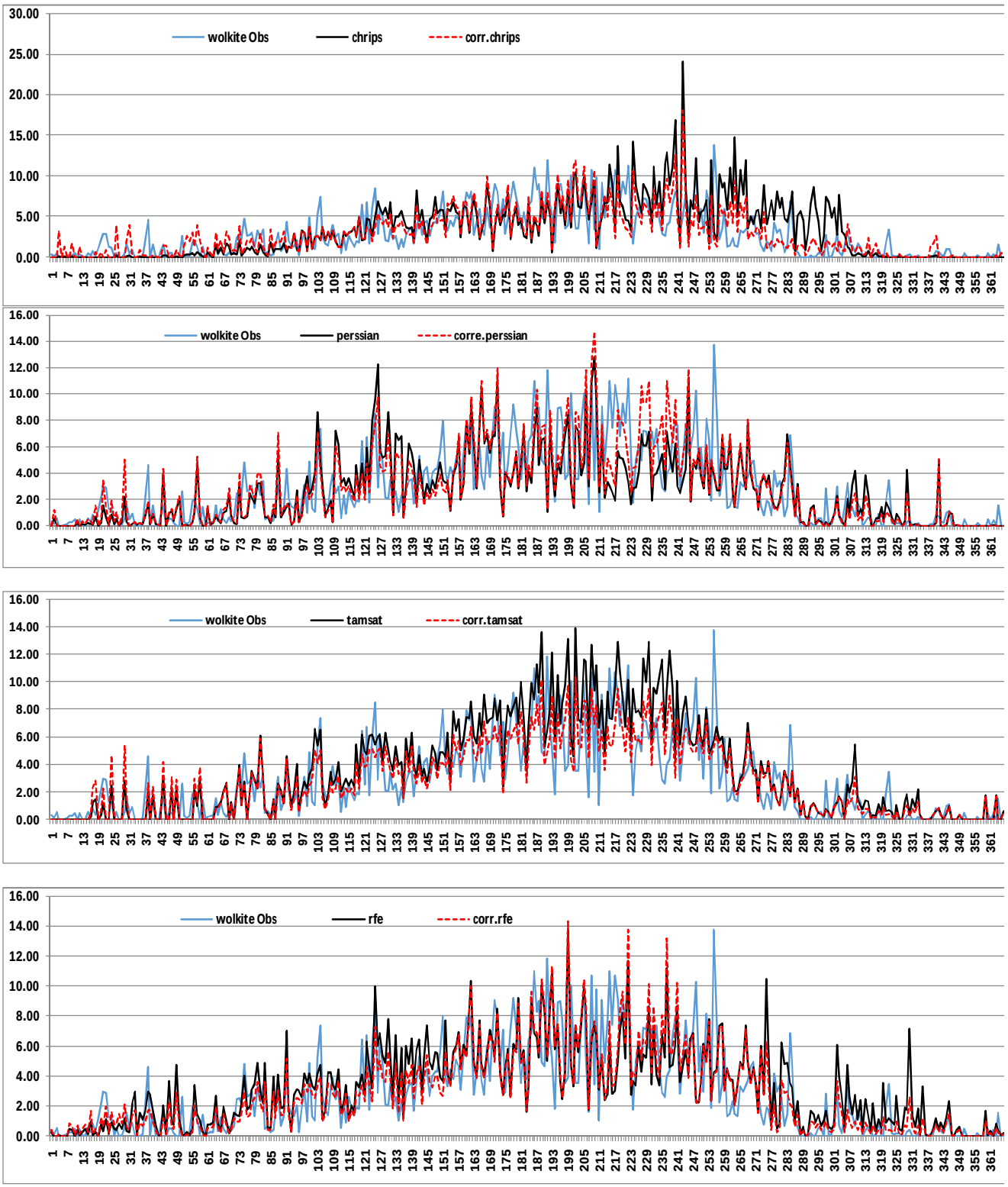

Figure 4-7 mean daily rainfall of Wolkite observed against SRPs

- for the remaining stations see **appendix III**

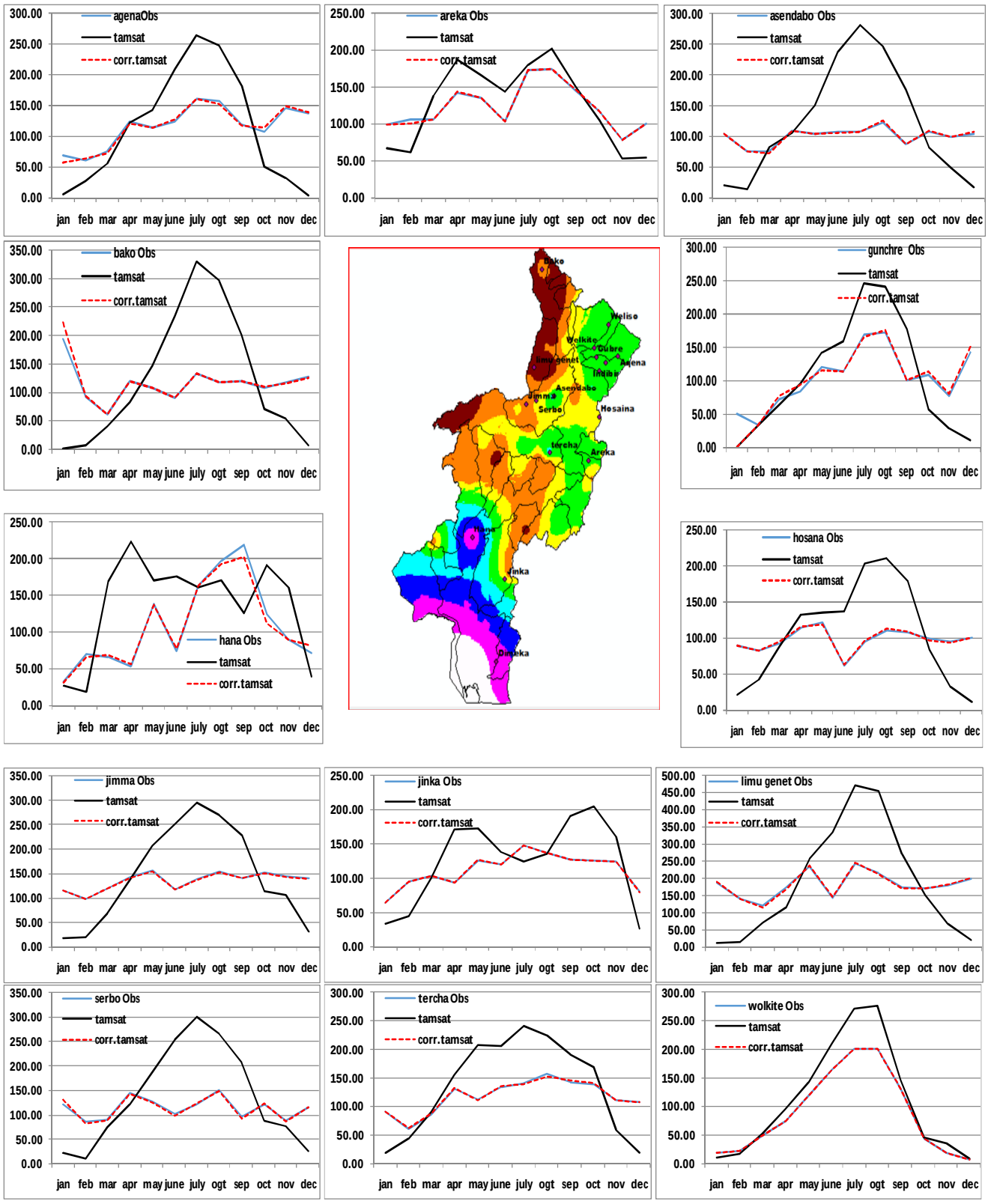

Figure 4-8 Mean monthly TAMSAT raw and corrected dataset with station observed data

4.2 HBV Hydrological Modeling Results for gauged observed rainfall data

4.2.1 Sensitivity Analysis

Sensitivity analysis determines which parameters of the model have the greatest impact on the model results. The effect of each model parameter was analyzed based on objective functions KGE. As shown in figure 4-9; Due to different consideration the most sensitive parameter for HBV-light model during simulations of the flows are FC, PERC, BETA, LP and k2 and fewer sensitivity parameters are UZL, K0, K1 and MAXBAS because of this parameter values are highly sensitive and a slight change of the parameters has great change on peak flows, volumes, and hydrograph shape. Similar to this study result Studies like (Abebe Temesgen Ayalew, 2019) clearly showed that K2 and BETA are most sensitive for their optimized parameter result and (Perera, 2017) stated FC, LP, and BETA were the most sensitive parameters, there is some variation with those study result this is due to study are and model objective function difference.

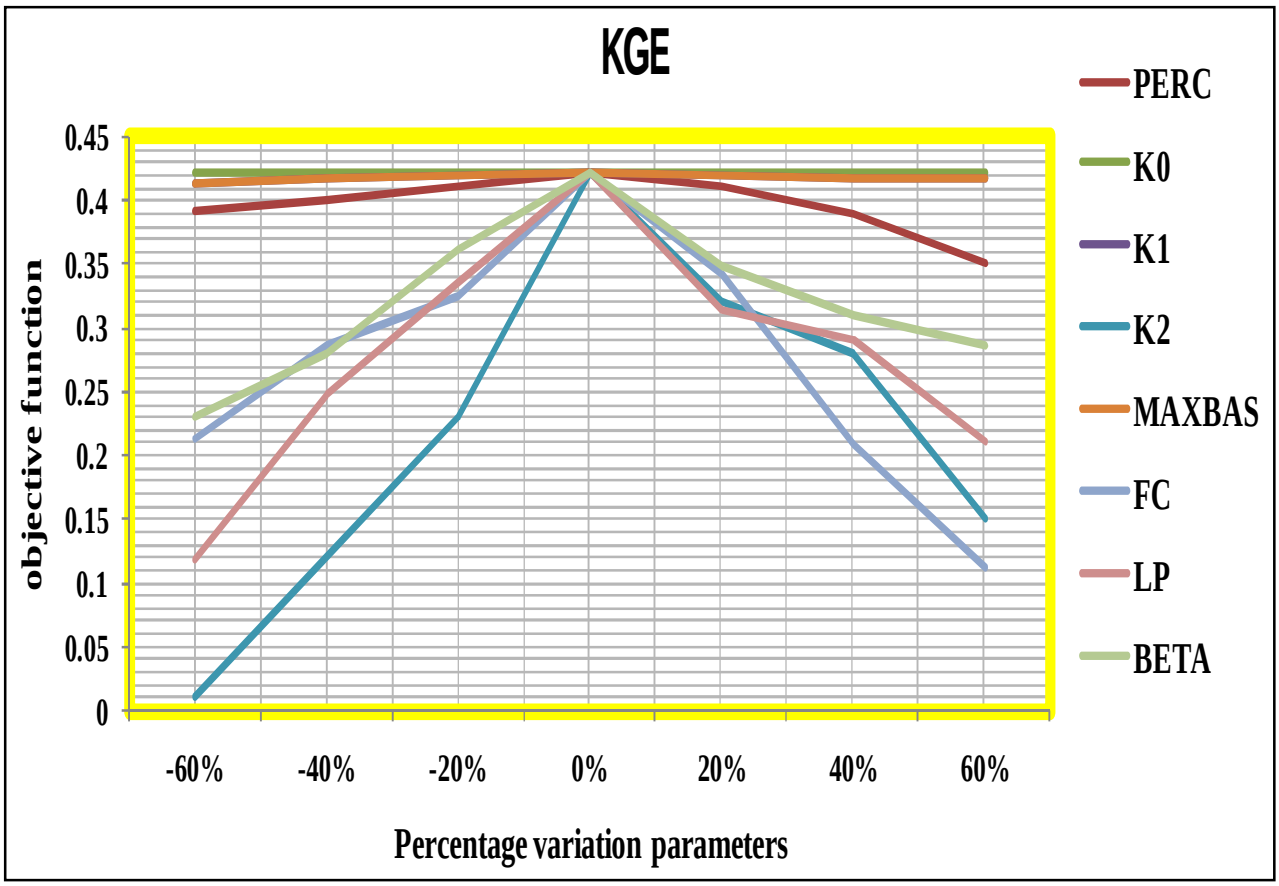

Figure 4-9 sensitivity analysis by considering KGE as the objective function

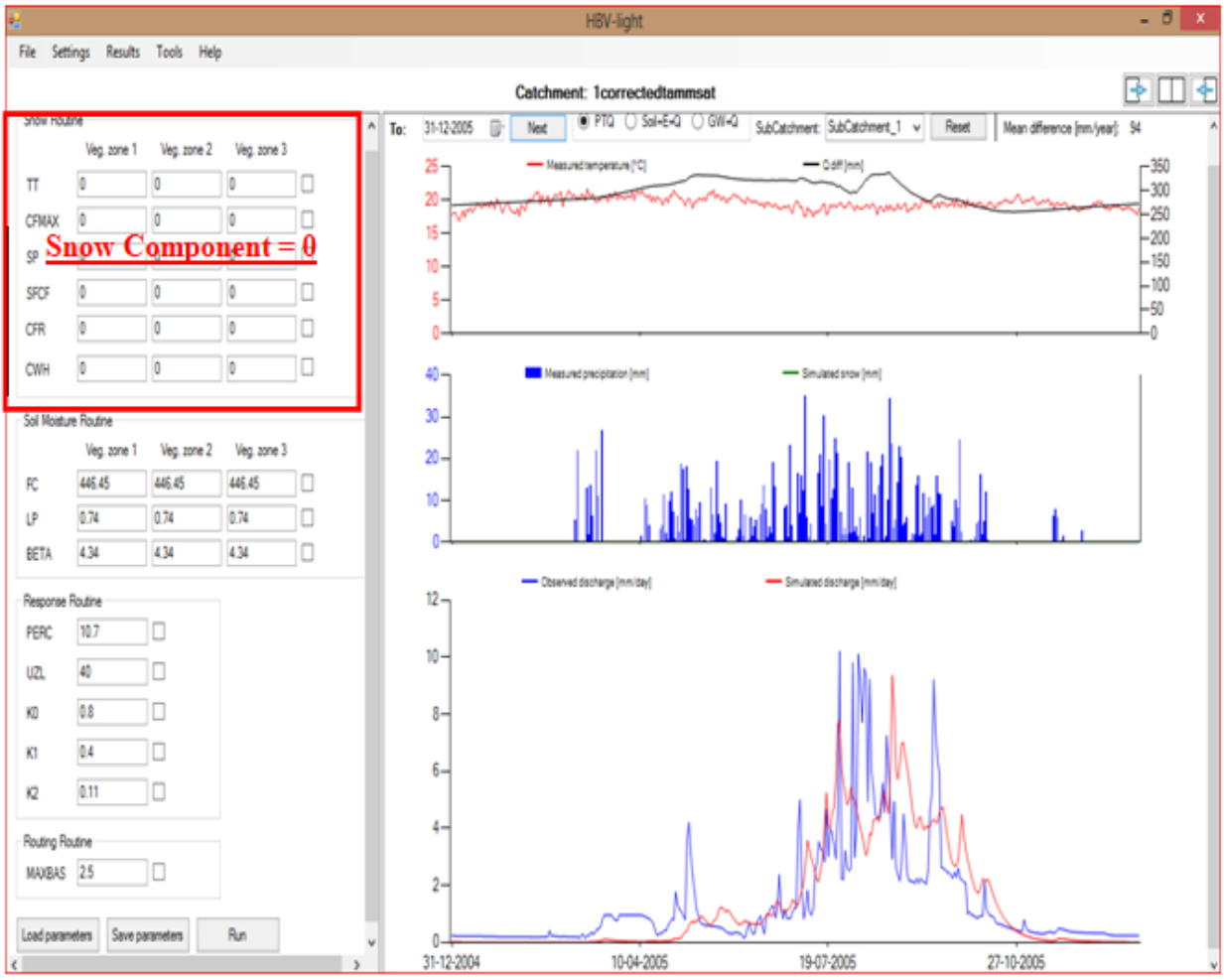

Figure 4-10 Sample HBV-light model result

4.2.2 Calibration and validation

The model parameters were optimized using rain gauged data as input for HBV-light software. The model was calibrated and validated for 10 years (2003-2012).for gauging station daily and monthly data from (2004-2009) and (2010-2012) were used as a calibration period and validation period respectively while 2003 was used as a warm-up period. Calibration was done automatically by optimizing the model parameters in each subroutine that have a significant effect on the performance of the model and by visualizing the KGE within the model itself. Based on this, several iterations were made to select the most optimum (best fitted) parameter set in order to match simulated discharges with the observed. Accordingly, the optimized values for the Wabe with the observed rainfall data simulated flow are tabulated below in table 4-4.

Table 4-4 HBV-light model optimized parameter value

	Sensetive Parameters							
Rainfall data type	PERC	K0	K1	K2	MAXBAS	FC	LP	BETA
Observed	1	0.8	0.248	0.15	1.86	198.5	0.8	3

The optimized parameters are nearly differing with the findings by (A. Y. JILLO ET AL., 2017). A strong reason for this slight difference is due to the calibration and validation period. in their study it clearly noted that the calibration and validation period have a significant influence on the optimized model value.

A result of daily and monthly simulated to daily and monthly observed streamflow (table 4-5) indicated a good agreement between the datasets with KGE=0.42 and KGE=0.61 for the calibration period (January 1-2004 to December 31- 2009) and KGE=0.54 AND KGE=0.71 for the validation period (January 1- 2010 to December 31- 2012) Respectively. This result showed better when compared with the result that was inferred from (A. Y. JILLO ET AL., 2017) for the study area,

The model captured well both the daily and monthly time series of streamflow as well as the trend during both calibration and validation periods.

Table 4-5 model performance using KGE for the calibration and validation period of Insitu based simulation

	Daily resullt					Monthly result				
rainfall type		cc	$\dot{\alpha}$	β	KGE		cc	$\dot{\alpha}$	β	KGE
Observed	Calibration	0.44	0.87	1.02	0.42	calbration	0.63	0.88	1.02	0.61
	Valdation	0.58	0.83	1.04	0.54	validation	0.75	0.85	1.04	0.71

A plot of daily simulated to daily observed streamflow (figure 4-11) shows a fair relationship between the observed and Insitu based simulated flow although a fair agreement between the observed and simulated discharge for most cases the simulated discharge underestimates the peak flows.

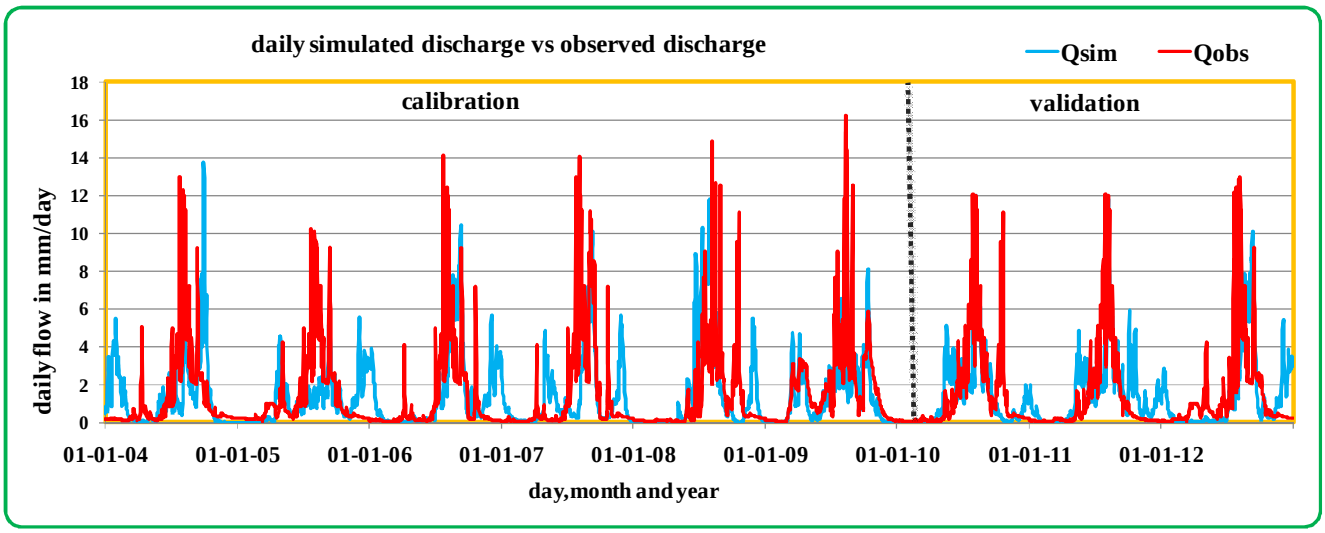

Figure 4-11 Daily calibrations and validation result for observed and Insitu based simulated flow

With the same analogy, the plot of monthly simulated to observed streamflow (figure 4-12) shows except for the year 2004 the simulated discharge underestimates the peak flow of the observed discharge.

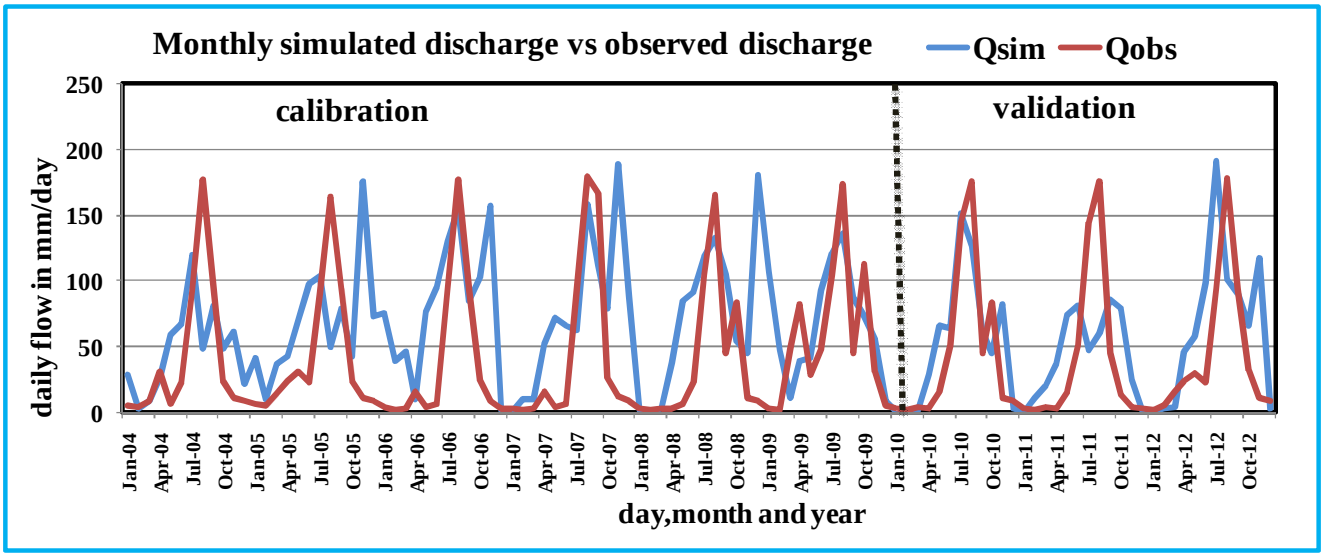

Figure 4-12 Monthly calibrations and validation result for observed and Insitu based simulated flow

4.3 HBV-light Modeling Results for Satellite Rainfall Products

For this part, the objectives were to test the HBV-light model performance with satellite rainfall products as an input. Thus, the four selected satellite rainfall estimates (CHRIPS, PERSSIAN-CCS, TAMSAT, and RFE) were used as input for the model independently using the same time windows. As noted before the model is first calibrating using rain gauged measured rainfall to establish model parameters. Secondly, satellite data is used also an input for the models using gauged optimized parameters**.**

HBV-light model is calibrated for a daily time series of six years (2004-2009) and validated for three years (2010-2012). Calibration was done automatically by optimized model parameters in each subroutine that have a significant effect on the performance of the model and by visualizing the KGE within the model itself. Based on this, several iterations were made to select the most optimum (best fitted) parameter set in order to match simulated discharges with the observed.

A plot of daily and monthly simulated to observe streamflow was prepared for all satellite rainfall products in figures (4-13 & 4-14) below respectively.

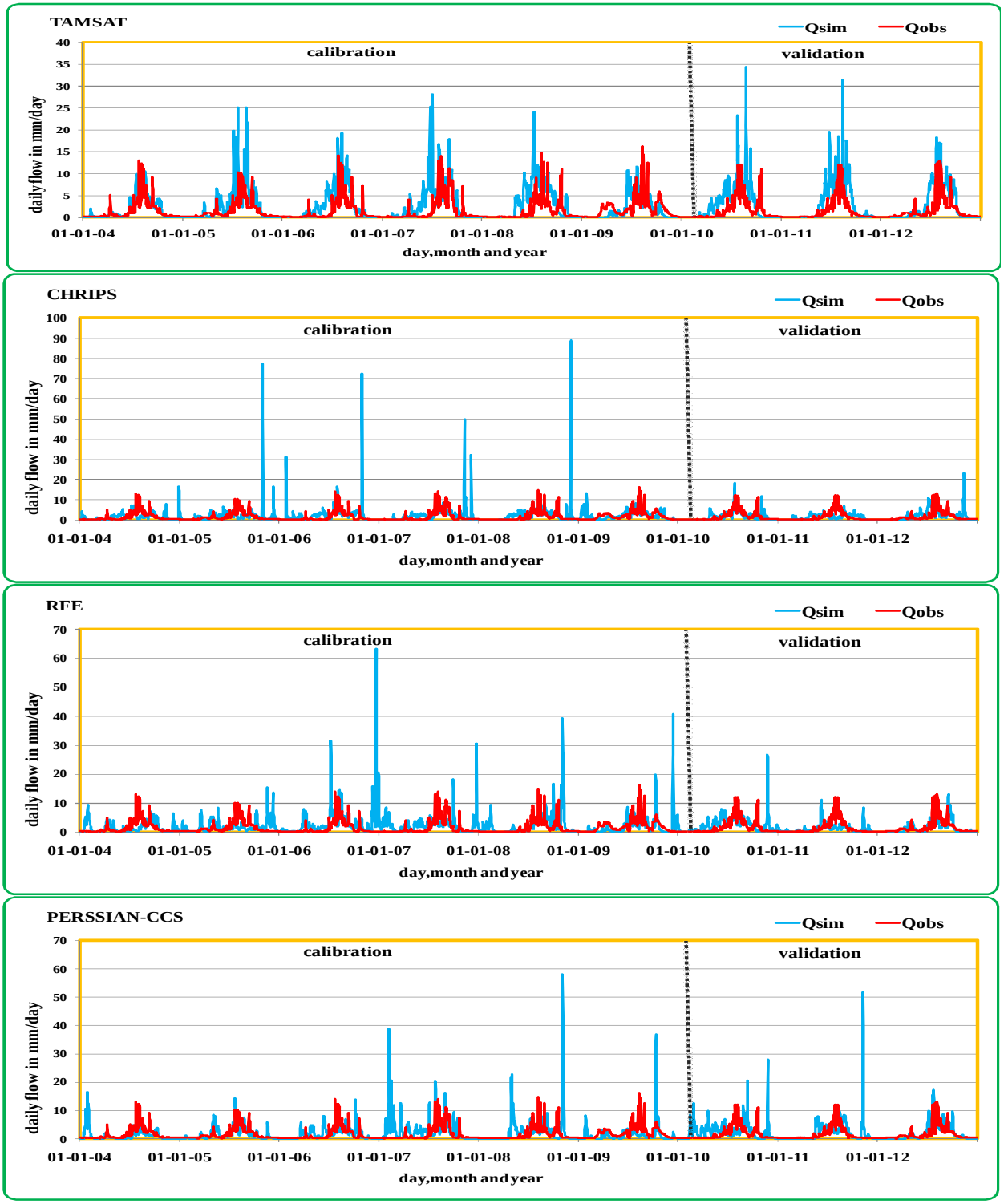

Figure 4-13 Daily calibrations and validation result for observed and satellite-based simulated flow

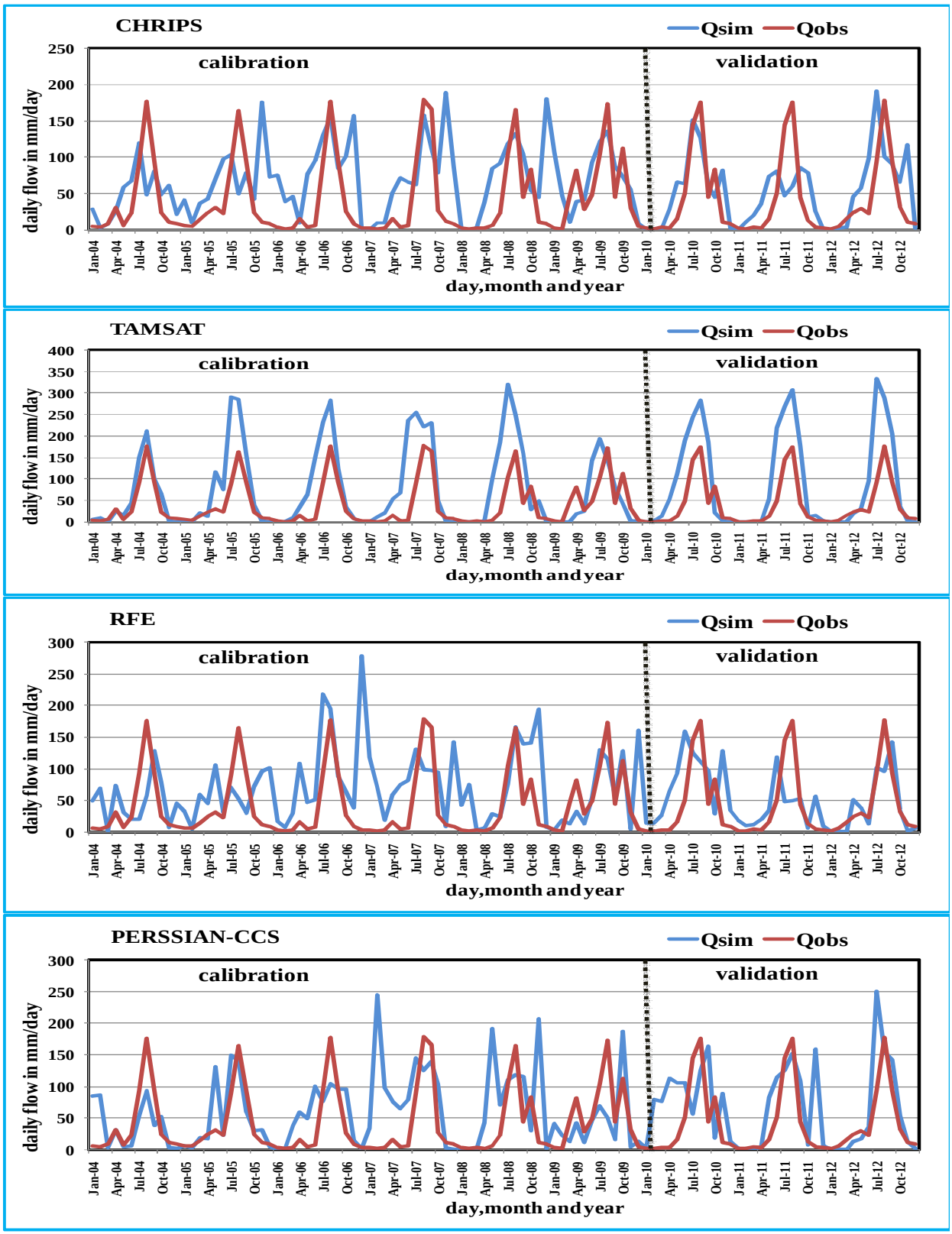

Figure 4-14 Monthly calibrations and validation result for observed and satellite-based simulated flow

Based on the final calibrated sensitive parameters to streamflow a final objective result is produced for all satellite rainfall products and summarized in Table 4-6 shown below

Table 4-6 model performance using KGE as an objective function for the calibration and validation period for the satellite rainfall-based simulation

rainfall type	Daily resullt					Monthly result				
		cc	$\dot{\alpha}$	β	KGE		cc	$\dot{\alpha}$	β	KGE
CHRIPS	calibration	0.47	1.65	1.77	-0.14	calbration	0.80	1.71	1.77	-0.06
	valdation	0.49	1.48	1.71	0.00	validation	0.79	1.49	1.71	0.11
PERSSIAN-CCS	calibration	0.19	1.54	1.37	-0.04	calbration	0.41	1.07	1.37	0.30
	valdation	0.30	1.51	1.57	-0.04	validation	0.57	1.17	1.57	0.27
TAMSAT	calibration	0.53	1.61	1.77	-0.09	calbration	0.76	1.74	1.77	-0.10
	valdation	0.63	1.90	2.08	-0.45	validation	0.87	2.02	2.08	-0.49
RFE	calibration	0.15	1.59	1.64	-0.21	calbration	0.35	1.08	1.64	0.08
	valdation	0.31	0.97	1.19	0.29	validation	0.52	0.84	1.19	0.46

From the summary table 4-6 CHRIPS score for daily and monthly calibration period (KGE=-0.14, r=0.47) and (KGE=-0.06, r=0.8) and validation period (KGE=0, r=0.49) and (KGE=0.11, r=0.79) respectively, PERSSIAN-CCS has scored for daily and monthly calibration period (KGE=-0.04, r=0.19) and (KGE=-0.3,r=0.41) and validation period (KGE=-0.04,r=0.3) and (KGE=0.27,r=0.57) respectively. TAMSAT has scored for daily and monthly calibration period (KGE=-0.09, r=0.53) and (KGE=-0.1, r=0.76) and validation period (KGE=-0.45, r=0.63) and (KGE=-0.49, r=0.87) respectively while RFE has scored for daily and monthly calibration period of (KGE=-0.21, r=0.15) and (KGE=0.08, r=0.35) and validation period (KGE=0.29, r=0.31) and (KGE=0.46, r=0.52) respectively.

TAMSAT showed a better result compared to other SRPs for both daily and monthly simulation because it has a better correlation with the Insitu rainfall data; this result was expected previously.

However, in few cases, the KGE in validation model slightly outperforms the one in calibration mode; a possible explanation is that the optimization algorithm may have converged to a local optimum; this scenario was previously seen in different studies including (A. Y. JILLO ET AL., 2017).

4.4 HBV- light model result for Bias adjusted SRPs

As expected before the result obtained from using SRPs for flow simulation has shown as an unsatisfactory result this enforces to apply bias-adjusted rainfall products for flow simulation and presented as follows.

Using bias-corrected satellite rainfall estimates as a model input; the HBV-light model is calibrated for daily time series of six years (2004-2009) and validated for three years (2010-2012). Calibration was done automatically by optimizing the model parameters in each subroutine that have a significant effect on the performance of the model and by visualizing the KGE within the model itself. The effect of bias-adjusted rainfall product in a change of the value of KGE is tabulated in table 4-7 below

Table 4-7 KGE value increment in % when the adjusted SRPs are used for modeling

KGE value increment in %				
	daily		monthly	
product type	calibartion	validation	calibartion	validation
CHRIPS	161.90	117.39	139.39	108.57
PERSSIAN-CCS	131.58	44.12	116.67	116.00
TAMSAT	50.00	30.19	38.18	37.10
RFE	115.79	144.44	93.75	106.67

As shown in the summarized table 4-7 above the highest KGE increment was observed when Chrips dataset is adjusted and used for the model while the lowest increment was shown for the TAMSAT data set but the best KGE was recorded by this data set and this s because this data set shows a good correlation with the Insitu rainfall data.

As it was previously noted the time step has great importance in meeting a better objective result, therefore, the monthly result for the dataset gives a satisfactory result.

A plot of daily and monthly simulated to observed streamflow was prepared for all bias-adjusted satellite rainfall products in figures (4-15 & 4-16) below respectively.

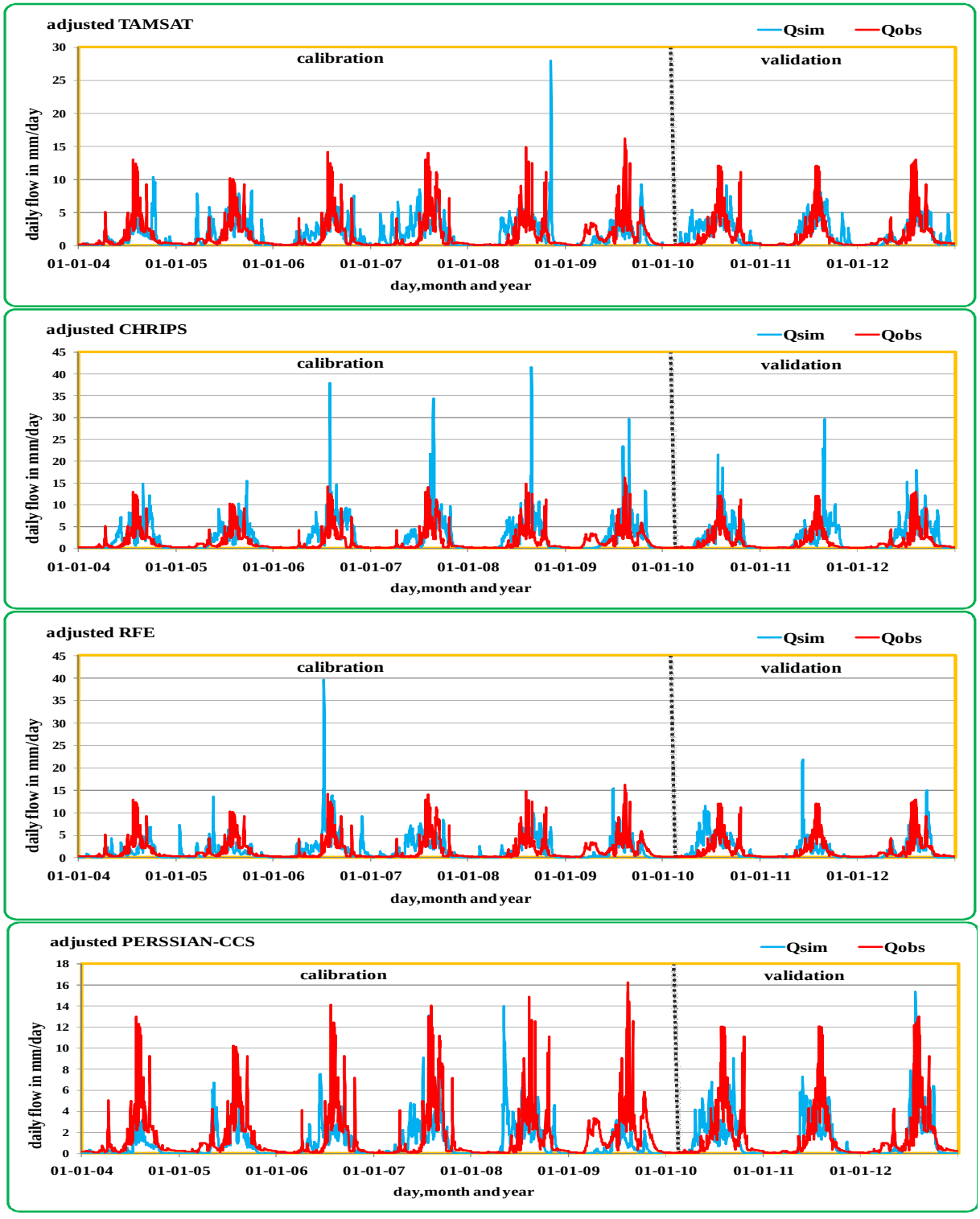

Figure 4-15 Daily calibrations and validation result for observed and bias-adjusted satellite rainfall product simulated flow

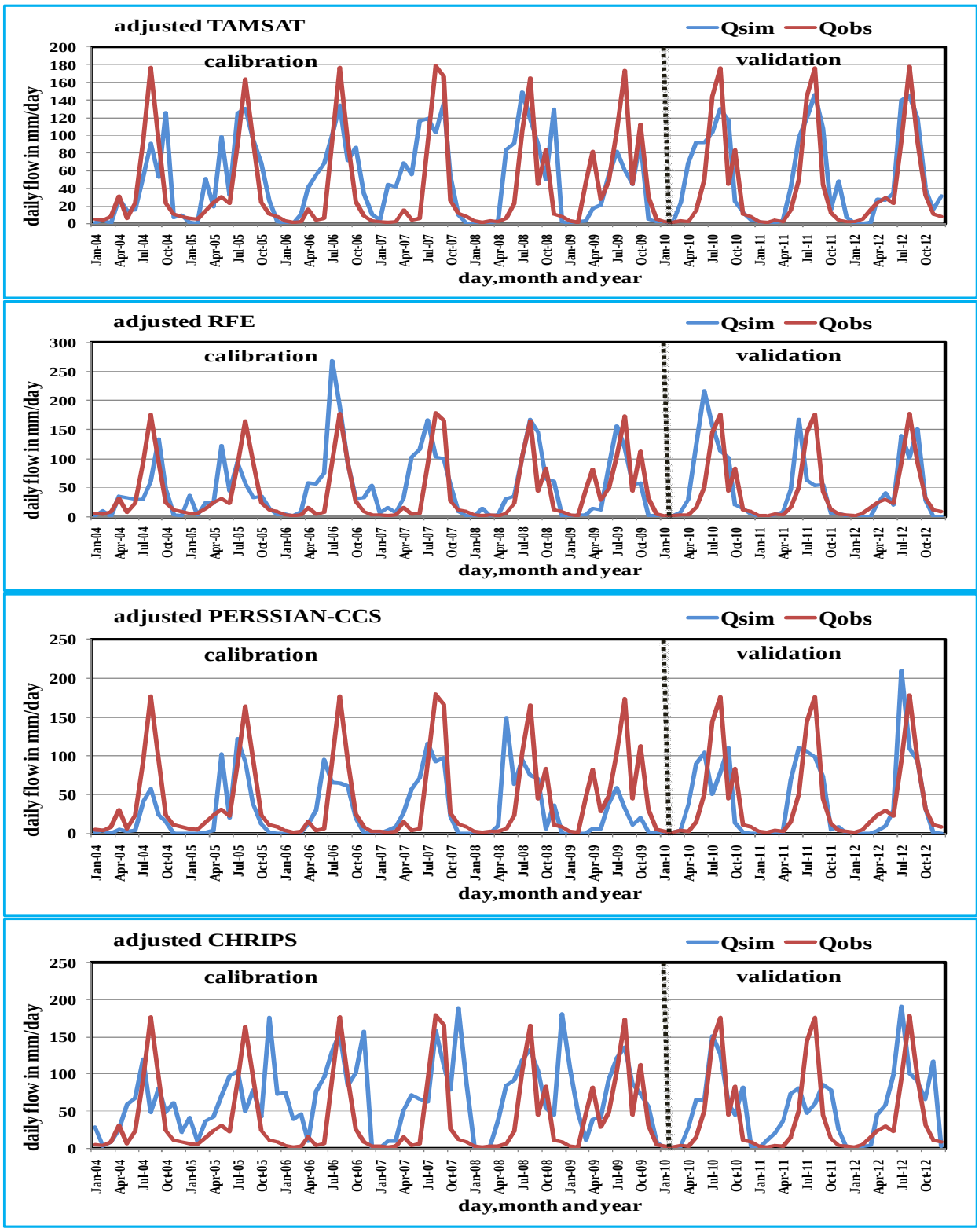

Figure 4-16 Monthly calibrations and validation result for observed and bias-adjusted satellite rainfall product

From the figure (4-20 and 4-21) a conclusion can be made that the simulated discharge underestimate the all observed peak discharges and adjusted TAMSAT nearly obtained a special result than the rest of the bias-adjusted satellite rainfall products

Based on the final calibrated stream flow a final objective result is produced for all satellite rainfall products and summarized in Table 4-8 shown below

Table 4-8 model performance using KGE as an objective function for the calibration and validation period for the bias-adjusted satellite rainfall based simulation

rainfall type		Daily resullt					Monthly result			
		cc	ά	β	KGE		cc	ά	β	KGE
Cor.CHRIPS	calibration	0.12	2.03	1.60	0.12	calbration	0.43	0.89	1.60	0.16
	valdation	0.35	0.96	0.79	0.32	validation	0.59	0.86	0.79	0.52
Cor. PERSSIAN-CCS	calibration	0.35	0.70	0.67	0.21	calbration	0.55	0.70	0.67	0.36
	valdation	0.47	0.87	0.95	0.45	validation	0.65	0.92	0.95	0.64
Cor.TAMSAT	calibration	0.41369	0.88993	1.13958	0.38733	calbration	0.65	0.85	1.14	0.60
	valdation	0.60288	0.85587	1.2029	0.53133	validation	0.82	0.92	1.20	0.72
Cor.RFE	calibration	0.38	1.06	1.17	0.36	calbration	0.63	1.03	1.17	0.59
	valdation	0.41	1.04	1.12	0.40	validation	0.58	1.08	1.12	0.56

From the summary table 4-8 Cor.CHIRPS score for daily and monthly calibration period (KGE=0.12, r=0.12) and (KGE=0.16, r=0.43) and validation period (KGE=0.32, r=0.35) and (KGE=0.52, r=0.59) respectively, Cor.PERSSIAN-CCS has scored for daily and monthly calibration period (KGE=0.21, r=0.35) and (KGE=0.16,r=0.43) and validation period (KGE=-0.32,r=0.35) and (KGE=0.36,r=0.55) respectively. Cor.TAMSAT has scored for daily and monthly calibration period (KGE=0.39, r=0.42) and (KGE=0.6, r=0.65) and validation period (KGE=-0.54, r=0.6) and (KGE=0.82, r=0.72) respectively while Cor.RFE has scored for daily and monthly calibration period of (KGE=0.36, r=0.38) and (KGE=0.59, r=0.63) and validation period (KGE=0.4, r=0.41) and (KGE=0.56, r=0.58) respectively.

Cor.TAMSAT showed a better result compared to other SRPs because it has a better correlation with the gauged observed rainfall data; this result was expected previously,

However, in few cases, the KGE in validation mode slightly outperforms the one in calibration mode; a possible explanation is that the optimization algorithm may have converged to a local optimum; this scenario was previously seen in different studies including (A. Y. JILLO ET AL., 2017).

4.5 Comparison of gauged observed and the bias-adjusted satellite rainfall products

4.5.1 Daily time scale

A plot of daily simulated to observed streamflow indicated a satisfactory agreement with KGE= 0.39 for the calibration period (Table 4-8) and with KGE=0.54 for the validation period for adjusted TAMSAT satellite rainfall estimates. Using the same time window size the calibration and validation of the observed streamflow with adjusted RFE based simulated flow revealed KGE=0.36 for the calibration period and KGE=0.4 for the validation period. For adjusted PERSSAIN-CCS based showed KGE=0.21 for the calibration period and KGE=0.45 for the validation period finally, the calibration and validation of the observed streamflow with adjusted CHRIPS based on simulated to observed flow showed that KGE=0.12 for the calibration period and KGE=0.32 for the validation period. While the gauged observed based was scored KGE=0.42 for the calibration period and KGE=0.54 for the validation period Hence from the result showed that **—Good**' for Cor.TAMSAT, and Cor.RFE **—satisfactory** for PERSSIAN-CCS and Cor.CHIRPS satellite rainfall estimates. Therefore, from this analysis, it can be concluded that the HBV-light model shows a good performance in streamflow simulation when adjusted satellite rainfall data were used as model input (specifically cor.TAMSAT) in the study area.

By considering their validation objective function value (KGE) the different rainfall dataset was ranked at daily scale for better understanding and tabulated by table 4-9 below

Table 4-9 Rank of different rainfall products based on their KGE result for flow simulation at the daily scale

product type	Rank
CHRIPS	4
PERSSIAN-CCS	3
TAMSAT	1
RFE	2

4.5.2 Monthly time scale

A plot of monthly simulated to observed streamflow indicated an excellent agreement with KGE= 0.6 for the calibration period (Table 4-6) and with KGE=0.72 for the validation period for adjusted TAMSAT satellite rainfall estimates Using the same time window size the calibration and validation of the observed streamflow with adjusted RFE based simulated flow revealed KGE=0.59 for the calibration period and KGE=0.56 for the validation period. For adjusted PERSSAIN-CCS based showed KGE=0.36 for the calibration period and KGE=0.64 for the validation period finally, the calibration and validation of the observed streamflow with adjusted CHRIPS based on simulated to observed flow showed that KGE=0.16 for the calibration period and KGE=0.52 for the validation period. While the gauged observed based was scored KGE=0.61 for the calibration period and KGE=0.71 for the validation period Hence from the result showed that **—Good**' for Cor.TAMSAT, and Cor.RFE **—satisfactory** for Cor.PERSSIAN-CCS and Cor.CHIRPS satellite rainfall estimates. Therefore, from this analysis, it can be concluded that the HBV-light model shows a good performance in streamflow simulation when adjusted satellite rainfall data were used as model input (specifically cor.TAMSAT) in the study area.

By considering their validation objective function value (KGE) the different rainfall dataset was ranked at monthly scale for better understanding and tabulated by table 4-10 below.

Table 4-10 Rank of different rainfall products based on their KGE result for flow simulation at a monthly scale

product type	Rank
CHRIPS	4
PERSSIAN-CCS	3
TAMSAT	1
RFE	2

From above all the results showed that when satellite rainfall products are aimed to validate for flow simulation there should be a bias adjustment to get a better result. so that the initial objective can be achieved easily, for this study area the performance of SRPs for flow simulation obtained an appreciable result, finally this study reveals that besides the Insitu rainfall data the bias-adjusted TAMSAT and RFE dataset can be used as an alternative dataset for hydrological modeling for the study area.

5. CONCLUSIONS AND RECOMMENDATIONS

5.1 Conclusions

The accuracy of satellite rainfall products over Omo- Gibe Basin using a statistical approach showed that all the daily satellite product data and the gauged observed data are weakly related and it was clearly seen that the time step has great importance to get a better correlation between the satellite rainfall data set and the gauged observed rainfall data.

Depending on the performance of the satellite products for different rain intensities at the daily scale; all of the satellite products indicated similar contribution as gauged observed data, This leads to the conclusion that all the satellite products, except RFE, were capable of detecting high-intensity rainfall events over 100 mm day^{-1} and determining the rainfall amount of those events.

The calibrations and validation of the HBV-light model using gauged observed rainfall data as well as satellite rainfall data gives a conclusion that when the SRPs were used for the flow simulation without adjustment the result was unsatisfactory. While the bias-adjusted satellite rainfall products gives satisfactory result. Because it has a better correlation with the gauged observed rainfall data adjusted TAMSAT showed a better result compared to other SRPs.

Finally, underestimation of the streamflow simulated by satellite rainfall estimates and the reduction of model performance statistics were due to the underestimation of the input satellite rainfall estimates and the contamination of satellite rainfall estimates with random and systematic errors. Thus this study tried to see the effect of bias correction of satellite rainfall estimates in order to improve their applicability for hydrological modeling. Bias corrected satellite rainfall estimates based simulations had significantly improved the model performance. This put in the picture that besides the gauged observed rainfall data the bias-adjusted TAMSAT and RFE dataset especially the TAMSAT can be used as alternative datasets for hydrological modeling for the study area.

5.2 Recommendations

Based on the final finding and assessments of this study the following points could be taken as recommendations and suggestions for future studies.

As previous works and studies, this study also recommends that to work with a comparison between the satellite rainfall products and Insitu rainfall: anyone should consider the application of a bias adjustment for the satellite rainfall products unless the result obtained from uncorrected satellite rainfall product will be unsatisfactory.

The selection of Statical indicators for the comparison has a positive impact on the final interpretation of the result so the continuous statics for estimation of rainfall amount and categorical statics for rain detection should be considered for the comparison aspect.

Analyzing and evaluating the performance of the satellite products for different rain intensities at the different time scale gives an insight for the SRPs in which rainfall intensity range give a perfect much with the Insitu rainfall data and the rainfall variation aspect for the given station on the intensity basis.

The main focus of this study was on comparing HBV-light model performances using satellite and in situ based rainfall products as an input to simulate streamflow hydrograph. As reported in the result section, their performance has been increased after bias correction; satellite rainfall estimates based on simulation do perform well like in situ based simulation. This further gives the insight to require more effort for assessing the importance of SRPs especially on high-resolution SRPs either for alternative usage for the gauged observed rainfall data or validation for hydrological modeling.
More studies using different hydrological models on different catchments need to be carried out in order to provide more general conclusions about the impact of choice of hydrological model on the evaluation and effectiveness of the SRPs and the final result and also simulation period also had a great importance on effectiveness of model efficiency and in future studies can be done with wide simulation period unless there is no data limitation.

As this study observed further attention should be given to the stations for better monitoring and effective usage. the active measure of the rainfall stations really gives reliable and on-time data’s and this study also recommend According to World Meteorological Organization (WMO) standard of one station for 100 to 250 km2 in area for mountainous regions (WMO, 1994) is if applied, and then the number of rainfall stations should become 8 to 19 for Wabe watershed. But now the existing number

of in and around is nearly 7 for the basin (1826.km2). Depending on the rainfall type and topography of the surrounding area, and the streamflow it is better to be added for a good representation of the rainfall pattern. Streamflow stations are highly required for water resources management and this needs well control points of inflow and outflow.

Finally, the study area is highly capable of small up to medium scale irrigation and hydropower projects so immediate collaboration amongst different sectors is required to utilize the available water resource wisely.

REFERENCE

Endalkachew Abebe & Asfaw Kebede. (2019). A Comparison of Hydrological Models Under Climate Change onthe Water Resources of Megech River Catchment, Abbay Basin,Ethiopia. *Journal of Natural Sciences Research* , 23.

A. Y. JILLO ET AL. (2017). Characterization of regional variability of seasonal water balance within Omo- Ghibe River Basin, Ethiopia. *Hydrological Sciences Journal* , 1203-1204.

Abebe Temesgen ayalew, . (2019). Rainfall - Runoff Modeling: A Comparative Analyses: Semi Distributed HBV Light and SWAT Models in Geba Catchment, Upper Tekeze Basin, Ethiopia. *American Journal of Science, Engineering and Technology* , 35-36.

Amr Elgamala, ∗. P. (2016). Impact analysis of satellite rainfall products on flow simulations in the Magdalena River Basin, Colombia. *Journal of Hydrology: Regional studies* .

B. Berhanu et al., Y. S. (2016). Bias correction and characterization of climate forecast system re-analysis daily precipitation in Ethiopia using fuzzy overlay. *Meteorol. Appl. 23:* , 230–243.

Bajwa, H., & Tim. (2002). Toward immersive virtual environments for GIS-basedfloodplain modeling and visualization,. *In: Proceedings of 22nd ESRI User Conference,*. SanDiego, TX, USA.

Bakary Faty, A. A. (2018). assesment of satellite rainfall products for stream flow simulation in Gambia watershed. *african journal of Environmental Science and Technology, Academic Journals* , 501-513.

Bergström, S. (1976.). Development and application of a conceptual runoff model for Scandinavian catchments. . *SMHI RHO 7. Norrköping. 134* , 134.

Beven, K. (2000). Changing ideas in hydrology—the case of physically-based models. . *Journal of hydrology 105:* , 157–172.

bitew et al, b. (2012). Evaluation of High-Resolution Satellite Rainfall Products through StreamflowSimulation in a Hydrological Modeling of a Small Mountainous watershed in Ethiopia. *JOURNAL OF HYDROMETEOROLOGY , 13*, 338.

Bitew G. Tassew, M. A. (2019). Application of HEC-HMS Model for Flow Simulationin the Lake Tana Basin: The Case of Gilgel AbayCatchment, Upper Blue Nile Basin, Ethiopia. *hydrology* .

Bushandi. (1982). Some methods for testing the homogeneity of rainfall records. *journal of hydrology* , 11 – 27.

Collischonn. (2008). hydrological modeling in the Amazon basin using TRMM rainfall estimates. *Journal of Hydrology* , 207-216.

Cunderlik, J. & Simonovia, S. P. (2007). Hydrological Models for Inverse climate change Impact Modelling. . *The 18th Canadian Hydro technical Conference on Challenge for Water Resources Engineering in a World.* Winnipeg, Manitoba,.

dinku. (2010).

Endalkachew Abebe & Asfaw Kebede . (2019). A Comparison of Hydrological Models Under Climate Change onthe Water Resources of Megech River Catchment, Abbay Basin, ethiopia. *Journal of Natural Sciences Research* .

F.Gao et al, Q. C. (2018). Comparison of two long-term and high-resolution satellite precipitation datasets in Xinjiang, China. *Atmospheric Research* , 150–157.

Feng Gaoa, Y. Z. (2018). Comparison of two long-term and high-resolution satellite precipitation datasets in Xinjiang, China . *atmospheric research* .

Franklin, J. B. (2016). Validating CHIRPS-based satellite precipitation estimates in Northeast Brazil,. *Journal of Arid Environments, Vol-139 (26.), Brazil* .

Gayathri K. Devi et al. (2015). A Review on Hydrological Models. *INTERNATIONAL CONFERENCE ON WATER RESOURCES, COASTAL AND OCEAN ENGINEERING (ICWRCOE 2015)* .

Gebre, S. L. (2015). Application of the HEC-HMS Model for Runoff Simulation of Upper Blue NileRiver Basin. *hydrology current reserch* .

Gebregiorgis, A., & Hossain, F. (2013). Understanding the dependence of satellite rainfall uncertainty on topography and climate for hydrologic model simulation. *Geosciences and Remote Sensing, IEEE Transactions on* , 51(1): pp704-718.

Gebremichael, T., & Romilly, G. (2010). Evaluation of satellite rainfall estimates over Ethiopian river basins. *Hydrol. Earth Syst. Sci* .

Gebresenbet, T. S. (2015). *Modeling of Cascade Dams and Reservoirs Operation for Optimal Water Use:*.

Getachew T., T. T. (2017). Validation of new satellite rainfall products over the Upper Blue Nile Basin, Ethiopia.

Gottschalk, Rodel, M., Hoser, P., & Meng.j. (2005). Analysis of multiple precipitation products and preliminary assessment of their impact on Global Land Data Assimilation System land surface states. *Journal of Hydrometeorology* , 6(5),573-598.

Grillakis, M. G., I. K. Tsanis, & Koutroulis, A. G. (2010). *Application of the HBV hydrological model in a flash flood case in Slovenia.* Natural hazaed and earth system science.

Grimes, D., Pardo-Igúzquiza, E., & Bonifacio, R. (1999). "Optimal Areal Rainfall Estimation Using Raingauges and Satellite Data. " *Journal of Hydrology* . , 222 (1–4): 93–108.

Gu H.et al. (2010). Hydrological assessment of TRMM rainfall data over Yangtze River Basin. *Water Science and Engineering,* , 3(4): pp.418.

Gupta, , et al.,. (2009). Decomposition of the mean squared error and NSE performance criteria: implications for improving hydrological modeling. JDecomposition of the mean squared error and NSE performance criteria: implications for improving hydrological modeling. Journal of Hyd. *Journal of Hydrology,* , 377 (1–2), 80–91.

Heidler, L. M. (2015). *thesiss :Evaluation of Different HydrologicalModels in Data Scarce Regions on the Island of Ceram, Indonesia.* technische universitat munchen Faculty of Civil, Geo and Environmental Engineering Hydrology and River Basin Managemen.

Hughes, D. (2006). Comparison of satellite rainfall data with observations from gauging station networks. . *J. Hydrol. 327, 399–410* .

Hylke E. Beck1, N. V. (2017). Global-scale evaluation of 22 precipitation datasets using gaugeobservations and hydrological modeling. *hydrology and earth system seience* .

IHMS. (2013). *INTEGRATED HYDROLOGICAL MODELING SYSTEM MANUAL VERSION 6.3.*

J. Seibert and M. J. P. Vis. (2012). Teaching hydrological modeling with a user-friendlycatchment-runoff-model software package. *hydrology and erath system science* .

J. Seibert1, 2., & Vis1, M. J. (2012). *Teaching hydrological modeling with a user-friendly catchment-runoff-model software package.* hydrology and earth system science .

Janowiak, J. E. (2001). A global satellite– rain gauge merged product for real-time precipitation monitoring applications. . *J. Climate* , 12, 3335–3342.

Laurent, H. J. (1998). Validation of satellite and ground based estimates of precipitation over the Sahel. . *Atmospheric Research, 47-48,* , 651-670.

Lenhart, T. E. (2002). Comparison of two different approaches of sensitivity analysis, Phys. Chem.

LIUJunzhiet.al. (2012). Evaluation of TRMM 3B42 Precipitation Product using Rain Gauge Data in Meichuan Watershed, Poyang Lake Basin, China. *Journal of Resources and Ecology* , (4) 359-366.

M. G. Grillakis, I. K. (2010.). Application of the HBV hydrological model in a flash flood case in Slovenia. NaturalHazards . *Earth System Sciences 10,* , 2713–2725.

M. M. Bitew and Gebremichael, M. M. (2011). Assessment of satellite rainfall products for streamflow simulation in medium watersheds of the Ethiopian highlands. *hydrology and erth system science* .

M.dembele, m., & S.J.Zwart. (2016). Evaluation and comparison of satellite-based rainfall products in Burkina Faso, West Africa. *journal of remote sensing* , 17.

Mauricio Zambrano-Bigiarini1, 2. A. (2017). Temporal and spatial evaluation of satellite-based rainfall estimates across the complex topographical and climatic gradients of Chile.

Mesfin Sahle, O. S. (2018). Future land use management effects on ecosystem services under differentscenarios in the Wabe River catchment of Gurage Mountain chain landscape,Ethiopia . *Elsevier* .

Nguyen P., A. S. (2015). A high resolution coupled hydrologic–hydraulic model (HiResFlood-UCI) for flash flood modeling. *Journal of Hydrology,* .

Odai et al, O. (2018). Evaluation of Satellite Rainfall Estimates in the Pra.

Odai1, C. O. (2018). Evaluation of Satellite Rainfall Estimates in the Pra basin of ghana. *springer* .

Oloche, J. (2010). Application of HEC-HMS for flood forecasting in Misai and Wan'an catchments in china. *Water science and Engineering* , 3(1):14-22.

perera, B. J. (2017). *ungaged catchment hydrology the case of lake tana basin.* enschede ,netherlands : international institues for geo-information science and earth observatin .

PÖYRY. (2018). *PÖYRY water resource.* Retrieved 7 11, 2018, from poyry: http://www.poyry.at

Raes, D. W. (2006). RAINBOW A software package for analyzing data and testing the homogeneity of historical data sets. *Proceedings of the 4t hInternational Workshop on 'Sustainable management of marginal dry lands'. Islamabad,Pakistan,* , 27-31 (In press).

Rientjes, T. H. (2011). Satellite based cloud detection and rainfall estimation in the upper Blue Nile basin. In.Nile river basin:. *Hydrology,climate and water use: e-book/editor A.M. Melese-dordreebt: Springer, 2* .

Rodrigo, V.-P. E.-C. (2016). Bias correction of daily satellite-based rainfall estimates for hydrologic forecasting in the Upper Zambezi, Africa. *Hydrol. Earth Syst. Sci* .

S_R_Kalsi. (2018). SATELLITE BASED WEATHER FORECASTING. *https://www.researchgate.net/scientific-contributions/80129464_S_R_Kalsi* , abstract.

Sandra Pombo, *. R. (2014). Validation of remote-sensing precipitation products for Angola.

SCHARFFENBERG W., F. M. (2016.). Hydrologic modelingsystem HEC-HMS v4.2: Users manual. *Davis, CA.USACE, Hydrologic Engineering Center* , 614.

Seibert, J. (2005). *HBV light version 2 User's Manual.*

Shrestha, M. S. (2011). *Bias-Adjustment of Satellite-Based Rainfall Estimates over the Central Himalayas of Nepal for Flood Prediction.* Kyoto University, Japan: Department of Civil and Earth Resources Engineering.

Su F., H. Y., & Lettenmaier, D. P. (2008). Evaluation of TRMM Multi-satellite Precipitation Analysis (TMPA) and its utility in hydrologic prediction in the La Plata basin. *J. Hydrometeor* , 9,622–640.

Subramanya. (1998). Engineering Hydrology, second edition. *Tata McGraw-Hill New Delhi, 110002, ISBN 0-07-462449-8.*

T. Cohen Liechti1, J. P.-L. (2012). Comparison and evaluation of satellite derived precipitation products for hydrological modeling of the Zambezi River Basin. *Copernicus Publications on behalf of the European Geosciences Union.*

T. Dinku et al. (2007). Validation of satellite rainfall products over East Africa's complex topography. *J. Remote Sens.* , , 28, 1503–1526.

Tesfay G., Y. A.-v. (2019). Evaluation of multiple satellite rainfall products over the rugged topography of Tekeze-Atbara Basin in Ethiopia. *International Journal of Remote Sensing* .

Toté et al, *. D. (2015). Evaluation of Satellite Rainfall Estimates for Drought and Flood Monitoring in Mozambique.

U.SACE. (2001). HEC-HMS Hydrologic Modeling System,User's Manual for Version 2.11. Report CPD-74A,. *Hydrologic Engineering Center:Davis, CA.US Army Corps of Engineer* .

USACE. (2016). *Hydrologic modeling system: user'smanual. U.S. Army Corps of engineers, Davis, CA.* Hydrologic Engineering Center.

Vera Thiemig, R. R.-B. (2013). Hydrological evaluation of satellite-based rainfall estimates over the Volta and Baro-Akobo Basin. *journal of hydrology* .

Vu Thi Thom1, D. N. (2018). Using gridded rainfall products in simulating streamflow in a tropical catchment – A case study of the Srepok River Catchment, Vietnam .

Ward, & Robinson. (2000). *Principles of hydrology (4th ed).* ,. London, Burr Ridge.

Wijngaard, J. K. (2003). Homogeneity of 20th century European daily temperature and precipitation series. *International Journal of Climatology,* , 23(6): pp.679-692.

Worqlul A. W., M. B. (2014). Comparison of rainfall estimations by TRMM 3B42, MPEG and CFSR with ground-observed. *Hydrol. Earth Syst. Sci* , 18, 4871-4881.

Yang, D. H. (2000.). comparison of different distributed hydrological models for characterisation of catchment spatialvariability. *Journal of Hydrological Procedia 14(3),* , 403-416.

Yared B., T. T. (2017). Evaluation of Satellite-Based Rainfall Estimates and Application to Monitor Meteorological Drought fo the Upper Blue Nile Basin, . *Ethiopia. National Drought Mitigation Center, University of Nebrask* .

Yves Tramblay, V. T. (2016). Evaluation of satellite-based rainfall products for hydrological modelling in Morocco. *Hydrological Sciences Journal* .

APPENDIX

I, Statical analysis for different Rainfall products

A, Pearson correlation for daily time series data

pearson correlation for daily time series data														
	woliso					jimma						gunchre		
	observed	chrips	perssian	tamsat		observed	chrips	perssian	tamsat		observed	chrips	perssian	tamsat
chrips	0.008				chrips	-0.005				chrips	0.009			
perssian	0.025	0.125			perssian	0.049	0.077			perssian	0.069	0.099		
tamsat	0.013	0.187	0.564		tamsat	0.041	0.16	0.574		tamsat	0.08	0.168	0.581	
rfe	0.024	0.108	0.385	0.485	rfe	0.051	0.092	0.389	0.484	rfe	0.058	0.095	0.468	0.587
	gercha						indibr					dimeka		
	observed	chrips	perssian	tamsat		observed	chrips	perssian	tamsat		observed	chrips	perssian	tamsat
chrips	-0.002				chrips	-0.002				chrips	0.065			
perssian	0.018	0.078			perssian	-0.009	0.091			perssian	0.058	0.571		
tamsat	0.028	0.114	0.544		tamsat	0.027	0.141	0.57		tamsat	0.036	0.504	0.467	
rfe	0.041	0.03	0.401	0.469	rfe	0.008	0.076	0.323	0.421	rfe	0.05	0.4	0.446	0.395
	serbo						hosana					bako		
	observed	chrips	perssian	tamsat		observed	chrips	perssian	tamsat		observed	chrips	perssian	tamsat
chrips	-0.017				chrips	-0.004				chrips	0.011			
perssian	0.008	0.097			perssian	0.045	0.028			perssian	0.023	0.143		
tamsat	-0.001	0.168	0.581		tamsat	0.032	0.108	0.544		tamsat	0.026	0.26	0.582	
rfe	0.006	0.086	0.435	0.515	rfe	0.028	0.055	0.39	0.458	rfe	0.019	0.141	0.435	0.559
	limu-genet						hana					areka		
	observed	chrips	perssian	tamsat		observed	chrips	perssian	tamsat		observed	chrips	perssian	tamsat
chrips	0.002				chrips	0.064				chrips	0.023			
perssian	0.043	0.137			perssian	-0.016	0.013			perssian	0.014	0.05		
tamsat	0.028	0.19	0.586		tamsat	-0.002	0.02	0.461		tamsat	0.007	0.093	0.575	
rfe	0.039	0.095	0.435	0.509	rfe	-0.016	-0.039	0.371	0.3	rfe	0.031	0.018	0.344	0.409
	jinka						gubre					agena		
	observed	chrips	perssian	tamsat		observed	chrips	perssian	tamsat		observed	chrips	perssian	tamsat
chrips	0.019				chrips	0.006				chrips	0.019			
perssian	0.009	-0.011			perssian	0.05	0.137			perssian	0.017	0.074		
tamsat	0.028	0.035	0.464		tamsat	0.035	0.17	0.577		tamsat	0.047	0.137	0.564	
rfe	0.01	-0.032	0.352	0.369	rfe	0.025	0.085	0.378	0.486	rfe	0.028	0.088	0.384	0.506

B, Mean daily statics of different rainfall products for the stations

Agena

Variable	N	N*	Mean	SE Mean	StDev	CoefVar	Minimum	Q1	Median	Q3	Maximum	IQR
agena Obs	366	0	3.833	0.141	2.7	70.44	0	1.743	3.241	5.339	19.243	3.596
chrips	366	0	3.419	0.207	3.954	115.63	0	0.051	2.137	5.314	22.153	5.263
corr.chrips	366	0	3.815	0.343	6.563	172.04	0	0.413	2.992	5.016	105.305	4.603
perssian	366	0	1.817	0.118	2.25	123.85	0	0	1	2.679	13	2.679
corre.perss	366	0	3.799	0.449	8.592	226.17	0	0	2.096	5.162	144.314	5.162
tamsat	366	0	3.681	0.193	3.686	100.12	0	0	2.813	6.18	17.42	6.18
corr.tamsa	366	0	3.796	0.243	4.643	122.3	0	0	3.407	5.206	48.748	5.206
rfe	366	0	2.804	0.133	2.547	90.84	0	0.608	2.316	4.33	14.404	3.723
corr.rfe	366	0	3.842	0.196	3.756	97.77	0	1.457	3.357	5.107	32.818	3.651

Areka

Variable	N	N*	Mean	SE Mean	StDev	CoefVar	Minimum	Q1	Median	Q3	Maximum	IQR
areka Obs	366	0	4.03	0.124	2.37	58.8	0	2.22	3.765	5.414	13.17	3.194
chrips	366	0	3.435	0.141	2.694	78.45	0	1.116	2.789	5.441	12.552	4.326
corr.chrips	366	0	4.011	0.129	2.461	61.37	0	2.114	3.752	5.576	13.16	3.462
perssian	366	0	3.277	0.148	2.825	86.23	0	1.2	2.523	4.6	16.111	3.4
corre.perss	366	0	4.029	0.166	3.171	78.7	0	1.653	3.477	5.739	24.719	4.087
tamsat	366	0	4.126	0.134	2.567	62.23	0	2.045	3.834	5.874	13.85	3.829
corr.tamsa	366	0	4.022	0.112	2.134	53.06	0	2.361	3.842	5.417	11.909	3.056
rfe	366	0	3.295	0.134	2.569	77.97	0	1.495	2.755	4.594	19.431	3.099
corr.rfe	366	0	4.023	0.148	2.84	70.6	0	1.929	3.527	5.422	18.317	3.493

Asendabo

Variable	N	N*	Mean	SE Mean	StDev	CoefVar	Minimum	Q1	Median	Q3	Maximum	IQR
asendabo (	366	0	3.307	0.113	2.164	65.44	0.16	1.73	2.84	4.487	12.67	2.757
chrips	366	0	3.688	0.202	3.873	105.03	0	0.194	2.79	5.926	23.71	5.733
corr.chrips	366	0	3.305	0.164	3.138	94.94	0	1.535	2.855	4.369	30.478	2.834
perssian	366	0	2.553	0.126	2.41	94.4	0	0.462	2.038	4.183	15.167	3.721
corre.perss	366	0	3.292	0.168	3.215	97.65	0	1.28	2.673	4.226	25.425	2.946
tamsat	366	0	3.995	0.179	3.42	85.61	0	1.096	3.5	6.306	14.873	5.21
corr.tamsa	366	0	3.307	0.159	3.036	91.81	0	1.68	3.02	4.225	24.908	2.545
rfe	366	0	3.136	0.119	2.269	72.35	0	1.386	2.802	4.606	14.703	3.22
corr.rfe	366	0	3.3	0.121	2.309	69.99	0	1.81	3.15	4.257	14.642	2.447

Bako

Variable	N	N*	Mean	SE Mean	StDev	CoefVar	Minimum	Q1	Median	Q3	Maximum	IQR
bako Obs	366	0	3.795	0.111	2.125	56	0	2.18	3.439	5.164	12	2.984
chrips	366	0	3.088	0.18	3.446	111.59	0	0.022	2.115	5.134	15.866	5.112
corr.chrips	366	0	3.781	0.305	5.829	154.17	0	0.729	3.02	4.566	61.523	3.836
perssian	366	0	2.886	0.15	2.875	99.6	0	0.182	2.127	4.621	11.846	4.439
corre.perss	366	0	3.815	0.33	6.322	165.7	0	1.038	2.784	4.615	96.726	3.577
tamsat	366	0	4.034	0.206	3.946	97.81	0	0.119	2.858	6.944	15.785	6.825
corr.tamsa	366	0	3.881	0.629	12.032	309.97	0	0.303	3.1	4.267	223.47	3.964
rfe	366	0	3.474	0.162	3.108	89.45	0	0.731	2.671	5.713	16.114	4.982
corr.rfe	366	0	3.815	0.19	3.641	95.44	0	1.966	3.293	4.48	37.459	2.514

Dimeka

Variable	N	N*	Mean	SE Mean	StDev	CoefVar	Minimum	Q1	Median	Q3	Maximum	IQR
dimeka Ob	366	0	2.43	0.104	1.982	81.56	0	0.829	2.148	3.531	11.75	2.702
chrips	366	0	2.621	0.138	2.648	101	0	0.571	1.787	3.844	13.617	3.273
corr.chrips	366	0	2.444	0.123	2.355	96.33	0	0.69	1.861	3.415	12.583	2.726
perssian	366	0	1.863	0.114	2.19	117.54	0	0.223	1	2.712	11	2.488
corre.pers	366	0	2.438	0.14	2.676	109.76	0	0.515	1.744	3.23	19.002	2.715
tamsat	366	0	2.934	0.12	2.301	78.42	0	1.115	2.576	4.291	11.569	3.176
corr.tamsa	366	0	2.4414	0.0924	1.7685	72.44	0	1.1491	2.3296	3.1728	11.2142	2.0237
rfe	366	0	2.034	0.123	2.356	115.86	0	0.454	1.237	2.68	19.291	2.226
corr.rfe	366	0	2.444	0.116	2.211	90.46	0	0.884	1.922	3.464	19.065	2.58

Gunchre

Variable	N	N*	Mean	SE Mean	StDev	CoefVar	Minimum	Q1	Median	Q3	Maximum	IQR
gunchre Ol	366	0	3.424	0.17	3.26	95.19	0	0.938	2.558	5	15.975	4.062
chrips	366	0	3.29	0.227	4.349	132.17	0	0	1.569	5.424	27.468	5.424
corr.chrips	366	0	3.383	0.304	5.822	172.12	0	0	1.932	5.103	71.896	5.103
perssian	366	0	2.287	0.165	3.155	137.97	0	0	0.8	3.617	18.25	3.617
corre.pers	366	0	3.555	0.363	6.945	195.38	0	0	1.217	4.846	93.179	4.846
tamsat	366	0	3.434	0.203	3.876	112.87	0	0	2.367	5.434	22.46	5.434
corr.tamsa	366	0	3.343	0.261	4.987	149.15	0	0	2.402	4.872	67.349	4.872
rfe	366	0	2.955	0.177	3.389	114.69	0	0.363	2.071	4.521	22.883	4.158
corr.rfe	366	0	3.52	0.21	4.024	114.3	0	0.711	2.605	4.916	37.982	4.205

Gubre

Variable	N	N*	Mean	SE Mean	StDev	CoefVar	Minimum	Q1	Median	Q3	Maximum	IQR
gubre Obs	366	0	3.994	0.127	2.437	61.01	0	2.182	3.5	5.771	12.283	3.589
chrips	366	0	3.292	0.186	3.567	108.34	0	0.105	2.453	5.505	25.141	5.4
corr.chrips	366	0	4.042	0.232	4.443	109.91	0	1.449	3.5	5.572	49.617	4.123
perssian	366	0	2.604	0.133	2.549	97.89	0	0.25	2	4.333	11.2	4.083
corre.pers	366	0	4.04	0.321	6.137	151.92	0	1.161	3.173	5.089	94.594	3.928
tamsat	366	0	3.675	0.184	3.52	95.79	0	0.349	2.821	6.295	15.055	5.946
corr.tamsa	366	0	4.026	0.212	4.062	100.88	0	1.037	3.66	5.477	28.453	4.44
rfe	366	0	3.211	0.143	2.743	85.4	0	0.821	2.877	4.721	19.801	3.9
corr.rfe	365	1	4.024	0.171	3.262	81.07	0	1.812	3.548	5.335	27.122	3.522

Hana

Variable	N	N*	Mean	StDev	CoefVar	Minimum	Q1	Median	Q3	Maximum	IQR
hana Obs	366	0	3.556	4.299	120.87	0	0	2.313	5.643	28.76	5.643
chrips	366	0	5.297	5.164	97.48	0	0.922	3.902	8.464	26.623	7.542
corr.chrips	366	0	3.546	3.223	90.89	0	1.237	2.626	4.993	15.778	3.756
perssian	366	0	3.02	4.237	140.29	0	0.167	1.5	4.35	38	4.183
corre.pers	366	0	3.545	4.787	135.05	0	0.171	1.861	5.117	36.22	4.946
tamsat	366	0	4.465	4.451	99.67	0	0.3	3.465	6.95	32.35	6.65
corr.tamsa	366	0	3.494	4.018	115.03	0	0.337	2.333	5.163	29.182	4.825
rfe	366	0	2.99	3.687	123.32	0	0.536	1.818	3.949	28.767	3.413
corr.rfe	366	0	3.53	4.161	117.88	0	0.703	1.961	4.751	27.662	4.048

Hosana

Variable	N	N*	Mean	StDev	CoefVar	Minimum	Q1	Median	Q3	Maximum	IQR
hosana Ob	366	0	3.191	2.284	71.57	0	1.509	2.655	4.428	13.889	2.918
chrips	366	0	3.474	3.506	100.91	0	0.258	2.731	5.972	22.485	5.714
corr.chrips	366	0	3.195	3.417	106.96	0	1.267	2.732	4.415	35.444	3.148
perssian	366	0	2.204	2.383	108.11	0	0.286	1.4	3.344	12.625	3.058
corre.perss	366	0	3.153	3.491	110.71	0	0.711	2.178	4.877	29.383	4.166
tamsat	366	0	3.472	2.972	85.61	0	0.808	3.149	5.478	18.887	4.671
corr.tamsa	366	0	3.203	2.93	91.49	0	1.327	2.772	4.458	27.54	3.131
rfe	366	0	2.639	2.282	86.44	0	0.793	2.228	3.873	12.693	3.081
corr.rfe	366	0	3.189	3.036	95.19	0	1.197	2.723	4.282	31.37	3.085

Indibr

Variable	N	N*	Mean	StDev	CoefVar	Minimum	Q1	Median	Q3	Maximum	IQR
indibr Obs	366	0	3.661	3.091	84.44	0	1.671	3.006	4.817	32.414	3.146
chrips	366	0	3.355	3.965	118.17	0	0.016	1.975	5.53	24.815	5.513
corr.chrips	366	0	3.767	5.235	138.98	0	0.304	2.992	5.039	48.512	4.735
perssian	366	0	2.22	2.808	126.53	0	0.125	1.225	3.518	22.75	3.393
corre.perss	366	0	3.761	5.419	144.08	0	0.526	2.391	4.984	51.691	4.458
tamsat	366	0	3.769	3.796	100.72	0	0	2.808	6.323	17.067	6.323
corr.tamsa	366	0	3.762	4.643	123.42	0	0	3.245	5.04	41.982	5.04
rfe	366	0	3.148	3.155	100.22	0	0.615	2.488	4.777	21	4.162
corr.rfe	366	0	3.765	4.905	130.28	0	1.231	2.833	4.822	52.969	3.591

Jimma

Variable	N	N*	Mean	StDev	CoefVar	Minimum	Q1	Median	Q3	Maximum	IQR
jimma Obs	366	0	4.423	2.166	48.97	0.323	2.785	4.122	5.648	13.331	2.864
chrips	366	0	3.773	3.742	99.18	0	0.263	3.122	6.305	23.856	6.042
corr.chrips	366	0	4.413	3.821	86.59	0	2.409	4.036	5.745	40.247	3.336
perssian	366	0	3.162	2.464	77.93	0	0.931	2.862	4.867	11.733	3.936
corre.perss	366	0	4.422	3.297	74.54	0	2.132	4.163	5.829	23.747	3.697
tamsat	366	0	4.806	3.612	75.16	0	1.51	4.49	7.557	16.123	6.047
corr.tamsa	366	0	4.419	2.894	65.49	0	2.847	4.256	5.737	20.213	2.889
rfe	366	0	3.763	2.616	69.52	0	1.402	3.7	5.597	10.998	4.196
corr.rfe	365	1	4.409	2.755	62.49	0	2.418	4.137	6.034	18.284	3.616

Jinka

Variable	N	N*	Mean	StDev	CoefVar	Minimum	Q1	Median	Q3	Maximum	IQR
jinka Obs	366	0	3.67	2.123	57.83	0.18	1.972	3.34	5.188	11.033	3.217
chrips	366	0	6.78	5.317	78.43	0	1.908	6.146	10.363	23.27	8.455
corr.chrips	366	0	3.6722	1.8584	50.61	0	2.4596	3.6132	4.6592	11.107	2.1996
perssian	366	0	2.101	2.209	105.16	0	0.467	1.4	3.15	16.933	2.683
corre.perss	366	0	3.678	3.216	87.44	0	1.392	2.876	5.123	16.389	3.731
tamsat	366	0	4.098	2.843	69.39	0	1.843	3.707	5.788	13.04	3.944
corr.tamsa	366	0	3.673	2.295	62.48	0	2.225	3.464	4.841	16.095	2.617
rfe	366	0	2.518	2.233	88.66	0	0.984	1.791	3.345	14.533	2.361
corr.rfe	366	0	3.683	2.615	71	0	1.761	3.171	4.803	17.835	3.042

Limugenet

Variable	N	N*	Mean	StDev	CoefVar	Minimum	Q1	Median	Q3	Maximum	IQR
limu genet	366	0	5.939	3.877	65.28	0.144	3.329	5.214	7.711	31.425	4.381
chrips	366	0	3.239	3.465	106.98	0	0.133	2.458	5.278	22.82	5.145
corr.chrips	366	0	5.948	5.842	98.22	0	2.394	5.276	7.506	53.798	5.112
perssian	366	0	4.004	3.613	90.23	0	0.659	3.392	6.5	15.917	5.841
corre.perss	366	0	5.959	5.56	93.3	0	2.392	5.227	8.314	47.297	5.922
tamsat	366	0	6.095	5.704	93.59	0	1.017	4.721	10.008	21.917	8.991
corr.tamsa	366	0	5.963	5.398	90.52	0	2.721	5.546	7.769	36.434	5.048
rfe	366	0	3.708	2.846	76.76	0	1.048	3.452	5.72	12.984	4.671
corr.rfe	366	0	5.945	4.697	79.01	0	2.97	5.202	7.666	35.337	4.695

Serbo

Variable	N	N*	Mean	StDev	CoefVar	Minimum	Q1	Median	Q3	Maximum	IQR
serbo Obs	366	0	3.722	2.577	69.23	0	1.762	3.317	5.313	14.367	3.551
chrips	366	0	3.715	3.987	107.32	0	0.185	2.686	6.05	22.112	5.865
corr.chrips	366	0	3.729	3.481	93.36	0	1.608	3.277	4.906	27.744	3.298
perssian	366	0	3.156	2.972	94.16	0	0.534	2.551	5	16.333	4.466
corre.perss	366	0	3.752	4.133	110.16	0	1.183	2.996	4.839	37.843	3.655
tamsat	366	0	4.484	3.769	84.04	0	1.156	3.728	7.229	19.371	6.073
corr.tamsa	366	0	3.742	3.577	95.6	0	1.949	3.306	4.756	34.075	2.807
rfe	366	0	3.419	2.547	74.49	0	1.17	3.197	5.045	12.239	3.875
corr.rfe	366	0	3.736	2.817	75.39	0	1.916	3.389	4.782	21.281	2.866

Tercha

Variable	N	N*	Mean	StDev	CoefVar	Minimum	Q1	Median	Q3	Maximum	IQR
tercha Obs	366.0	0.0	3.866	2.5	64.3	0.0	2.0	3.6	5.5	11.9	3.6
chrips	366.0	0.0	3.438	3.2	94.4	0.0	0.5	2.7	5.8	15.1	5.3
corr.chrips	366.0	0.0	3.855	3.2	84.1	0.0	1.8	3.5	5.3	32.7	3.5
perssian	366.0	0.0	3.779	3.6	94.0	0.0	1.0	3.0	5.6	17.9	4.6
corre.perss	366.0	0.0	3.859	3.3	84.7	0.0	1.5	3.3	5.5	21.0	4.0
tamsat	366.0	0.0	4.433	3.3	74.0	0.0	1.6	4.6	6.6	20.8	5.0
corr.tamsa	366.0	0.0	3.849	2.5	65.5	0.0	2.4	3.8	5.2	18.8	2.9
rfe	366.0	0.0	3.554	2.7	76.6	0.0	1.6	3.0	5.1	16.2	3.5
corr.rfe	366.0	0.0	3.839	2.4	62.6	0.0	2.2	3.6	5.2	16.8	3.0

Woliso

Variable	N	N*	Mean	StDev	CoefVar	Minimum	Q1	Median	Q3	Maximum	IQR
woliso Obs	366	0	3.2724	1.7192	52.54	0	1.9504	2.9335	4.3295	9.7077	2.3791
chrips	366	0	3.532	3.93	111.29	0	0.084	2.351	5.681	22.153	5.597
corr.chrips	366	0	3.285	4.298	130.83	0	0.912	2.962	4.342	59.794	3.43
perssian	366	0	2.501	2.61	104.39	0	0.143	1.462	4.277	10.846	4.134
corre.perss	366	0	3.287	3.961	120.51	0	0.583	2.839	4.376	47.535	3.793
tamsat	366	0	3.456	3.663	105.98	0	0.276	2.161	6.083	16.886	5.807
corr.tamsa	366	0	3.282	3.038	92.55	0	0.99	3.043	4.458	18.988	3.468
rfe	366	0	2.974	2.683	90.24	0	0.691	2.414	4.659	14.73	3.967
corr.rfe	366	0	3.279	3.078	93.88	0	1.627	2.88	4.275	41.129	2.648

Wolkite

Variable	N	Mean	StDev	Variance	Minimum	Q1	Median	Q3	Maximum	IQR
wolkite Ob	366	2.891	2.915	8.5	0	0.376	1.948	4.64	13.767	4.263
chrips	366	3.337	3.573	12.77	0	0.126	2.497	5.707	24.047	5.581
corr.chrips	366	2.892	2.86	8.177	0	0.496	2.156	4.451	18.111	3.955
perssian	366	2.69	2.682	7.195	0	0.25	2.192	4.188	12.818	3.938
corre.pers	366	2.895	2.985	8.908	0	0.304	2.104	4.588	14.768	4.284
tamsat	366	3.576	3.455	11.938	0	0.382	2.633	5.995	13.855	5.614
corr.tamsa	366	2.892	2.626	6.894	0	0.368	2.435	4.943	10.307	4.576
rfe	366	3.229	2.7	7.289	0	0.799	2.822	4.965	13.76	4.166
corr.rfe	366	2.893	2.759	7.615	0	0.559	2.198	4.437	14.32	3.877

II, Mean daily correlations of different rainfall products for the stations

Correlations

agena

	Obs	chrips	corr.chrips	perssian	corre.perssian	tamsat	corr.tamsat
chrips	0.162						
corr.chrips	0.094	0.258					
perssian	0.198	0.371	0.065				
corre.perssian	0.068	0.043	0.003	0.348			
tamsat	0.184	0.538	0.069	0.721	0.181		
corr.tamsat	0.046	0.077	-0.026	0.275	0.165	0.398	
rfe	0.152	0.453	0.072	0.596	0.135	0.713	0.260
corr.rfe	0.066	0.112	0.045	0.231	0.089	0.278	0.479

	rfe
chrips	
corr.chrips	
perssian	
corre.perssian	
tamsat	
corr.tamsat	
rfe	
corr.rfe	0.580

Correlations

areka

	Obs	chrips	corr.chrips	perssian	corre.perssian	tamsat	corr.tamsat
chrips	0.208						
corr.chrips	0.145	0.776					
perssian	0.131	0.209	0.105				
corre.perssian	0.139	0.125	0.092	0.875			
tamsat	0.197	0.374	0.164	0.614	0.512		
corr.tamsat	0.171	0.182	0.080	0.520	0.553	0.896	
rfe	0.061	0.177	0.111	0.448	0.330	0.535	0.466
corr.rfe	0.124	0.145	0.101	0.368	0.403	0.541	0.567

	rfe
chrips	
corr.chrips	
perssian	
corre.perssian	
tamsat	
corr.tamsat	
rfe	
corr.rfe	0.877

Correlations

asendabo

	Obs	chrips	corr.chrips	perssian	corre.perssian	tamsat	corr.tamsat
chrips	0.079						
corr.chrips	0.053	0.265					
perssian	0.023	0.413	-0.005				
corre.perssian	-0.027	0.033	-0.079	0.503			
tamsat	0.048	0.650	0.050	0.718	0.276		
corr.tamsat	0.046	0.071	-0.077	0.269	0.683	0.353	
rfe	0.081	0.441	0.045	0.643	0.260	0.651	0.246
corr.rfe	0.068	0.077	0.025	0.219	0.454	0.230	0.459

	rfe
chrips	
corr.chrips	
perssian	
corre.perssian	
tamsat	
corr.tamsat	
rfe	
corr.rfe	0.651

Correlations

bako

	Obs	chrips	corr.chrips	perssian	corre.perssian	tamsat	corr.tamsat
chrips	-0.050						
corr.chrips	0.002	0.098					
perssian	-0.047	0.626	0.020				
corre.perssian	0.048	0.000	0.156	0.217			
tamsat	0.006	0.804	0.020	0.781	0.059		
corr.tamsat	-0.005	-0.003	0.078	0.070	0.820	0.050	
rfe	-0.023	0.667	-0.005	0.776	0.046	0.815	0.015
corr.rfe	0.191	0.002	0.124	0.070	0.205	0.069	0.102

	rfe
chrips	
corr.chrips	
perssian	
corre.perssian	
tamsat	
corr.tamsat	
rfe	
corr.rfe	0.273

Correlations

dimeka

	Obs	chrips	corr.chrips	perssian	corre.perssian	tamsat	corr.tamsat
chrips	0.089						
corr.chrips	0.175	0.697					
perssian	0.072	0.663	0.351				
corre.perssian	0.108	0.453	0.676	0.519			
tamsat	0.082	0.602	0.332	0.543	0.317		
corr.tamsat	0.156	0.286	0.508	0.257	0.494	0.680	
rfe	0.008	0.601	0.243	0.714	0.215	0.506	0.200
corr.rfe	0.165	0.361	0.523	0.280	0.457	0.374	0.547

	rfe
chrips	
corr.chrips	
perssian	
corre.perssian	
tamsat	
corr.tamsat	
rfe	
corr.rfe	0.541

Correlations

gunchre

	Obs	chrips	corr.chrips	perssian	corre.perssian	tamsat	corr.tamsat
chrips	0.133						
corr.chrips	0.094	0.439					
perssian	0.126	0.299	0.094				
corre.perssian	0.082	0.081	-0.013	0.513			
tamsat	0.210	0.464	0.152	0.605	0.286		
corr.tamsat	0.145	0.153	0.016	0.344	0.717	0.545	
rfe	0.156	0.321	0.122	0.547	0.208	0.681	0.333
corr.rfe	0.167	0.157	0.357	0.308	0.352	0.430	0.436

	rfe
chrips	
corr.chrips	
perssian	
corre.perssian	
tamsat	
corr.tamsat	
rfe	
corr.rfe	0.603

Correlations

gubre

	Obs	chrips	corr.chrips	perssian	corre.perssian	tamsat	corr.tamsat
chrips	0.133						
corr.chrips	0.099	0.290					
perssian	0.085	0.547	0.105				
corre.perssian	0.009	0.066	0.066	0.377			
tamsat	0.076	0.645	0.096	0.782	0.174		
corr.tamsat	0.086	0.084	0.133	0.285	0.600	0.325	
rfe	0.039	0.524	0.067	0.682	0.144	0.729	0.214
corr.rfe	0.094	0.101	0.101	0.229	0.234	0.209	0.396

	rfe
chrips	
corr.chrips	
perssian	
corre.perssian	
tamsat	
corr.tamsat	
rfe	
corr.rfe	0.598

Correlations

hana

	Obs	chrips	corr.chrips	perssian	corre.perssian	tamsat	corr.tamsat
chrips	0.167						
corr.chrips	0.193	0.806					
perssian	-0.100	0.099	0.021				
corre.perssian	0.071	0.248	0.335	0.509			
tamsat	0.032	0.196	0.100	0.575	0.401		
corr.tamsat	0.160	0.204	0.236	0.228	0.547	0.701	
rfe	-0.102	-0.021	-0.012	0.460	0.207	0.331	0.132
corr.rfe	0.164	0.224	0.304	0.169	0.446	0.331	0.460

	rfe
chrips	
corr.chrips	
perssian	
corre.perssian	
tamsat	
corr.tamsat	
rfe	
corr.rfe	0.624

Correlations

hosana

	Obs	chrips	corr.chrips	perssian	corre.perssian	tamsat	corr.tamsat
chrips	0.061						
corr.chrips	0.022	0.289					
perssian	0.023	0.319	0.009				
corre.perssian	0.034	0.017	-0.060	0.570			
tamsat	0.054	0.567	0.032	0.629	0.326		
corr.tamsat	0.090	0.044	-0.062	0.301	0.647	0.490	
rfe	0.048	0.345	0.020	0.630	0.314	0.596	0.309
corr.rfe	0.078	0.027	0.000	0.270	0.374	0.274	0.396

	rfe
chrips	
corr.chrips	
perssian	
corre.perssian	
tamsat	
corr.tamsat	
rfe	
corr.rfe	0.705

Correlations

indibr

	Obs	chrips	corr.chrips	perssian	corre.perssian	tamsat
chrips	0.019					
corr.chrips	0.076	0.282				
perssian	0.104	0.322	0.096			
corre.perssian	0.118	0.034	0.213	0.521		
tamsat	0.038	0.509	0.043	0.692	0.242	
corr.tamsat	0.093	0.022	0.198	0.246	0.408	0.322
rfe	0.015	0.355	0.015	0.492	0.207	0.591
corr.rfe	-0.002	0.015	-0.028	0.138	0.203	0.139

	corr.tamsat	rfe
chrips		
corr.chrips		
perssian		
corre.perssian		
tamsat		
corr.tamsat		
rfe	0.190	
corr.rfe	0.183	0.720

Correlations

	jimma Obs	chrips	corr.chrips	perssian	corre.perssian	tamsat	corr.tamsat
chrips	0.076						
corr.chrips	0.042	0.263					
perssian	0.116	0.507	0.075				
corre.perssian	0.031	0.108	-0.000	0.543			
tamsat	0.103	0.710	0.104	0.714	0.288		
corr.tamsat	0.030	0.112	0.097	0.346	0.686	0.406	
rfe	0.108	0.543	0.069	0.678	0.260	0.724	0.276
corr.rfe	0.052	0.088	0.088	0.268	0.409	0.241	0.486

	rfe
chrips	
corr.chrips	
perssian	
corre.perssian	
tamsat	
corr.tamsat	
rfe	
corr.rfe	0.633

Correlations

	jinka Obs	chrips	corr.chrips	perssian	corre.perssian	tamsat	corr.tamsat
chrips	0.198						
corr.chrips	0.126	0.648					
perssian	-0.016	0.012	0.062				
corre.perssian	0.023	0.198	0.208	0.568			
tamsat	0.137	0.427	0.248	0.467	0.459		
corr.tamsat	0.068	0.256	0.253	0.251	0.551	0.789	
rfe	-0.048	-0.043	0.052	0.632	0.200	0.389	
corr.rfe	0.078	0.235	0.225	0.217	0.396	0.447	

	corr.tamsat	rfe
chrips		
corr.chrips		
perssian		
corre.perssian		
tamsat		
corr.tamsat		
rfe	0.237	
corr.rfe	0.504	0.622

Correlations

	limu genet Obs	chrips	corr.chrips	perssian	corre.perssian	tamsat	corr.tamsat
chrips	0.064						
corr.chrips	0.075	0.303					
perssian	0.142	0.596	0.109				
corre.perssian	0.166	0.090	0.095	0.411			
tamsat	0.147	0.709	0.137	0.757	0.224		
corr.tamsat	0.079	0.093	0.122	0.228	0.579	0.304	
rfe	0.127	0.579	0.103	0.743	0.212	0.752	0.217
corr.rfe	0.148	0.090	0.200	0.213	0.371	0.226	0.422

	rfe
chrips	
corr.chrips	
perssian	
corre.perssian	
tamsat	
corr.tamsat	
rfe	
corr.rfe	0.513

Correlations

	serbo Obs	chrips	corr.chrips	perssian	corre.perssian	tamsat	corr.tamsat
chrips	0.130						
corr.chrips	-0.015	0.311					
perssian	0.075	0.405	0.018				
corre.perssian	-0.014	0.052	-0.098	0.496			
tamsat	0.068	0.621	0.050	0.669	0.256		
corr.tamsat	-0.004	0.070	-0.047	0.295	0.730	0.358	
rfe	0.103	0.441	0.075	0.651	0.265	0.653	0.248
corr.rfe	0.064	0.083	0.096	0.258	0.440	0.220	0.428

	rfe
chrips	
corr.chrips	
perssian	
corre.perssian	
tamsat	
corr.tamsat	
rfe	
corr.rfe	0.666

Correlations

	tercha Obs	chrips	corr.chrips	perssian	corre.perssian	tamsat	corr.tamsat
chrips	0.269						
corr.chrips	0.141	0.501					
perssian	0.118	0.364	0.084				
corre.perssian	0.119	0.178	0.070	0.581			
tamsat	0.230	0.620	0.186	0.572	0.403		
corr.tamsat	0.157	0.238	0.122	0.357	0.653	0.644	
rfe	0.116	0.407	0.104	0.636	0.290	0.582	0.345
corr.rfe	0.113	0.231	0.075	0.281	0.407	0.426	0.502

	rfe
chrips	
corr.chrips	
perssian	
corre.perssian	
tamsat	
corr.tamsat	
rfe	
corr.rfe	0.725

Correlations

	wolkite Obs	chrips	corr.chrips	perssian	corre.perssian	tamsat	corr.tamsat
chrips	0.531						
corr.chrips	0.593	0.886					
perssian	0.611	0.514	0.575				
corre.perssian	0.659	0.573	0.636	0.957			
tamsat	0.770	0.632	0.719	0.770	0.837		
corr.tamsat	0.763	0.627	0.699	0.776	0.838	0.987	
rfe	0.667	0.546	0.591	0.719	0.722	0.786	0.785
corr.rfe	0.720	0.599	0.663	0.712	0.774	0.854	0.845

	rfe
chrips	
corr.chrips	
perssian	
corre.perssian	
tamsat	
corr.tamsat	
rfe	
corr.rfe	0.957

III Graphical intepretationfor mean daily

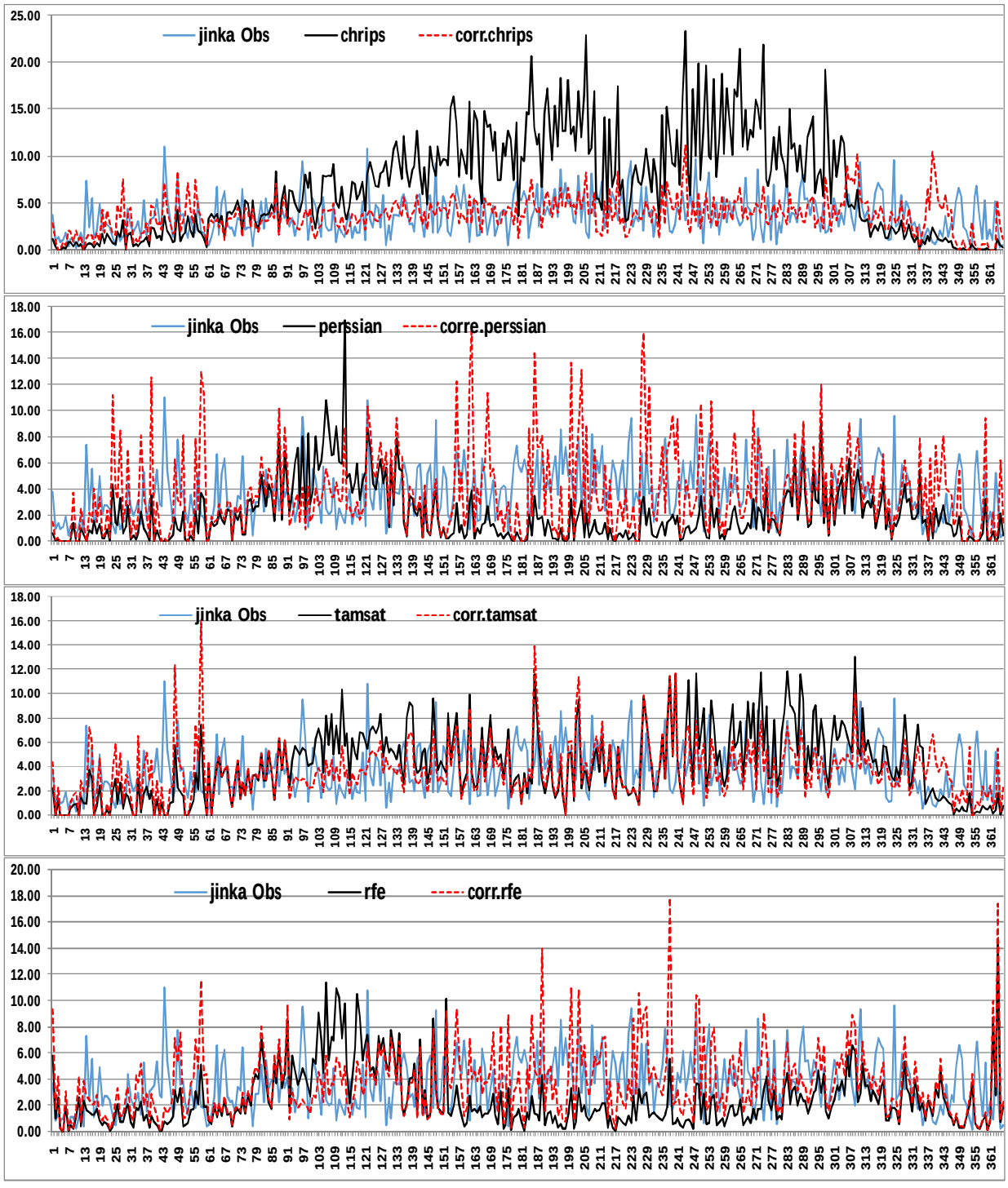

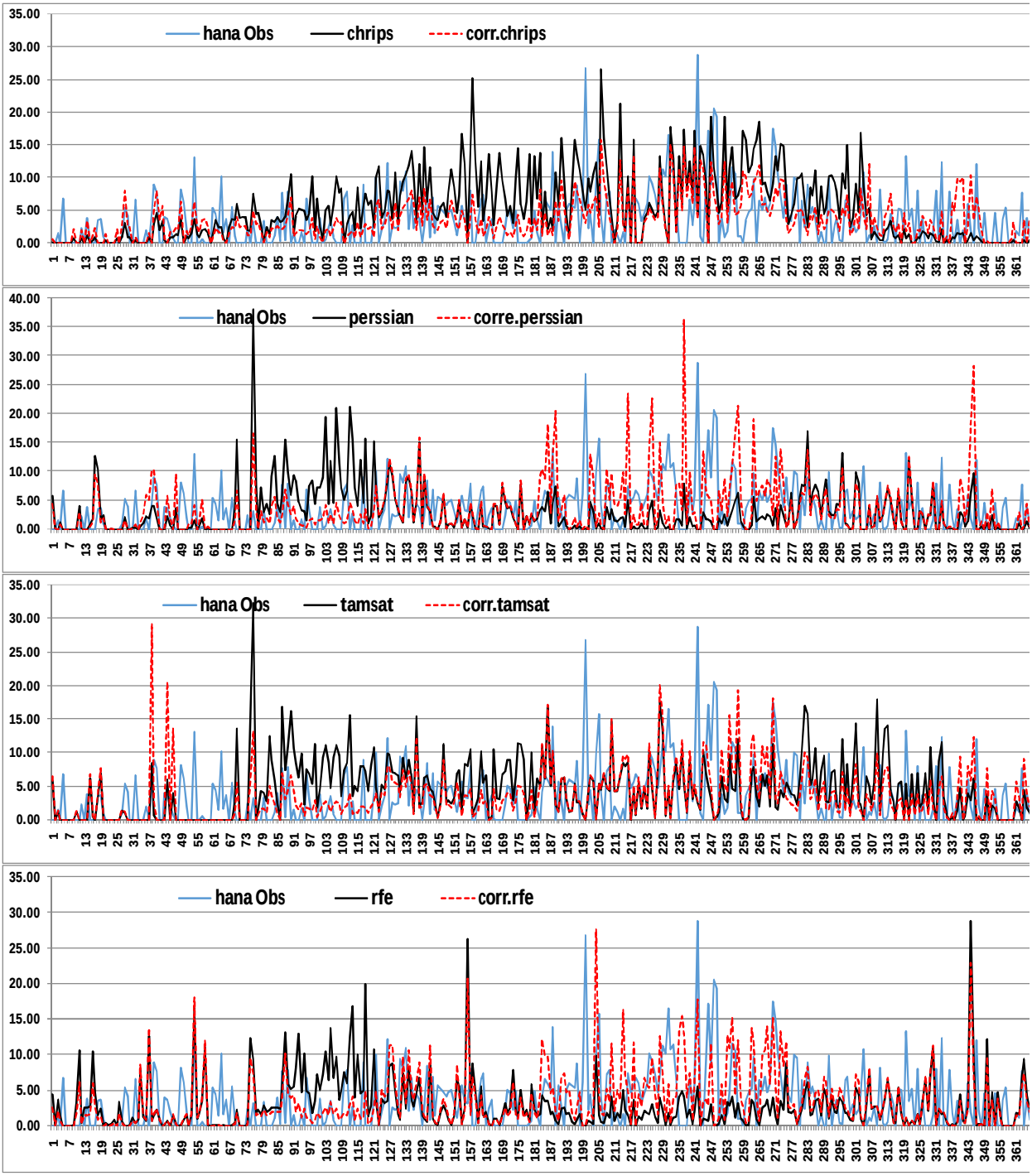
hana Obs
chrips
corr.chrips
hana Obs
perssian
corre.perssian
hana Obs
tamsat
corr.tamsat
hana Obs
rfe
corr.rfe

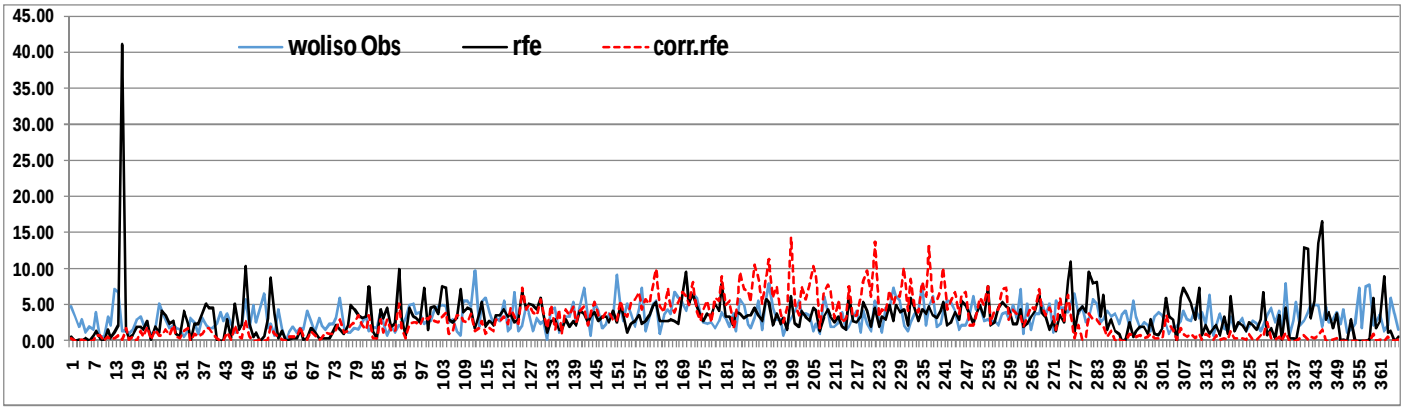
woliso Obs
rfe
corr.rfe

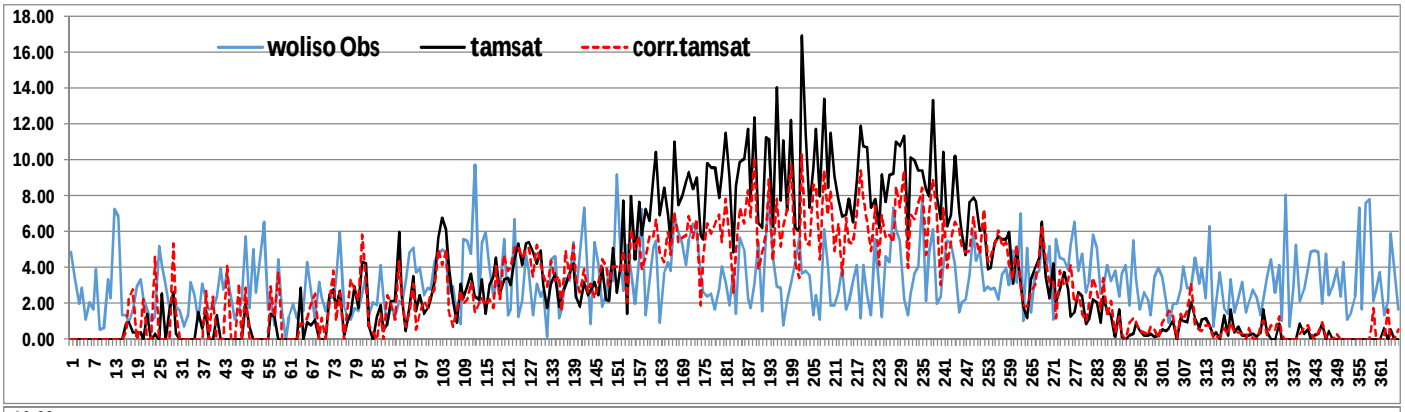
woliso Obs
tamsat
corr.tamsat

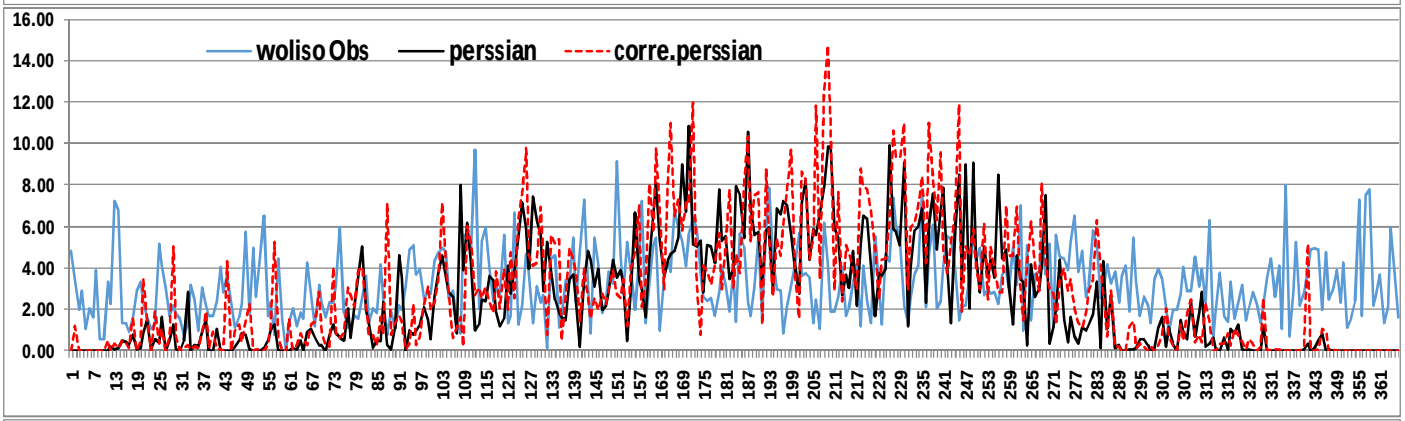
woliso Obs
perssian
corre.perssian

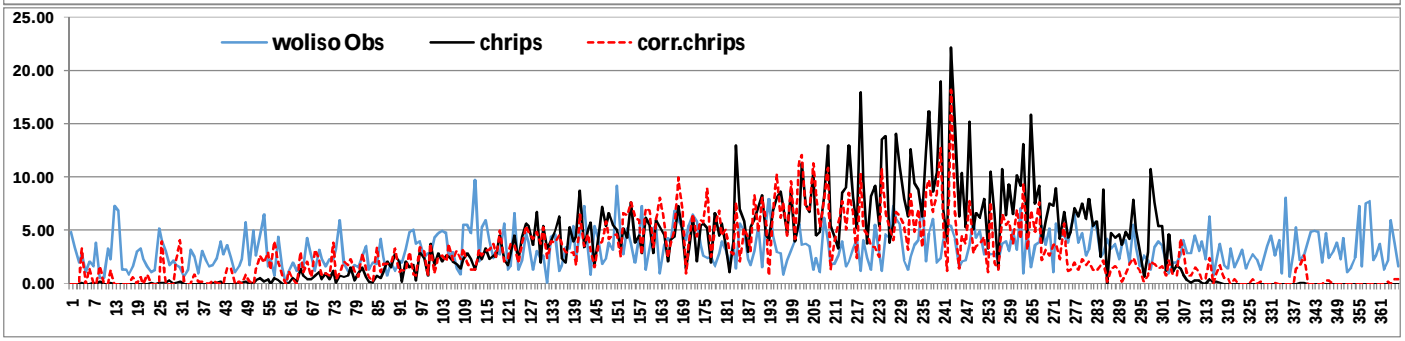
woliso Obs
chrips
corr.chrips

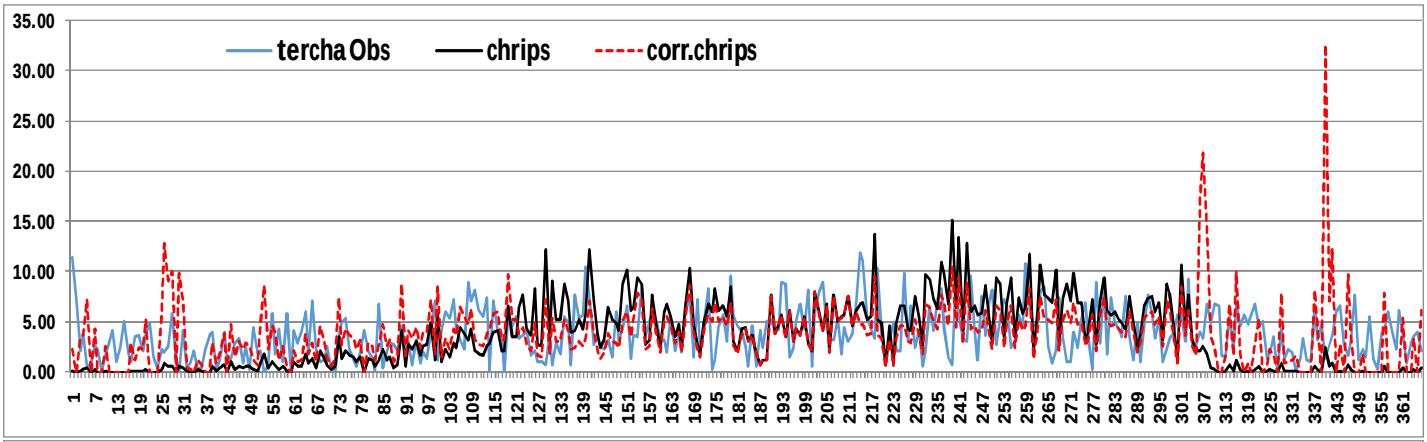
tercha Obs
chrips
corr.chrips

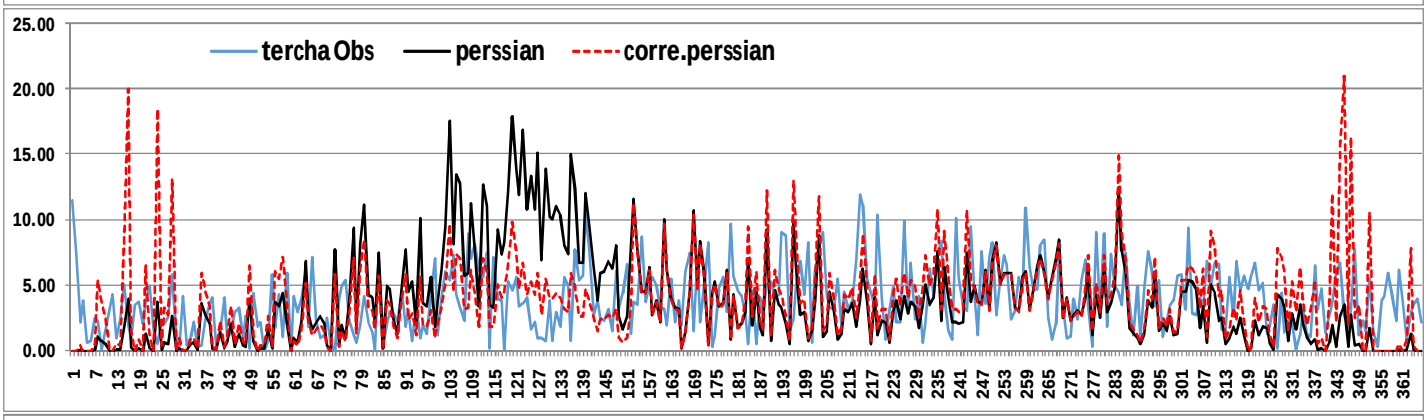
tercha Obs
perssian
corre.perssian

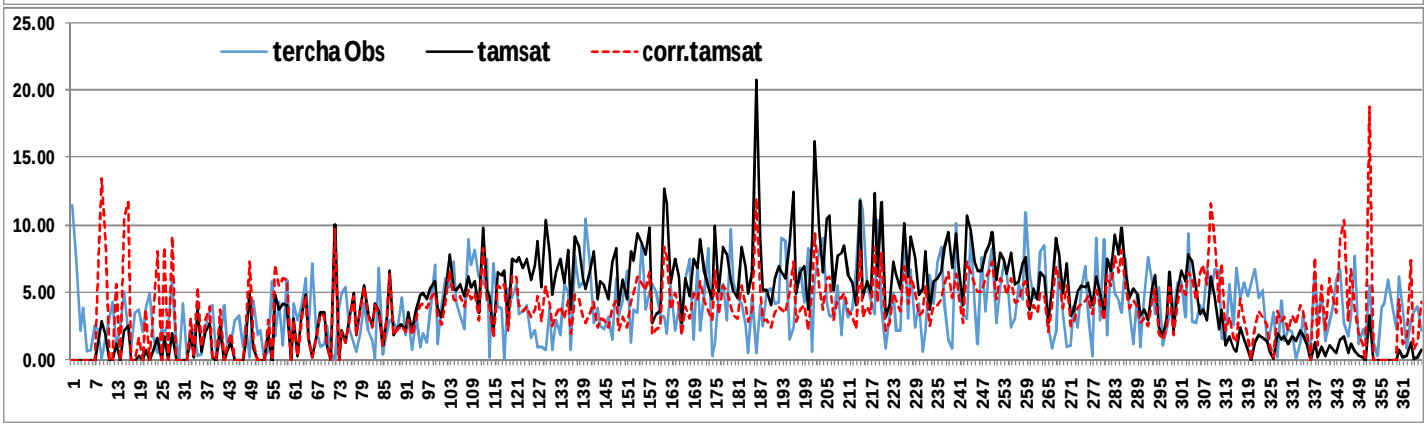
tercha Obs
tamsat
corr.tamsat

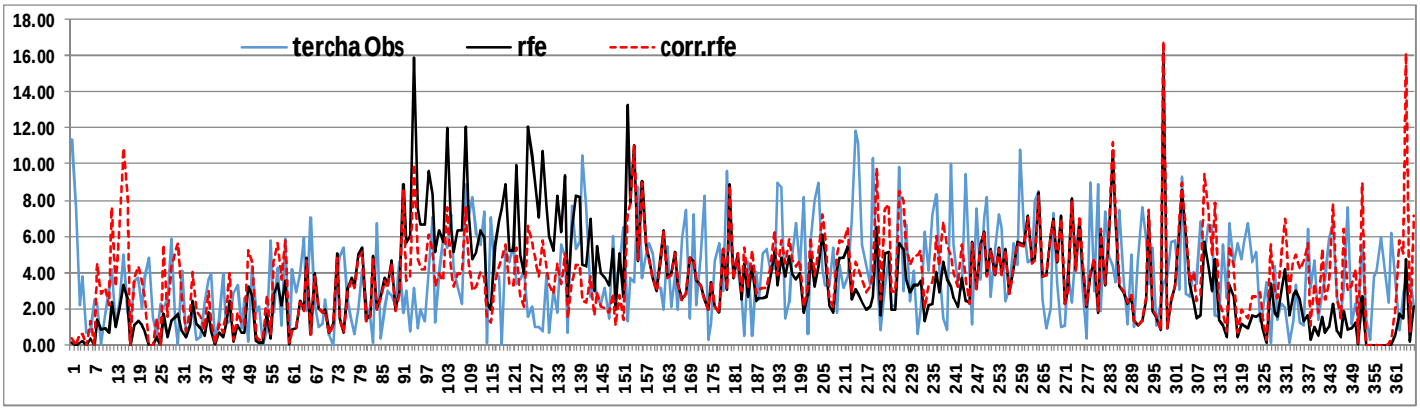
tercha Obs
rfe
corr.rfe

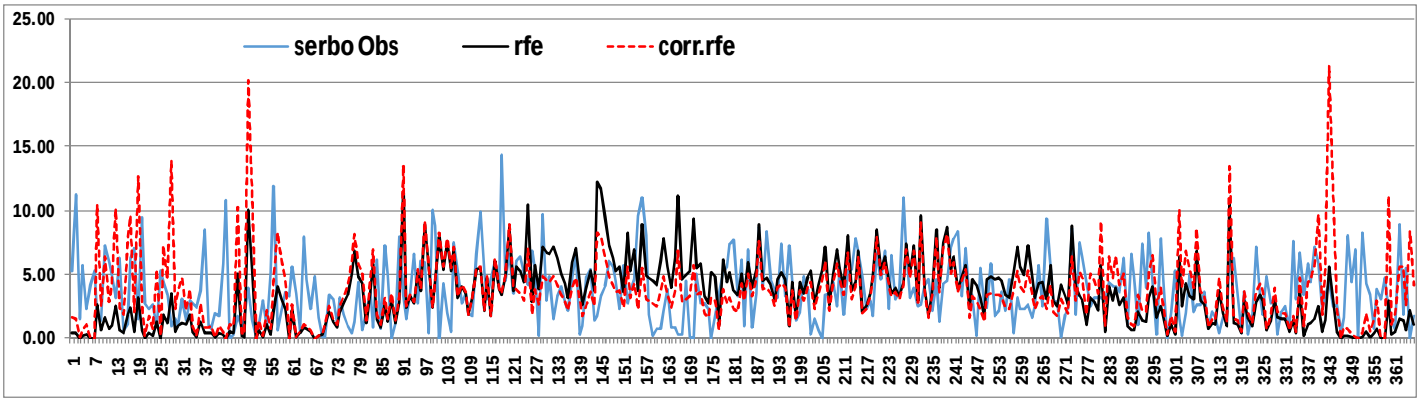
serbo Obs
rfe
corr.rfe

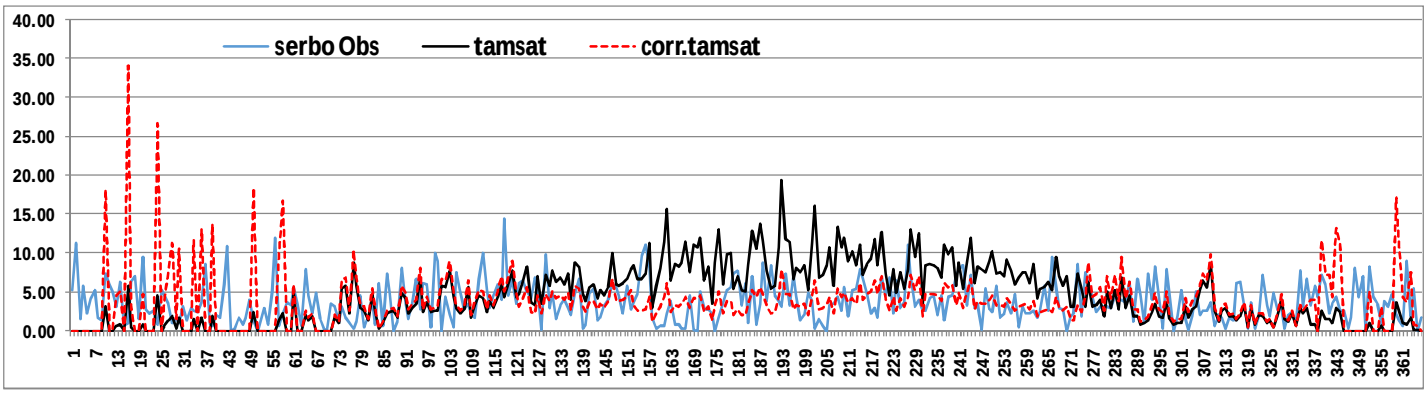
serbo Obs
tamsat
corr.tamsat

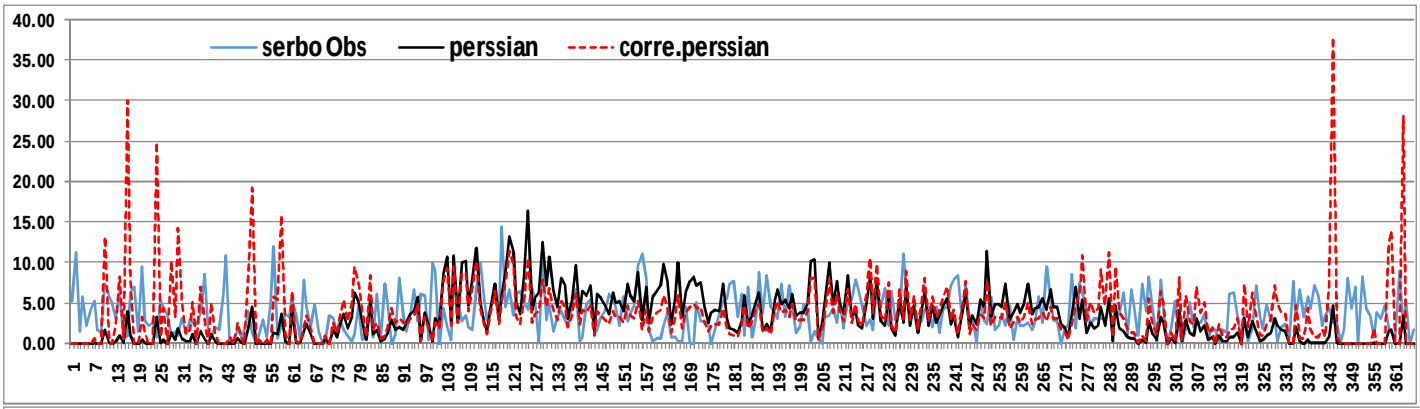
serbo Obs
perssian
corre.perssian

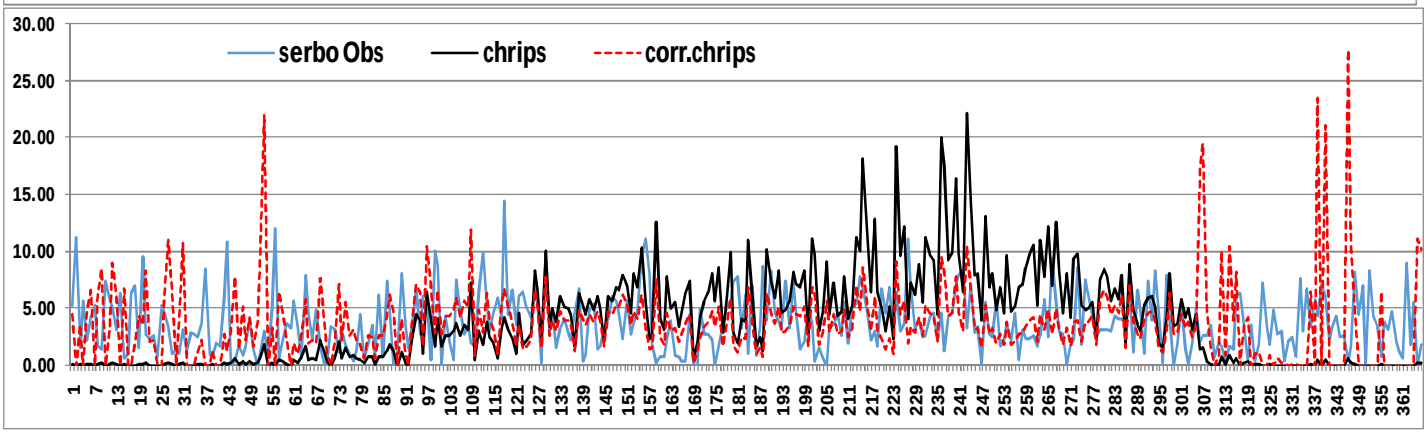
serbo Obs
chrips
corr.chrips

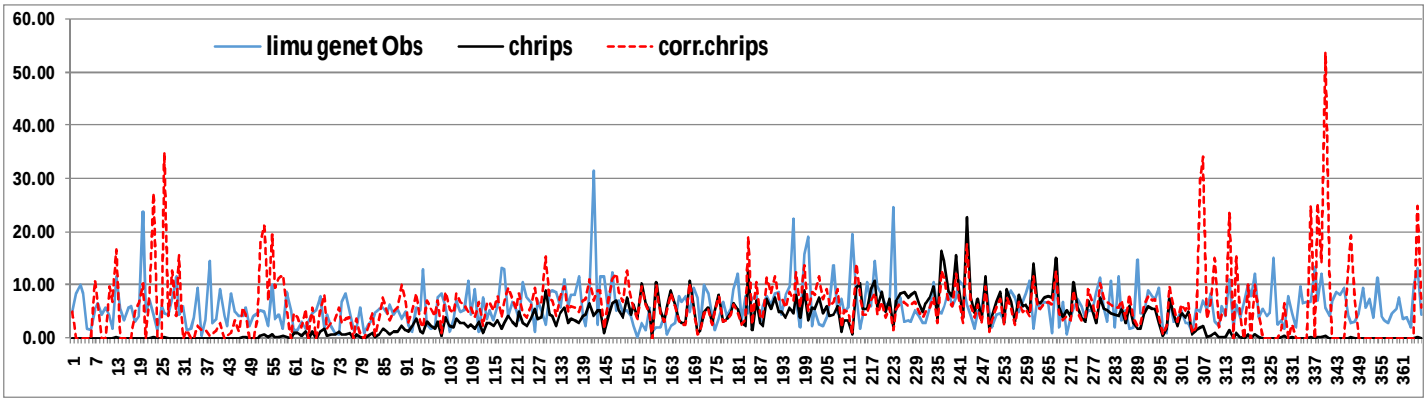
limu genet Obs
chrips
corr.chrips

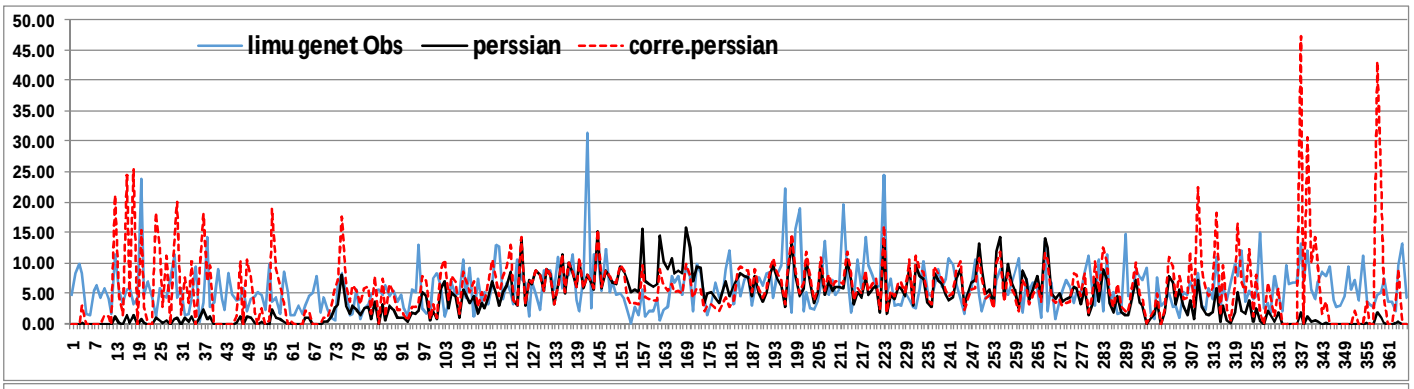
limu genet Obs
perssian
corre.perssian

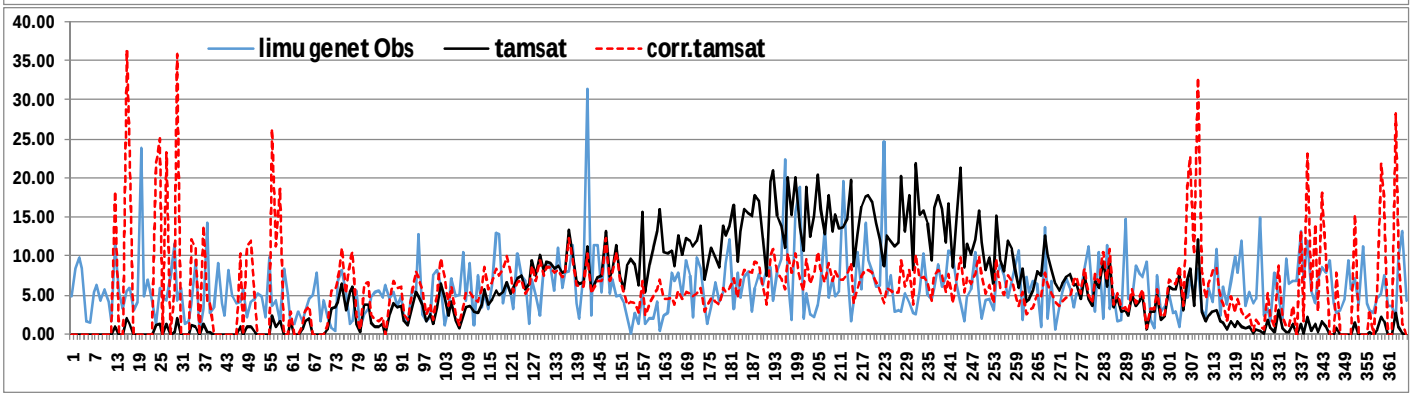
limu genet Obs
tamsat
corr.tamsat

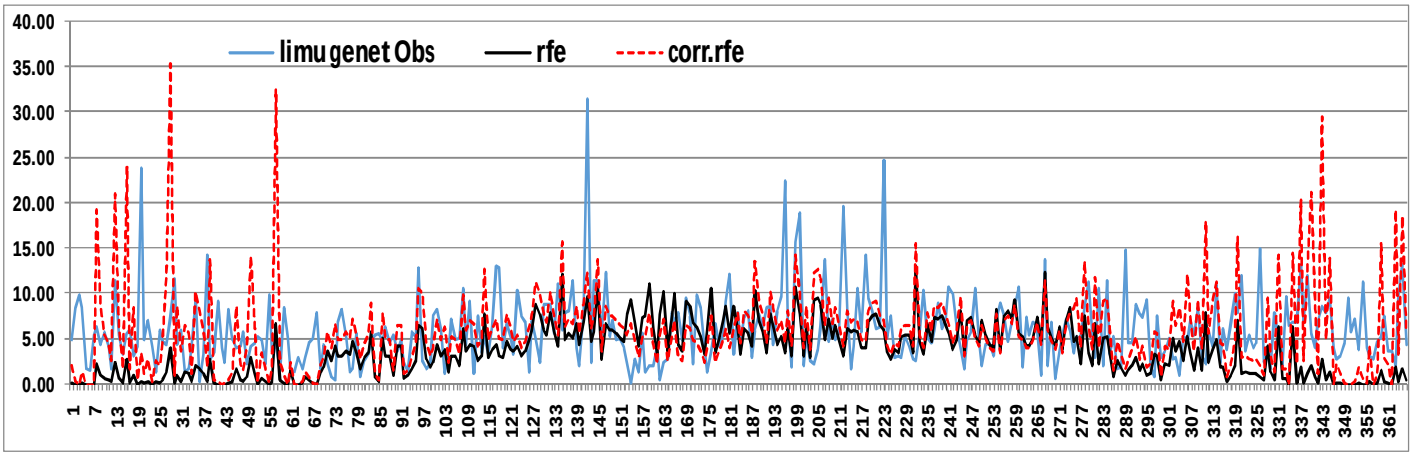
limu genet Obs
rfe
corr.rfe

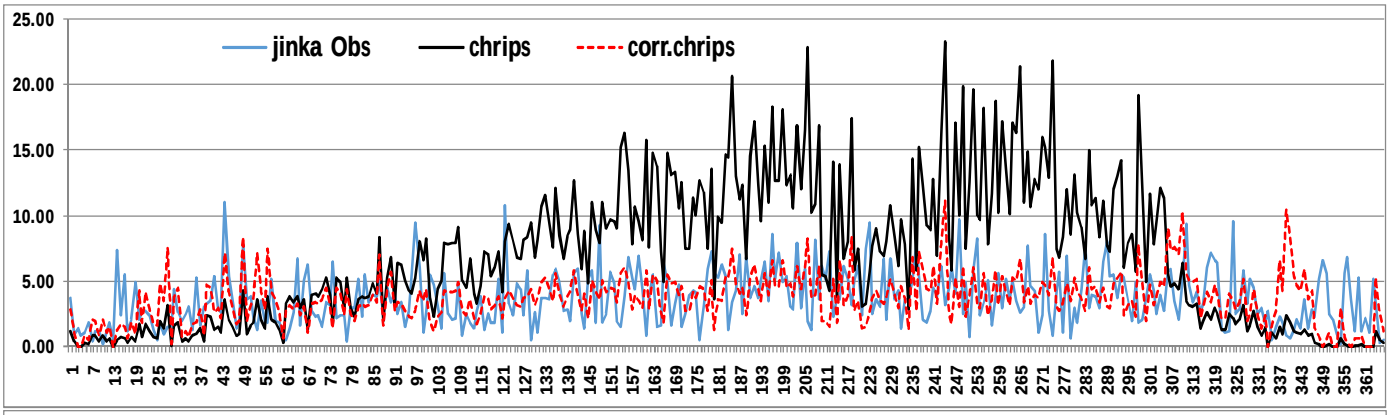
jinka Obs
chrips
corr.chrips

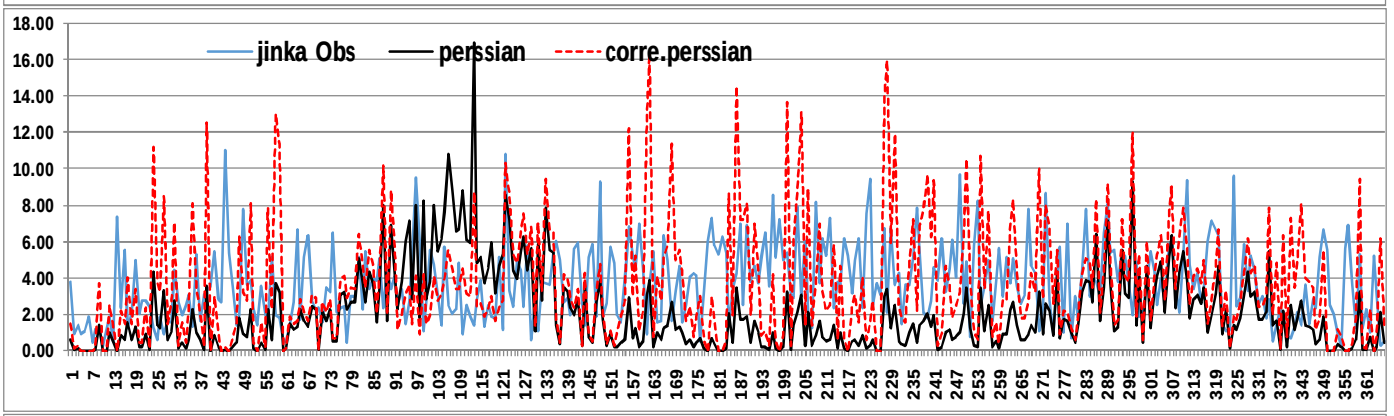
jinka Obs
perssian
corre.perssian

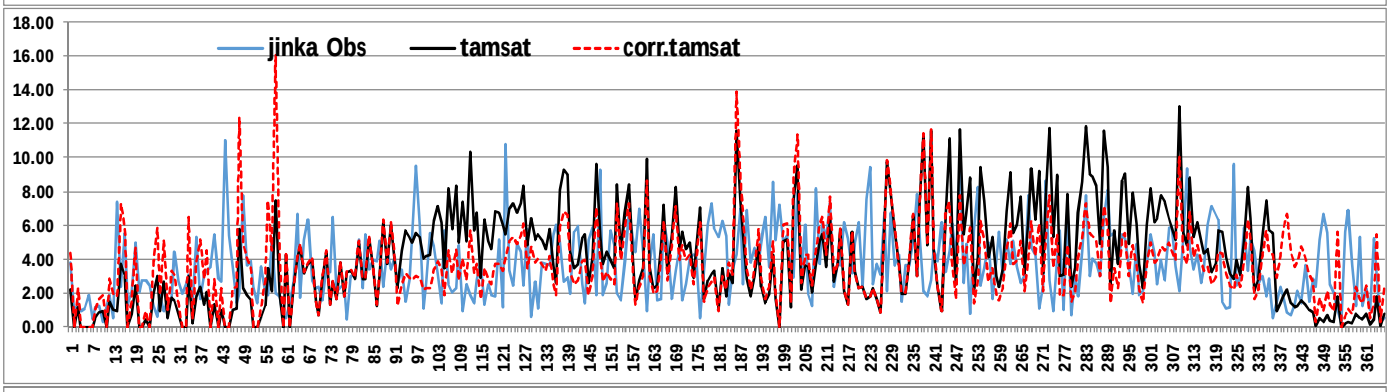
jinka Obs
tamsat
corr.tamsat

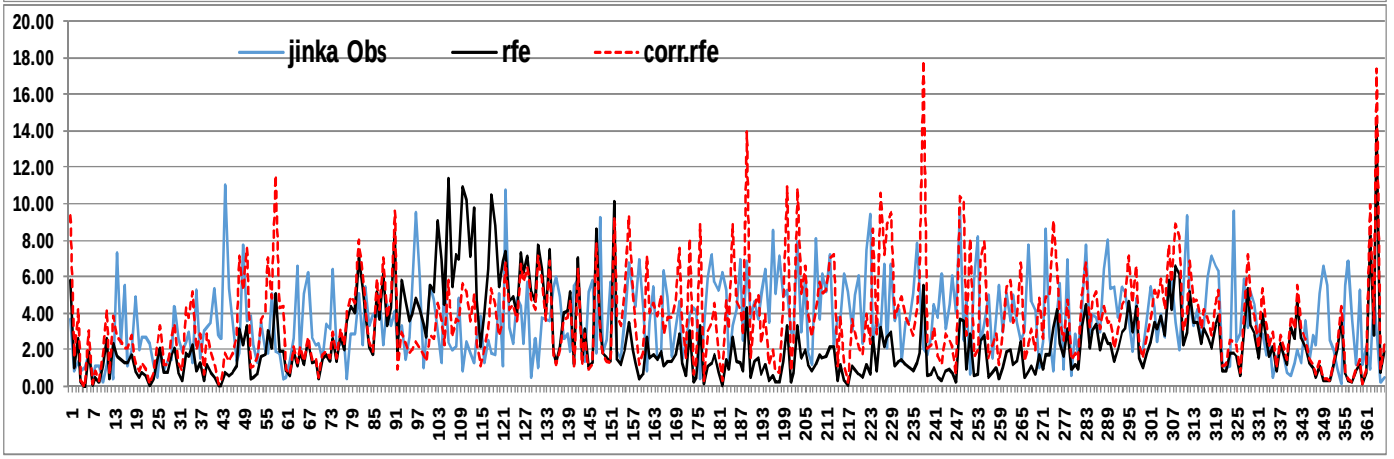
jinka Obs
rfe
corr.rfe

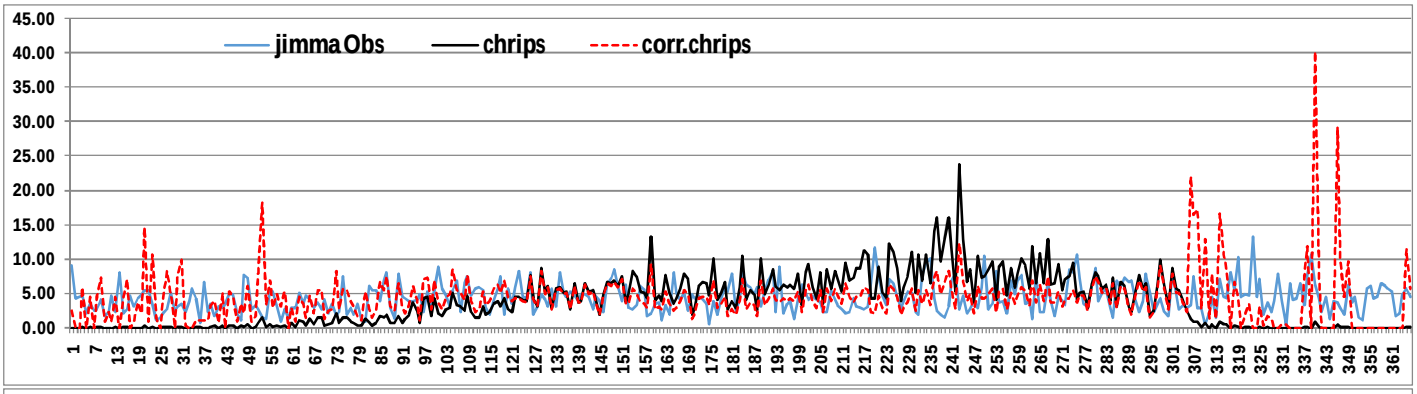
jimma Obs
chrips
corr.chrips

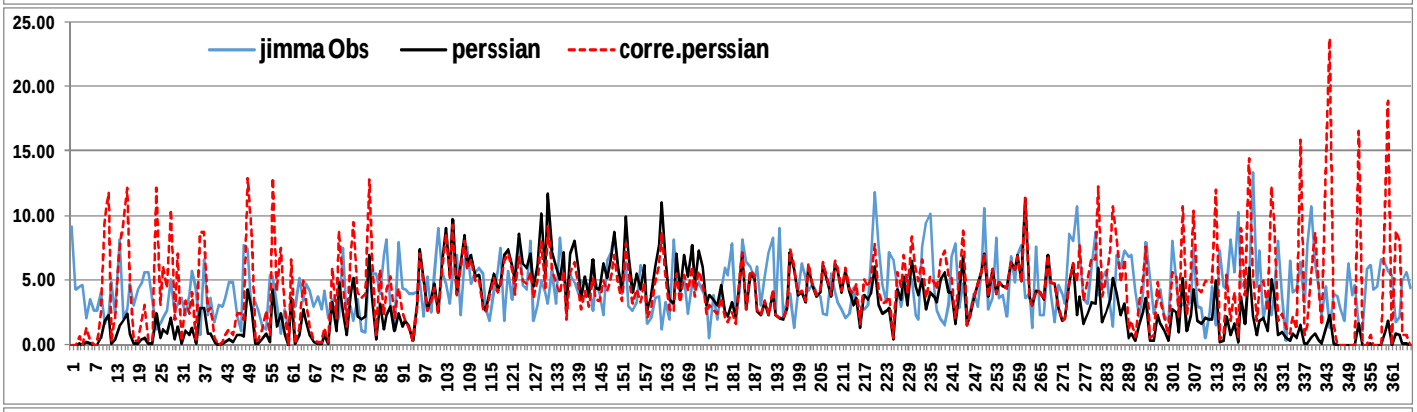
jimma Obs
perssian
corre.perssian

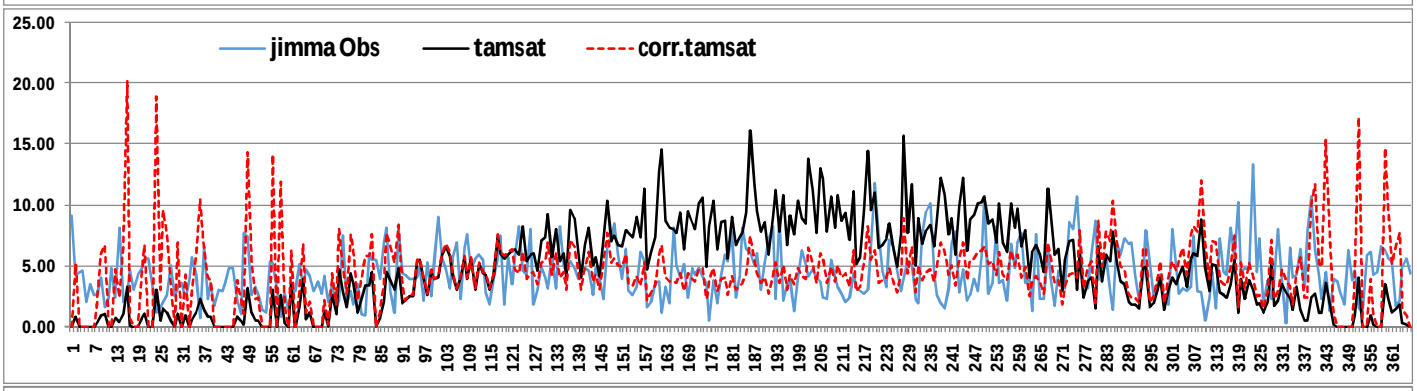
jimma Obs
tamsat
corr.tamsat

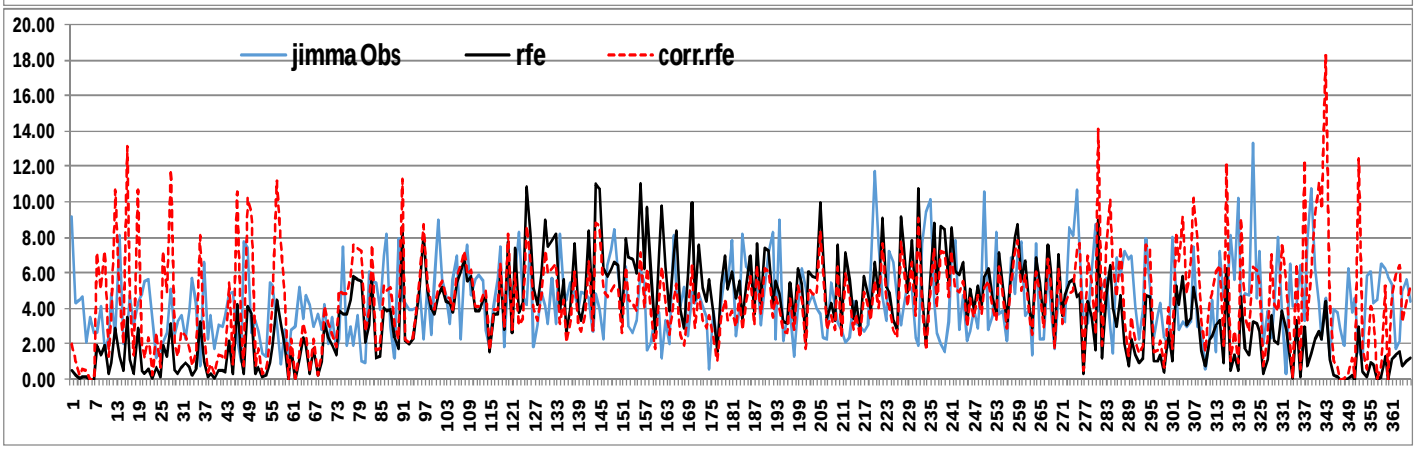
jimma Obs
rfe
corr.rfe

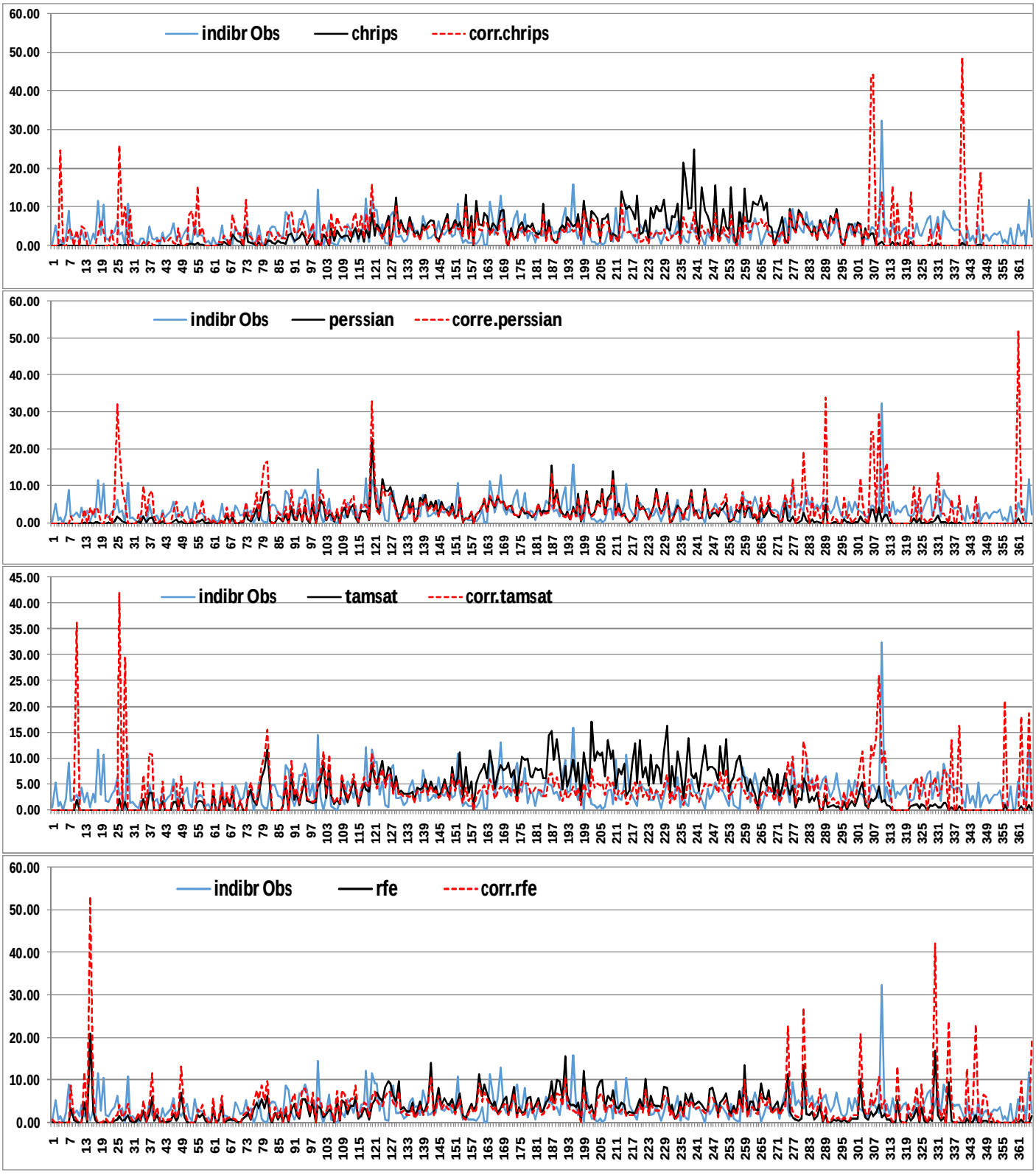
indibr Obs
chrips
corr.chrips
indibr Obs
perssian
corre.perssian
indibr Obs
tamsat
corr.tamsat
indibr Obs
rfe
corr.rfe

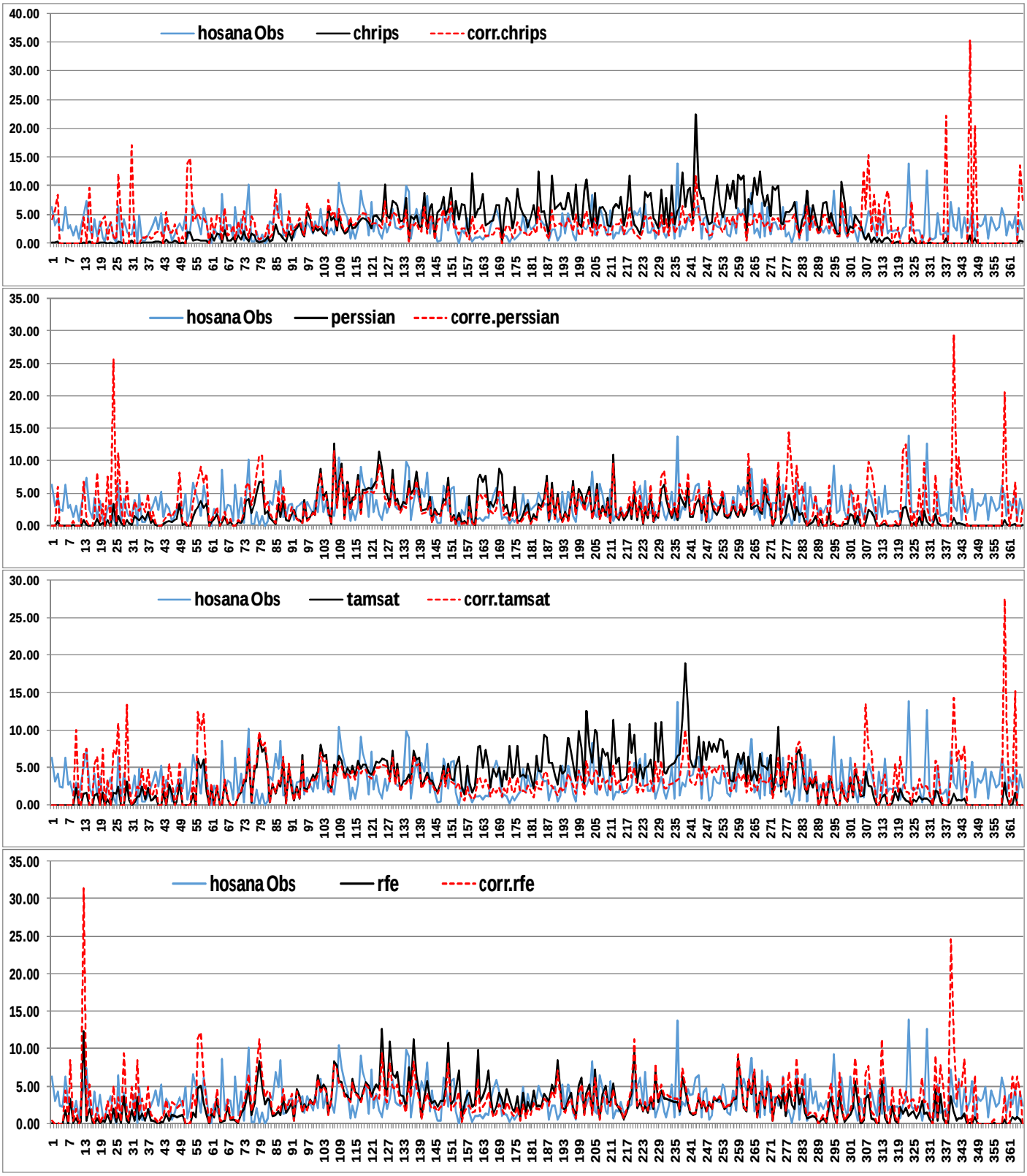
hosana Obs
chrips
corr.chrips
hosana Obs
perssian
corre.perssian
hosana Obs
tamsat
corr.tamsat
hosana Obs
rfe
corr.rfe

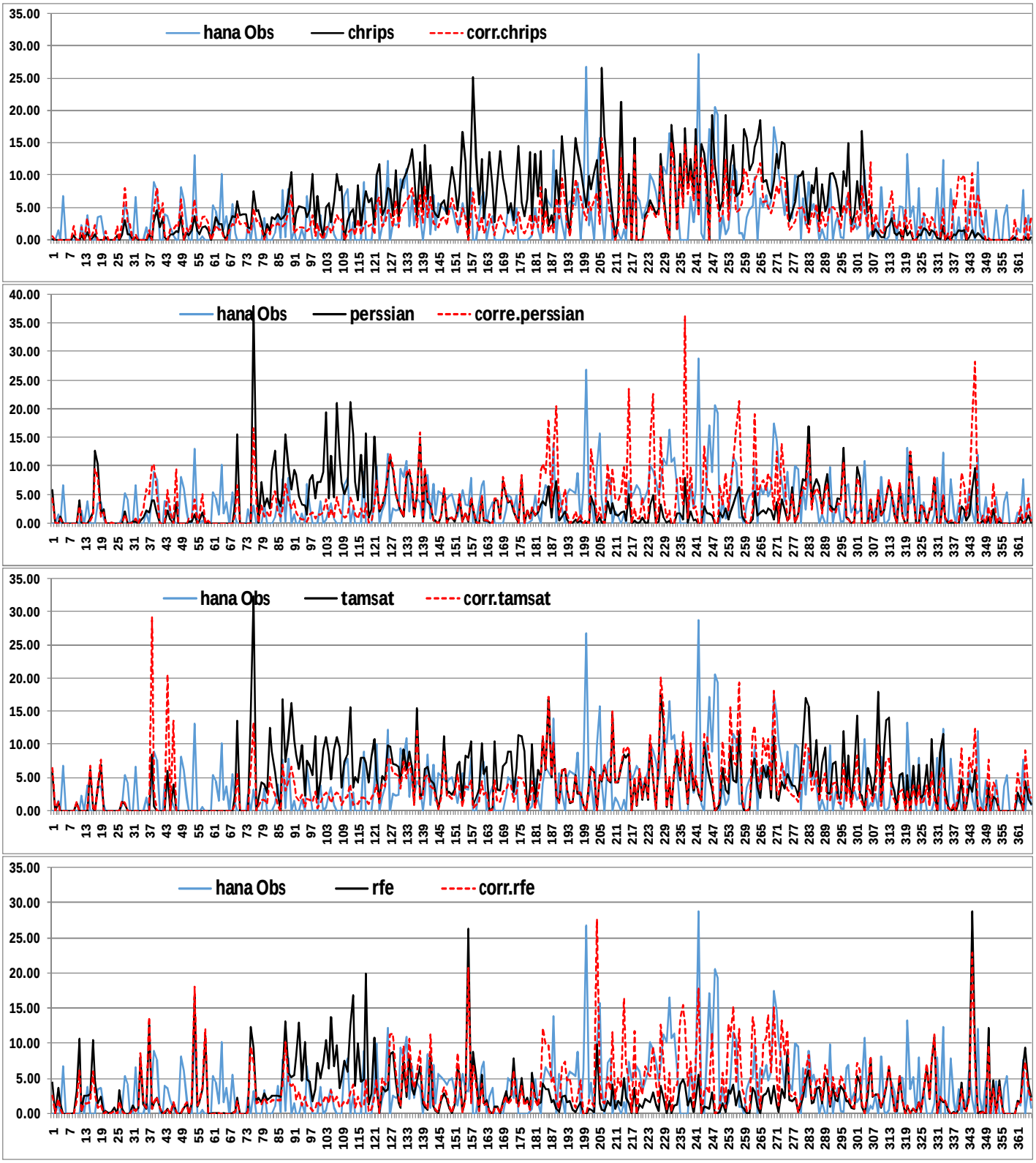
hana Obs
chrips
corr.chrips
hana Obs
perssian
corre.perssian
hana Obs
tamsat
corr.tamsat
hana Obs
rfe
corr.rfe

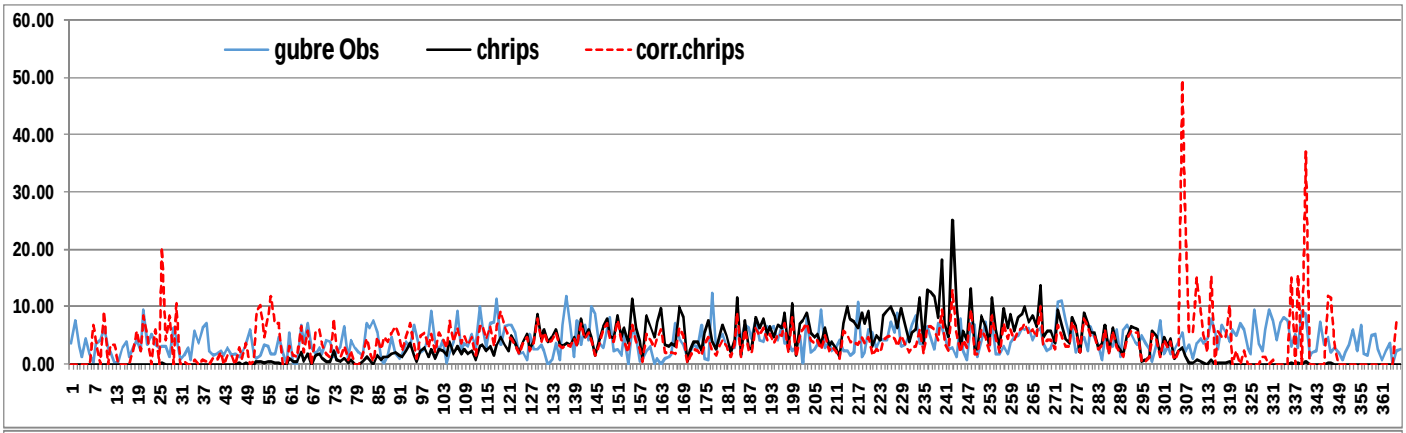
gubre Obs
chrips
corr.chrips

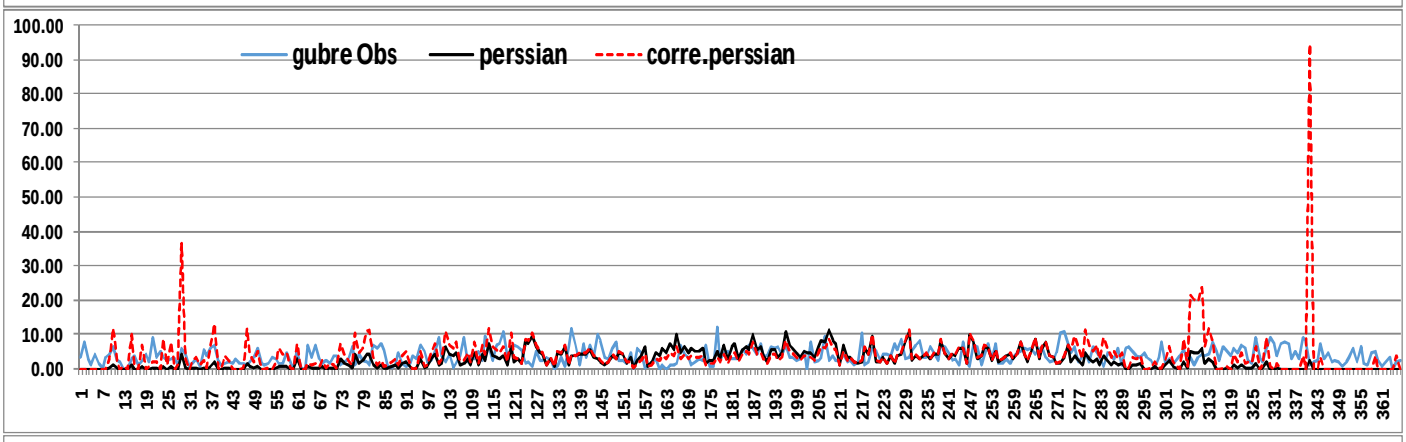
gubre Obs
perssian
corre.perssian

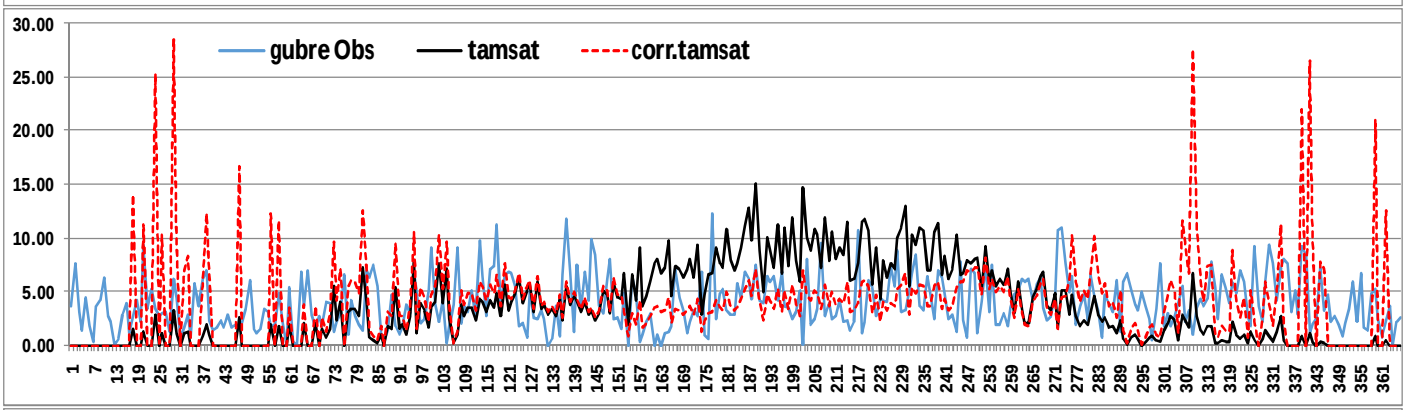
gubre Obs
tamsat
corr.tamsat

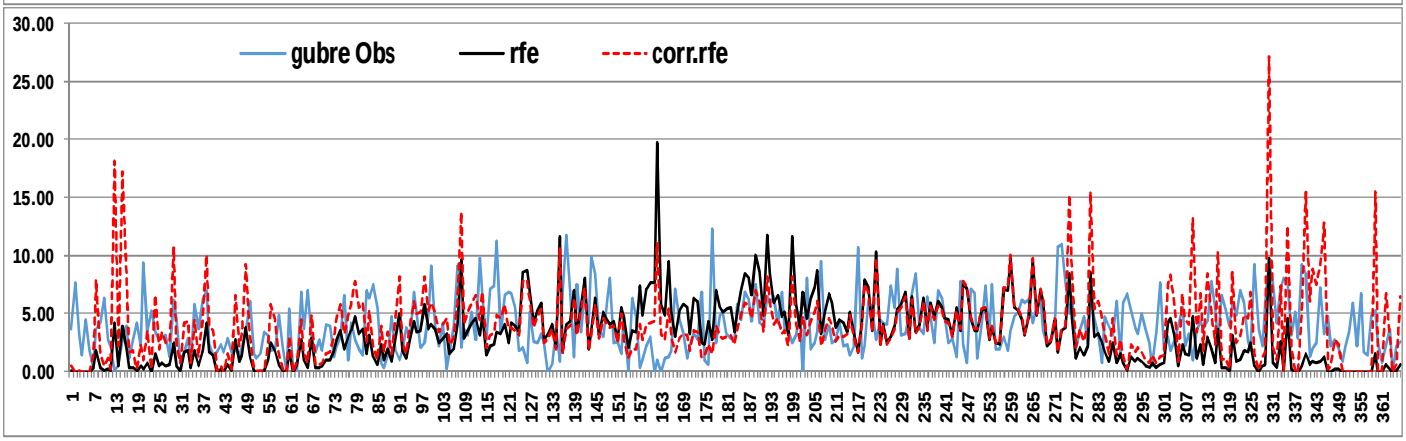
gubre Obs
rfe
corr.rfe

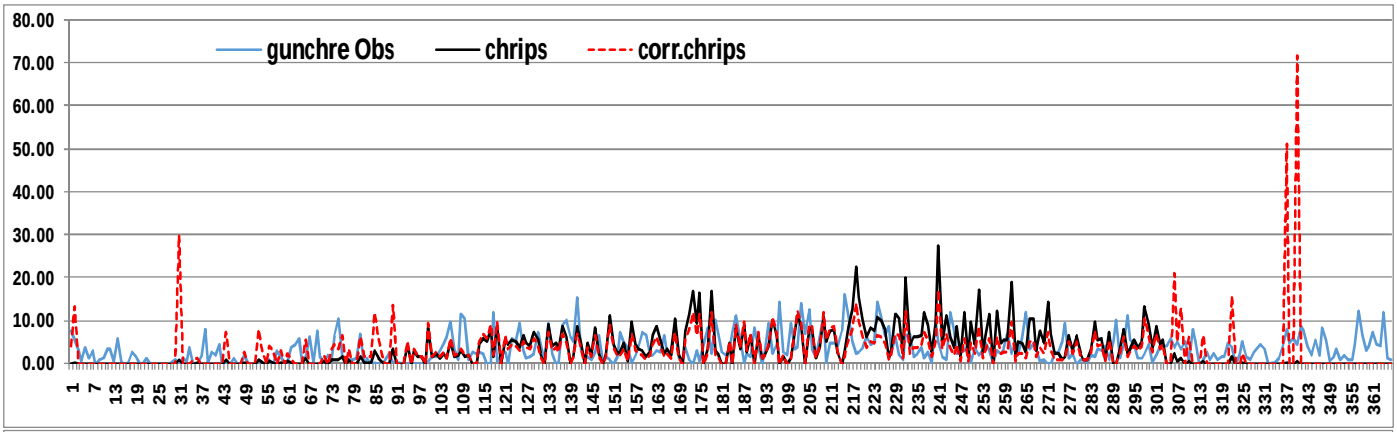
gunchre Obs
chrips
corr.chrips

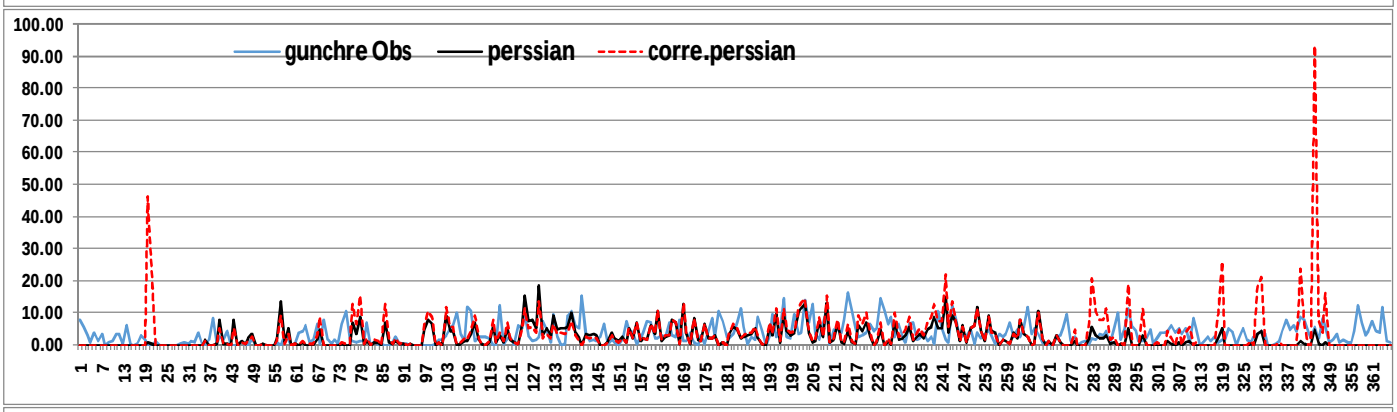
gunchre Obs
perssian
corre.perssian

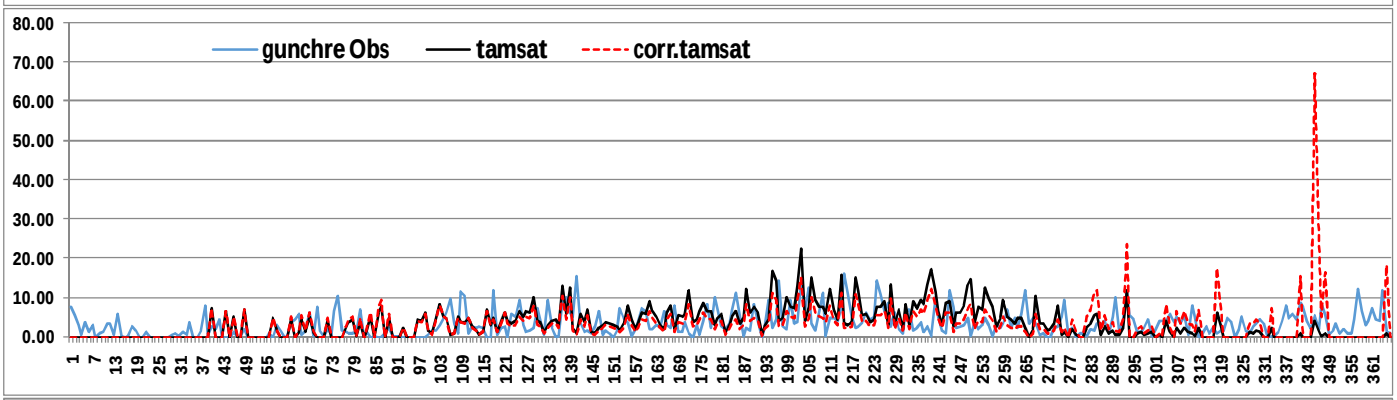
gunchre Obs
tamsat
corr.tamsat

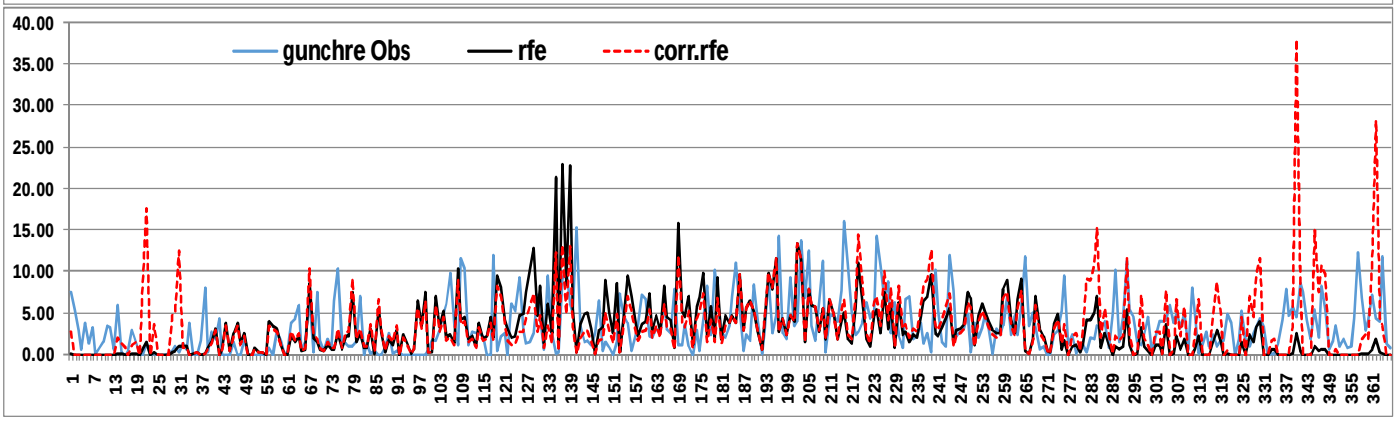
gunchre Obs
rfe
corr.rfe

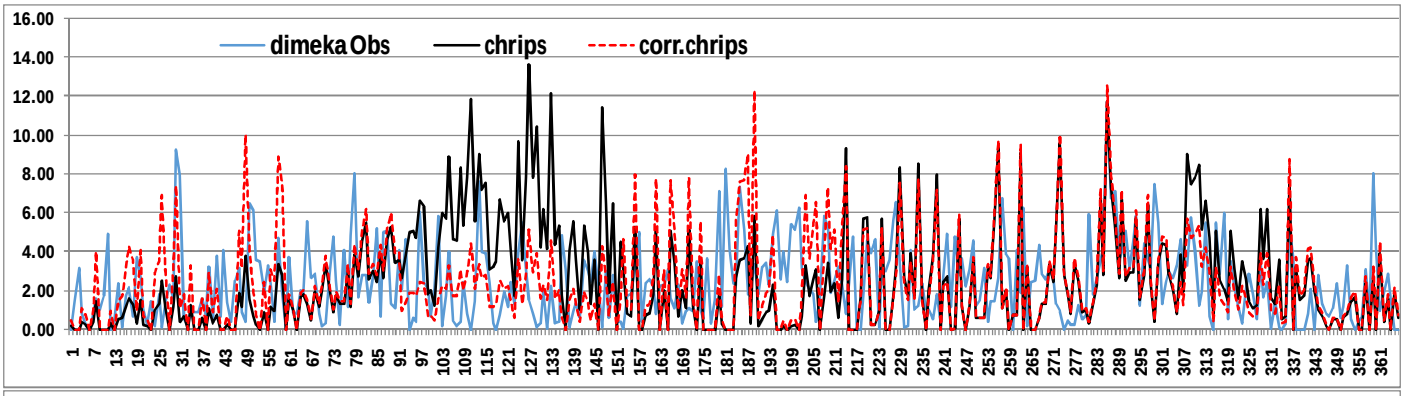
dimeka Obs
chrips
corr.chrips

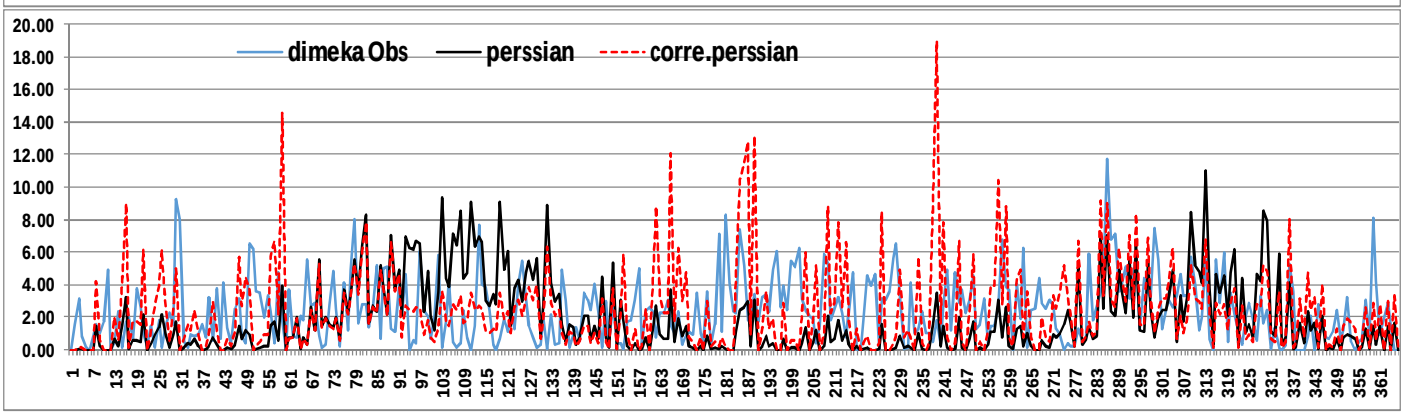
dimeka Obs
perssian
corre.perssian

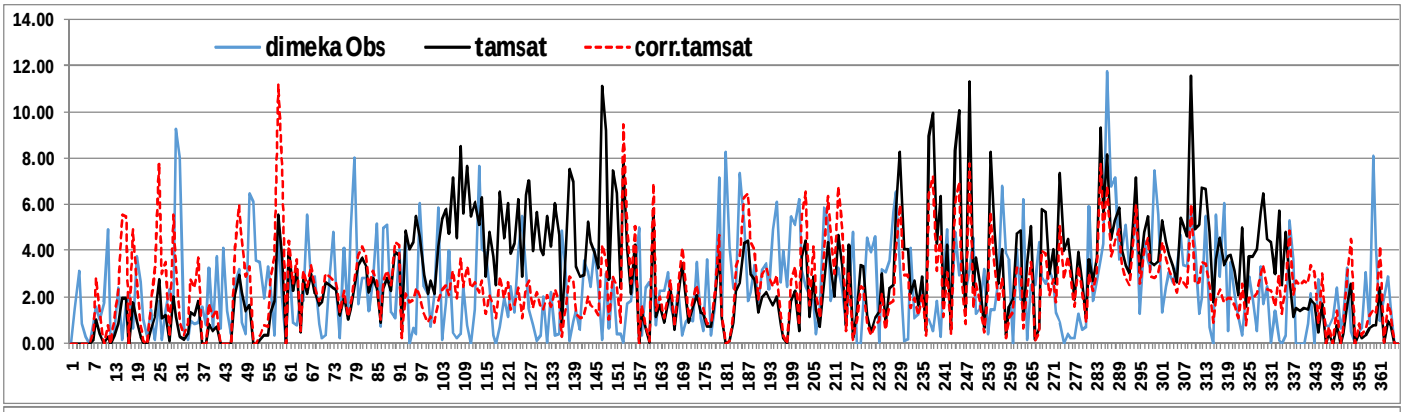
dimeka Obs
tamsat
corr.tamsat

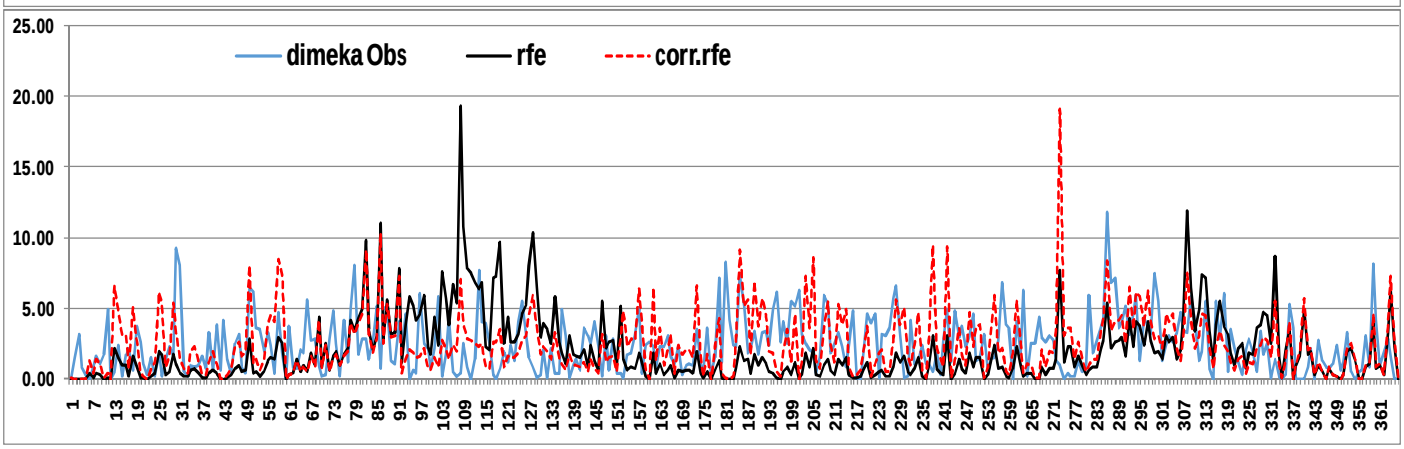
dimeka Obs
rfe
corr.rfe

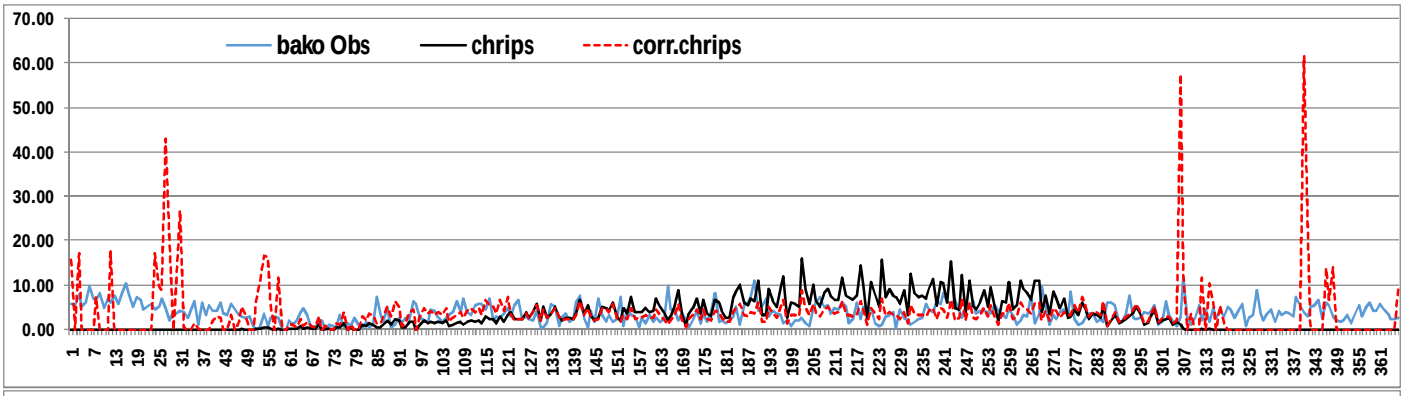
bako Obs
chrips
corr.chrips
70.00
60.00
50.00
40.00
30.00
20.00
10.00
0.00

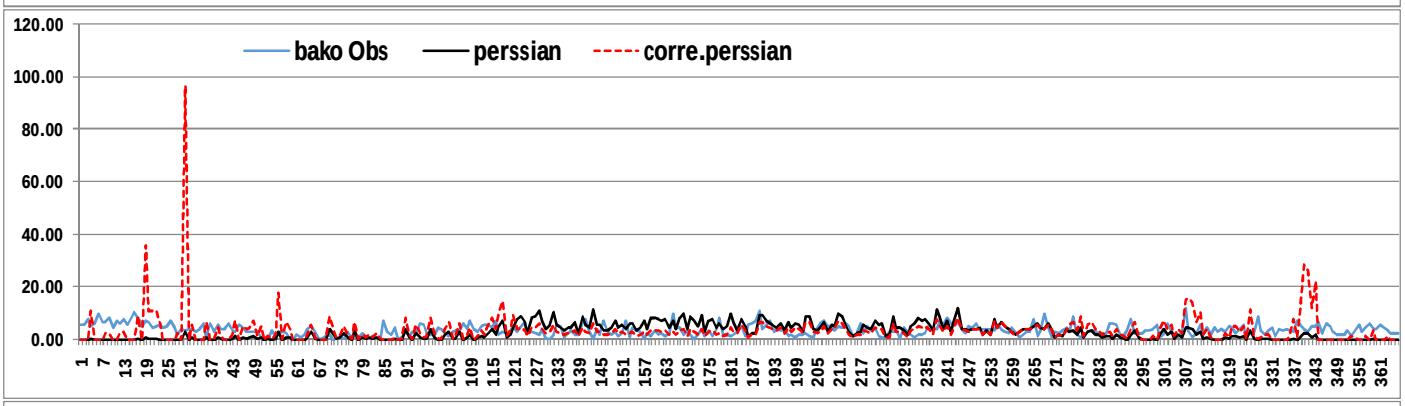
bako Obs
perssian
corre.perssian
120.00
100.00
80.00
60.00
40.00
20.00
0.00

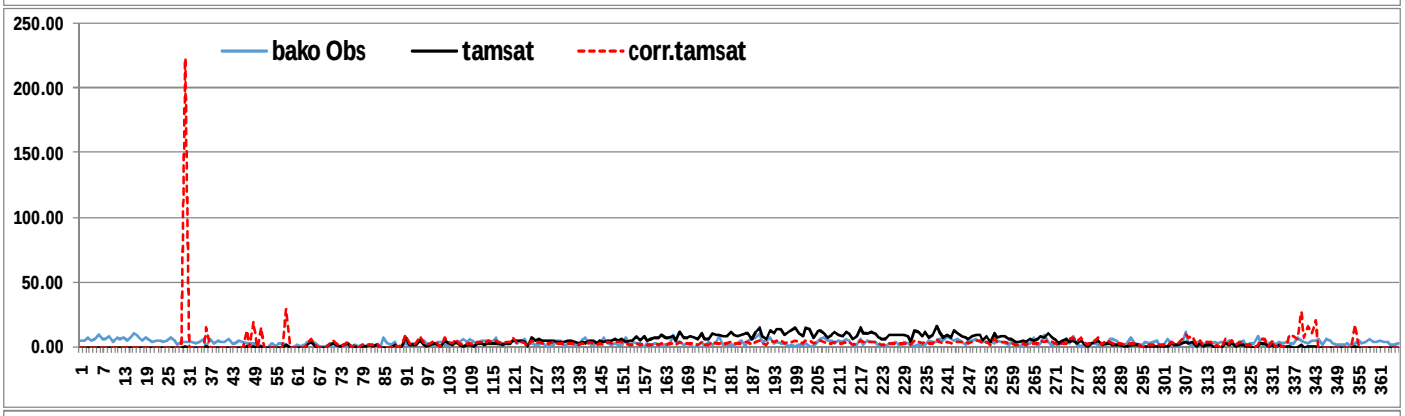
bako Obs
tamsat
corr.tamsat
250.00
200.00
150.00
100.00
50.00
0.00

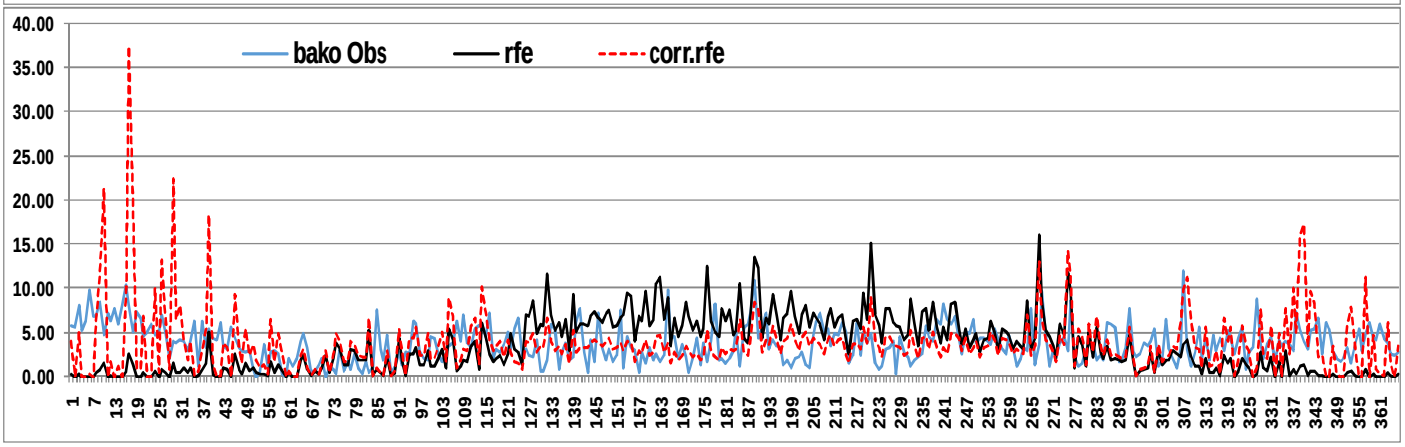
bako Obs
rfe
corr.rfe
40.00
35.00
30.00
25.00
20.00
15.00
10.00
5.00
0.00

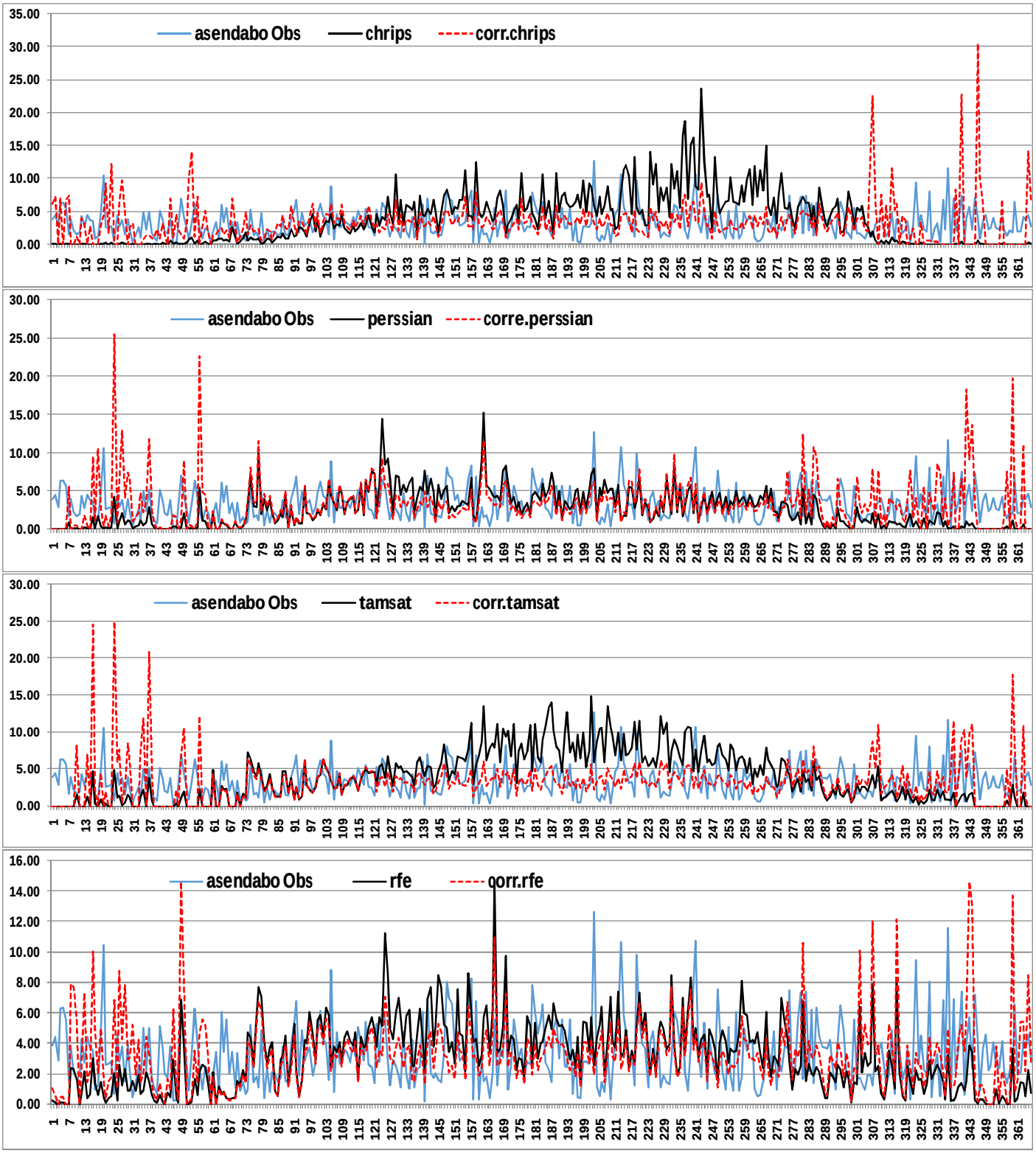
asendabo Obs
chrips
corr.chrips
asendabo Obs
perssian
corre.perssian
asendabo Obs
tamsat
corr.tamsat
asendabo Obs
rfe
corr.rfe

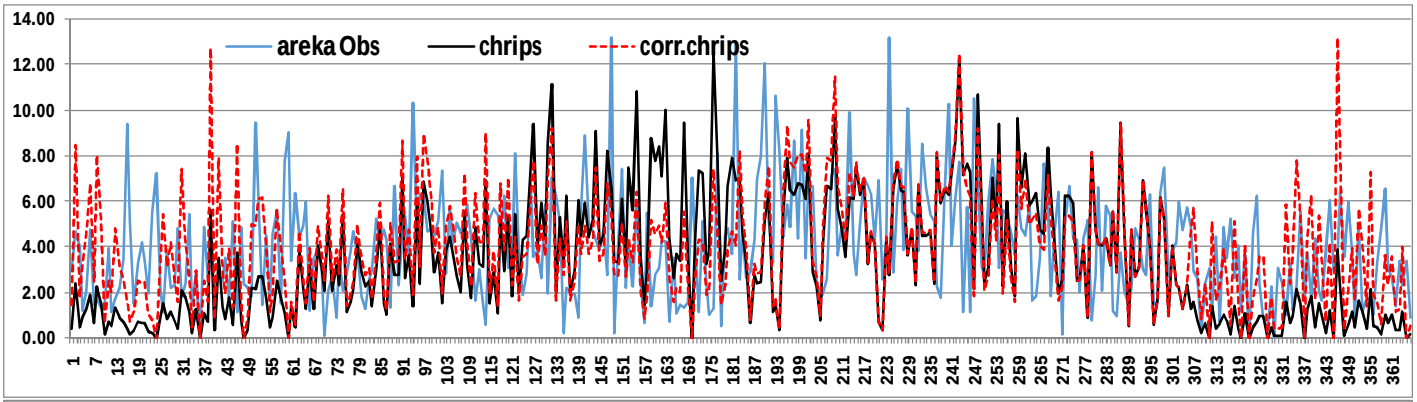
areka Obs
chrips
corr.chrips

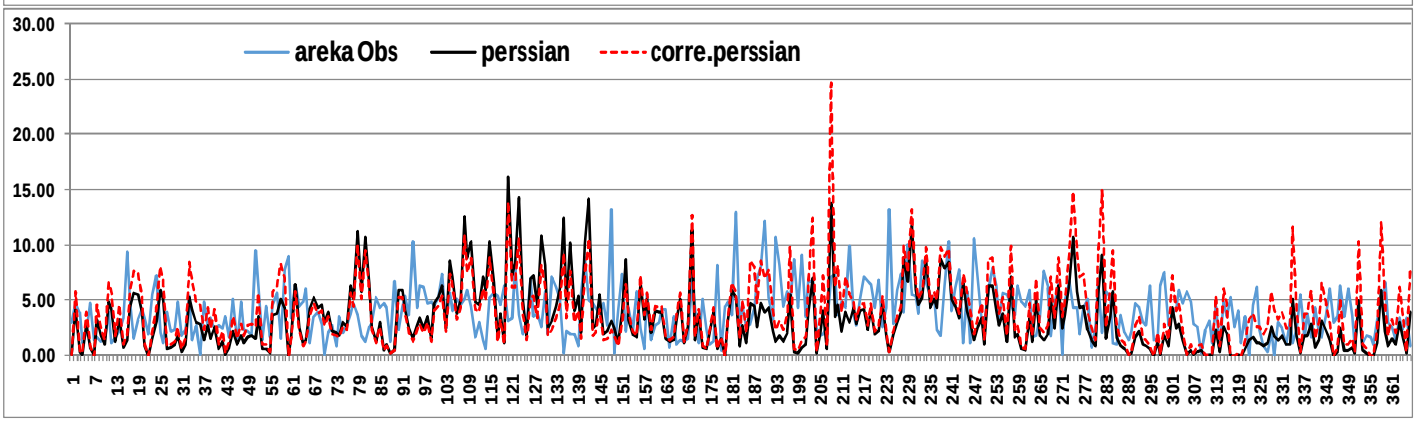
areka Obs
perssian
corre.perssian

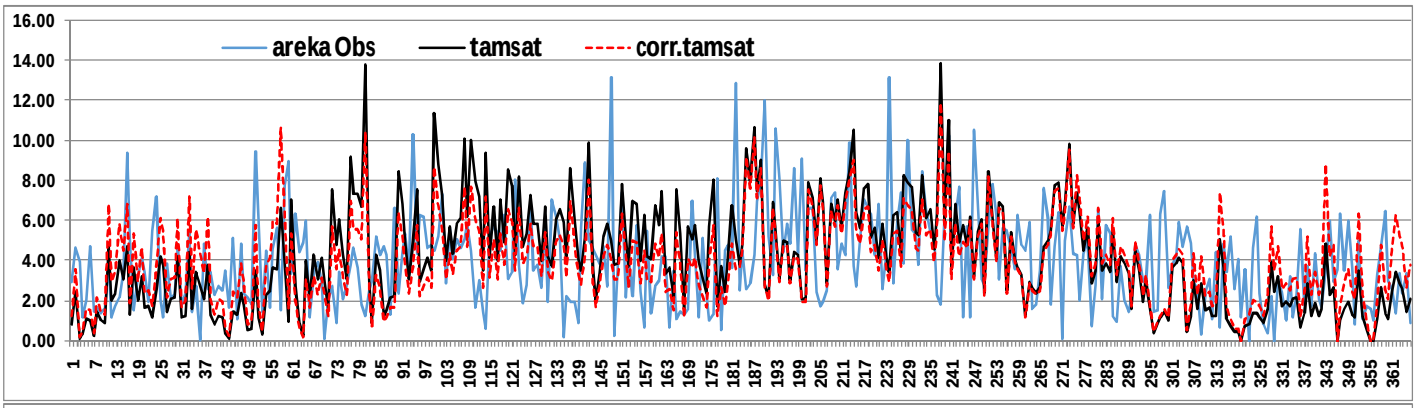
areka Obs
tamsat
corr.tamsat

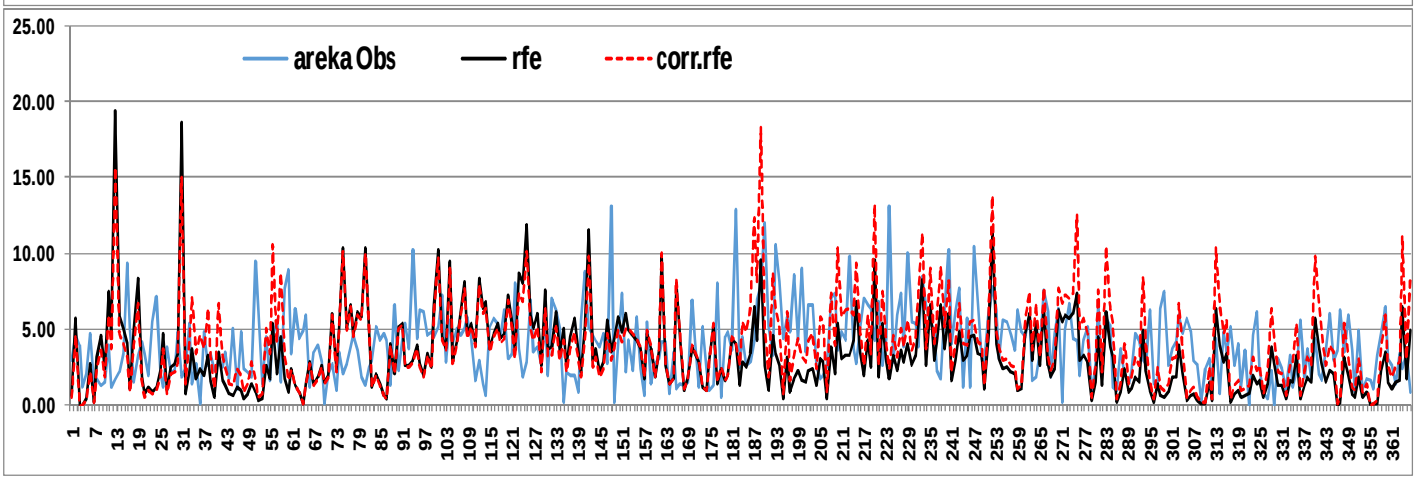
areka Obs
rfe
corr.rfe

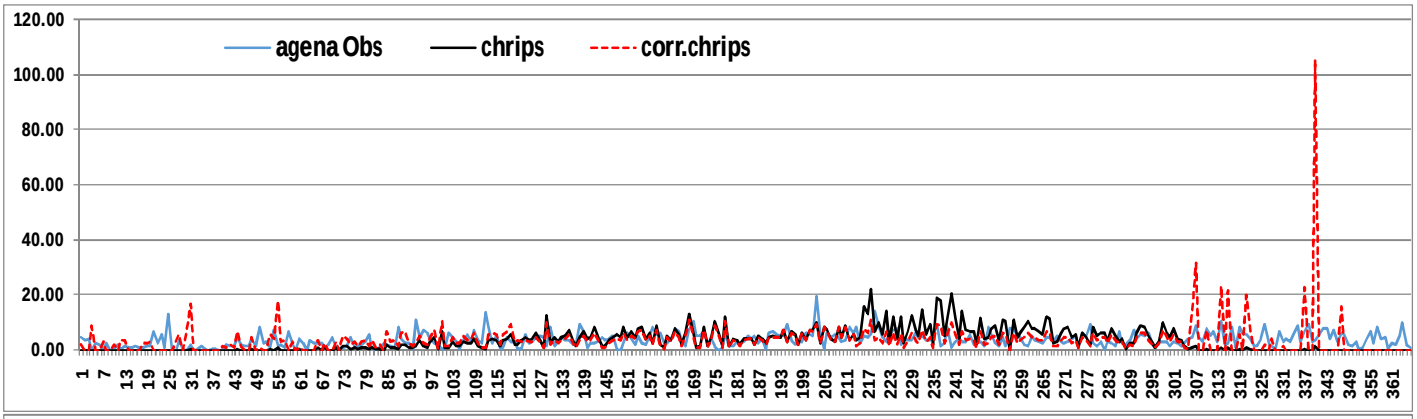
agena Obs
chrips
corr.chrips
120.00
100.00
80.00
60.00
40.00
20.00
0.00

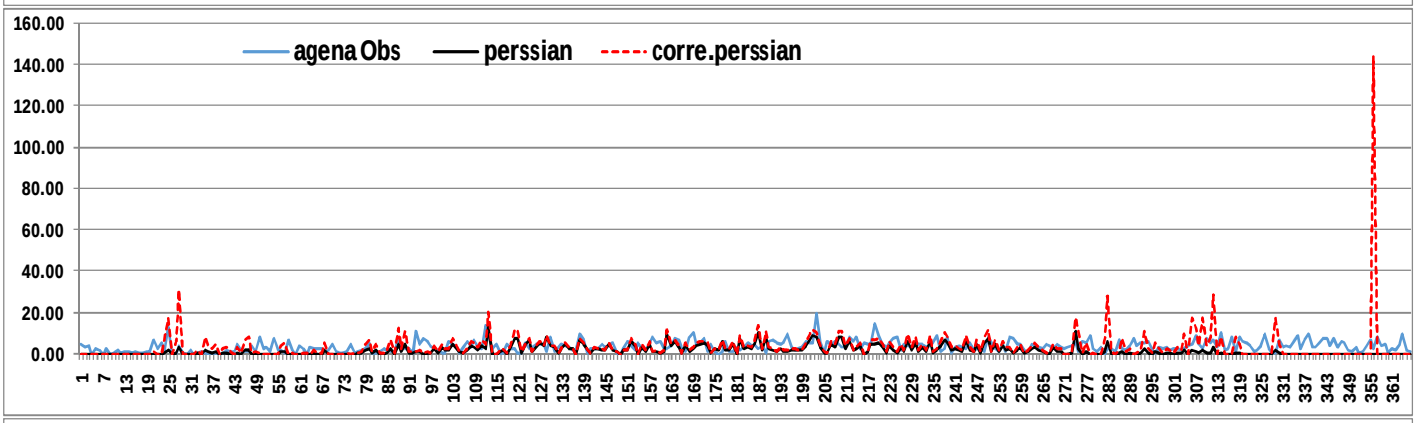
agena Obs
perssian
corre.perssian
160.00
140.00
120.00
100.00
80.00
60.00
40.00
20.00
0.00

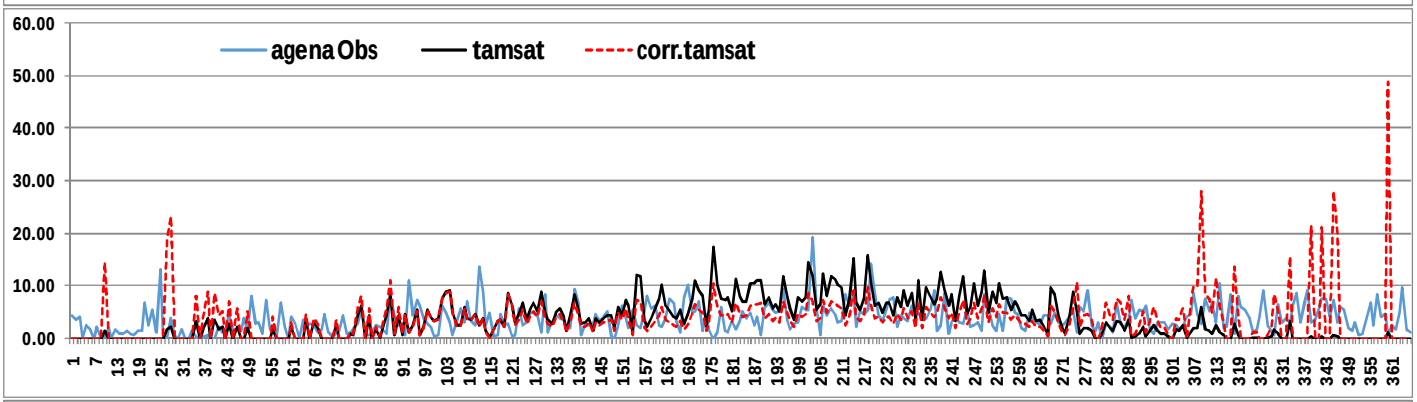
agena Obs
tamsat
corr.tamsat
60.00
50.00
40.00
30.00
20.00
10.00
0.00

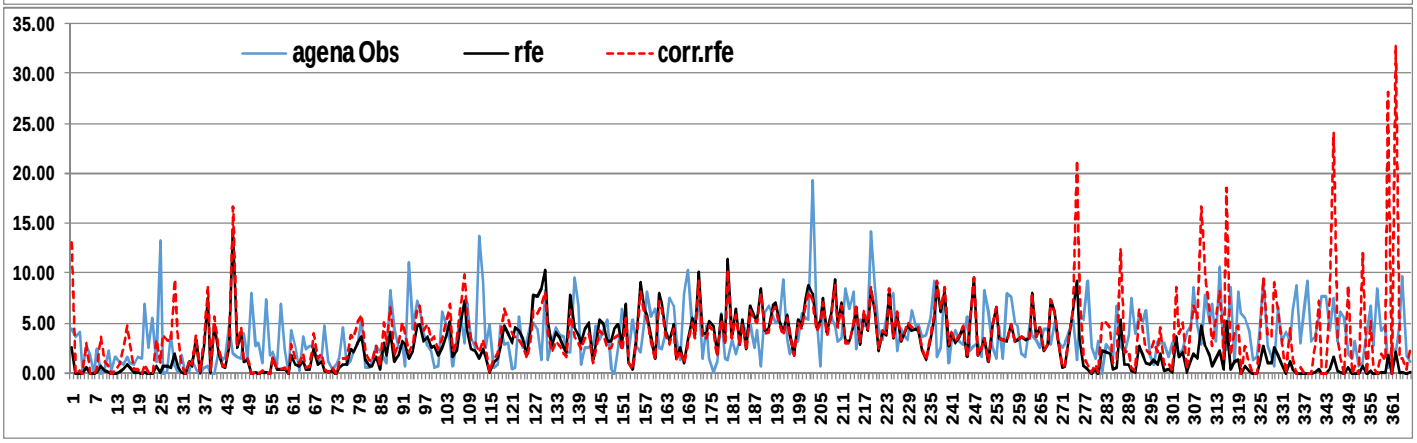
agena Obs
rfe
corr.rfe
35.00
30.00
25.00
20.00
15.00
10.00
5.00
0.00

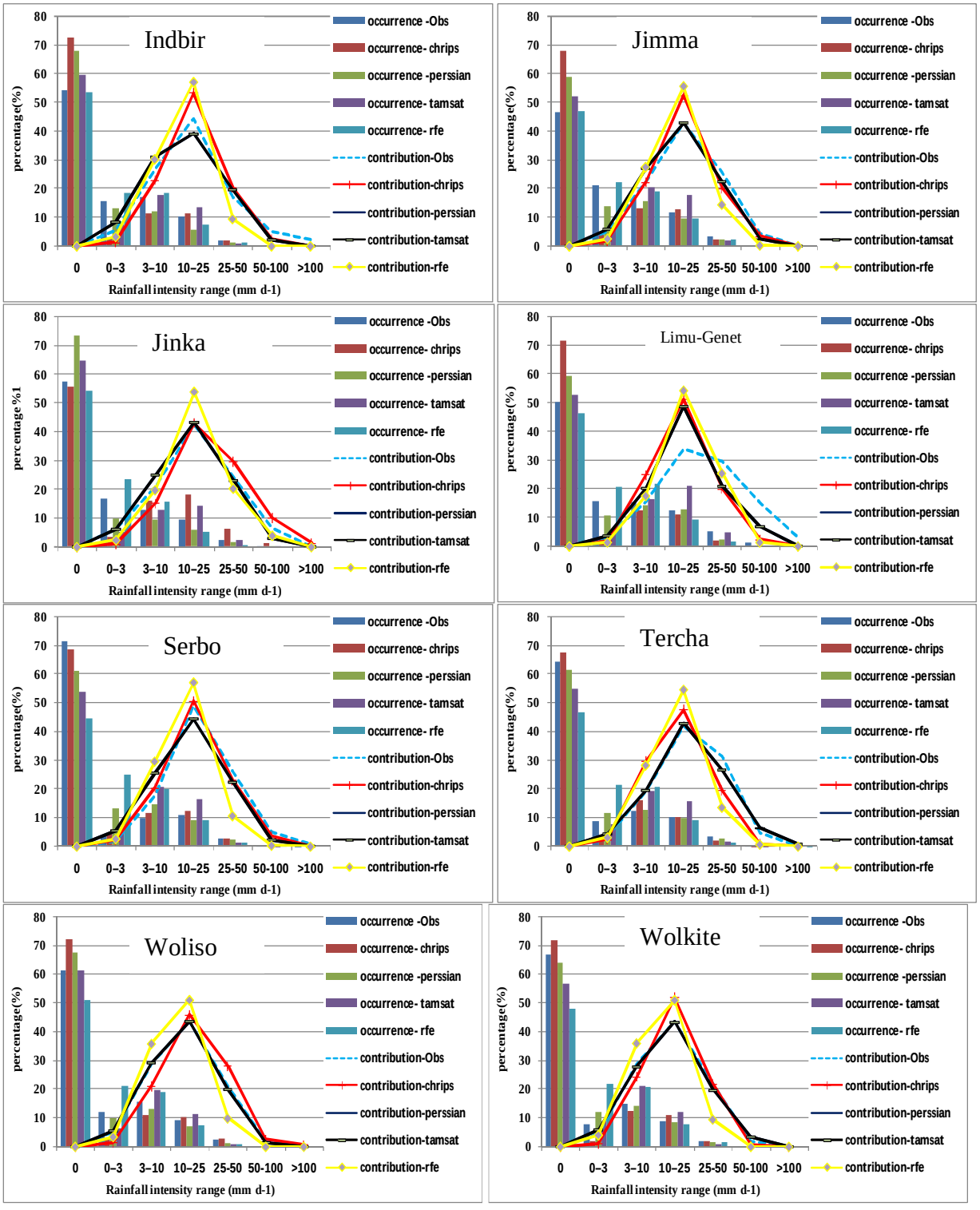
Indbir
Jimma
Jinka
Limu-Genet
Serbo
Tercha
Woliso
Wolkite
percentage(%)
Rainfall intensity range (mm d-1)
0
0–3
3–10
10–25
25-50
50-100
>100
occurrence -Obs
occurrence- chrips
occurrence -perssian
occurrence- tamsat
occurrence- rfe
contribution-Obs
contribution-chrips
contribution-perssian
contribution-tamsat
contribution-rfe

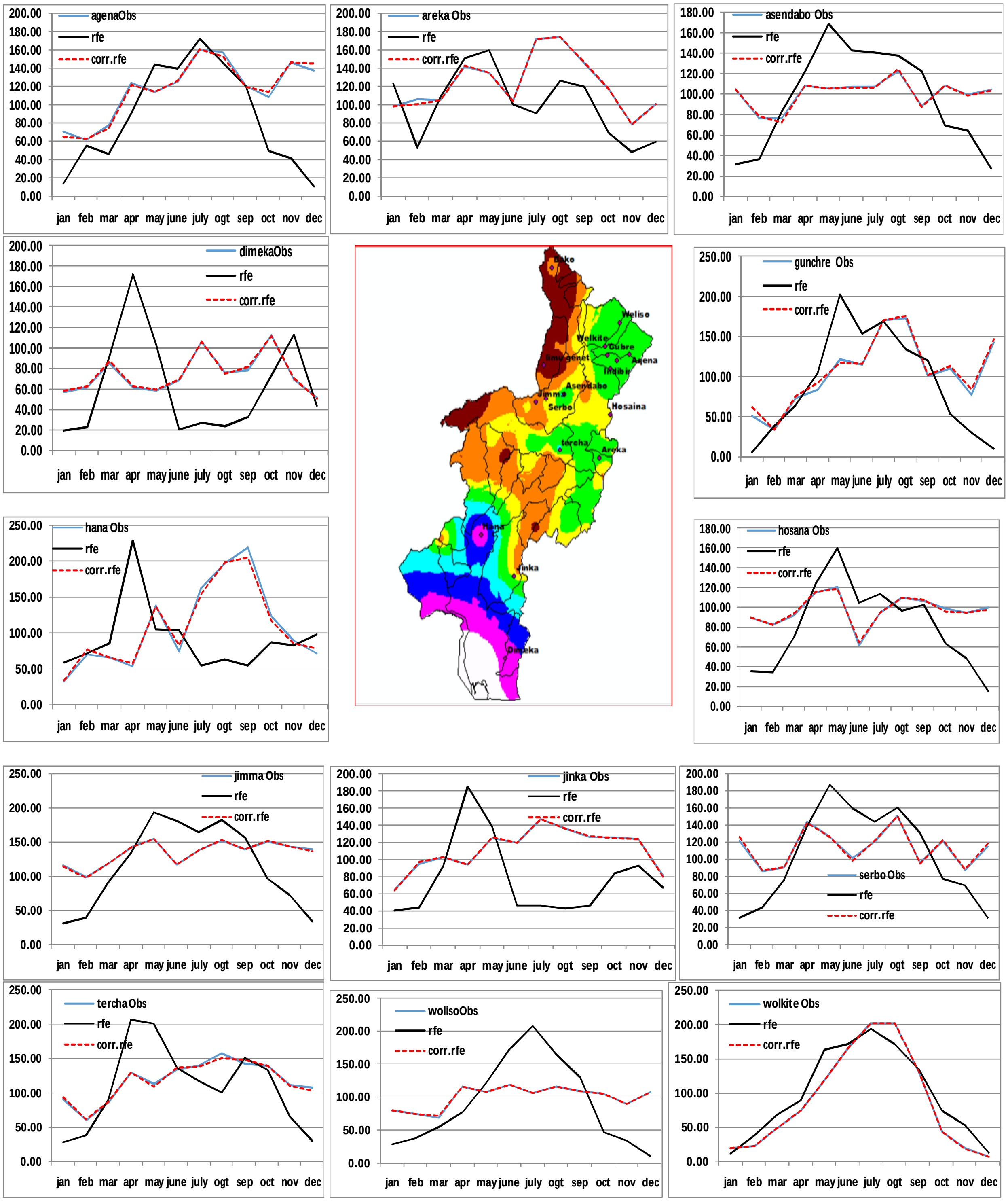
agenaObs
rfe
corr.rfe
arekaObs
rfe
corr.rfe
asendabo Obs
rfe
corr.rfe
dimekaObs
rfe
corr.rfe
gunchre Obs
rfe
corr.rfe
hana Obs
rfe
corr.rfe
hosana Obs
rfe
corr.rfe
jimma Obs
rfe
corr.rfe
jinka Obs
rfe
corr.rfe
serbo Obs
rfe
corr.rfe
tercha Obs
rfe
corr.rfe
wolisoObs
rfe
corr.rfe
wolkite Obs
rfe
corr.rfe
jan feb mar apr may june july ogt sep oct nov dec
Bako
Weliso
Welkite
Gubre
Agena
Imdibir
Asendabo
Jimma
Serbo
Hosaina
tercha
Areka
Hana
Jinka
Dimeka

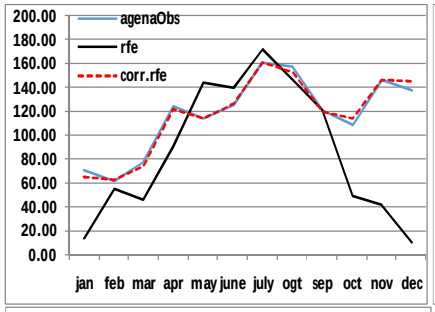
agenaObs
rfe
corr.rfe
jan feb mar apr may june july ogt sep oct nov dec

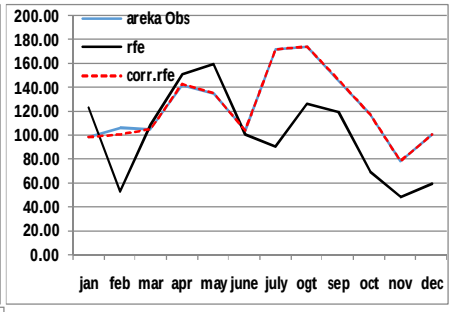
areka Obs
rfe
corr.rfe
jan feb mar apr may june july ogt sep oct nov dec

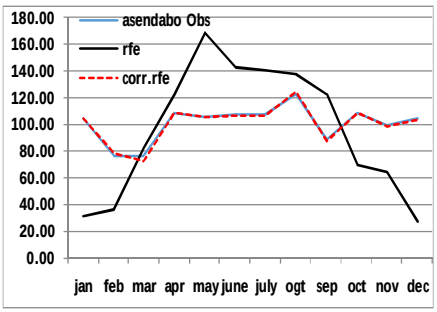
asendabo Obs
rfe
corr.rfe
jan feb mar apr may june july ogt sep oct nov dec

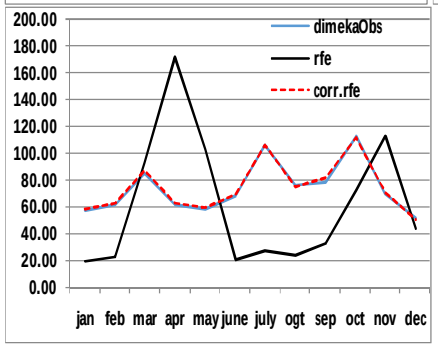
dimekaObs
rfe
corr.rfe
jan feb mar apr may june july ogt sep oct nov dec

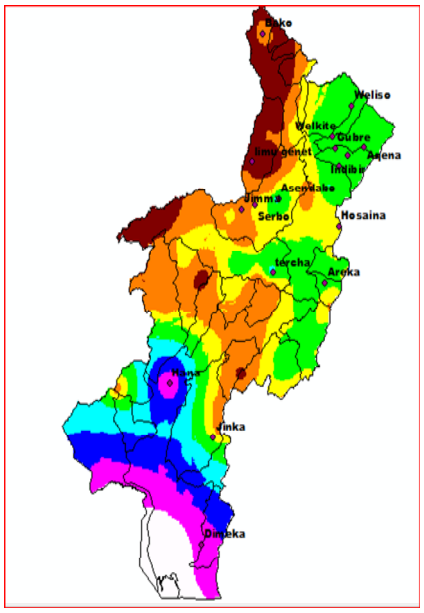
Bako
Weliso
Wolkite
Gubre
Agena
Ilubabi
Asendabo
Jimma
Serbo
Hosaina
tercha
Aroka
Hana
Jinka
Dimeka

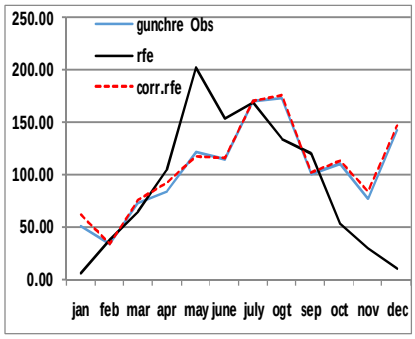
gunchre Obs
rfe
corr.rfe
jan feb mar apr may june july ogt sep oct nov dec

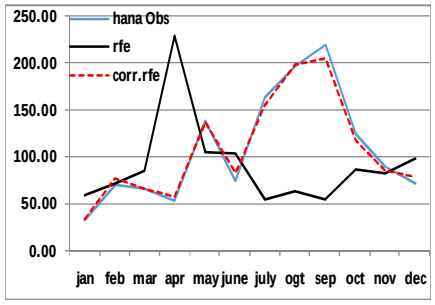
hana Obs
rfe
corr.rfe
jan feb mar apr may june july ogt sep oct nov dec

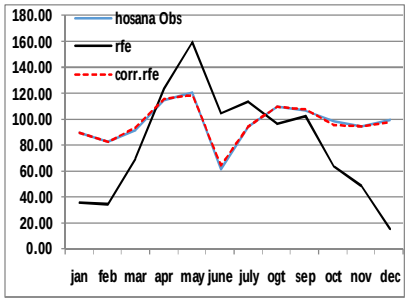
hosana Obs
rfe
corr.rfe
jan feb mar apr may june july ogt sep oct nov dec

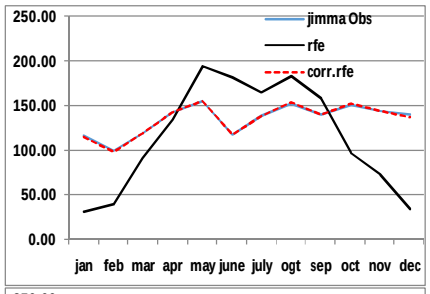
jimma Obs
rfe
corr.rfe
jan feb mar apr may june july ogt sep oct nov dec

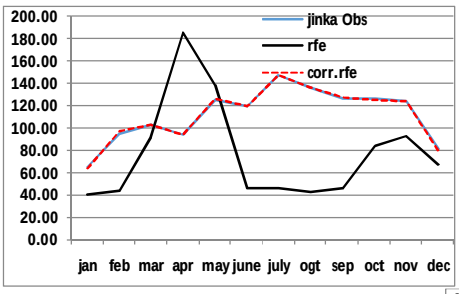
jinka Obs
rfe
corr.rfe
jan feb mar apr may june july ogt sep oct nov dec

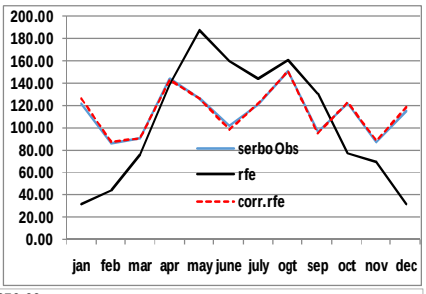
serbo Obs
rfe
corr.rfe
jan feb mar apr may june july ogt sep oct nov dec

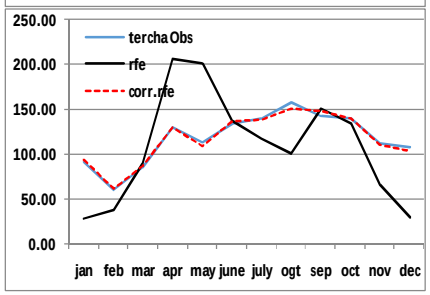
tercha Obs
rfe
corr.rfe
jan feb mar apr may june july ogt sep oct nov dec

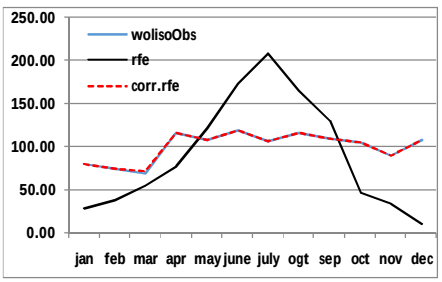
wolisoObs
rfe
corr.rfe
jan feb mar apr may june july ogt sep oct nov dec

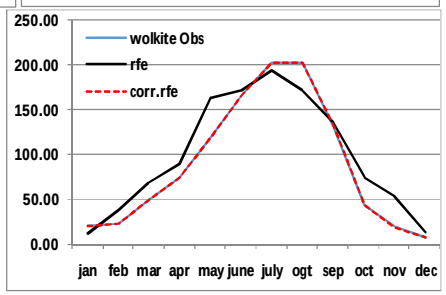
wolkite Obs
rfe
corr.rfe
jan feb mar apr may june july ogt sep oct nov dec

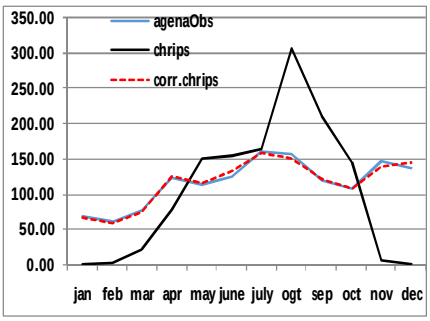
agenaObs
chrips
corr.chrips
jan feb mar apr may june july ogt sep oct nov dec

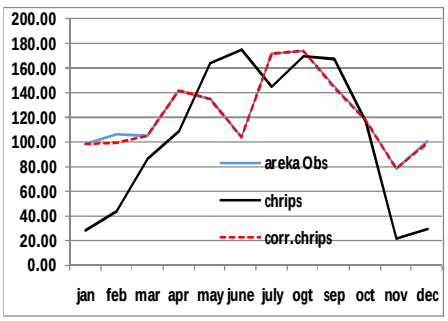
areka Obs
chrips
corr.chrips
jan feb mar apr may june july ogt sep oct nov dec

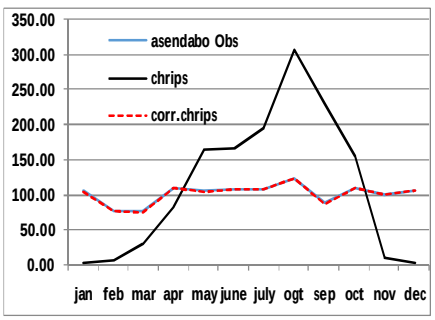
asendabo Obs
chrips
corr.chrips
jan feb mar apr may june july ogt sep oct nov dec

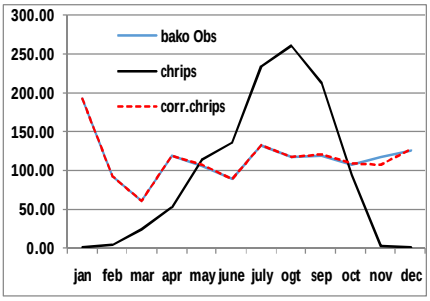
bako Obs
chrips
corr.chrips
jan feb mar apr may june july ogt sep oct nov dec

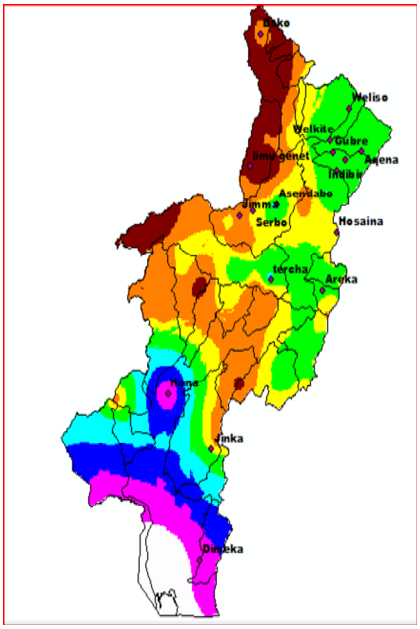
Bako
Welkite
Gubre
Agena
Indibir
Asendabo
Jimma
Serbe
Hosaina
Areka
Jinka
Dimeka

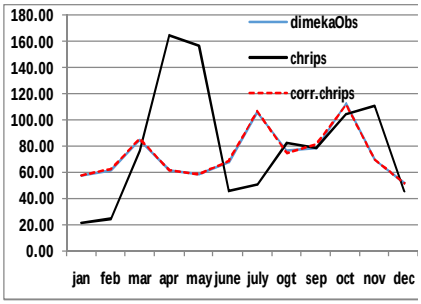
dimekaObs
chrips
corr.chrips
jan feb mar apr may june july ogt sep oct nov dec

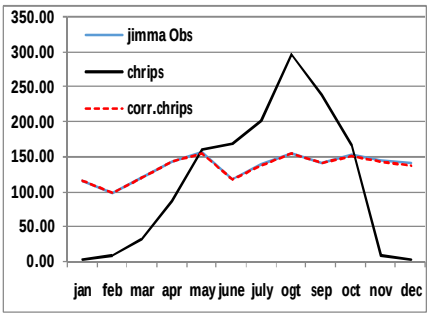
jimma Obs
chrips
corr.chrips
jan feb mar apr may june july ogt sep oct nov dec

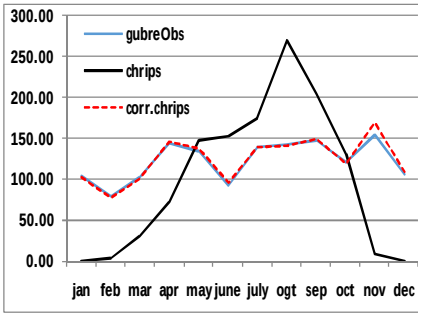
gubreObs
chrips
corr.chrips
jan feb mar apr may june july ogt sep oct nov dec

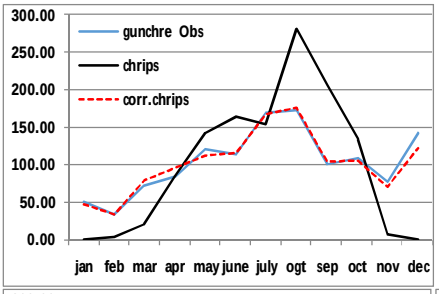
gunchre Obs
chrips
corr.chrips
jan feb mar apr may june july ogt sep oct nov dec

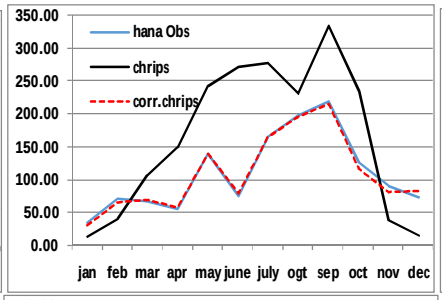
hana Obs
chrips
corr.chrips
jan feb mar apr may june july ogt sep oct nov dec

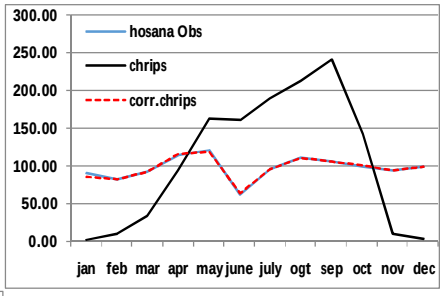
hosana Obs
chrips
corr.chrips
jan feb mar apr may june july ogt sep oct nov dec

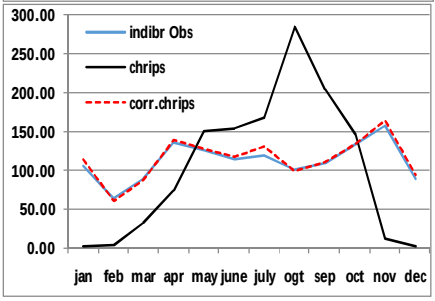
indibr Obs
chrips
corr.chrips
jan feb mar apr may june july ogt sep oct nov dec

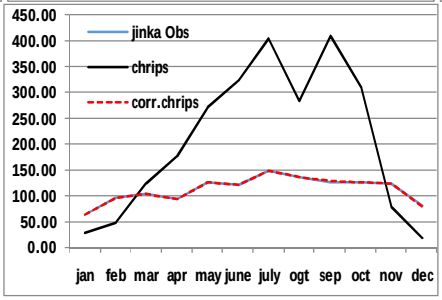
jinka Obs
chrips
corr.chrips
jan feb mar apr may june july ogt sep oct nov dec

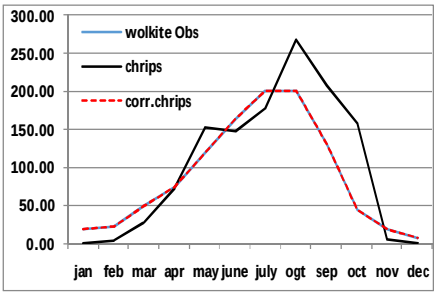
wolkite Obs
chrips
corr.chrips
jan feb mar apr may june july ogt sep oct nov dec

IV statistical indicators for mean daily and monthly data's

	station name		Areka					Station name		Agena			
	statical indicators							statical indicators					
product type	Bias	ME	RMSE	E	POD	FAR	product type	Bias	ME	RMSE	E	POD	FAR
CHIRPS	0.85	-0.58	3.24	-0.88	0.97	0.00	CHIRPS	0.89	-0.4	4.43	-1.69	0.76	0
co.CHIRPS	1.00	-0.02	3.15	-0.78	0.97	0.00	co.CHIRPS	1	-0.02	6.85	-5.45	0.76	0
PERSIANN-CCS	0.81	-0.75	3.52	-1.21	0.97	0.01	PERSIANN-CCS	0.47	-2.02	3.74	-0.92	0.74	0
co.PERSIANN-C	1.00	0.00	3.68	-1.42	0.97	0.01	co.PERSIANN-CCS	0.99	-0.03	8.82	-9.7	0.74	0
TAMSAT	1.02	0.10	3.13	-0.75	0.99	0.01	TAMSAT	0.96	-0.14	4.15	-1.36	0.74	0
co.TAMSAT	1.00	-0.01	2.90	-0.50	0.99	0.01	co.TAMSAT	0.99	-0.04	5.26	-2.8	0.74	0
RFE	0.82	-0.73	3.46	-1.14	1.00	0.01	RFE	0.73	-1.03	3.57	-0.75	0.93	0.01
co.RFE	1.00	-0.01	3.46	-1.14	1.00	0.01	co.RFE	1	0.01	4.47	-1.75	0.93	0.01
	station name		Asendabo					station name		Bako			
	statical indicators							statical indicators					
product type	Bias	ME	RMSE	E	POD	FAR	product type	Bias	ME	RMSE	E	POD	FAR
CHIRPS	1.12	0.39	4.30	-2.95	0.86	0.00	CHIRPS	0.81	-0.68	4.18	-2.87	0.77	0.00
co.CHIRPS	1.00	0.00	3.71	-1.95	0.86	0.00	co.CHIRPS	1.00	-0.01	6.19	-7.51	0.77	0.00
PERSIANN-CCS	0.77	-0.75	3.28	-1.31	0.89	0.00	PERSIANN-CCS	0.76	-0.91	3.76	-2.14	0.83	0.00
co.PERSIANN-C	1.00	-0.01	3.92	-2.29	0.89	0.00	co.PERSIANN-CCS	1.01	0.02	6.56	-8.56	0.83	0.00
TAMSAT	1.21	0.70	4.01	-2.45	0.83	0.00	TAMSAT	1.06	0.26	4.46	-3.41	0.76	0.00
co.TAMSAT	1.00	0.00	3.64	-1.84	0.83	0.00	co.TAMSAT	1.02	0.09	12.21	-32.11	0.76	0.00
RFE	0.95	-0.17	3.01	-0.94	0.97	0.00	RFE	0.92	-0.32	3.81	-2.23	0.94	0.00
co.RFE	1.00	-0.01	3.05	-0.99	0.97	0.00	co.RFE	1.01	0.02	3.84	-2.28	0.94	0.00
	station name		Dimeka					station name		Gunchre			
	statical indicators							statical indicators					
product type	Bias	ME	RMSE	E	POD	FAR	product type	Bias	ME	RMSE	E	POD	FAR
CHIRPS	1.08	0.21	3.15	-1.54	0.83	0.06	CHIRPS	0.96	-0.12	5.07	-1.43	0.64	0.08
co.CHIRPS	1.01	0.01	2.80	-1.00	0.83	0.06	co.CHIRPS	0.99	-0.04	6.39	-2.86	0.64	0.08
PERSIANN-CCS	0.77	-0.57	2.90	-1.14	0.88	0.04	PERSIANN-CCS	0.67	-1.14	4.39	-0.82	0.66	0.08
co.PERSIANN-C	1.00	0.01	3.15	-1.53	0.88	0.04	co.PERSIANN-CCS	1.04	0.13	7.42	-4.19	0.66	0.08
TAMSAT	1.21	0.52	2.94	-1.21	0.94	0.04	TAMSAT	1.00	0.02	4.50	-0.91	0.71	0.05
co.TAMSAT	1.00	0.01	2.44	-0.52	0.94	0.04	co.TAMSAT	0.98	-0.08	5.54	-1.90	0.71	0.05
RFE	0.84	-0.40	3.09	-1.43	0.96	0.05	RFE	0.86	-0.47	4.34	-0.78	0.85	0.09
co.RFE	1.01	0.01	2.71	-0.88	0.96	0.05	co.RFE	1.03	0.10	4.73	-1.11	0.85	0.09
	station name		Gubre					station name		Hana			
	statical indicators							statical indicators					
product type	Bias	ME	RMSE	E	POD	FAR	product type	Bias	ME	RMSE	E	POD	FAR
CHIRPS	0.82	-0.69	4.10	-1.83	0.83	0.02	CHIRPS	1.49	1.75	6.38	-1.21	0.87	0.33
co.CHIRPS	1.01	0.05	4.85	-2.96	0.83	0.02	co.CHIRPS	1.00	-0.01	4.84	-0.27	0.87	0.33
PERSIANN-CCS	0.65	-1.39	3.64	-1.24	0.83	0.01	PERSIANN-CCS	0.85	-0.54	6.34	-1.18	0.79	0.32
co.PERSIANN-C	1.01	0.05	6.57	-6.30	0.83	0.01	co.PERSIANN-CCS	1.00	-0.01	6.19	-1.08	0.79	0.32
TAMSAT	0.92	-0.31	4.13	-1.88	0.79	0.01	TAMSAT	1.26	0.91	6.15	-1.05	0.83	0.28
co.TAMSAT	1.01	0.03	4.55	-2.49	0.79	0.01	co.TAMSAT	0.98	-0.06	5.39	-0.58	0.83	0.28
RFE	0.80	-0.79	3.67	-1.28	0.95	0.01	RFE	0.84	-0.57	5.96	-0.93	0.94	0.33
co.RFE	1.01	0.04	3.88	-1.54	0.95	0.01	co.RFE	0.99	-0.03	5.46	-0.62	0.94	0.33
	station name		Hosana					station name		Indibr			
	statical indicators							statical indicators					
product type	Bias	ME	RMSE	E	POD	FAR	product type	Bias	ME	RMSE	E	POD	FAR
CHIRPS	1.09	0.29	4.07	-2.19	0.83	0.00	CHIRPS	0.92	-0.30	4.98	-1.61	0.75	0.01
co.CHIRPS	1.00	0.00	4.06	-2.17	0.83	0.00	co.CHIRPS	1.03	0.11	5.87	-2.61	0.75	0.01
PERSIANN-CCS	0.69	-0.99	3.40	-1.23	0.83	0.00	PERSIANN-CCS	0.61	-1.44	4.20	-0.85	0.78	0.01
co.PERSIANN-C	0.99	-0.04	4.10	-2.23	0.83	0.00	co.PERSIANN-CCS	1.03	0.10	5.91	-2.66	0.78	0.01
TAMSAT	1.09	0.29	3.66	-1.57	0.82	0.00	TAMSAT	1.03	0.12	4.80	-1.42	0.74	0.01
co.TAMSAT	1.00	0.01	3.54	-1.42	0.82	0.00	co.TAMSAT	1.03	0.10	5.33	-1.98	0.74	0.01
RFE	0.83	-0.55	3.19	-0.96	0.94	0.00	RFE	0.86	-0.51	4.41	-1.04	0.90	0.01
co.RFE	1.00	0.00	3.65	-1.56	0.94	0.00	co.RFE	1.03	0.10	5.80	-2.53	0.90	0.01

	station name		Jimma					station name		Jinka			
	statical indicators							statical indicators					
product type	Bias	ME	RMSE	E	POD	FAR	product type	Bias	ME	RMSE	E	POD	FAR
CHIRPS	0.85	-0.64	4.22	-2.81	0.89	0.00	CHIRPS	1.85	3.12	6.16	-7.44	0.97	0.00
co.CHIRPS	1.00	-0.01	4.31	-2.97	0.89	0.00	co.CHIRPS	1.00	0.00	2.64	-0.55	0.97	0.00
PERSIANN-CCS	0.71	-1.26	3.33	-1.37	0.95	0.00	PERSIANN-CCS	0.57	-1.57	3.46	-1.66	0.93	0.00
co.PERSIANN-C	1.00	0.00	3.88	-2.22	0.95	0.00	co.PERSIANN-CCS	1.00	0.01	3.81	-2.23	0.93	0.00
TAMSAT	1.09	0.39	4.03	-2.47	0.89	0.00	TAMSAT	1.12	0.44	3.33	-1.47	0.94	0.00
co.TAMSAT	1.00	0.00	3.56	-1.71	0.89	0.00	co.TAMSAT	1.00	0.00	3.01	-1.02	0.94	0.00
RFE	0.85	-0.66	3.27	-1.29	0.99	0.00	RFE	0.69	-1.15	3.35	-1.50	1.00	0.00
co.RFE	1.00	-0.01	3.41	-1.49	0.99	0.00	co.RFE	1.00	0.01	3.23	-1.32	1.00	0.00
	station name		limugenet					station name		Serbo			
	statical indicators							statical indicators					
product type	Bias	ME	RMSE	E	POD	FAR	product type	Bias	ME	RMSE	E	POD	FAR
CHIRPS	0.55	-2.68	5.70	-1.17	0.84	0.00	CHIRPS	1.00	0.01	4.44	-1.98	0.85	0.03
co.CHIRPS	1.00	0.01	6.76	-2.04	0.84	0.00	co.CHIRPS	1.00	0.01	4.36	-1.87	0.85	0.03
PERSIANN-CCS	0.67	-1.94	5.27	-0.85	0.86	0.00	PERSIANN-CCS	0.85	-0.57	3.82	-1.21	0.87	0.02
co.PERSIANN-C	1.00	0.02	6.22	-1.58	0.86	0.00	co.PERSIANN-CCS	1.01	0.03	4.89	-2.62	0.87	0.02
TAMSAT	1.03	0.17	6.40	-1.73	0.83	0.00	TAMSAT	1.20	0.78	4.47	-2.02	0.83	0.02
co.TAMSAT	1.00	0.02	6.38	-1.72	0.83	0.00	co.TAMSAT	1.01	0.02	4.41	-1.94	0.83	0.02
RFE	0.62	-2.23	5.02	-0.68	0.97	0.00	RFE	0.92	-0.30	3.44	-0.79	0.98	0.02
co.RFE	1.00	0.01	5.62	-1.11	0.97	0.00	co.RFE	1.00	0.01	3.69	-1.06	0.98	0.02
	station name		Tercha					station name		Woliso			
	statical indicators							statical indicators					
product type	Bias	ME	RMSE	E	POD	FAR	product type	Bias	ME	RMSE	E	POD	FAR
CHIRPS	0.89	-0.41	3.53	-1.03	0.87	0.01	CHIRPS	1.08	0.27	4.06	-4.60	0.79	0.00
co.CHIRPS	1.00	-0.01	3.79	-1.34	0.87	0.01	co.CHIRPS	1.00	0.01	4.59	-6.15	0.79	0.00
PERSIANN-CCS	0.98	-0.09	4.08	-1.71	0.92	0.01	PERSIANN-CCS	0.76	-0.77	3.00	-2.06	0.81	0.00
co.PERSIANN-C	1.00	-0.01	3.86	-1.42	0.92	0.01	co.PERSIANN-CCS	1.00	0.01	4.28	-5.21	0.81	0.00
TAMSAT	1.15	0.58	3.67	-1.19	0.89	0.01	TAMSAT	1.06	0.20	3.72	-3.69	0.79	0.00
co.TAMSAT	1.00	-0.02	3.25	-0.71	0.89	0.01	co.TAMSAT	1.00	0.01	3.37	-2.86	0.79	0.00
RFE	0.92	-0.31	3.48	-0.96	0.97	0.01	RFE	0.91	-0.30	2.95	-1.95	0.96	0.00
co.RFE	0.99	-0.03	3.25	-0.72	0.97	0.01	co.RFE	1.00	0.01	3.45	-3.03	0.96	0.00

	station name		Wolkite			
	statical indicators					
product type	Bias	ME	RMSE	E	POD	FAR
CHIRPS	1.15	0.45	3.22	-0.23	0.87	0.07
co.CHIRPS	1.00	0.00	2.60	0.20	0.87	0.07
PERSIANN-CCS	0.93	-0.20	2.48	0.27	0.91	0.07
co.PERSIANN-C	1.00	0.00	2.43	0.30	0.91	0.07
TAMSAT	1.24	0.69	2.32	0.36	0.85	0.06
co.TAMSAT	1.00	0.00	1.92	0.56	0.85	0.06
RFE	1.12	0.34	2.32	0.36	0.97	0.11
co.RFE	1.00	0.00	2.12	0.47	0.97	0.11

	station name		Agena					station name		Areka			
	statical indicators							statical indicators					
product type	Bias	ME	RMSE	E	POD	FAR	product type	Bias	ME	RMSE	E	POD	FAR
CHIRPS	0.89	-0.86	73.41	-4.36	1.00	0.00	CHIRPS	0.85	-13.27	43.38	-1.25	1.00	0.00
co.CHIRPS	1.00	-0.55	4.59	0.98	1.00	0.00	co.CHIRPS	1.00	-0.58	1.92	1.00	1.00	0.00
PERSIANN-CCS	0.47	-61.48	71.39	-4.07	1.00	0.00	PERSIANN-CCS	0.81	-22.97	41.05	-1.02	1.00	0.00
co.PERSIANN-CCS	0.99	-1.03	5.21	0.97	1.00	0.00	co.PERSIANN-CC	1.00	-0.02	2.15	0.99	1.00	0.00
TAMSAT	0.96	5.09	69.20	-3.76	1.00	0.00	TAMSAT	1.02	5.10	31.21	-0.16	1.00	0.00
co.TAMSAT	0.99	-1.12	4.83	0.98	1.00	0.00	co.TAMSAT	1.00	-0.24	1.66	1.00	1.00	0.00
RFE	0.73	-31.39	55.83	-2.10	1.00	0.00	RFE	0.82	-22.41	39.39	-0.86	1.00	0.00
co.RFE	1.00	0.28	3.64	0.99	1.00	0.00	co.RFE	1.00	-0.21	1.64	1.00	1.00	0.00
	station name		Asendabo					station name		Bako			
	statical indicators							statical indicators					
product type	Bias	ME	RMSE	E	POD	FAR	product type	Bias	ME	RMSE	E	POD	FAR
CHIRPS	1.12	19.33	91.16	-45.83	1.00	0.00	CHIRPS	0.81	-11.75	94.93	-9.06	1.00	0.00
co.CHIRPS	1.00	-0.05	0.69	1.00	1.00	0.00	co.CHIRPS	1.00	-0.43	2.67	0.99	1.00	0.00
PERSIANN-CCS	0.77	-23.00	55.02	-16.06	1.00	0.00	PERSIANN-CCS	0.76	-27.72	86.86	-7.42	1.00	0.00
co.PERSIANN-CCS	1.00	-0.44	1.66	0.98	1.00	0.00	co.PERSIANN-CC	1.01	0.62	4.09	0.98	1.00	0.00
TAMSAT	1.21	25.39	87.29	-41.93	1.00	0.00	TAMSAT	1.06	12.82	116.14	-14.06	1.00	0.00
co.TAMSAT	1.00	0.01	1.45	0.99	1.00	0.00	co.TAMSAT	1.02	2.64	8.81	0.91	1.00	0.00
RFE	0.95	-5.20	44.43	-10.12	1.00	0.00	RFE	0.92	-9.78	88.42	-7.73	1.00	0.00
co.RFE	1.00	-0.22	1.34	0.99	1.00	0.00	co.RFE	1.01	0.59	1.39	1.00	1.00	0.00
	station name		Dimeka					station name		Gunchre			
	statical indicators							statical indicators					
product type	Bias	ME	RMSE	E	POD	FAR	product type	Bias	ME	RMSE	E	POD	FAR
CHIRPS	1.08	2.61	47.07	-5.72	1.00	0.00	CHIRPS	0.96	1.87	66.07	-1.53	1.00	0.00
co.CHIRPS	1.01	0.43	1.23	1.00	1.00	0.00	co.CHIRPS	0.99	-1.27	7.91	0.96	1.00	0.00
PERSIANN-CCS	0.77	-17.30	52.01	-7.20	1.00	0.00	PERSIANN-CCS	0.67	-34.69	54.52	-0.72	1.00	0.00
co.PERSIANN-CCS	1.00	0.23	1.25	1.00	1.00	0.00	co.PERSIANN-CC	1.04	3.98	9.86	0.94	1.00	0.00
TAMSAT	1.21	9.97	42.89	-4.57	1.00	0.00	TAMSAT	1.00	4.62	59.39	-1.04	0.92	0.00
co.TAMSAT	1.00	0.34	1.01	1.00	1.00	0.00	co.TAMSAT	0.98	-2.47	15.39	0.86	0.92	0.00
RFE	0.84	-12.10	53.23	-7.59	1.00	0.00	RFE	0.86	-14.31	54.48	-0.72	1.00	0.00
co.RFE	1.01	0.40	1.32	0.99	1.00	0.00	co.RFE	1.03	2.93	5.12	0.98	1.00	0.00
	station name		Gubre					station name		Hana			
	statical indicators							statical indicators					
product type	Bias	ME	RMSE	E	POD	FAR	product type	Bias	ME	RMSE	E	POD	FAR
CHIRPS	0.82	-9.23	72.13	-8.39	1.00	0.00	CHIRPS	1.49	57.65	92.99	-1.67	1.00	0.00
co.CHIRPS	1.01	1.45	4.86	0.96	1.00	0.00	co.CHIRPS	1.00	-0.33	5.17	0.99	1.00	0.00
PERSIANN-CCS	0.65	-42.42	66.63	-7.01	1.00	0.00	PERSIANN-CCS	0.85	-16.35	97.05	-1.91	1.00	0.00
co.PERSIANN-CCS	1.01	1.39	2.89	0.98	1.00	0.00	co.PERSIANN-CC	1.00	-0.36	8.14	0.98	1.00	0.00
TAMSAT	0.92	-0.06	83.17	-11.49	1.00	0.00	TAMSAT	1.26	21.97	75.18	-0.75	1.00	0.00
co.TAMSAT	1.01	0.98	2.55	0.99	1.00	0.00	co.TAMSAT	0.98	-1.92	6.79	0.99	1.00	0.00
RFE	0.80	-23.96	59.85	-5.47	1.00	0.00	RFE	0.84	-17.29	87.50	-1.37	1.00	0.00
co.RFE	1.01	1.11	2.03	0.99	1.00	0.00	co.RFE	0.99	-0.82	6.18	0.99	1.00	0.00
	station name		Hosana					station name		Indibir			
	statical indicators							statical indicators					
product type	Bias	ME	RMSE	E	POD	FAR	product type	Bias	ME	RMSE	E	POD	FAR
CHIRPS	1.09	15.77	80.19	-27.50	1.00	0.00	CHIRPS	0.92	2.93	79.79	-10.33	1.00	0.00
co.CHIRPS	1.00	0.12	1.73	0.99	1.00	0.00	co.CHIRPS	1.03	3.23	5.39	0.95	1.00	0.00
PERSIANN-CCS	0.69	-30.10	51.41	-10.71	1.00	0.00	PERSIANN-CCS	0.61	-43.96	68.28	-7.30	1.00	0.00
co.PERSIANN-CCS	0.99	-1.16	2.90	0.96	1.00	0.00	co.PERSIANN-CC	1.03	3.06	7.77	0.89	1.00	0.00
TAMSAT	1.09	13.96	62.79	-16.48	1.00	0.00	TAMSAT	1.03	14.19	85.09	-11.89	1.00	0.00
co.TAMSAT	1.00	0.36	1.70	0.99	1.00	0.00	co.TAMSAT	1.03	3.08	4.72	0.96	1.00	0.00
RFE	0.83	-16.82	41.30	-6.56	1.00	0.00	RFE	0.86	-15.64	54.44	-4.28	1.00	0.00
co.RFE	1.00	-0.07	1.68	0.99	1.00	0.00	co.RFE	1.03	3.17	4.49	0.96	1.00	0.00

	station name		Jimma					station name		Jinka			
	statical indicators							statical indicators					
product type	Bias	ME	RMSE	E	POD	FAR	product type	Bias	ME	RMSE	E	POD	FAR
CHIRPS	0.85	-8.40	85.47	-23.66	1.00	0.00	CHIRPS	1.85	98.83	153.25	-41.66	1.00	0.00
co.CHIRPS	1.00	-0.32	0.96	1.00	1.00	0.00	co.CHIRPS	1.00	0.05	0.41	1.00	1.00	0.00
PERSIANN-CCS	0.71	-38.47	64.08	-12.86	1.00	0.00	PERSIANN-CCS	0.57	-47.88	70.51	-8.03	1.00	0.00
co.PERSIANN-CCS	1.00	-0.03	0.83	1.00	1.00	0.00	co.PERSIANN-CC	1.00	0.22	0.61	1.00	1.00	0.00
TAMSAT	1.09	15.04	90.17	-26.45	1.00	0.00	TAMSAT	1.12	10.21	46.70	-2.96	1.00	0.00
co.TAMSAT	1.00	-0.13	0.46	1.00	1.00	0.00	co.TAMSAT	1.00	0.07	0.41	1.00	1.00	0.00
RFE	0.85	-20.17	56.53	-9.79	1.00	0.00	RFE	0.69	-35.14	62.15	-6.02	1.00	0.00
co.RFE	1.00	-0.27	0.89	1.00	1.00	0.00	co.RFE	1.00	0.37	0.99	1.00	1.00	0.00

	station name		Limu-genet					station name		Serbo			
	statical indicators							statical indicators					
product type	Bias	ME	RMSE	E	POD	FAR	product type	Bias	ME	RMSE	E	POD	FAR
CHIRPS	0.55	-68.28	104.06	-7.42	1.00	0.00	CHIRPS	1.00	6.61	90.12	-18.39	1.00	0.00
co.CHIRPS	1.00	0.28	2.52	1.00	1.00	0.00	co.CHIRPS	1.00	0.20	2.79	0.98	1.00	0.00
PERSIANN-CCS	0.67	-59.02	99.28	-6.66	1.00	0.00	PERSIANN-CCS	0.85	-17.25	61.75	-8.10	1.00	0.00
co.PERSIANN-CCS	1.00	0.61	3.09	0.99	1.00	0.00	co.PERSIANN-CC	1.01	0.93	4.05	0.96	1.00	0.00
TAMSAT	1.03	14.26	141.74	-14.61	1.00	0.00	TAMSAT	1.20	24.25	95.84	-20.93	1.00	0.00
co.TAMSAT	1.00	0.74	2.32	1.00	1.00	0.00	co.TAMSAT	1.01	0.60	3.58	0.97	1.00	0.00
RFE	0.62	-68.05	93.86	-5.85	1.00	0.00	RFE	0.92	-9.24	48.63	-4.65	1.00	0.00
co.RFE	1.00	0.19	2.04	1.00	1.00	0.00	co.RFE	1.00	0.44	1.95	0.99	1.00	0.00

	station name		Tercha					station name		Woliso			
	statical indicators							statical indicators					
product type	Bias	ME	RMSE	E	POD	FAR	product type	Bias	ME	RMSE	E	POD	FAR
CHIRPS	0.89	-4.74	56.23	-3.36	1.00	0.00	CHIRPS	1.08	15.12	89.96	-28.84	1.00	0.00
co.CHIRPS	1.00	-0.35	3.16	0.99	1.00	0.00	co.CHIRPS	1.00	0.40	1.01	1.00	1.00	0.00
PERSIANN-CCS	0.98	-2.67	71.22	-5.99	1.00	0.00	PERSIANN-CCS	0.76	-23.53	60.45	-12.47	1.00	0.00
co.PERSIANN-CCS	1.00	-0.21	2.17	0.99	1.00	0.00	co.PERSIANN-CC	1.00	0.45	1.32	0.99	1.00	0.00
TAMSAT	1.15	21.85	61.69	-4.24	1.00	0.00	TAMSAT	1.06	11.54	91.74	-30.03	1.00	0.00
co.TAMSAT	1.00	-0.51	2.15	0.99	1.00	0.00	co.TAMSAT	1.00	0.30	0.73	1.00	1.00	0.00
RFE	0.92	-9.53	49.65	-2.40	1.00	0.00	RFE	0.91	-9.11	56.36	-10.71	1.00	0.00
co.RFE	0.99	-0.82	3.24	0.99	1.00	0.00	co.RFE	1.00	0.19	0.97	1.00	1.00	0.00

	station name		Wolkite			
	statical indicators					
product type	Bias	ME	RMSE	E	POD	FAR
CHIRPS	1.15	14.88	46.74	0.55	1.00	0.00
co.CHIRPS	1.00	0.02	0.12	1.00	1.00	0.00
PERSIANN-CCS	0.93	-6.14	24.95	0.87	1.00	0.00
co.PERSIANN-CCS	1.00	0.11	0.37	1.00	1.00	0.00
TAMSAT	1.24	19.83	33.77	0.76	1.00	0.00
co.TAMSAT	1.00	0.04	0.14	1.00	1.00	0.00
RFE	1.12	10.32	22.08	0.90	1.00	0.00
co.RFE	1.00	0.06	0.13	1.00	1.00	0.00

\

V Mean monthly statics of different rainfall products for the stations

Agena

Variable	N	N*	Mean	SE Mean	StDev	CoefVar	Minimum	Q1	Median	Q3	Maximum	IQR
agenaObs	12	0	116.9	9.56	33.13	28.34	61.29	84.65	122.18	144.47	161.23	59.82
chrips	12	0	104.3	28.8	99.8	95.67	1.6	4.8	112.3	162.4	305.9	157.6
corr.chrips	12	0	116.35	9.69	33.55	28.84	58.3	82.53	123.5	143.01	159.07	60.48
perssian	12	0	55.4	12.6	43.8	78.96	0.1	16.2	50.9	98.5	121.9	82.3
corre.perss	12	0	115.87	9.83	34.05	29.38	63.39	80.84	120.17	143.01	165.14	62.17
tamsat	12	0	112.3	27.6	95.7	85.25	4.1	28.4	89.3	203.4	264.7	174.9
corr.tamsa	12	0	115.8	10	34.7	30.01	56.9	82.8	119.1	146.8	161.2	64
rfe	12	0	85.5	16.4	56.7	66.32	9.9	42.6	72.5	142.6	171.7	100
corr.rfe	12	0	117.18	9.76	33.79	28.84	62.81	83.89	121.23	146.36	160.87	62.47

Areka

Variable	N	N*	Mean	SE Mean	StDev	CoefVar	Minimum	Q1	Median	Q3	Maximum	IQR
areka Obs	12	0	122.91	8.72	30.2	24.57	78.2	101.37	111.12	143.86	173.8	42.49
chrips	12	0	104.8	17.6	61.1	58.29	21.6	33	112.6	166.8	175.6	133.9
corr.chrips	12	0	122.33	8.85	30.66	25.07	78.2	99.26	110.99	143.64	173.8	44.39
perssian	12	0	99.9	13.6	47	46.98	34.8	63.5	94.5	144	181.3	80.6
corre.perss	12	0	122.89	8.93	30.92	25.16	78.2	99.53	110.99	145.87	173.8	46.34
tamsat	12	0	125.8	15.9	54.9	43.65	54	63.2	141	176.1	202.1	112.9
corr.tamsa	12	0	122.68	8.88	30.75	25.07	78.2	99.96	110.99	145.11	173.8	45.15
rfe	12	0	100.5	10.9	37.6	37.42	47.8	61.4	104.4	125.2	159.6	63.8
corr.rfe	12	0	122.7	8.87	30.74	25.06	78.2	100.08	110.99	145.12	173.8	45.05

Asendabo

Variable	N	N*	Mean	SE Mean	StDev	CoefVar	Minimum	Q1	Median	Q3	Maximum	IQR
asendabo (	12	0	100.86	4.02	13.91	13.8	76.16	90.78	105.12	108.27	123.02	17.5
chrips	12	0	112.5	30.1	104.4	92.82	2.2	7	118.3	188.1	306.8	181.1
corr.chrips	12	0	100.81	4.04	14.01	13.9	75.55	90.52	105.19	108.93	122.73	18.41
perssian	12	0	77.9	15.9	55.1	70.8	6.3	20.6	83	129.8	163.6	109.2
corre.perss	12	0	100.42	4.19	14.5	14.44	72.16	90.29	104.96	108.02	124.65	17.73
tamsat	12	0	121.8	27.5	95.1	78.07	14	27.5	93.7	222.3	280.8	194.9
corr.tamsa	12	0	100.86	4.3	14.91	14.78	72.99	90.95	105.79	108.24	125.8	17.29
rfe	12	0	95.7	14.3	49.4	51.64	27.6	43.9	102.3	140	168.7	96
corr.rfe	12	0	100.64	4.13	14.31	14.22	72.76	90.67	105.15	108.31	124.41	17.64

Bako

Variable	N	N*	Mean	SE Mean	StDev	CoefVar	Minimum	Q1	Median	Q3	Maximum	IQR
bako Obs	12	0	115.75	9.02	31.26	27.01	61.35	96.55	118.06	125.13	193.13	28.58
chrips	12	0	94.2	28.1	97.2	103.24	0.2	2.4	72.7	192.7	260.6	190.4
corr.chrips	12	0	115.32	9.04	31.3	27.14	61.49	96.56	113.82	126.05	193.24	29.49
perssian	12	0	88	21.7	75.3	85.57	6.2	20	55.9	172.8	193.9	152.8
corre.perss	12	0	116.37	9.91	34.35	29.51	61.07	96.7	116.81	124	206.89	27.3
tamsat	12	0	123	33.8	117	95.08	1.2	15.8	77.2	226.5	330.5	210.7
corr.tamsa	12	0	118.4	11.1	38.3	32.35	61.2	98.3	117.3	124.5	223.5	26.2
rfe	12	0	106	23.5	81.4	76.85	10.1	30.4	81.8	197	214.9	166.6
corr.rfe	12	0	116.34	9.27	32.1	27.59	61.79	96.9	117.48	125.42	197.39	28.52

Dimeka

Variable	N	N*	Mean	SE Mean	StDev	CoefVar	Minimum	Q1	Median	Q3	Maximum	IQR
dimekaObs	12	0	74.13	5.48	18.97	25.6	51.96	59.59	69.08	83.4	112.77	23.82
chrips	12	0	80	13.6	47	58.83	21.4	45.1	77.5	109	164.3	63.9
corr.chrips	12	0	74.56	5.52	19.12	25.64	51.97	59.85	69.4	85.24	111.91	25.38
perssian	12	0	56.8	13.9	48.2	84.79	13.8	20.7	25.8	89.7	158.8	69.1
corre.perss	12	0	74.36	5.48	18.97	25.52	51.65	59.97	69.19	84.91	111.21	24.94
tamsat	12	0	89.5	13.8	47.7	53.35	20.8	38	89.7	135.9	153.8	98
corr.tamsa	12	0	74.46	5.41	18.74	25.16	51.78	60.2	70.55	84.21	111.52	24.01
rfe	12	0	62	14.1	49	79.01	19.2	22.6	38.4	100.4	172.2	77.8
corr.rfe	12	0	74.53	5.51	19.08	25.6	50.43	60.25	70.02	85.4	111.7	25.15

Gunchre

Variable	N	N*	Mean	SE Mean	StDev	CoefVar	Minimum	Q1	Median	Q3	Maximum	IQR
gunchre O	12	0	104.4	12.5	43.4	41.57	34.5	74	105.8	137.4	172.8	63.3
chrips	12	0	100.4	27.2	94.2	93.84	1.1	5.8	109.7	161.8	281.4	156
corr.chrips	12	0	103.2	12.3	42.4	41.14	34.2	73.3	105.4	121.4	176.6	48.1
perssian	12	0	69.8	15	52	74.6	1	22.2	59.6	115.6	144.1	93.4
corre.perss	12	0	108.4	12	41.5	38.27	32.8	80.1	104.2	142.6	178.2	62.6
tamsat	12	0	104.7	25.2	87.4	83.41	0	29.4	80	173.1	246.8	143.7
corr.tamsa	12	0	102	14.7	51.1	50.09	0	78.3	107.2	142.3	176.5	64
rfe	12	0	90.1	19.1	66	73.22	5.5	31.1	84.5	148.8	202.4	117.7
corr.rfe	12	0	107.4	12.2	42.1	39.22	33.9	78.4	107.6	139.3	175.8	60.9

Gubre

Variable	N	N*	Mean	SE Mean	StDev	CoefVar	Minimum	Q1	Median	Q3	Maximum	IQR
gubreObs	12	0	121.83	7.1	24.58	20.18	79.05	102.3	126.84	143.26	153.68	40.96
chrips	12	0	100.4	26.7	92.7	92.26	1	5.3	102.4	169.6	270.2	164.3
corr.chrips	12	0	123.29	7.78	26.93	21.85	77.18	100.1	127.92	143.54	168.86	43.44
perssian	12	0	79.4	17.6	60.9	76.75	2.8	18.9	67.2	136.7	179	117.8
corre.perss	12	0	123.22	7.29	25.24	20.49	79.76	102.22	127.12	144.18	160.52	41.96
tamsat	12	0	112.1	29	100.5	89.7	4.7	19.6	82.8	193.2	292.6	173.6
corr.tamsa	12	0	122.81	7.27	25.18	20.5	80.68	100.7	128.05	143.25	159.84	42.55
rfe	12	0	97.9	18.3	63.5	64.88	10.8	39.3	85.4	151	198.2	111.6
corr.rfe	12	0	122.94	7.17	24.84	20.21	79.91	102.78	128.62	145.53	155.73	42.75

Hana

Variable	N	N*	Mean	StDev	CoefVar	Minimum	Q1	Median	Q3	Maximum	IQR
hana Obs	12	0	108.5	59.4	54.75	33	67.2	82	157.2	218.4	90
chrips	12	0	161.6	116.7	72.2	11.5	37.1	188.6	263.6	333	226.6
corr.chrips	12	0	108.1	58.1	53.74	30.8	66.8	82.3	157.7	214.5	90.9
perssian	12	0	92.1	67.8	73.56	27.9	43.4	64.4	137.9	256.3	94.5
corre.perss	12	0	108.1	55.1	50.97	33.6	70	88.3	159.6	201.1	89.6
tamsat	12	0	136.2	68.4	50.21	19.2	61.7	164.6	174.4	223.2	112.8
corr.tamsa	12	0	106.6	55.5	52.12	31	66.9	85.2	157.1	202.6	90.2
rfe	12	0	91.2	46.8	51.35	55	60	84	102.3	228.3	42.3
corr.rfe	12	0	107.7	55.3	51.33	33.9	68.3	83.7	150.8	204.7	82.5

Hosana

Variable	N	N*	Mean	StDev	CoefVar	Minimum	Q1	Median	Q3	Maximum	IQR
hosana Ob	12	0	97.32	15.69	16.12	61.89	90.38	97.1	109.56	121.11	19.18
chrips	12	0	106	90.1	85	2.9	11	119.3	183.4	241.4	172.4
corr.chrips	12	0	97.44	15.61	16.02	63.81	87.52	97.18	110.8	119.89	23.28
perssian	12	0	67.2	46.6	69.26	4	24.2	71.1	107	140.5	82.9
corre.perss	12	0	96.17	15.69	16.31	61.11	88.22	94.68	110.54	116.53	22.31
tamsat	12	0	105.9	70.5	66.59	11	34.3	109.8	167.6	210.1	133.2
corr.tamsa	12	0	97.68	15.24	15.6	63.49	90.25	96.48	111.26	118.11	21.02
rfe	12	0	80.5	43.2	53.72	15	38.4	82.9	111.2	160	72.8
corr.rfe	12	0	97.26	14.99	15.42	64.66	90.65	95.58	109.66	119.04	19

Indibr

Variable	N	N*	Mean	StDev	CoefVar	Minimum	Q1	Median	Q3	Maximum	IQR
indibr Obs	12	0	111.65	24.75	22.17	63.75	92.4	111.36	131.19	156.87	38.78
chrips	12	0	102.3	94.5	92.38	1.5	5.4	109.4	163.1	283.9	157.7
corr.chrips	12	0	114.88	27.27	23.74	60.47	95.68	115.69	133.26	164.24	37.58
perssian	12	0	67.7	55.5	82.01	2.1	13.8	64.9	110.2	150.3	96.5
corre.perss	12	0	114.71	28.39	24.75	67.08	99.1	112	135.77	167.24	36.67
tamsat	12	0	115	97.2	84.52	4.3	22.8	92.9	206.7	276.1	183.9
corr.tamsa	12	0	114.73	25.54	22.26	66.31	98.39	112.28	133.02	162.07	34.63
rfe	12	0	96	57.2	59.56	7.7	47.1	81.8	146.8	185	99.6
corr.rfe	12	0	114.82	24.9	21.69	68.88	96.73	111.75	131.79	164.54	35.06

Jimma

Variable	N	N*	Mean	StDev	CoefVar	Minimum	Q1	Median	Q3	Maximum	IQR
jimma Obs	12	0	134.91	17.98	13.33	98.76	117.73	140.62	150.14	155.69	32.41
chrips	12	0	115.1	104.2	90.55	3	8.6	124.9	194.3	297.7	185.8
corr.chrips	12	0	134.58	18.17	13.5	97.82	117.7	139.32	150.2	155.59	32.5
perssian	12	0	96.4	59.4	61.6	13.9	39.1	96.2	147.6	195.6	108.5
corre.perss	12	0	134.88	18.17	13.47	97.82	117.93	141.69	149.71	155.45	31.77
tamsat	12	0	146.6	101.2	69.01	19.1	42.6	126.9	246.6	295.5	204
corr.tamsa	12	0	134.77	18.16	13.47	97.82	117.77	140.69	150.33	155.59	32.55
rfe	12	0	114.7	61.6	53.71	31.2	47.7	115.3	176.6	193.7	128.9
corr.rfe	12	0	134.64	18.2	13.52	97.82	117.7	139.43	150.55	155.57	32.85

Jinka

Variable	N	N*	Mean	StDev	CoefVar	Minimum	Q1	Median	Q3	Maximum	IQR
jinka Obs	12	0	111.95	24.51	21.89	64.43	93.83	121.91	126.65	147.74	32.82
chrips	12	0	206.8	145.7	70.48	18.4	55.9	224.4	320.5	410.5	264.6
corr.chrips	12	0	112	24.62	21.98	64.4	94.42	121.91	127.08	147.74	32.66
perssian	12	0	64.1	48.3	75.36	25.4	28.1	38.6	94.9	182.5	66.8
corre.perss	12	0	112.17	24.65	21.98	64.61	94.16	121.91	127.73	147.74	33.57
tamsat	12	0	125	61.8	49.46	26.3	58	136.4	171.9	205	113.9
corr.tamsa	12	0	112.02	24.64	22	64.35	94.29	121.91	127.21	147.74	32.92
rfe	12	0	76.8	45.6	59.33	40.1	43.8	56.4	92.5	185.6	48.6
corr.rfe	12	0	112.32	24.46	21.78	64.37	95.45	121.91	127.31	147.74	31.87

Limugenet

Variable	N	N*	Mean	StDev	CoefVar	Minimum	Q1	Median	Q3	Maximum	IQR
limu genet	12	0	181.1	37.5	20.68	119.5	149.7	175.6	209.9	243	60.1
chrips	12	0	98.8	90.4	91.54	1.6	6.7	102.6	161.4	267.6	154.7
corr.chrips	12	0	181.4	37.8	20.84	120	152.8	175.9	206.9	244.8	54.1
perssian	12	0	122.1	90.8	74.38	9.2	26.6	118.6	213.4	236.6	186.8
corre.perss	12	0	181.7	38.8	21.32	115.2	152.8	175.1	210.5	243.7	57.7
tamsat	12	0	185.9	167.5	90.1	11.4	32.2	132.5	317.1	470.5	284.9
corr.tamsa	12	0	181.9	38.6	21.24	115.7	151.6	176.7	209.9	245.1	58.3
rfe	12	0	113.1	70.8	62.59	19.2	40.1	100.5	184.2	204.9	144.1
corr.rfe	12	0	181.3	38.3	21.12	117.1	152.8	175.5	207.9	245.8	55.1

Serbo

Variable	N	N*	Mean	StDev	CoefVar	Minimum	Q1	Median	Q3	Maximum	IQR
sebo Obs	12	0	113.52	21.37	18.83	86.37	91.98	117.75	125.46	150.4	33.48
chrips	12	0	113.3	105.9	93.43	2.7	7.5	122.8	187	315.2	179.5
corr.chrips	12	0	113.72	21.13	18.58	86.89	91.54	120.8	124.2	149.64	32.66
perssian	12	0	96.3	68.1	70.71	14.1	24.5	91.1	161.2	198.2	136.7
corre.perss	12	0	114.45	23.73	20.74	85.67	89.8	117.91	131.67	150.49	41.88
tamsat	12	0	136.8	102.7	75.08	11.4	38.4	105.7	242.2	301.2	203.8
corr.tamsa	12	0	114.12	22.61	19.81	83.51	90.46	120.32	130.2	149.59	39.74
rfe	12	0	104.3	55.4	53.16	31.3	49.8	103.9	156.2	187.7	106.4
corr.rfe	12	0	113.96	21.7	19.05	86.88	91.7	120.01	126.39	150.72	34.69

Tercha

Variable	N	N*	Mean	StDev	CoefVar	Minimum	Q1	Median	Q3	Maximum	IQR
tercha Obs	12.0	0.0	117.9	28.1	23.86	61.03	95	121.78	139.97	157.38	45.0
chrips	12.0	0.0	104.8	84.8	80.85	6.2	13	115.2	182	215.6	169.0
corr.chrips	12.0	0.0	117.6	28.2	23.94	60.68	96.26	121.63	139.39	151.02	43.1
perssian	12.0	0.0	115.3	80.9	70.16	18.3	43.7	109.7	146.4	277.5	102.7
corre.perss	12.0	0.0	117.7	27.6	23.45	61.77	96.02	121.9	139.36	152.22	43.3
tamsat	12.0	0.0	135.2	83.8	61.95	18.6	46.8	162.4	206.6	240.8	159.7
corr.tamsa	12.0	0.0	117.4	27.7	23.6	61.85	94.47	120.6	139.7	152.12	45.2
rfe	12.0	0.0	108.4	61.0	56.26	28.9	45.1	109	147.3	205.9	102.2
corr.rfe	12.0	0.0	117.1	27.6	23.6	61.66	95.7	119.91	138.7	150.57	43.0

Woliso

Variable	N	N*	Mean	StDev	CoefVar	Minimum	Q1	Median	Q3	Maximum	IQR
wolisoObs	12	0	99.81	17.2	17.23	68.56	82.35	106.73	113.93	118.6	31.2
chrips	12	0	107.7	107.2	99.5	0.3	3.5	100.9	195.9	317.3	217.7
corr.chrips	12	0	100.21	16.84	16.81	70.06	84.6	106.56	113.94	118.91	29.5
perssian	12	0	76.3	67.6	88.68	1.9	13.8	56.2	143	191.2	138
corre.perss	12	0	100.25	16.83	16.78	70.36	83.3	106.3	114.45	118.53	30.5
tamsat	12	0	105.4	107.3	101.83	4.9	13.8	67.6	212	292.9	239.9
corr.tamsa	12	0	100.11	16.76	16.74	70.01	83.8	106.77	114.09	118.46	30
rfe	12	0	90.7	66.5	73.28	10.1	35.2	65.9	156.5	208.5	133.6
corr.rfe	12	0	100	16.83	16.83	71.45	81.91	106.61	114.5	118.54	31.9

Wolkite

Variable	N	Mean	StDev	Variance	Minimum	Q1	Median	Q3	Maximum	IQR
wolkiteObs	12	88.2	72.7	5283.6	7.8	20.8	62	156.9	201.8	136.1
chrips	12	101.8	94.2	8868.7	0.6	4.6	110.1	172	267.9	167.4
corr.chrips	12	88.2	72.7	5288.4	7.8	20.8	62	157	201.8	136.2
perssian	12	82	62.6	3921.8	7.3	23.9	68.5	145.6	174.7	121.7
corre.perss	12	88.3	72.8	5292.7	7.8	20.8	62	157	201.8	136.2
tamsat	12	109.1	99.1	9824.2	8.2	21.5	73.9	194.6	275.6	173.1
corr.tamsa	12	88.2	72.7	5285.8	7.9	20.8	61.9	157	201.8	136.2
rfe	12	98.5	65.8	4328.5	11.5	42.2	81.5	169.5	193.4	127.3
corr.rfe	12	88.2	72.7	5286.4	7.9	20.8	62.1	157	201.8	136.2